Weak mixing angle at low Q^2 (JLab/Mainz parity violating electron scattering experiments)

Frank Maas
(Helmholtz Institute Mainz,
Institute for Nuclear Phyiscs,
PRISMA cluster of excellence
Johannes Gutenberg University Mainz)

Ultimate Precision at Hadron Colliders, November 29, 2019

Møller Scattering

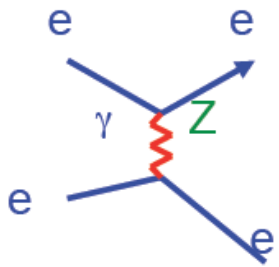

- Purely Leptonic

Q-Weak (JLab)
P2 (Mainz/MESA)

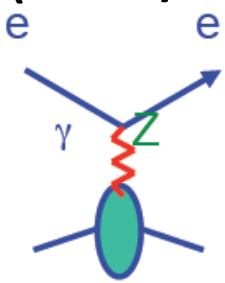

- Coherent quarks in p
- in operation now
- $2(2C_{1u}+C_{1d})$

e-DIS

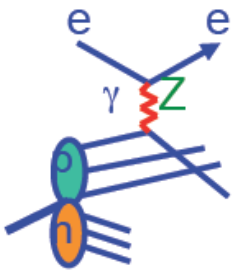

- Isoscaler quark scattering
- $(2C_{1u}-C_{1d})+Y(2C_{2u}-C_{2d})$

Atomic Parity Violation

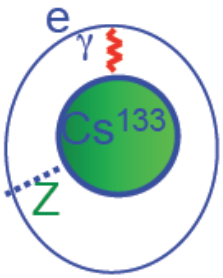

- Coherent quarks in entire nucleus
- Nuclear structure uncertainties
- $-376\ C_{1u} - 422\ C_{1d}$

Neutrino Scattering

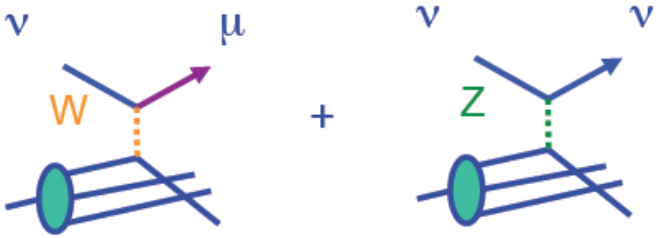

- Quark scattering (from nucleus)
- Weak charged and neutral current difference

S. Su

Courtesy of P. Reimer and R. Arnold

Weak charge $Q_W(p)$ and weak mixing angle $\sin^2\theta_W$

The relative strength between the weak and electromagnetic interaction is determined by the weak mixing angle: $\sin^2\theta_W$

left-right symmetric

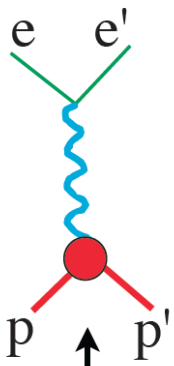

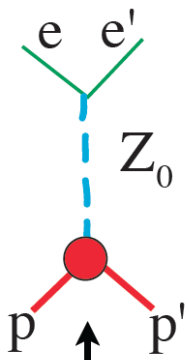

left-right symmetry violated: „parity violation“, measure A_{LR}^{exp}

$Q_e(p) = +1$
electric charge of the proton

$Q_W(p) = 1 - 4\sin^2\theta_W = 0.05$
weak charge of the proton
small modification of $\sin^2\theta_W$: amplified in $Q_W(p)$

$\sin^2\theta_W$: a central parameter of the standard model, sensitive to physics beyond the standard model

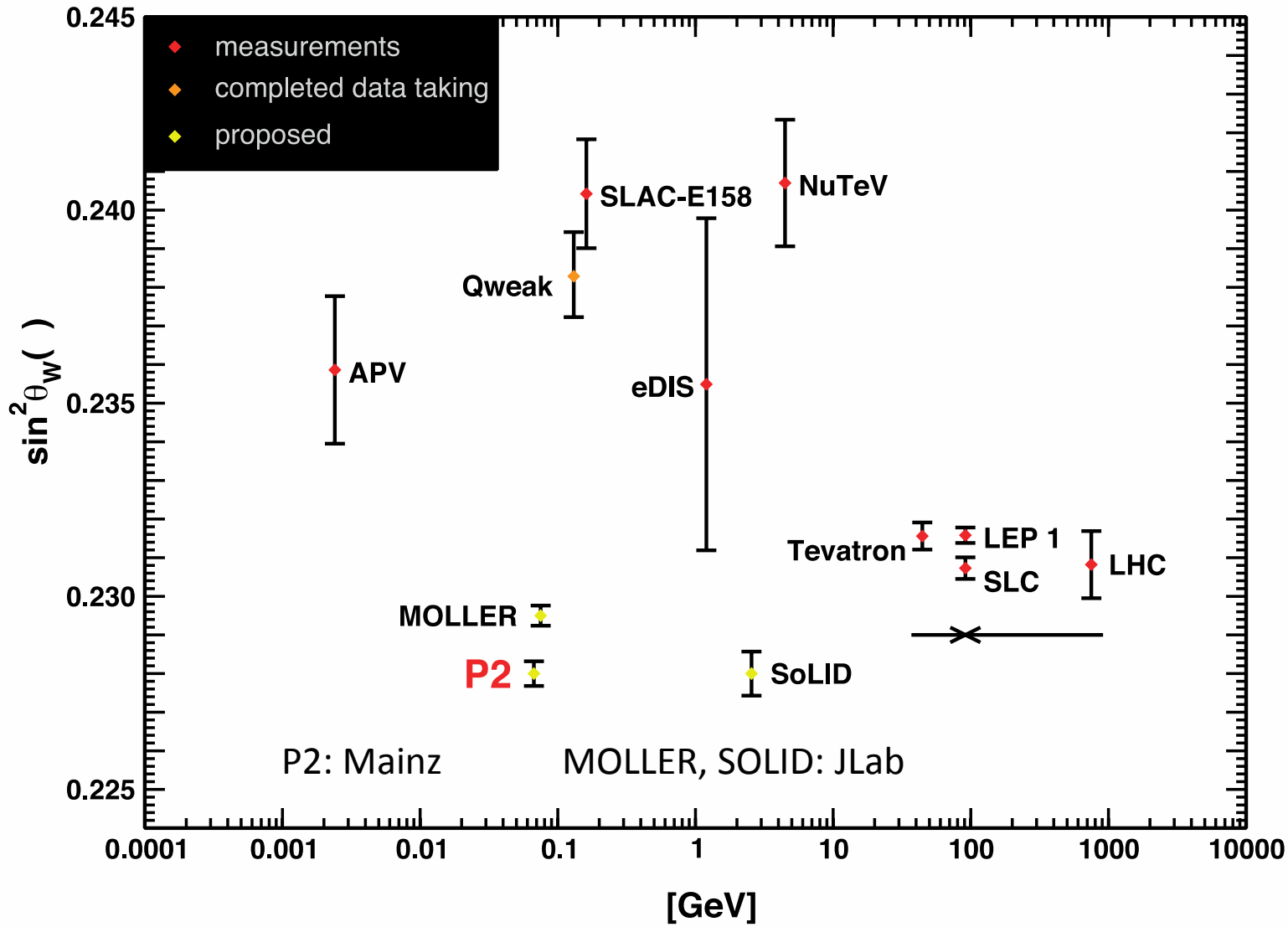
measurements
completed data taking
proposed
0.245
0.240
0.235
0.230
0.225
$\sin^2\theta_W(\ )$
APV
Qweak
SLAC-E158
NuTeV
eDIS
Tevatron
LEP 1
SLC
LHC
MOLLER
P2
SoLID
P2: Mainz
MOLLER, SOLID: JLab
0.0001
0.001
0.01
0.1
1
10
100
1000
10000
[GeV]

Universal quantum corrections: can be absorbed into a scale dependent, „running“ $\sin^2\theta_{eff}$ or $\sin^2\theta_W(\mu)$

On Z resonance: A_Z is imaginary

$$\left|A_Z + A_{new}\right|^2 \rightarrow A_Z^2\left[1+\left(\frac{A_{new}}{A_Z}\right)^2\right]$$

No interference term

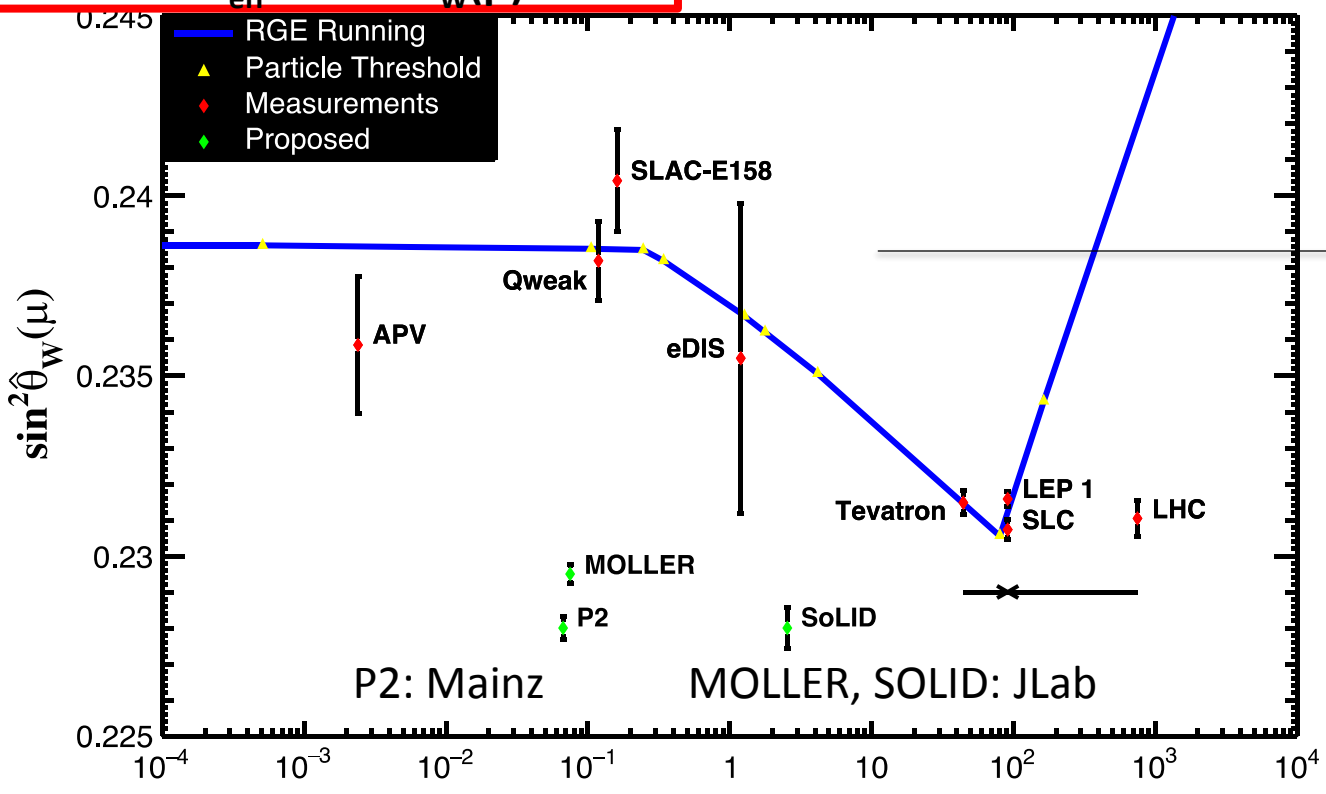

3 %

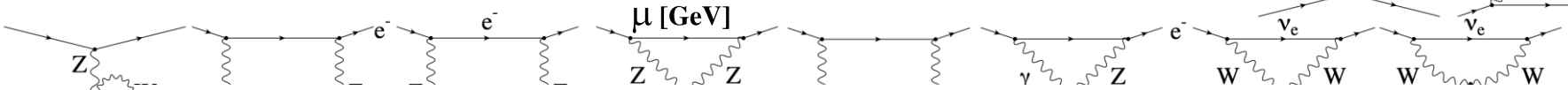

$\delta(Q^e_W)$ (theory) = 0.6%, factor of 2 improvement with full two-loop calculation

Sensitivity to new physics beyond the Standard Model

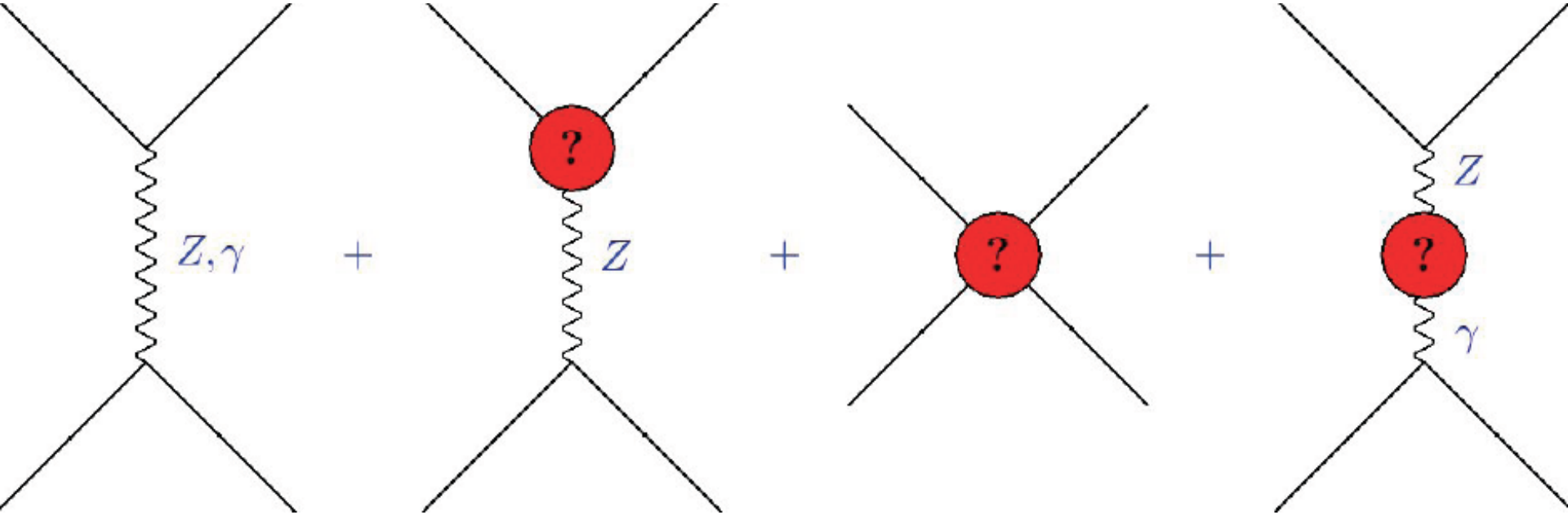

Extra Z

Mixing with
Dark photon or
Dark Z

Contact interaction

New
Fermions

Running $\sin^2\theta_W$ and Dark Parity Violation

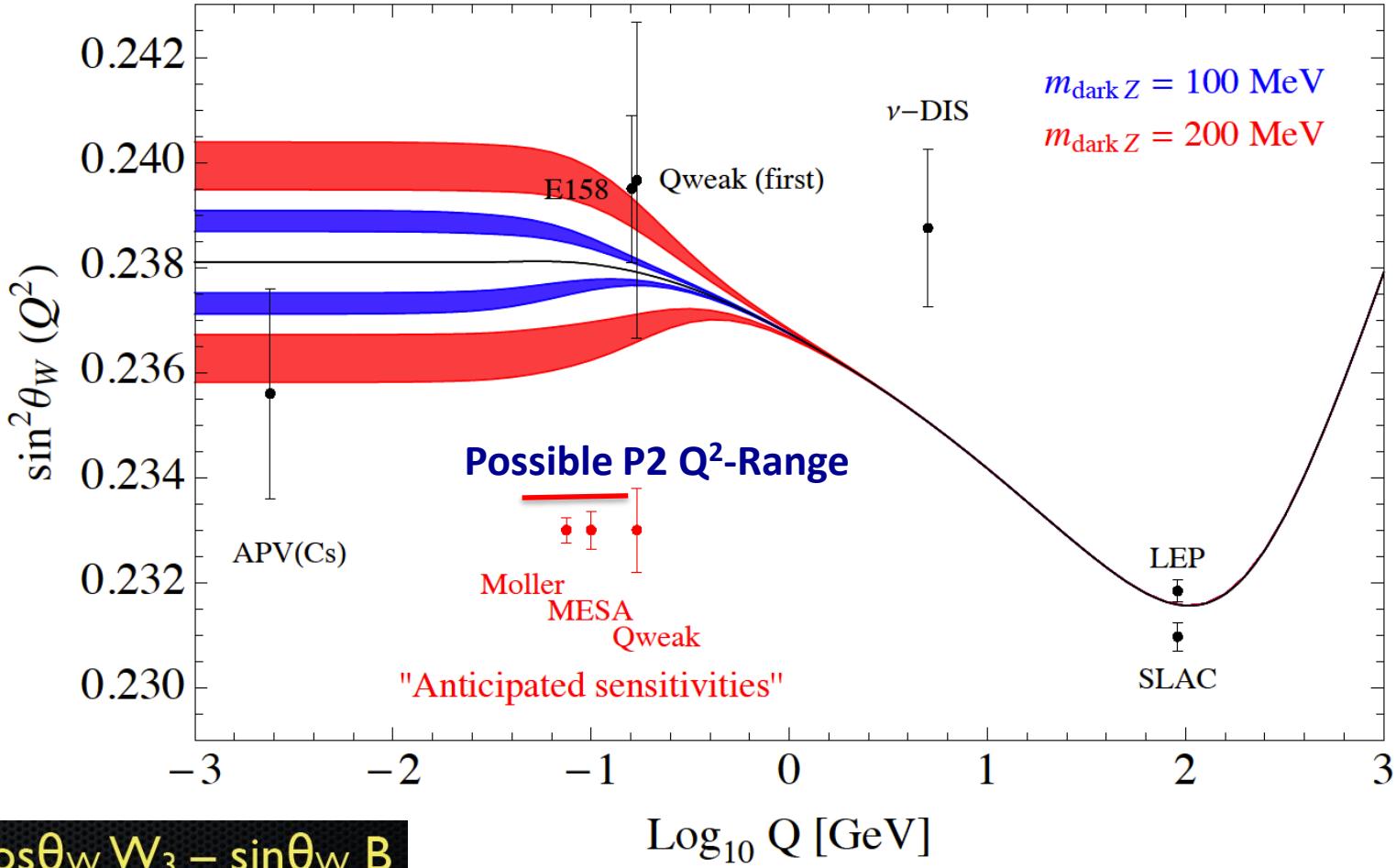

$Z = \cos\theta_W W_3 - \sin\theta_W B$

$A = \sin\theta_W W_3 + \cos\theta_W B$

Bill Marciano

- Complementary access by weak charges of proton and electron

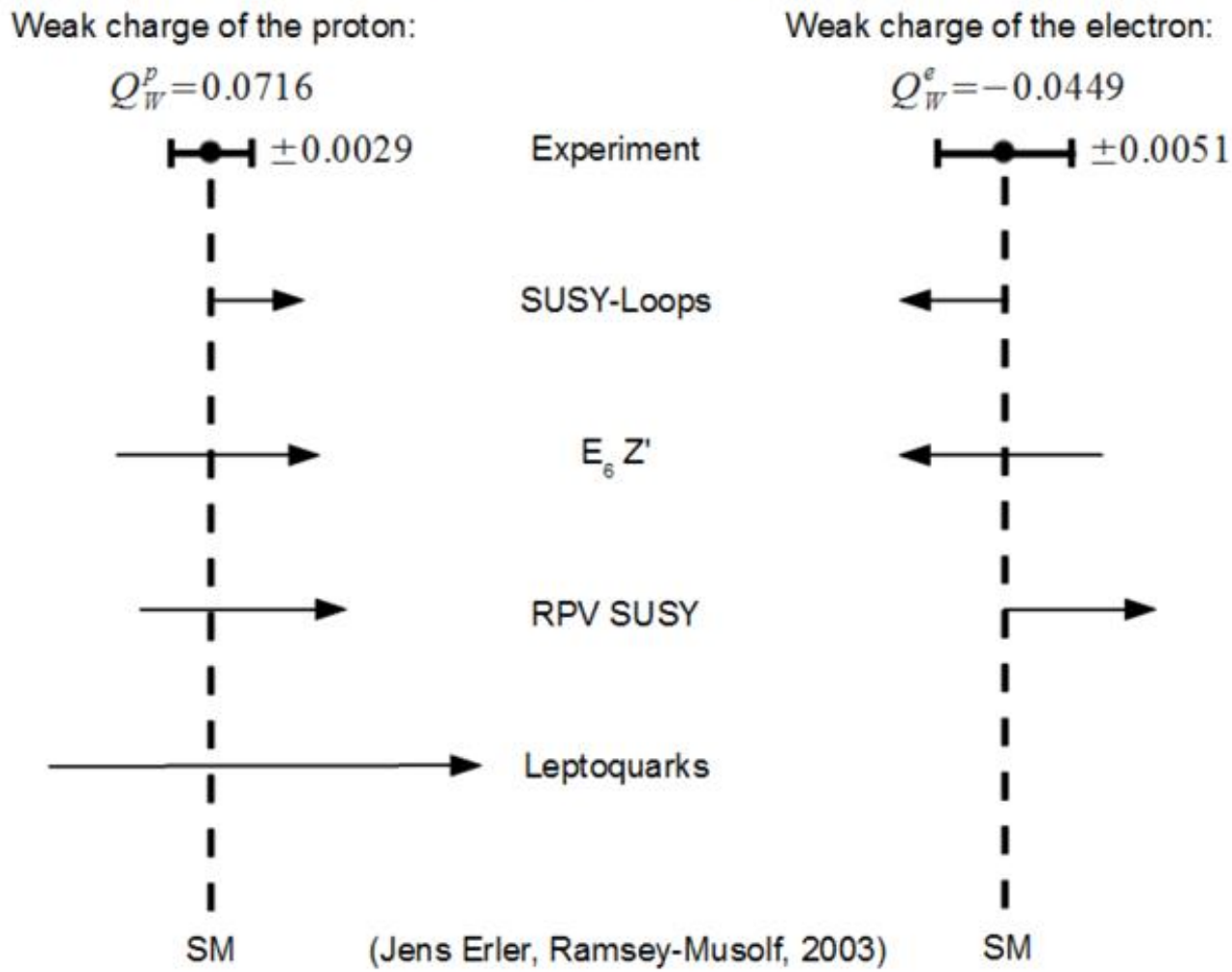

(Jens Erler, Ramsey-Musolf, 2003)

Weak Charge Of Proton: Qweak (Jlab), P2 (MESA)

Weak Charge Of Electron: MOELLER (JLAB)

Weak Charge Of Quarks: SOLID (PVDIS) (JLAB)

Proton: special case

Proton Weak charge:	$Q_W(p)$	=	$1 - 4 \sin^2 \theta_W$
Error:	$\Delta Q_W(p)$	=	$4\, \Delta\sin^2 \theta_W$
Rel. error:	$\Delta Q_W(p)/Q_W(p)$	=	$4/(\ (1/\sin^2 \theta_W) - 4\ )\ \ (\Delta\sin^2 \theta_W/\sin^2 \theta_W)$
Rel. error	$\Delta\sin^2 \theta_W/\sin^2 \theta_W$	=	$(\ (1/\sin^2 \theta_W) - 4\ )/4\ \ \Delta Q_W(p)/Q_W(p)$
Example:	$\sin^2 \theta_W$ (50 MeV)	=	0.238
	$4/(\ (1/\sin^2 \theta_W) - 4\ )$	~	20
	$\Delta Q_W(p)/Q_W(p)$	=	2% from Experiment
	$\Delta\sin^2 \theta_W/\sin^2 \theta_W$	=	0.1 % same precision as LEP, SLAC
Neutron Weak charge:	$\Delta Q_W(p)/Q_W(n)$	=	$\Delta\sin^2 \theta_W/\sin^2 \theta_W$

Physics sensitivity from contact interaction (LEP2 convention, g^2= 4pi)

	precision	$\Delta \sin^2\bar{\theta}_W(0)$	Λ_{new} (expected)
APV Cs	0.58 %	0.0019	32.3 TeV
E158	14 %	0.0013	17.0 TeV
Qweak I	19 %	0.0030	17.0 TeV
Qweak final	4.5 %	0.0008	33 TeV
PVDIS	4.5 %	0.0050	7.6 TeV
SoLID	0.6 %	0.00057	22 TeV
MOLLER	2.3 %	0.00026	39 TeV
P2	2.0 %	0.00036	49 TeV
PVES ^{12}C	0.3 %	0.0007	49 TeV

Jens Erler

Parity Violating Asymmetry in elastic electron proton scattering

$\sigma \approx$

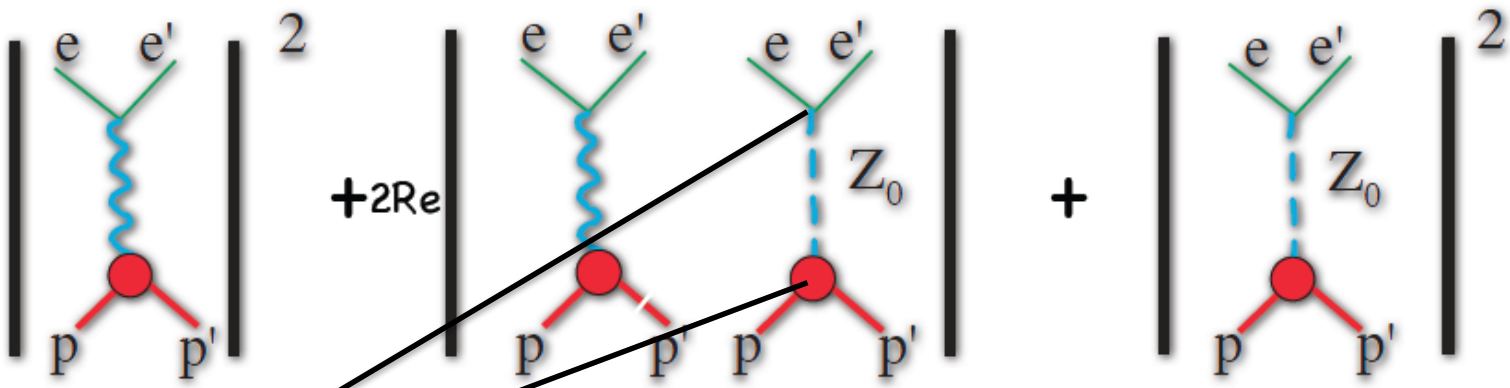

$(V\text{-}A)_e(V\text{-}A)_p$

$A_eV_p+V_eA_p$

V-A coupling:
parity-violating
cross section asymmetry A_{LR}
longitudinally pol. electrons
unpolarised protons

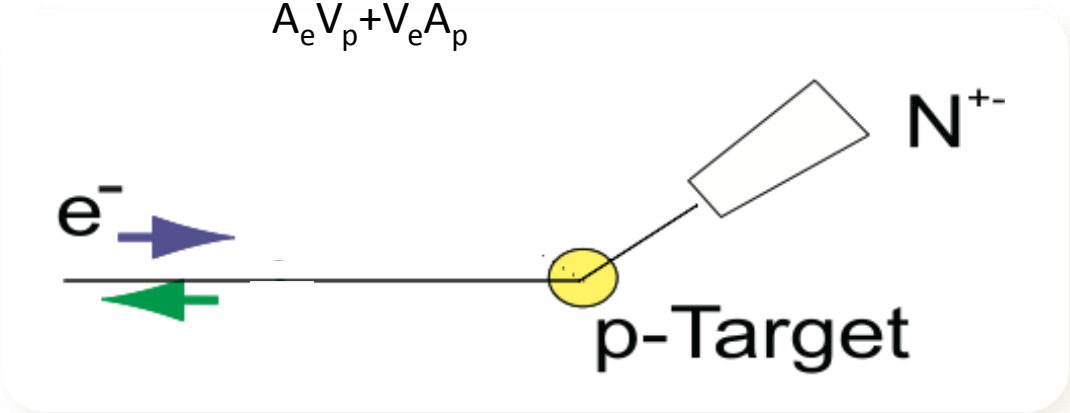

Conceptually very simple experiments

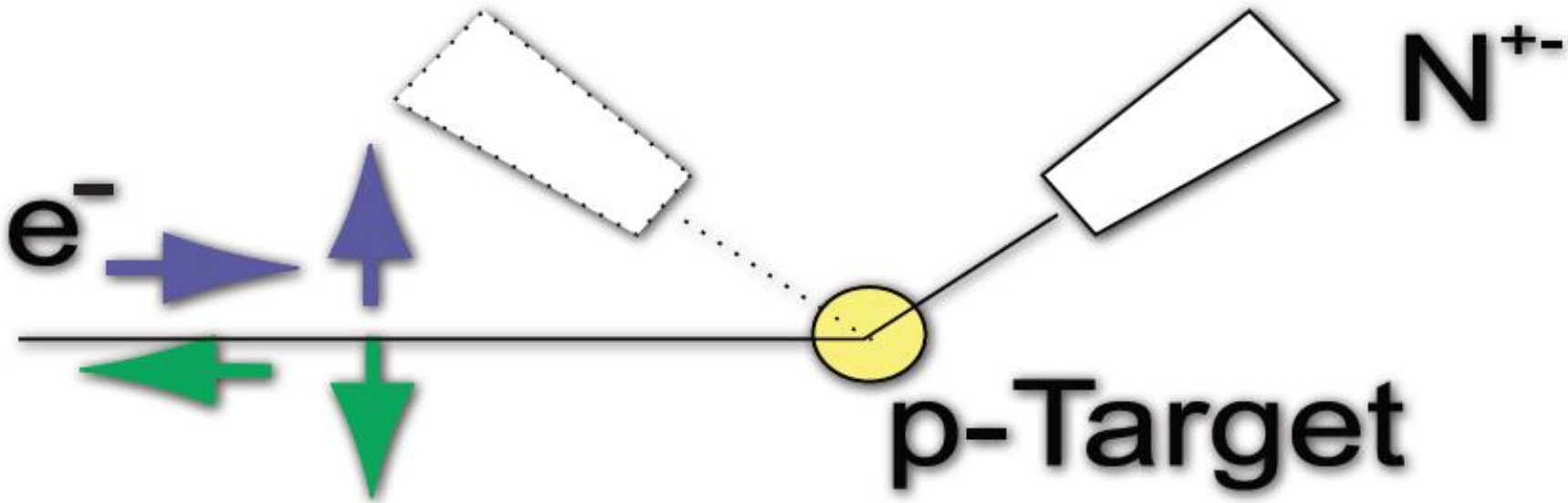

$A = (N^+ - N^-)/(N^+ + N^-)$ $\Delta A = (N^+ + N^-)^{-1/2} = N^{-1/2}$

$A = 20 \times 10^{-9}$ 2% Measurement $N = 6.25 \times 10^{18}$ events

Highest rate, measure Q^2: Large Solid Angle Spectrometers

Apparative (false) asymmetries:

Extreme good control of beam and target

Flip Helicity fast

Extra spin flip

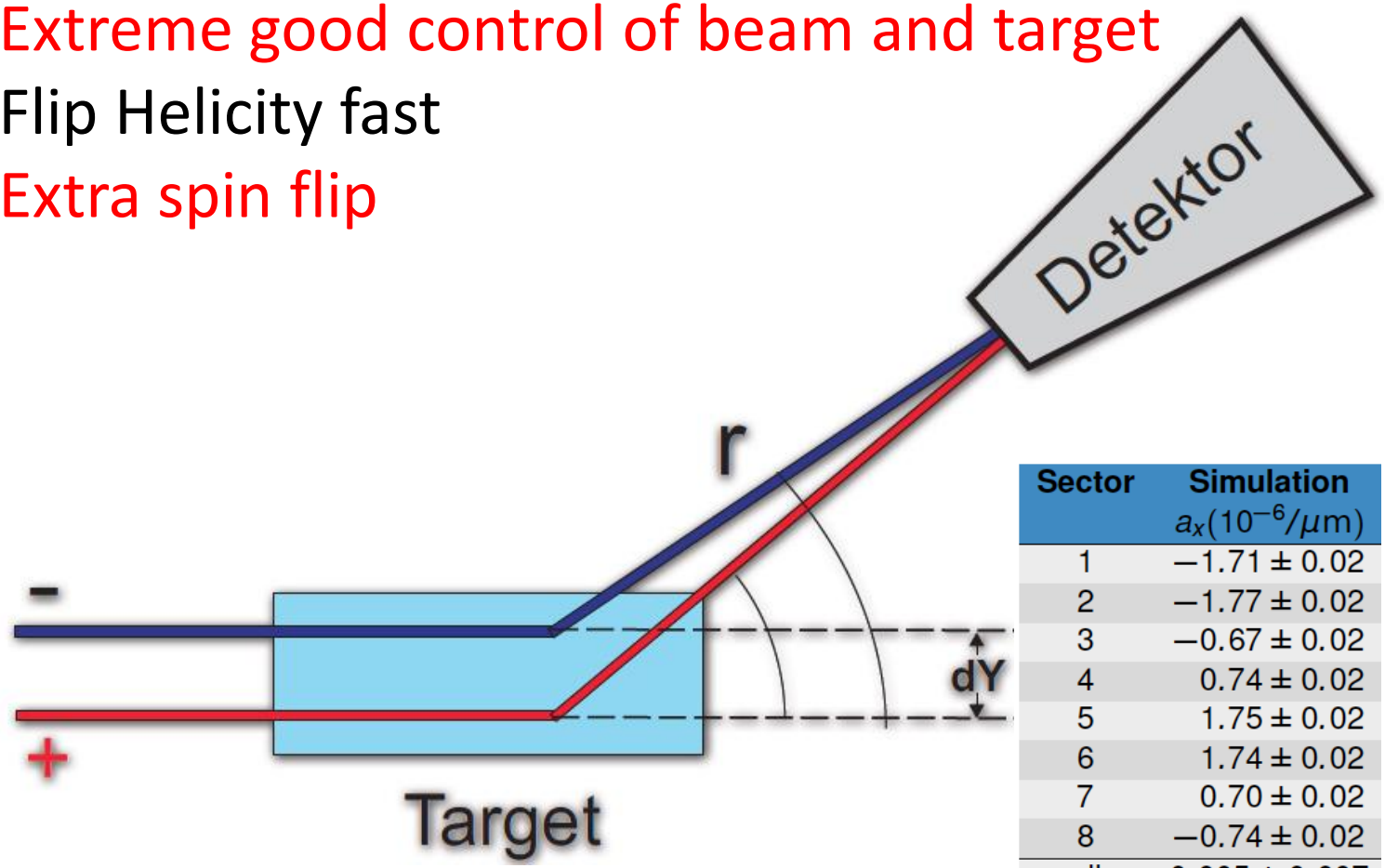

Sector	Simulation $a_x(10^{-6}/\mu m)$	Sector	Simulation $a_E(10^{-9}/eV)$
1	-1.71 ± 0.02	1	-11.4 ± 0.1
2	-1.77 ± 0.02	2	-11.4 ± 0.1
3	-0.67 ± 0.02	3	-11.5 ± 0.1
4	0.74 ± 0.02	4	-11.4 ± 0.1
5	1.75 ± 0.02	5	-11.5 ± 0.1
6	1.74 ± 0.02	6	-11.4 ± 0.1
7	0.70 ± 0.02	7	-11.3 ± 0.1
8	-0.74 ± 0.02	8	-11.5 ± 0.1
all	0.005 ± 0.007	all	-11.42 ± 0.04

Counting Technique

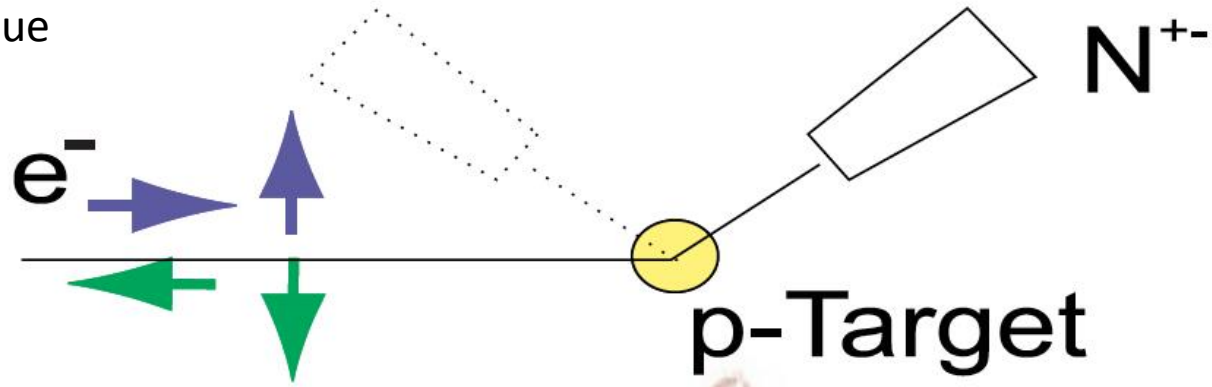

Count scattered electrons:
- pile-up (double count losses)
- Background Asymmetry
- Very Fast Counting (MHz)
- Measure TOF or Energy

Analogue Technique

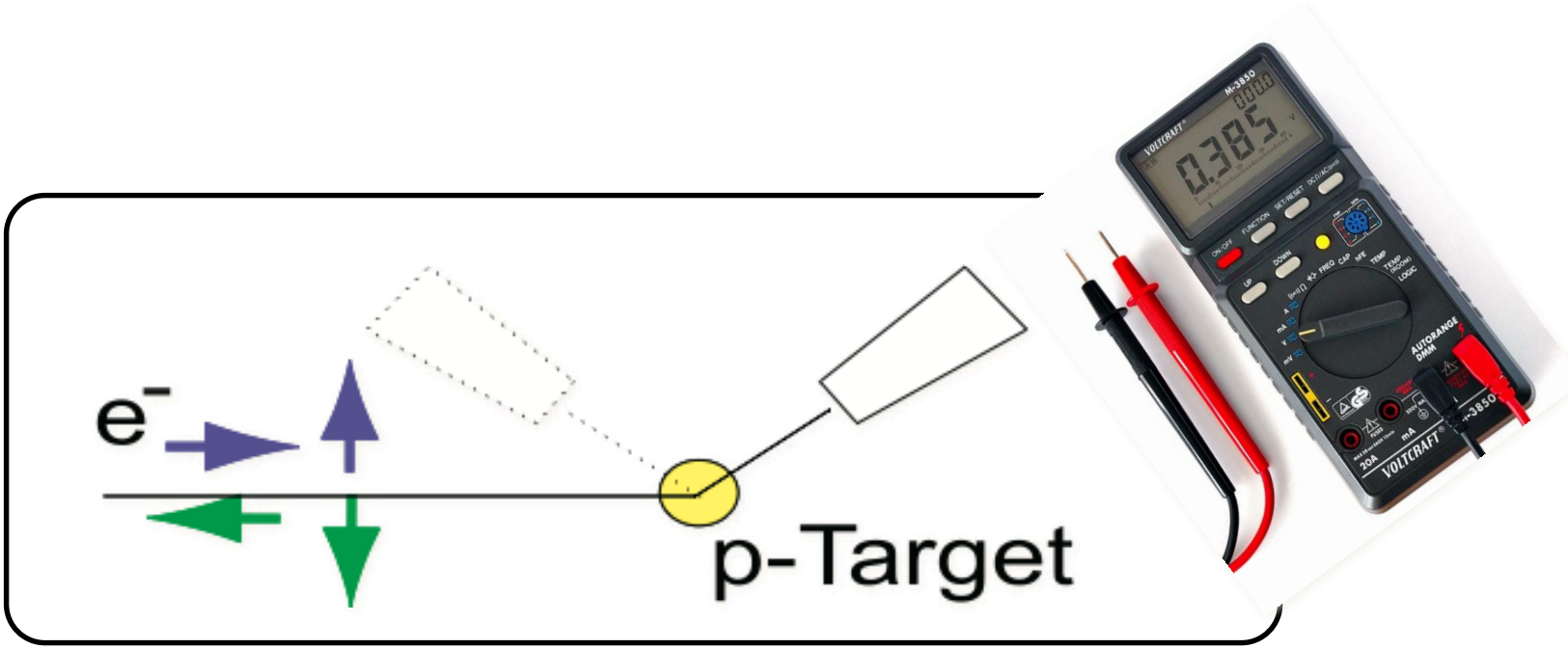

Measure Flux of Scattered electrons:
- no pile-up (double count losses)
- sensitive to small electr. fields.
- no separation of phys. process

PVeS Experiment Summary

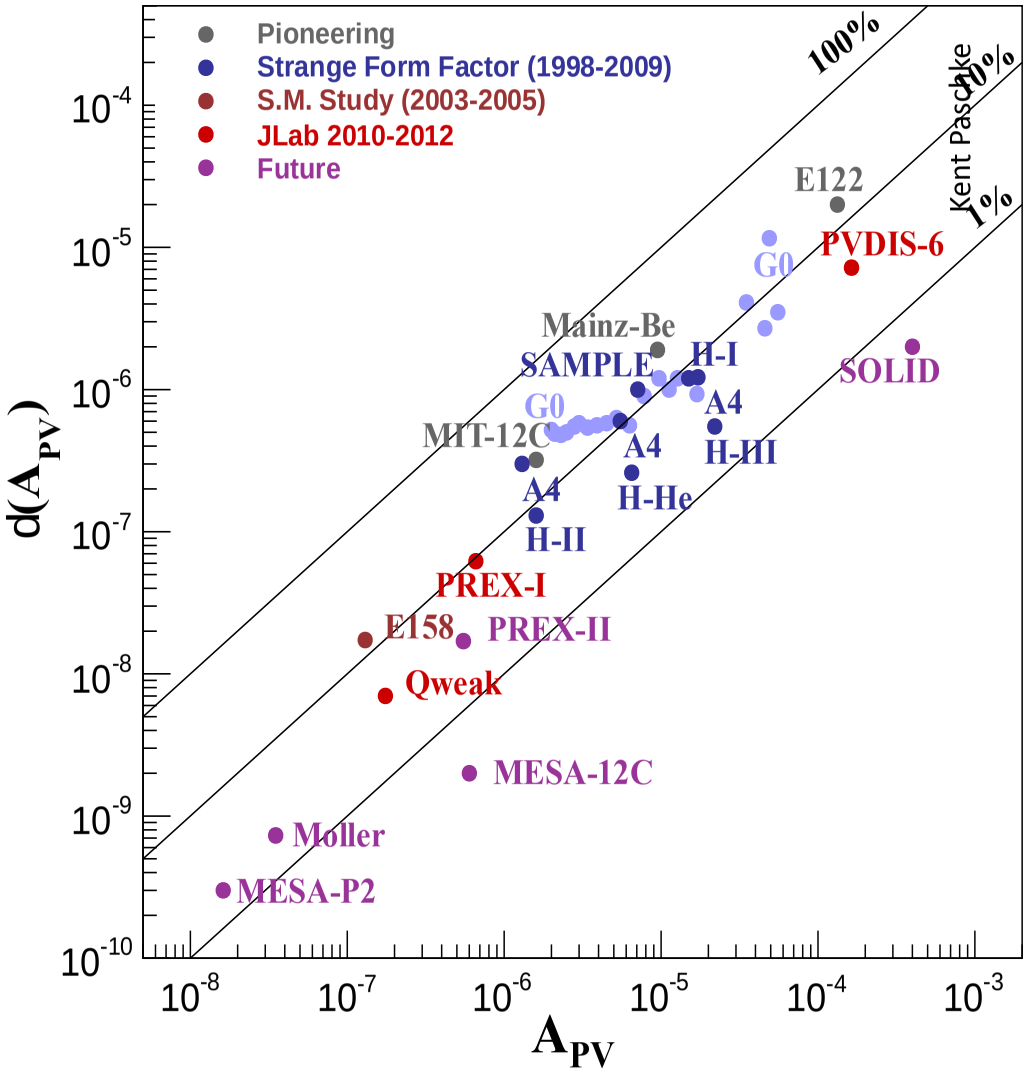

Mainz Energy-Recovering Superconducting Accelerator (MESA)

Key parameters electron accelerator MESA

- Max. beam energy 155 MeV
- Beam current >1 mA (ERL mode)
- Superconducting cavities
- **Commissioning 2021**

New underground (-11m) experimental hall currently under construction

(Art. 91b *Forschungsbau*)

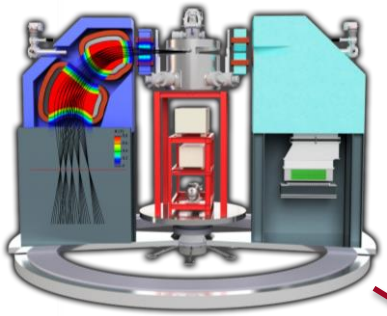

MAGIX experiment
(internal gas target)

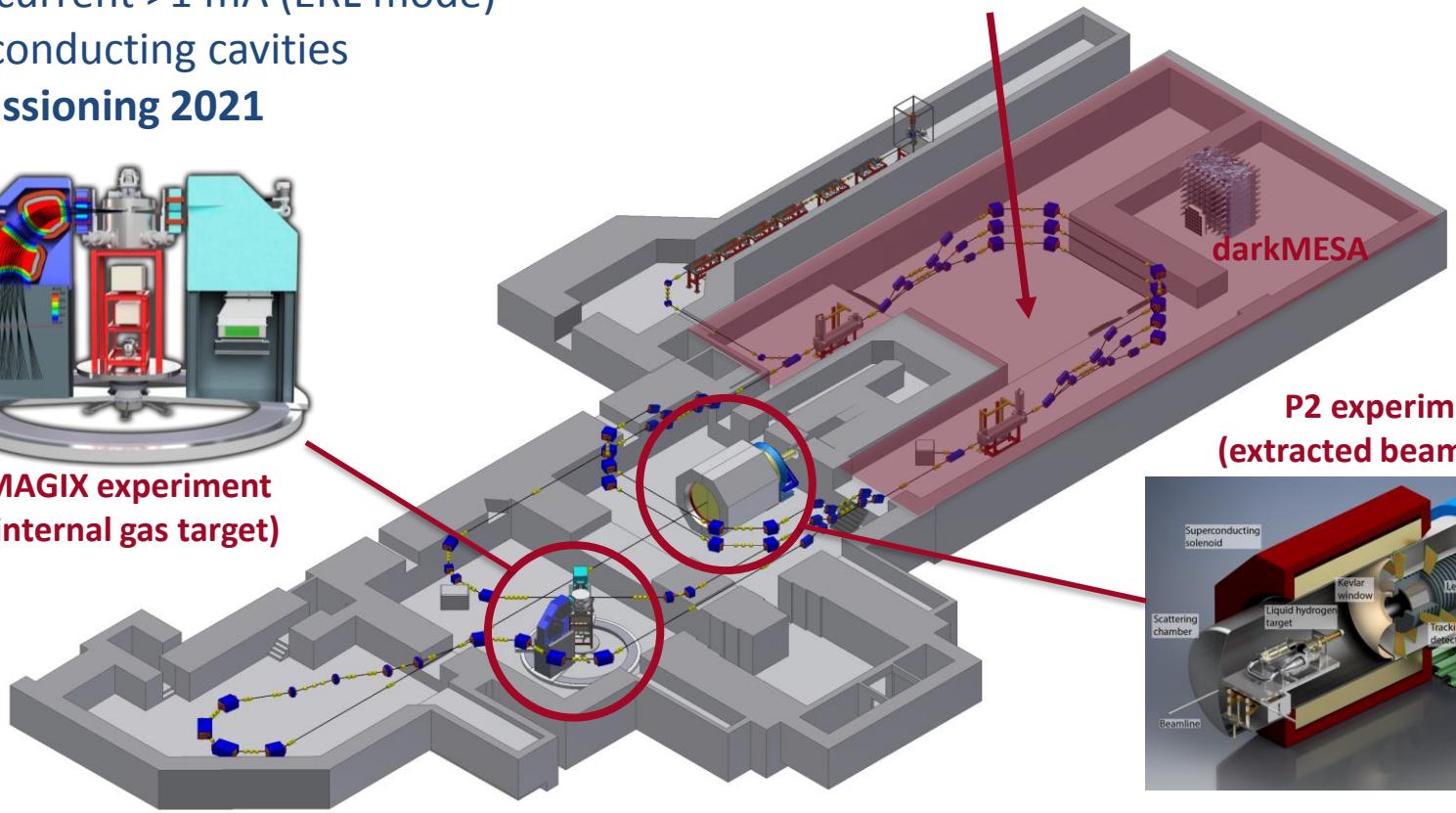

P2 experiment
(extracted beam mode)

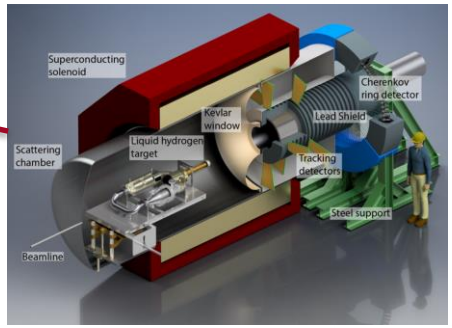

$$A_{LR}^{exp} = \frac{\sigma(e^{\rightarrow}) - \sigma(e^{\leftarrow})}{\sigma(e^{\rightarrow}) + \sigma(e^{\leftarrow})} = -P\,\frac{G_F Q^2}{4\sqrt{2}\pi\alpha}\left(Q_W(p) - F(Q^2)\right)$$

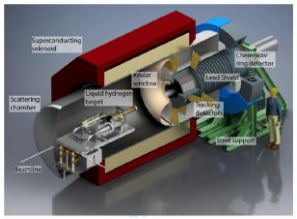

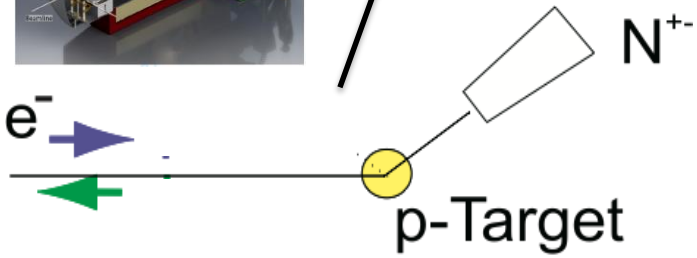

Cross section asymmetry A_{LR}^{exp}
Magnetic spectrometer
Cherenkov detector
Read-out electronics
Data acquisition

Momentum transfer Q^2
Tracking system

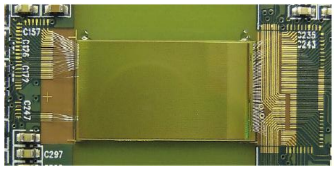

Beam polarisation P
Polarimetry

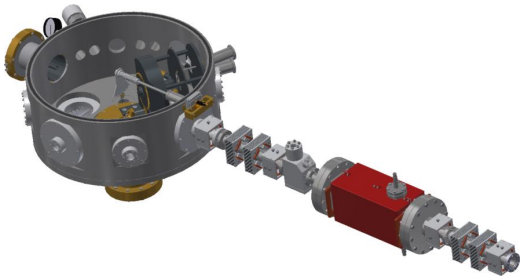

Hadron structure $F(Q^2)$,
Strangeness form factors
Axial form factor
QED and EW corrections
Theory

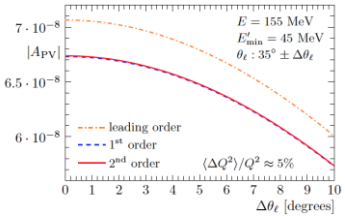

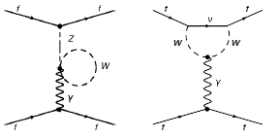

- Contributions to $\Delta\sin^2\Theta_W$ for 35° central scattering angle, E=150 MeV, 10000 h of data taking

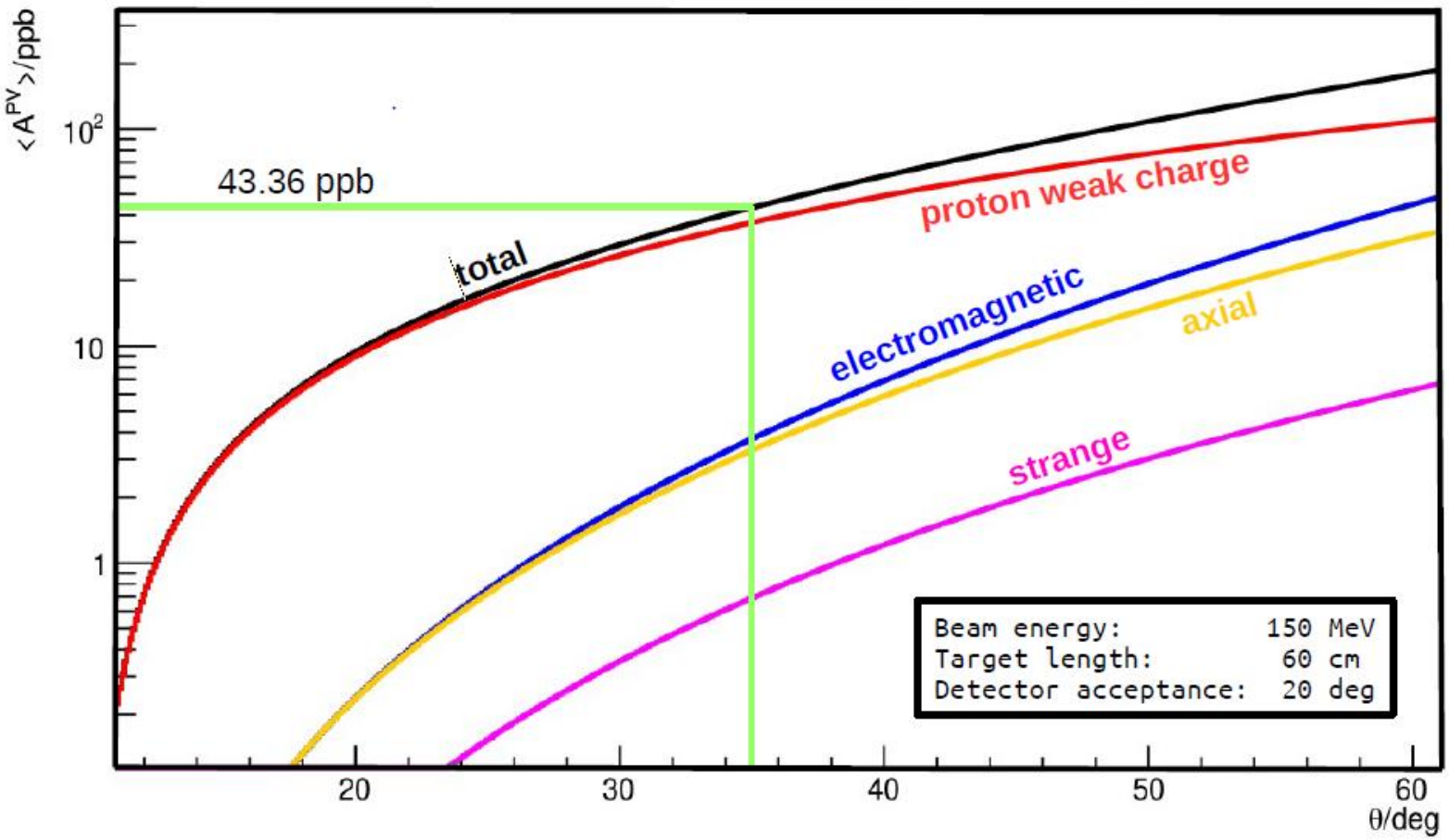

A_{exp}	-24.03 ppb
ΔA_{stat} (2.1 %)	± 0.50 ppb
ΔA_{P} (0.50 %)	± 0.12 ppb
ΔA_{false} (0.42 %)	± 0.10 ppb
$\Delta A_{t.w.}$ (0.79 %)	± 0.19 ppb
$\Delta A_{t.p.}$ (0.04 %)	± 0.01 ppb
ΔA_{tot} (2.4 %)	± 0.58 ppb
$\sin^2\theta_W$	0.23116
$\Delta_{\square_{\gamma Z}} \sin^2\theta_W$ (0.02 %)	± 0.0004
$\Delta_{FF} \sin^2\theta_W$ (0.05 %)	± 0.00012
$\Delta \sin^2\theta_W$	± 0.00037
$\Delta \sin^2\theta_W / \sin^2\theta_W$	0.16 %

Including:
- Detector response
- Validated by MAMI test beam measurements
- Effects from target
- Measured field map
- 10,000 h data taking
- Additional backward angle measurement
- 1 loop corrections

(10,000 h) data taking →

$\int \mathcal{L} dt \simeq 8.6\ \mathrm{ab}^{-1}$

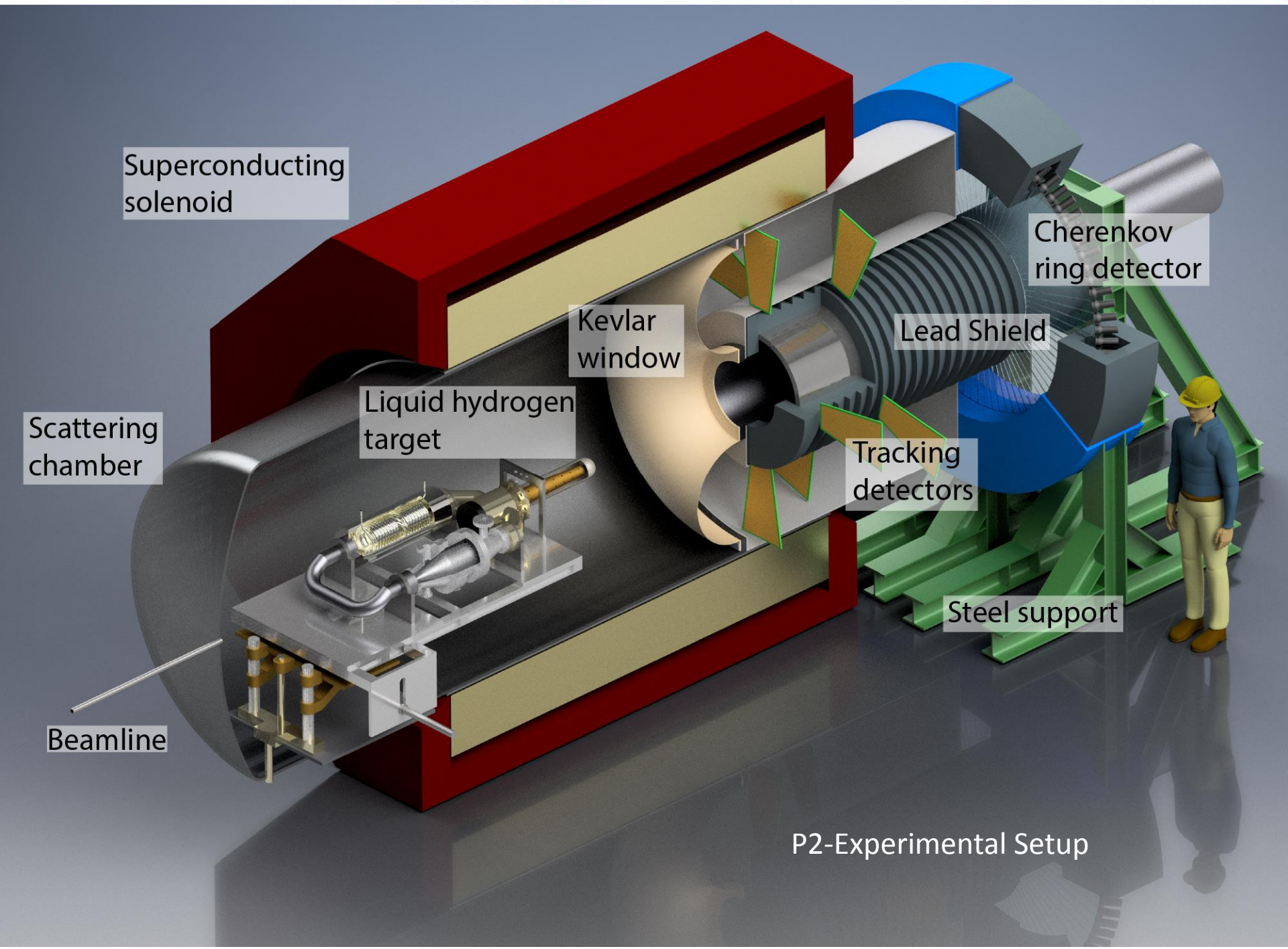
Superconducting solenoid
Cherenkov ring detector
Kevlar window
Lead Shield
Liquid hydrogen target
Scattering chamber
Tracking detectors
Steel support
Beamline
P2-Experimental Setup

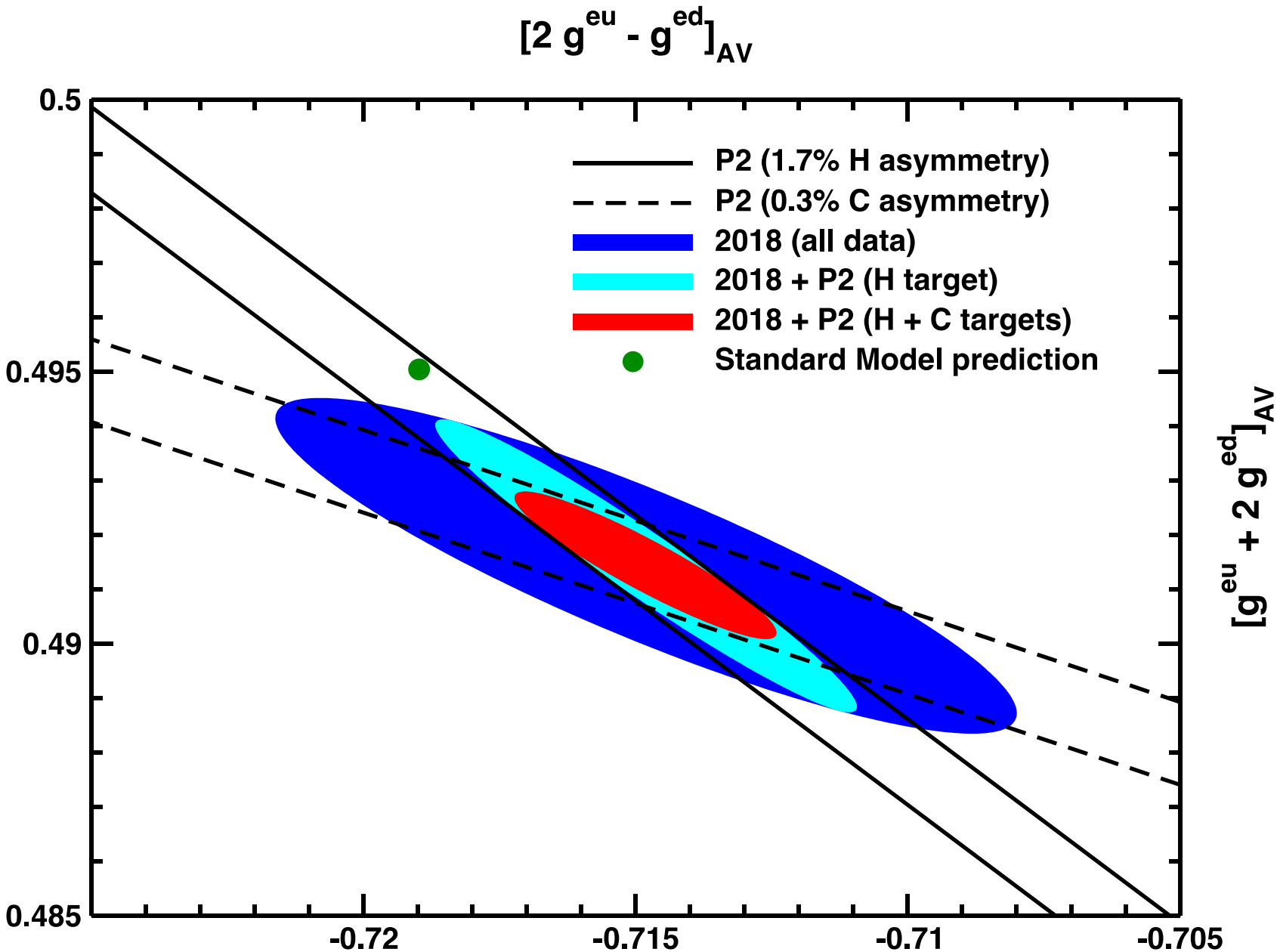

Combine measurements on Hydrogen with a measurement on Carbon

Neutron skins and neutron stars in the multi-messenger era

PHYSICAL REVIEW LETTERS **120**, 172702 (2018)

Editors' Suggestion Featured in Physics

Neutron Skins and Neutron Stars in the Multimessenger Era

F. J. Fattoyev,[1,*] J. Piekarewicz,[2,†] and C. J. Horowitz[1,‡]

[1]*Center for Exploration of Energy and Matter and Department of Physics, Indiana University, Bloomington, Indiana 47405, USA*

[2]*Department of Physics, Florida State University, Tallahassee, Florida 32306, USA*

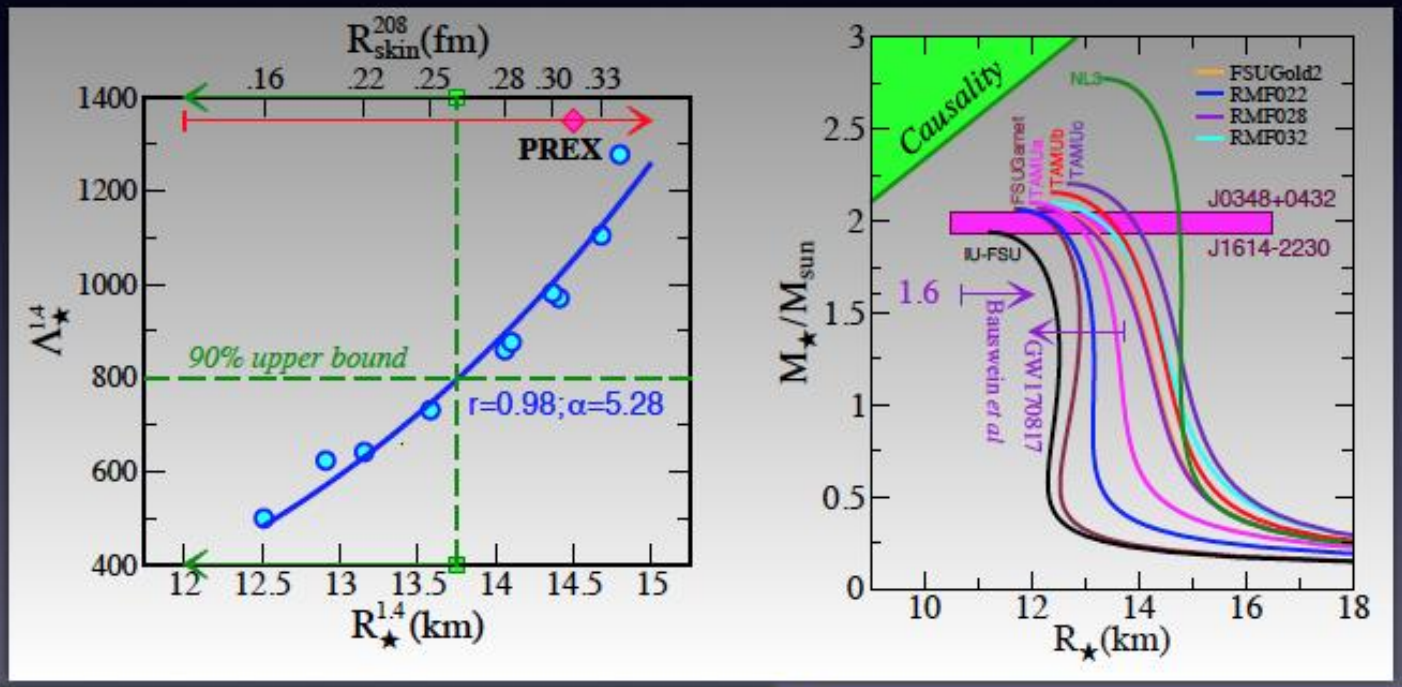

Exciting possibility: If PREX confirms that Rskin is large and LIGO-Virgo that NS-radius is small, this may be evidence of a softening of the EOS at high densities (phase transition?)

The very first observation of a BNS merger already provides a treasure trove of insights into the nature of dense matter!

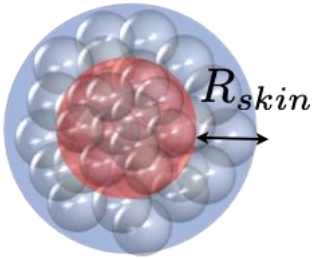

Equation of state of heavy neuclei describes also neutron stars (NS)

→ Correlation btw. **radius R_{NS}** and **neutron skin thickness** of nuclei ^{208}Pb

→ Neutron star deformability correlated with R_{NS} and measured in neutron star merger via gravitational waves

$$E(\rho,\delta) = E(\rho,0) + \boxed{E_{sym}(\rho)}\delta^2 +$$

$$\delta = (\rho_n - \rho_p)/(\rho_n + \rho_p)$$

MREX@MESA (modified P2 detector):

Programme to measure neutron thickness of heavy nuclei (^{208}Pb) via parity violation

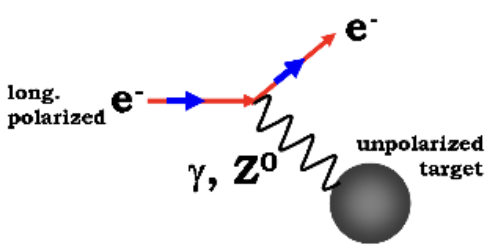

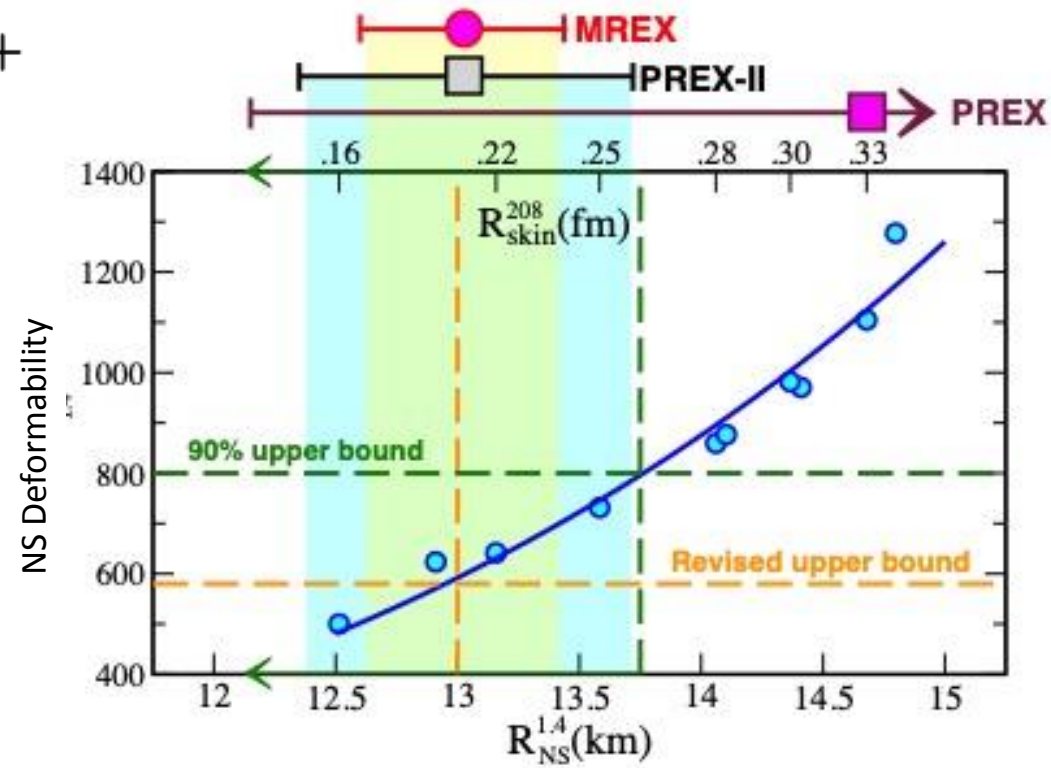

P2: Design report published

The P2 Experiment arXiv:1802.04759

A future high-precision measurement of the electroweak mixing angle at low momentum transfer

Dominik Becker[1,2], Razvan Bucoveanu[1,3], Carsten Grzesik[1,2], Ruth Kempf[1,2], Kathrin Imai[1,2], Matthias Molitor[1,2], Alexey Tyukin[1,2], Marco Zimmermann[1,2], David Armstrong[4], Kurt Aulenbacher[1,2,5], Sebastian Baunack[1,2], Rakitha Beminiwattha[6], Niklaus Berger[1,2], Peter Bernhard[1,7], Andrea Brogna[1,7], Luigi Capozza[1,2,5], Silviu Covrig Dusa[8], Wouter Deconinck[4], Jürgen Diefenbach[1,2], James Dunne[17], Jens Erler[9], Ciprian Gal[10], Boris Gläser[1,2], Boxing Gou[1,2,5], Wolfgang Gradl[1,2], Michael Gericke[11], Mikhail Gorchtein[1,2], Yoshio Imai[1,2], Krishna S. Kumar[12], Frank Maas[1,2,5,a], Juliette Mammei[11], Jie Pan[11], Preeti Pandey[11], Kent Paschke[10], Ivan Perić[13], Mark Pitt[14], Sakib Rahman[11], Seamus Riordan[15], David Rodríguez Piñeiro[1,2,5], Concettina Sfienti[1,2,3,7], Iurii Sorokin[1,2], Paul Souder[16], Hubert Spiesberger[1,3], Michaela Thiel[1,2], Valery Tyukin[1,2], and Quirin Weitzel[1,7]

[1] PRISMA Cluster of Excellence, Johannes Gutenberg-Universität Mainz, Germany
[2] Institute of Nuclear Physics, Johannes Gutenberg-Universität Mainz, Germany
[3] Institute of Physics, Johannes Gutenberg-Universität, Mainz, Germany
[4] College of William and Mary, Williamsburg, Virginia, USA
[5] Helmholtz Institute Mainz, Johannes Gutenberg-Universität Mainz, Germany
[6] Louisiana Tech University, Ruston, Louisiana, USA
[7] Detector Laboratory, PRISMA Cluster of Excellence, Johannes Gutenberg-Universität Mainz, Germany
[8] Thomas Jefferson National Accelerator Facility, Newport News, Virginia, USA
[9] Departamento de Física Teórica, Instituto de Física, Universidad Nacional Autónoma de México, CDMX, México
[10] University of Virginia, Charlottesville, Virginia, USA
[11] Department of Physics and Astronomy, University of Manitoba, Winnipeg, Canada
[12] Department of Physics and Astronomy, Stony Brook University, Stony Brook, USA
[13] Institute for Data Processing and Electronics, Karlsruhe Institute of Technology, Karlsruhe, Germany
[14] Virginia Tech University, Blacksburg, Virginia, USA
[15] Physics Division, Argonne National Laboratory, Argonne, USA
[16] Physics Department, Syracuse University, Syracuse, USA
[17] Mississippi State University, Mississippi State, MS, USA

The 12 GeV Upgrade of JLab

First physics beams to Hall A in 2014

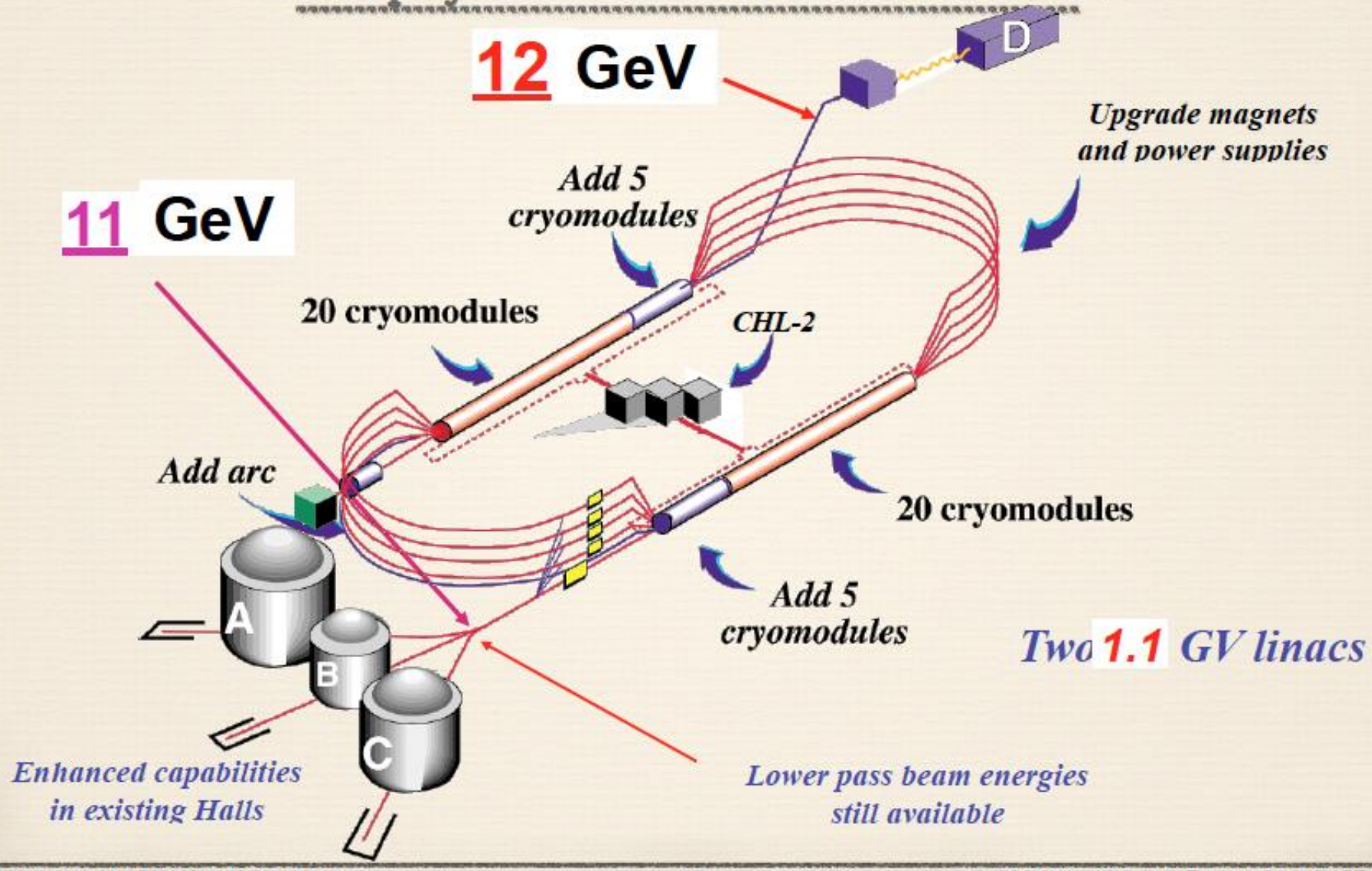

Parity-Violating Fixed Target 11 GeV electron-electron (Møller) scattering

MOLLER at JLab

Unique opportunity leveraging the 12 GeV Upgrade investment

Evolutionary progression to extraordinary luminosity and electron beam stability with high longitudinal beam polarization

60 μA 90% polarized electrons

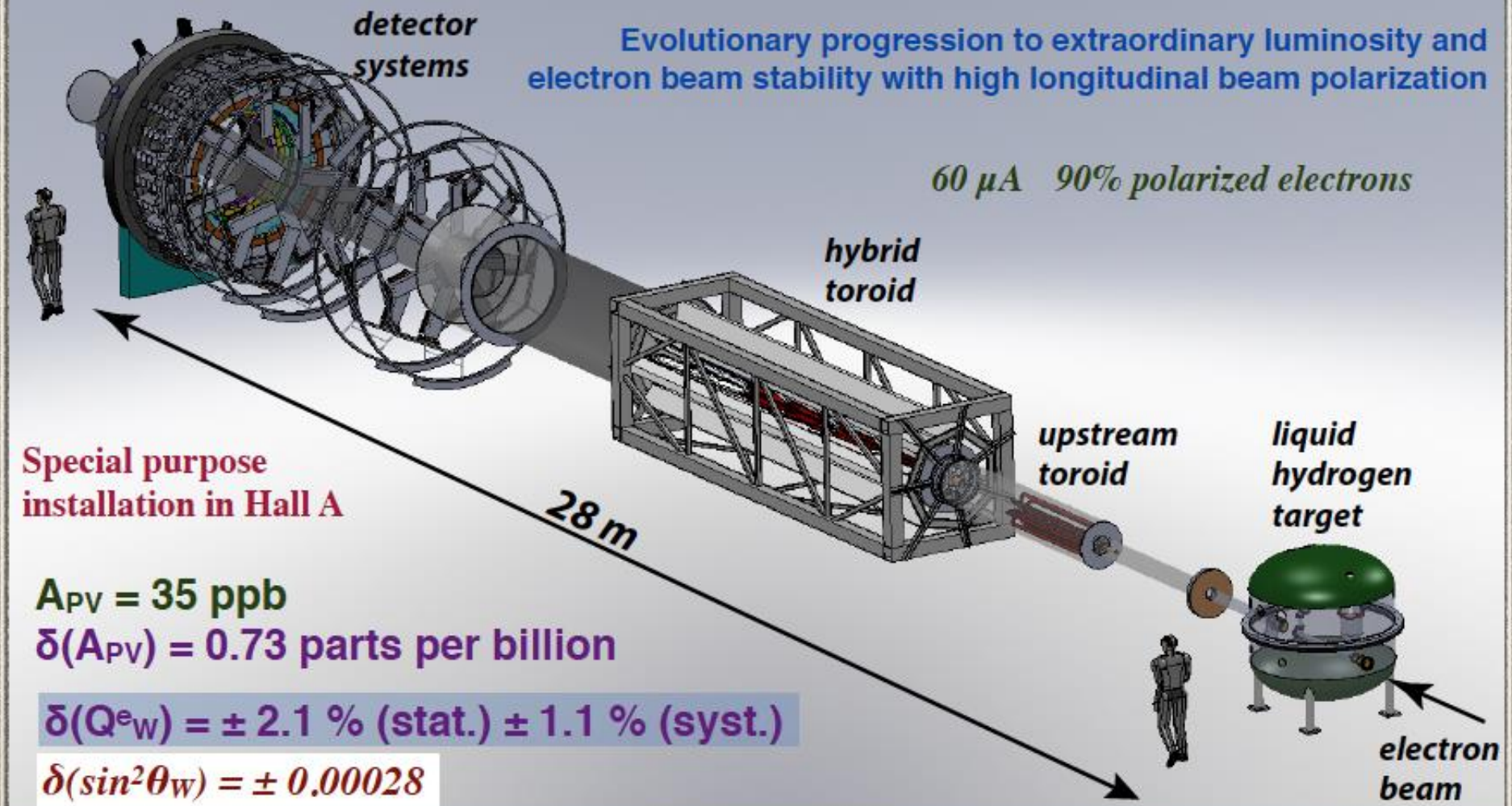

Special purpose installation in Hall A

A_{PV} = 35 ppb

$\delta(A_{PV})$ = 0.73 parts per billion

$\delta(Q^e_W) = \pm 2.1\ \%$ (stat.) $\pm 1.1\ \%$ (syst.)

$\delta(\sin^2\theta_W) = \pm 0.00028$

MOLLER Apparatus

Technical Challenges

Evolutionary Improvements from Technology of Third Generation Experiments

- ~ 150 GHz scattered electron rate
- 1 nm control of beam centroid on target
- > 10 gm/cm² liquid hydrogen target
  - 1.5 m: ~ 5 kW @ 85 μA
- Full Azimuthal acceptance with θ_{lab} ~ 5 mra
  - novel toroidal spectrometer pair
  - radiation hard, highly segmented integrating detectors
- Robust and Redundant 0.4% beam polarimetry

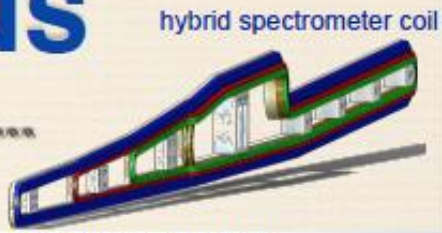

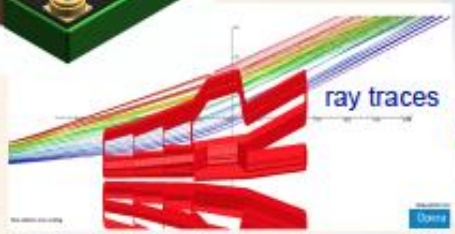

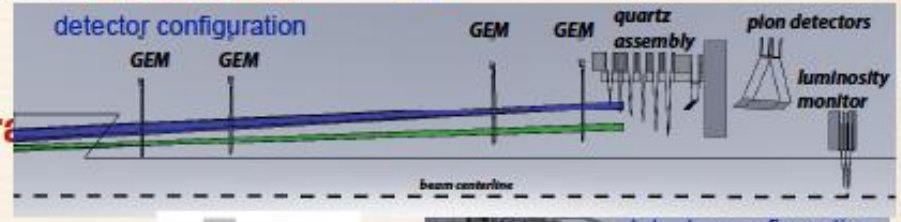

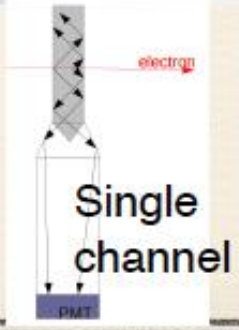

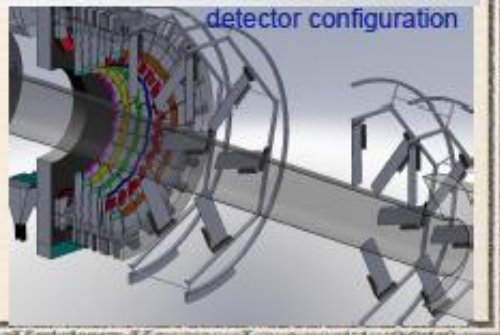

- Parity violating electron scattering: "Low energy frontier" comprises a sensitive test of the standard model complementary to LHC
- 7 years of R&D in Mainz, components are ready to be built
- P2-Experiment is funded to 90%, Q1/2021 building will be ready
- Determination of $\sin^2(\theta_W)$ with high precision (similar to Z-pole)
- New MESA energy recovering accelerator at 155 MeV, target precision is 2 % in weak proton charge i.e. 0.15% in $\sin^2(\theta_W)$
- Sensitivity to new physics up to a scale of 50 MeV up to 50 (70) TeV
- Much more physics from PV electron scattering
- Together with Moeller@Jlab (electron weak charge) and SOLID@Jlab (quark weak charge) very sensitive test of standard model and possibility to narrow in on Standard Model Extension

Cherenkov "Quartz" detectors

SFB 1044
Institut für Kernphysik

Full GEANT4 simulation

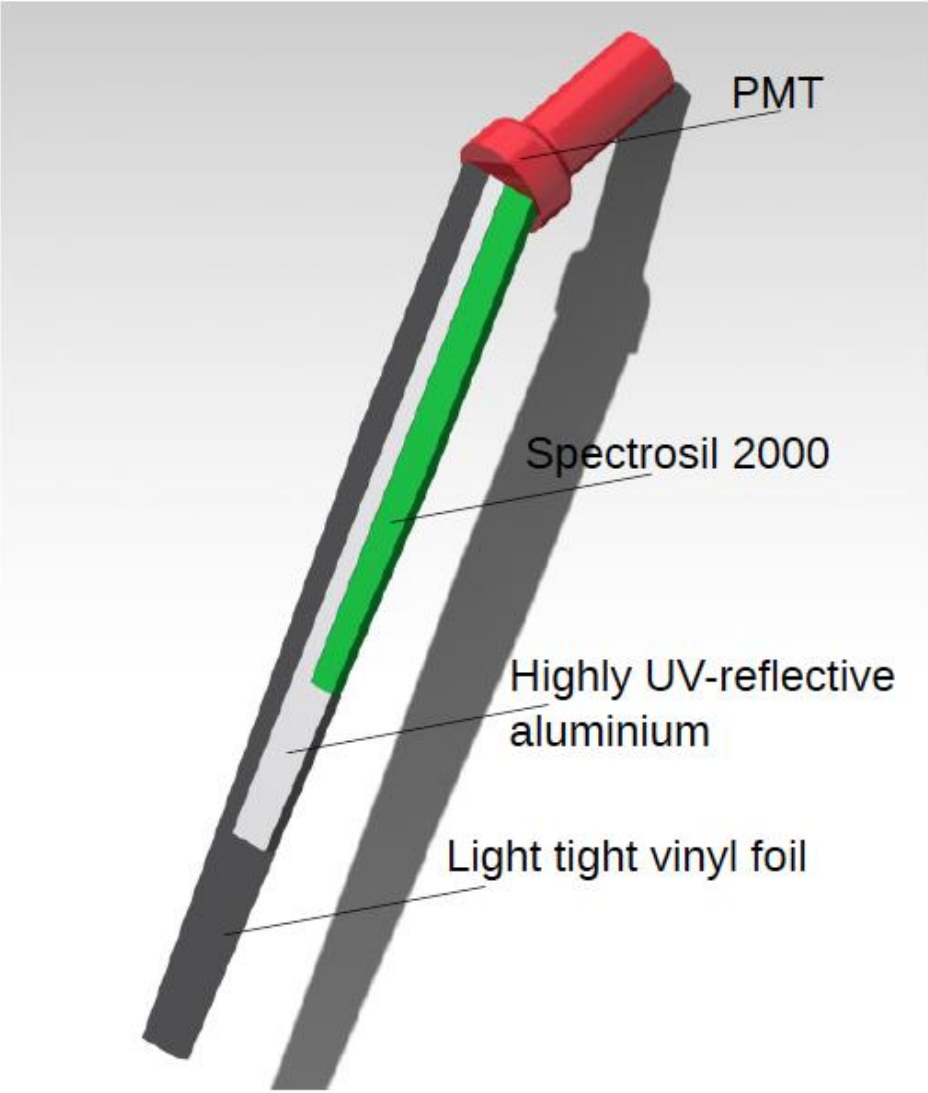

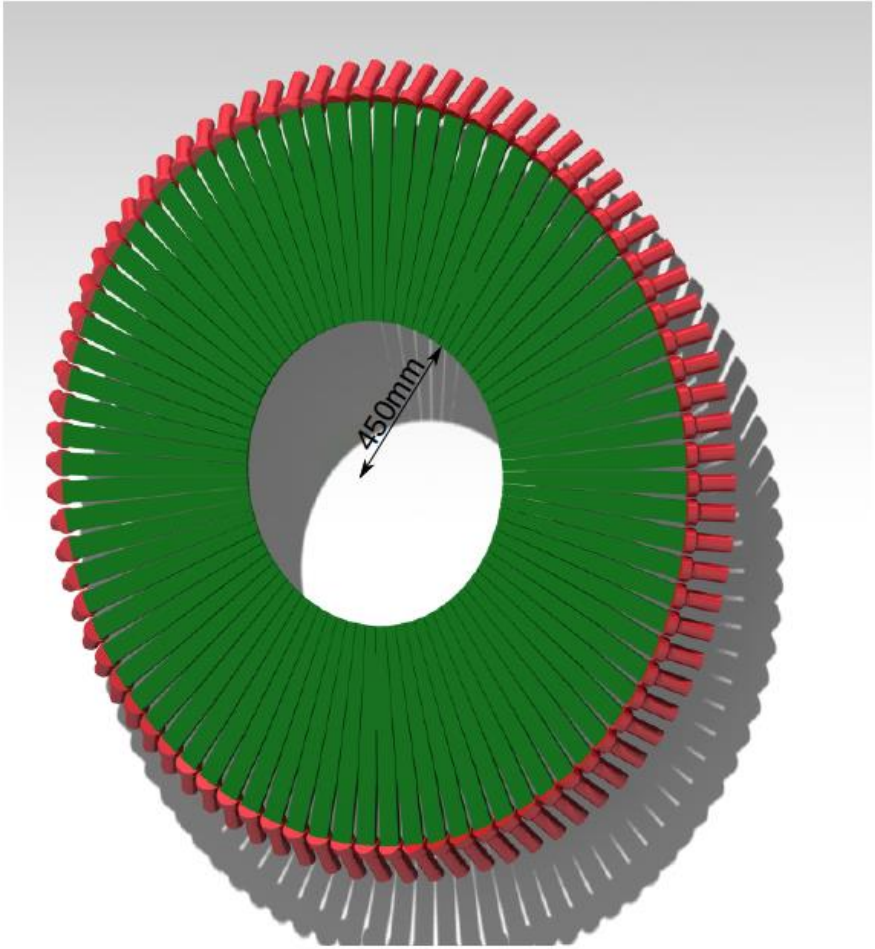

Kathrin Gerz

P2-Detector response

SFB 1044
Institut für Kernphysik

Full GEANT4 simulation

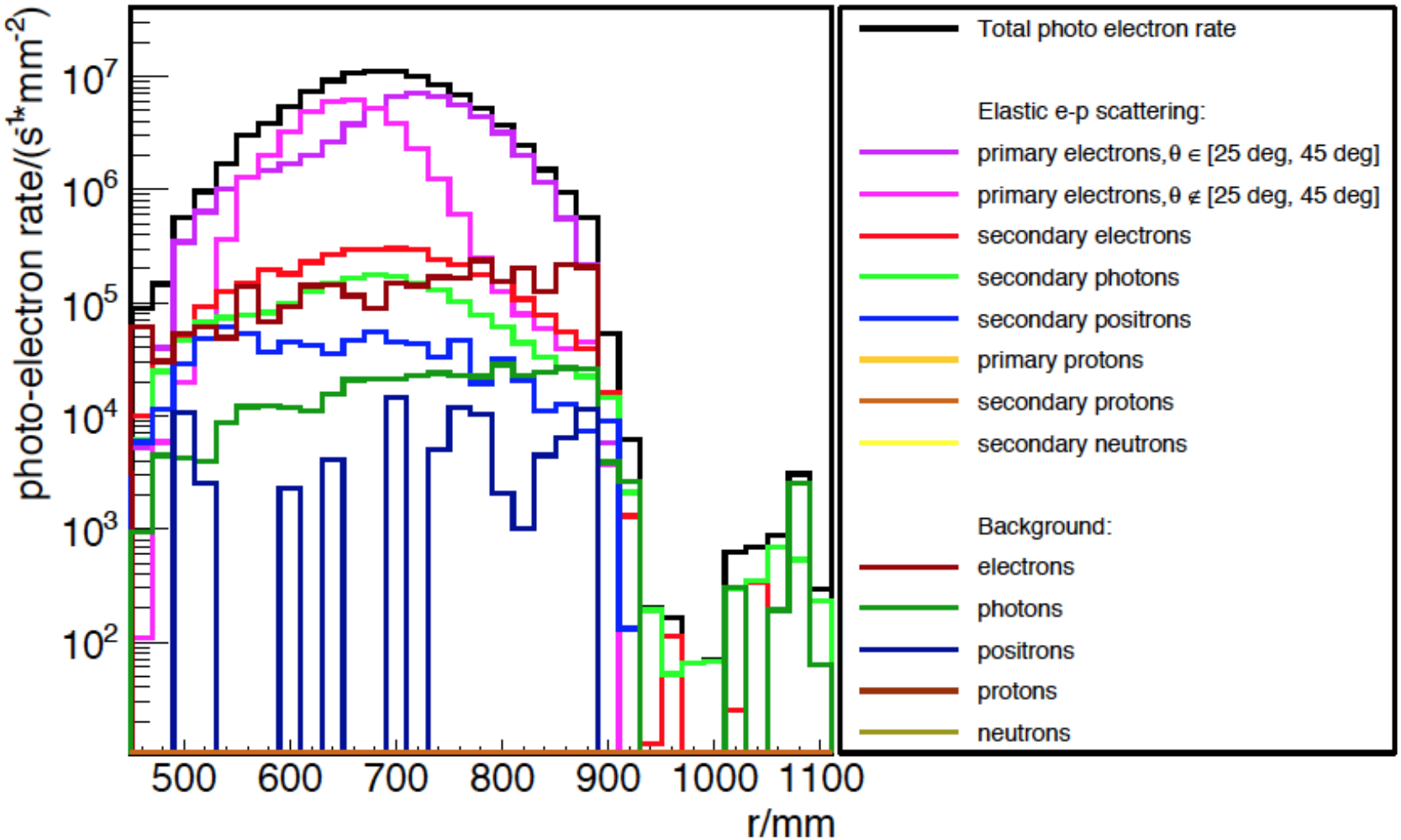


SFB 1044
Institut für Kernphysik
JG|U

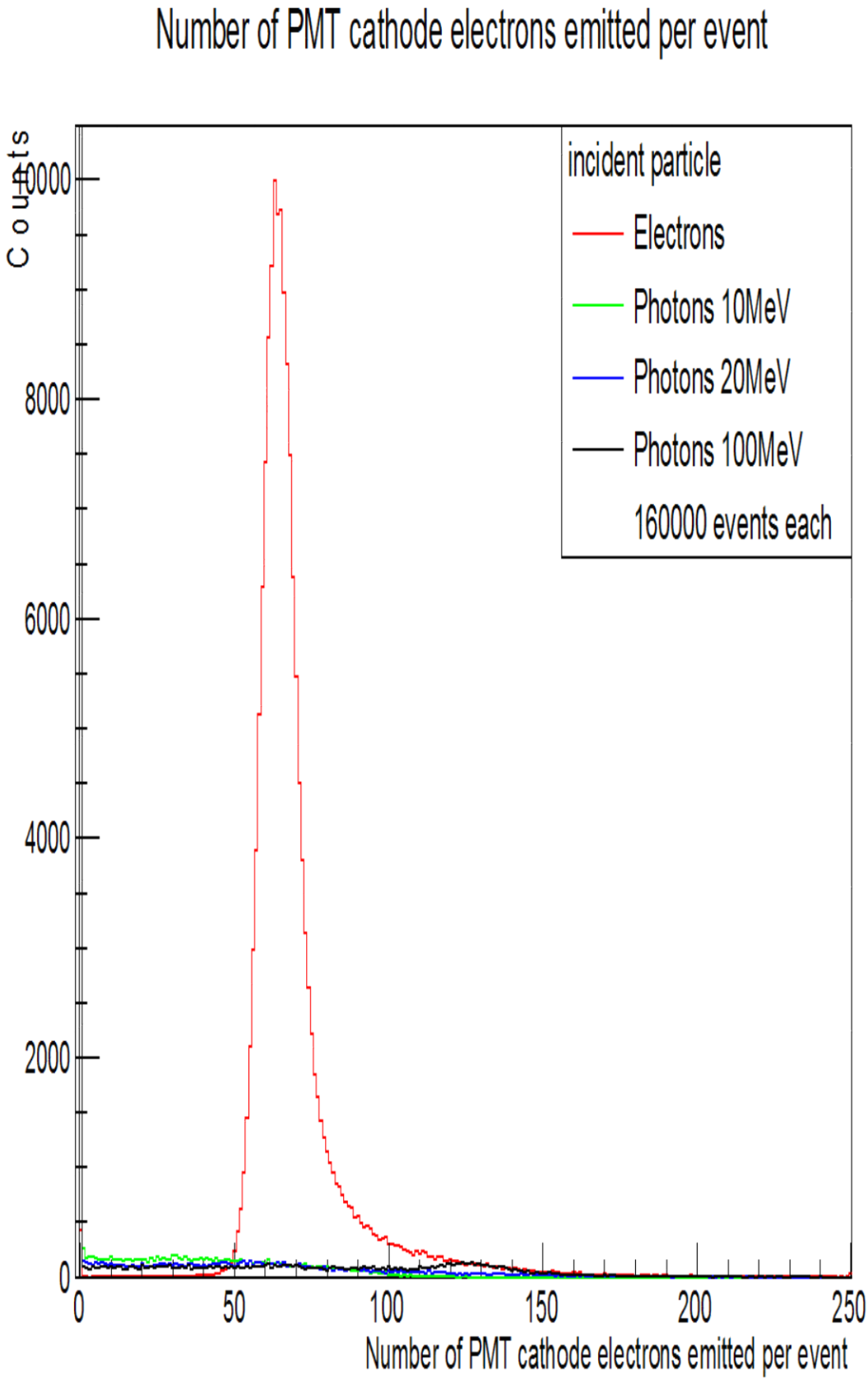
Number of PMT cathode electrons emitted per event
Counts
10000
8000
6000
4000
2000
0
0
50
100
150
200
250
Number of PMT cathode electrons emitted per event
incident particle
Electrons
Photons 10MeV
Photons 20MeV
Photons 100MeV
160000 events each

Collaboration

EPJ manuscript No.
(will be inserted by the editor)

The P2 Experiment

A future high-precision measurement of the electroweak mixing angle at low momentum transfer

Dominik Becker[1,2], Razvan Bucoveanu[1,3], Carsten Grzesik[1,2], Kathrin Imai[1,2], Ruth Kempf[1,2], Matthias Molitor[1,2], Alexey Tyukin[1,2], Marco Zimmermann[1,2], David Armstrong[4], Kurt Aulenbacher[1,2,5], Sebastian Baunack[1,2], Rakitha Beminiwattha[6], Niklaus Berger[1,2], Peter Bernhard[1,7], Andrea Brogna[1,7], Luigi Capozza[1,2,5], Silviu Covrig Dusa[8], Wouter Deconinck[4], Jürgen Diefenbach[1,2], James Dunne[9], Jens Erler[10], Ciprian Gal[11], Michael Gericke[12], Boris Gläser[1,2], Mikhail Gorchtein[1,2], Boxing Gou[1,2,5], Wolfgang Gradl[1,2], Yoshio Imai[1,2], Krishna S. Kumar[13], Frank Maas[1,2,5,a], Juliette Mammei[12], Jie Pan[12], Preeti Pandey[12], Kent Paschke[11], Ivan Perić[14], Mark Pitt[15], Sakib Rahman[12], Seamus Riordan[16], David Rodríguez Piñeiro[1,2,5], Concettina Sfienti[1,2,5,7], Iurii Sorokin[1,2], Paul Souder[17], Hubert Spiesberger[1,3], Michaela Thiel[1,2], Valery Tyukin[1,2], and Quirin Weitzel[1,7]

[1] PRISMA Cluster of Excellence, Johannes Gutenberg-Universität Mainz, Germany
[2] Institute of Nuclear Physics, Johannes Gutenberg-Universität Mainz, Germany
[3] Institute of Physics, Johannes Gutenberg-Universität, Mainz, Germany
[4] College of William and Mary, Williamsburg, Virginia, USA
[5] Helmholtz Institute Mainz, Johannes Gutenberg-Universität Mainz, Germany
[6] Louisiana Tech University, Ruston, Louisiana, USA
[7] Detector Laboratory, PRISMA Cluster of Excellence, Johannes Gutenberg-Universität Mainz, Germany
[8] Thomas Jefferson National Accelerator Facility, Newport News, Virginia, USA
[9] Mississippi State University, Mississippi State, MS, USA
[10] Departamento de Física Teórica, Instituto de Física, Universidad Nacional Autónoma de México, CDMX, México
[11] University of Virginia, Charlottesville, Virginia, USA
[12] Department of Physics and Astronomy, University of Manitoba, Winnipeg, Canada
[13] Department of Physics and Astronomy, Stony Brook University, Stony Brook, USA
[14] Institute for Data Processing and Electronics, Karlsruhe Institute of Technology, Karlsruhe, Germany
[15] Virginia Tech U
[16] Physics Division
[17] Physics Departm

Accepted for publication, will be EPJ A highlight

$\sin^2\theta_W$

Møller Scattering

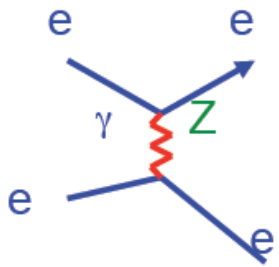

- Purely Leptonic

Q-Weak (JLab)
P2 (Mainz/MESA)

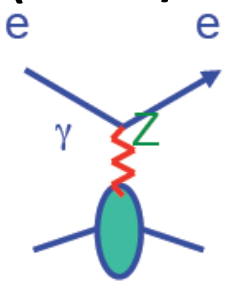

- Coherent quarks in p
- in operation now
- $2(2C_{1u}+C_{1d})$

e-DIS

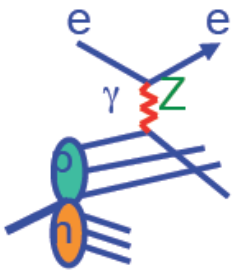

- Isoscaler quark scattering
- $(2C_{1u}-C_{1d})+Y(2C_{2u}-C_{2d})$

Atomic Parity Violation

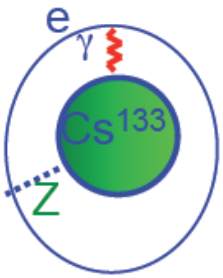

- Coherent quarks in entire nucleus
- Nuclear structure uncertainties
- $-376\ C_{1u} - 422\ C_{1d}$

Neutrino Scattering

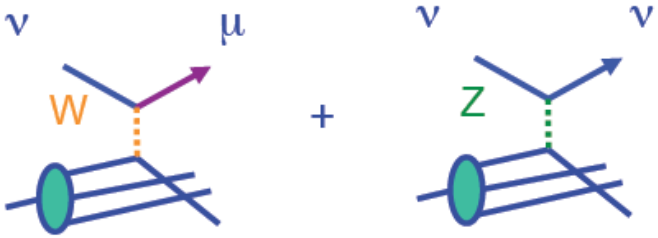

- Quark scattering (from nucleus)
- Weak charged and neutral current difference

S. Su

Courtesy of P. Reimer and R. Arnold

Summary: Measurements of $\sin^2\theta_{W(effective)}$

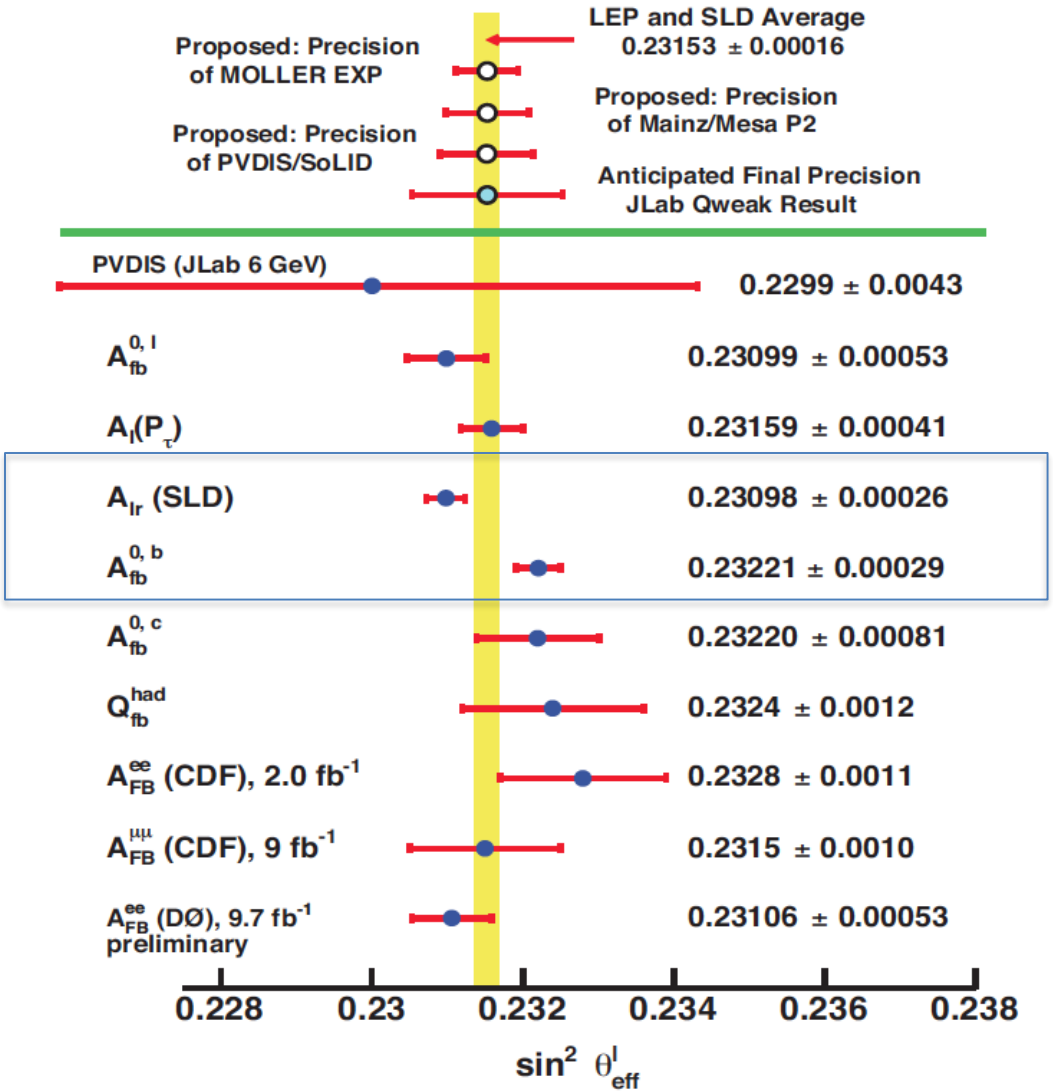

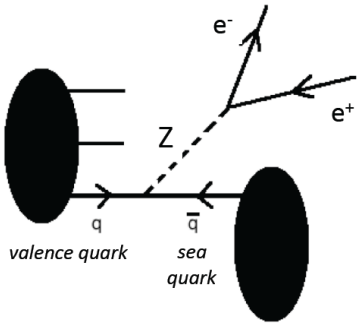

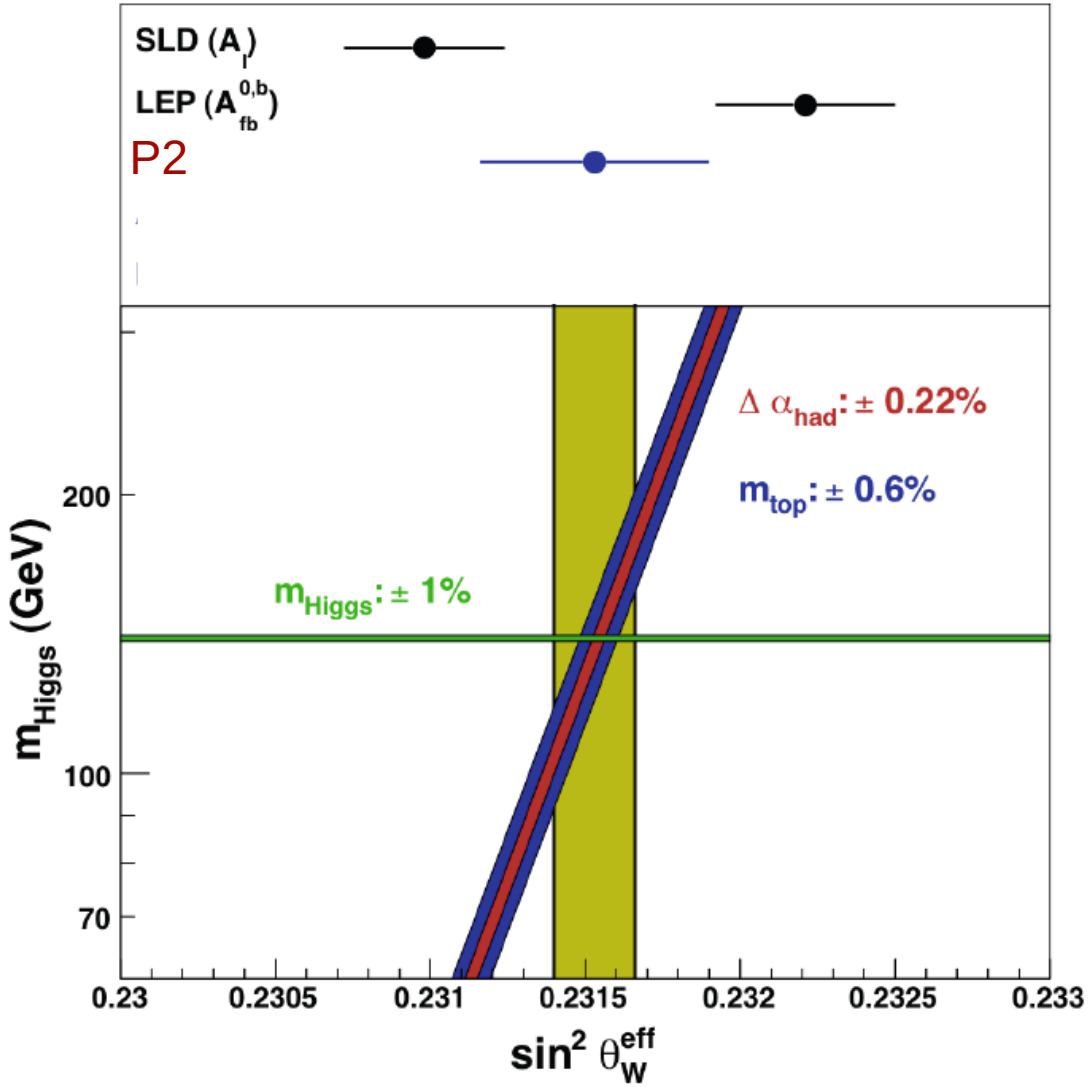
SLD (A_l)
LEP ($A_{fb}^{0,b}$)
P2
$\Delta\alpha_{had}$: ± 0.22%
m_{top}: ± 0.6%
m_{Higgs}: ± 1%
m_{Higgs} (GeV)
200
100
70
0.23
0.2305
0.231
0.2315
0.232
0.2325
0.233
$\sin^2\theta_W^{eff}$

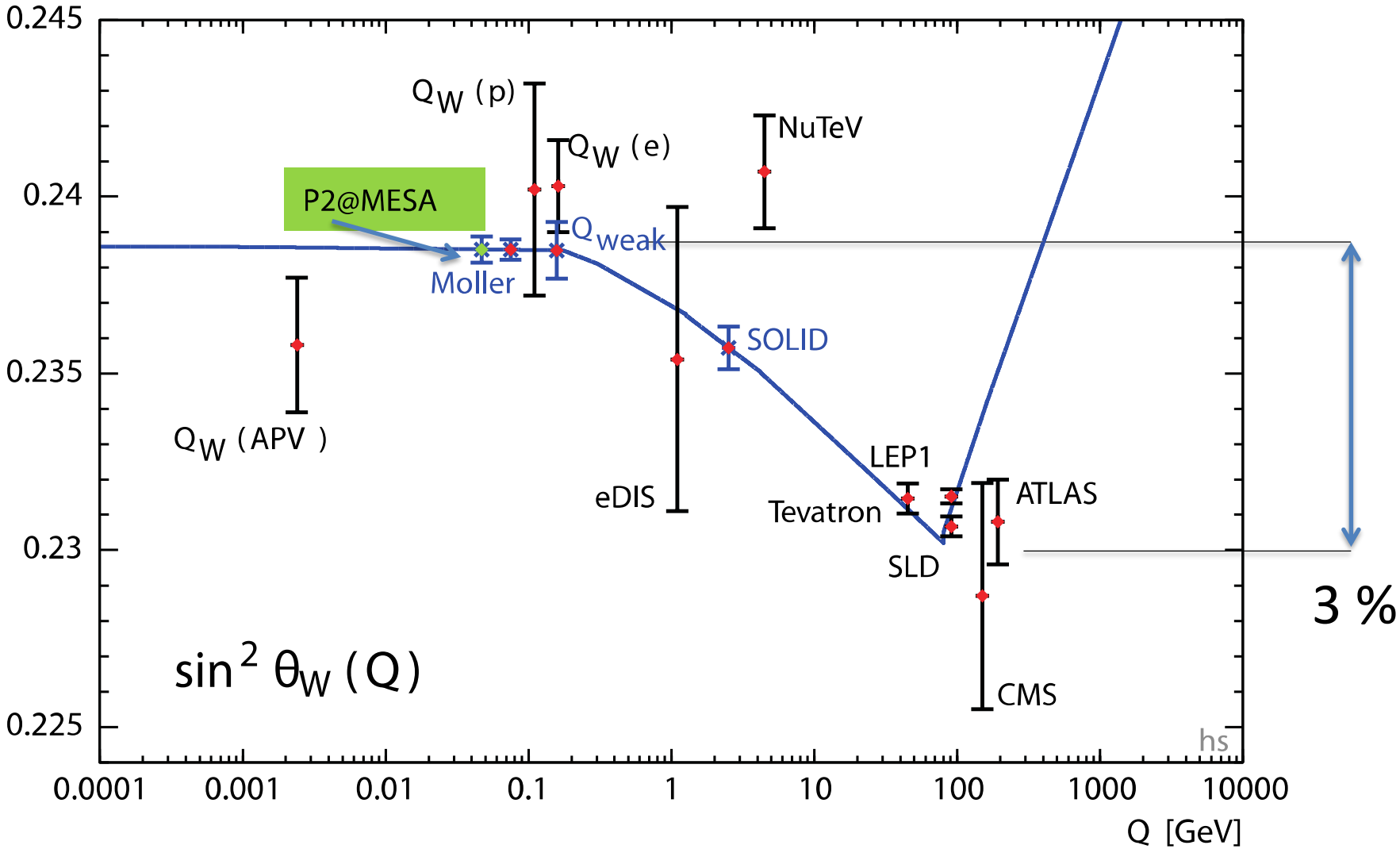
0.245
0.24
0.235
0.23
0.225
0.0001
0.001
0.01
0.1
1
10
100
1000
10000
Q [GeV]
Q_W (p)
Q_W (e)
NuTeV
P2@MESA
Q_{weak}
Moller
SOLID
Q_W (APV)
eDIS
LEP1
Tevatron
ATLAS
SLD
CMS
3 %
$\sin^2\theta_W(Q)$
hs

Electroweak:

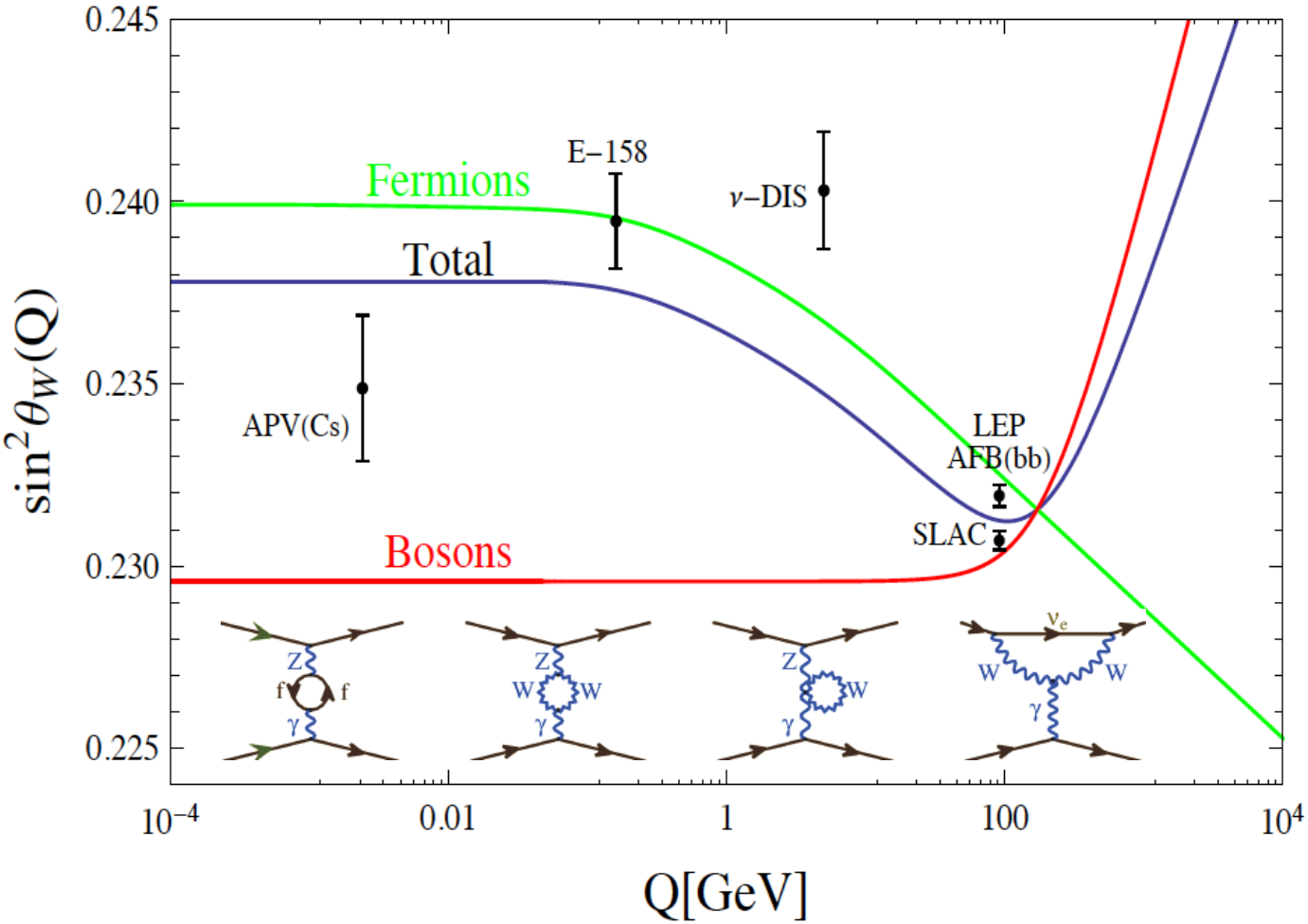

γZ-box

- γZ box graph contributions obtained by modelling hadronic effects:

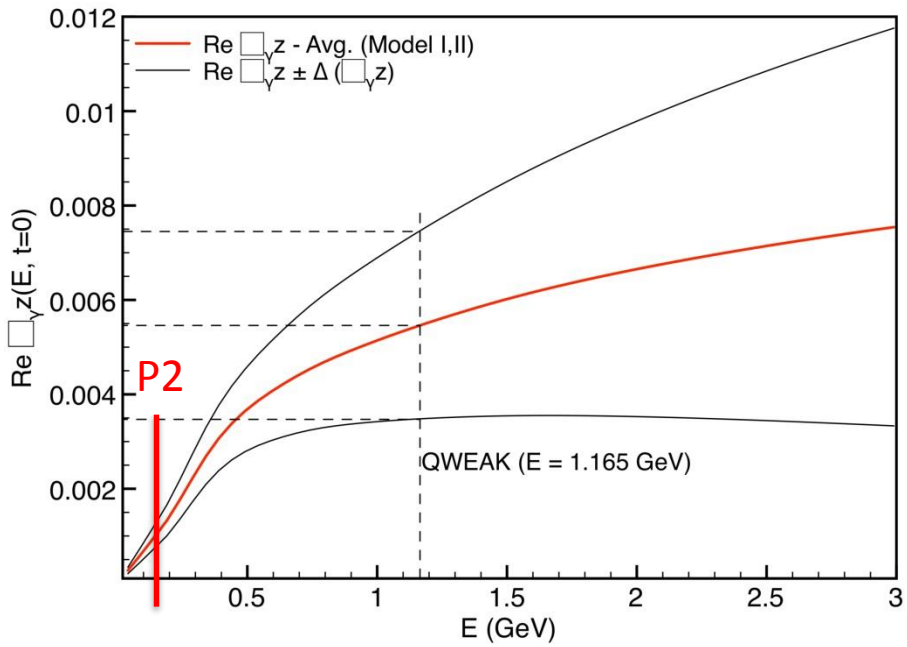

[Gorchstein, Horowitz & Ramsey-Musolf 2011]

- Hadronic uncertainties suppressed at lower energies
- Low beam energy experiment: **P2 @ MESA**

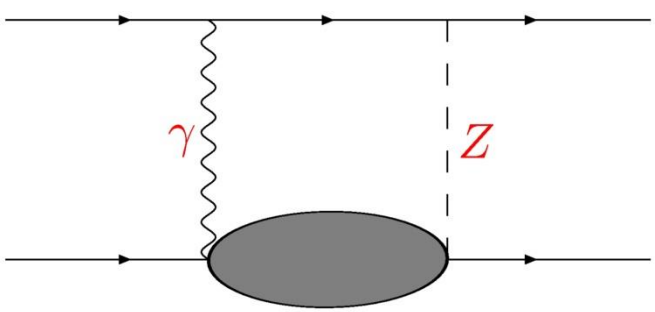

Progress in Theory
- Theory uncertainties in box diagrams
- 2 loop corrections
- Hadronic contributions in loops
- Auxiliary measurements
- PV-asymmetry in Carbon

Isospin breaking

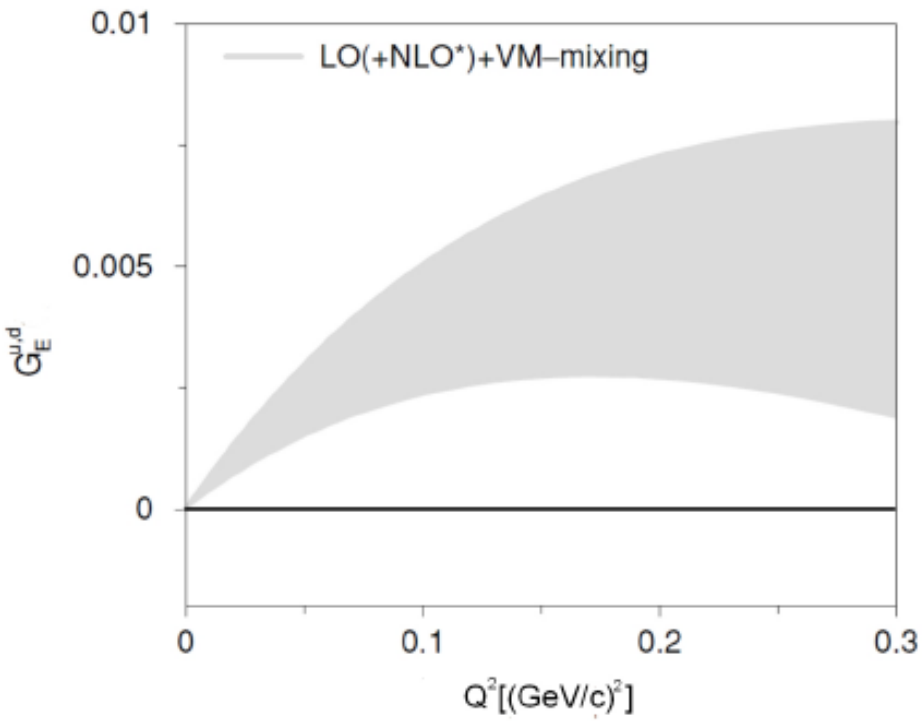
0.01
0.005
0
LO(+NLO*)+VM–mixing
$G_E^{u,d}$
0
0.1
0.2
0.3
$Q^2[(GeV/c)^2]$

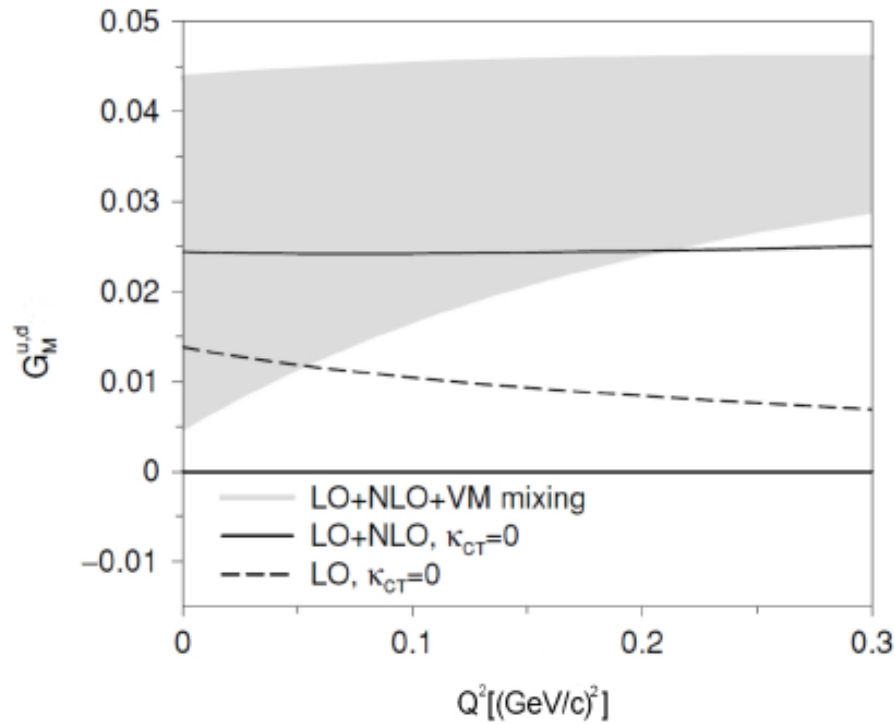
0.05
0.04
0.03
0.02
0.01
0
–0.01
$G_M^{u,d}$
LO+NLO+VM mixing
LO+NLO, κ_{CT}=0
LO, κ_{CT}=0
0
0.1
0.2
0.3
$Q^2[(GeV/c)^2]$

Strange quarks

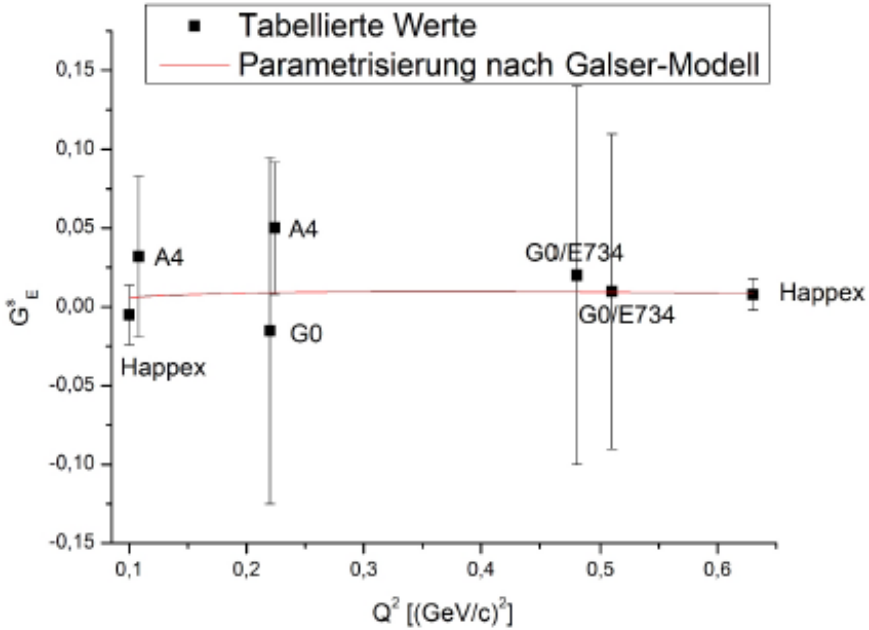

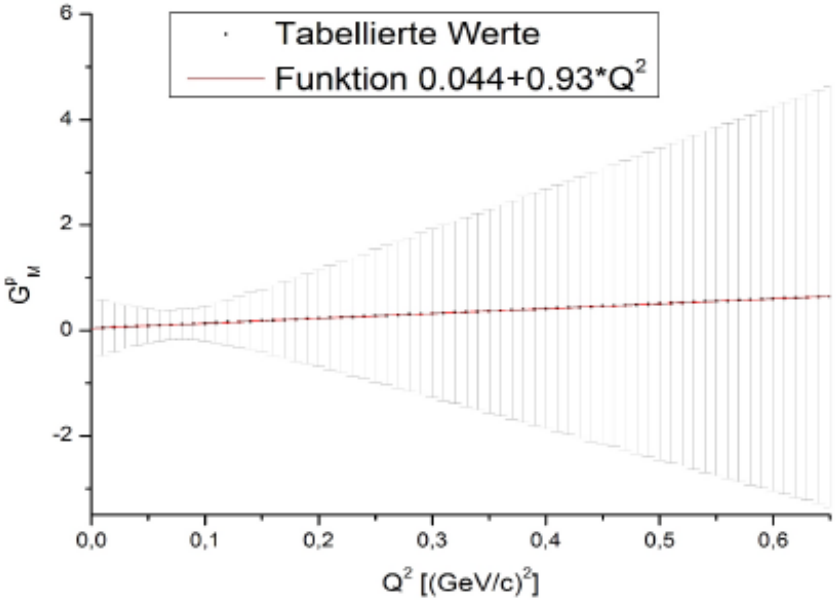

present A4: reduce old SAMPLE error in G_M^s, G_A^e by factor 2

$G_A^p(Q^2 = 0\ \mathrm{GeV}^2/c^2) = -\ 1.135(411)$ 36% Error

Sensitivity to new physics

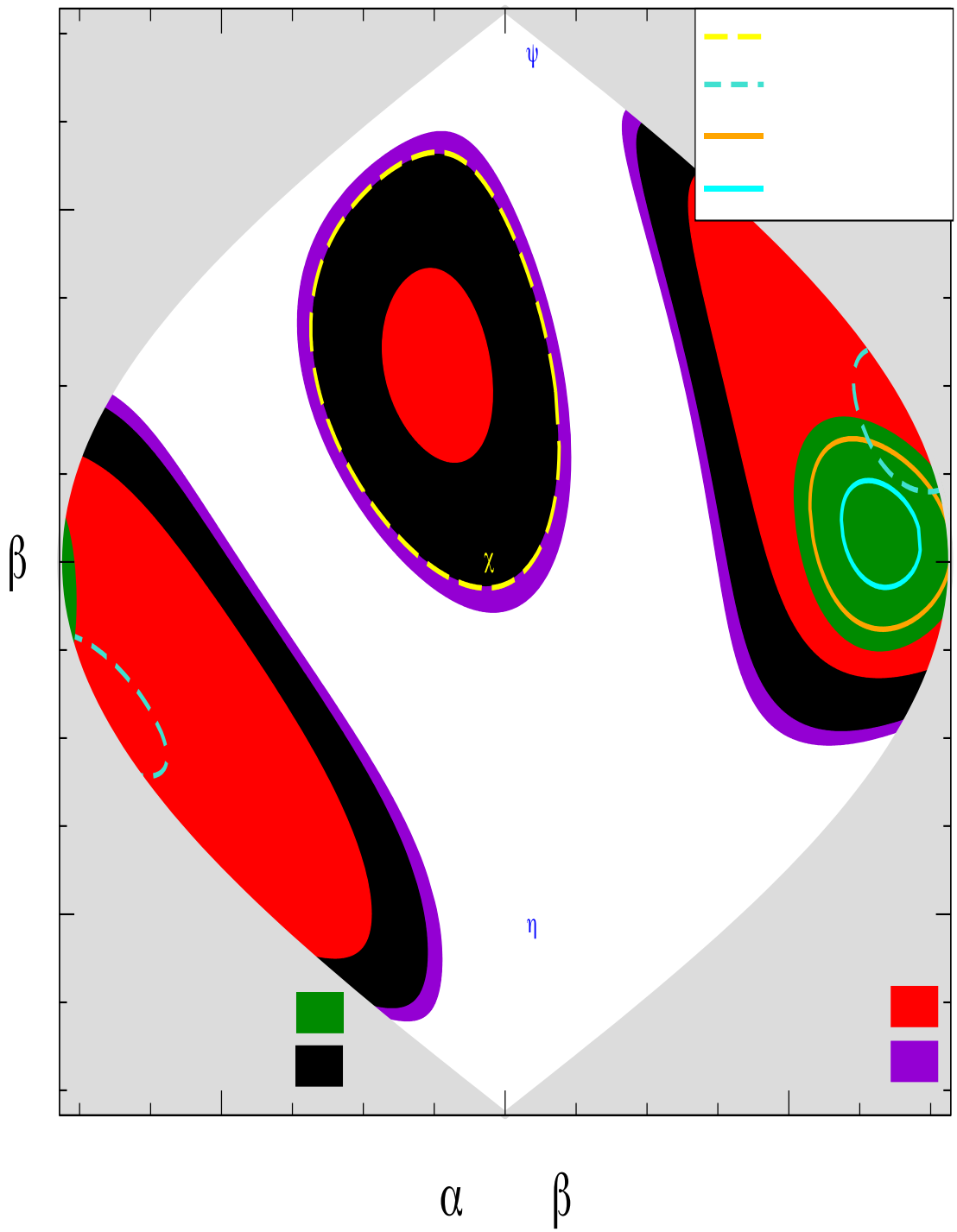
ψ
χ
η
β
α
β

Example: supersymmetric Standard Model extensions

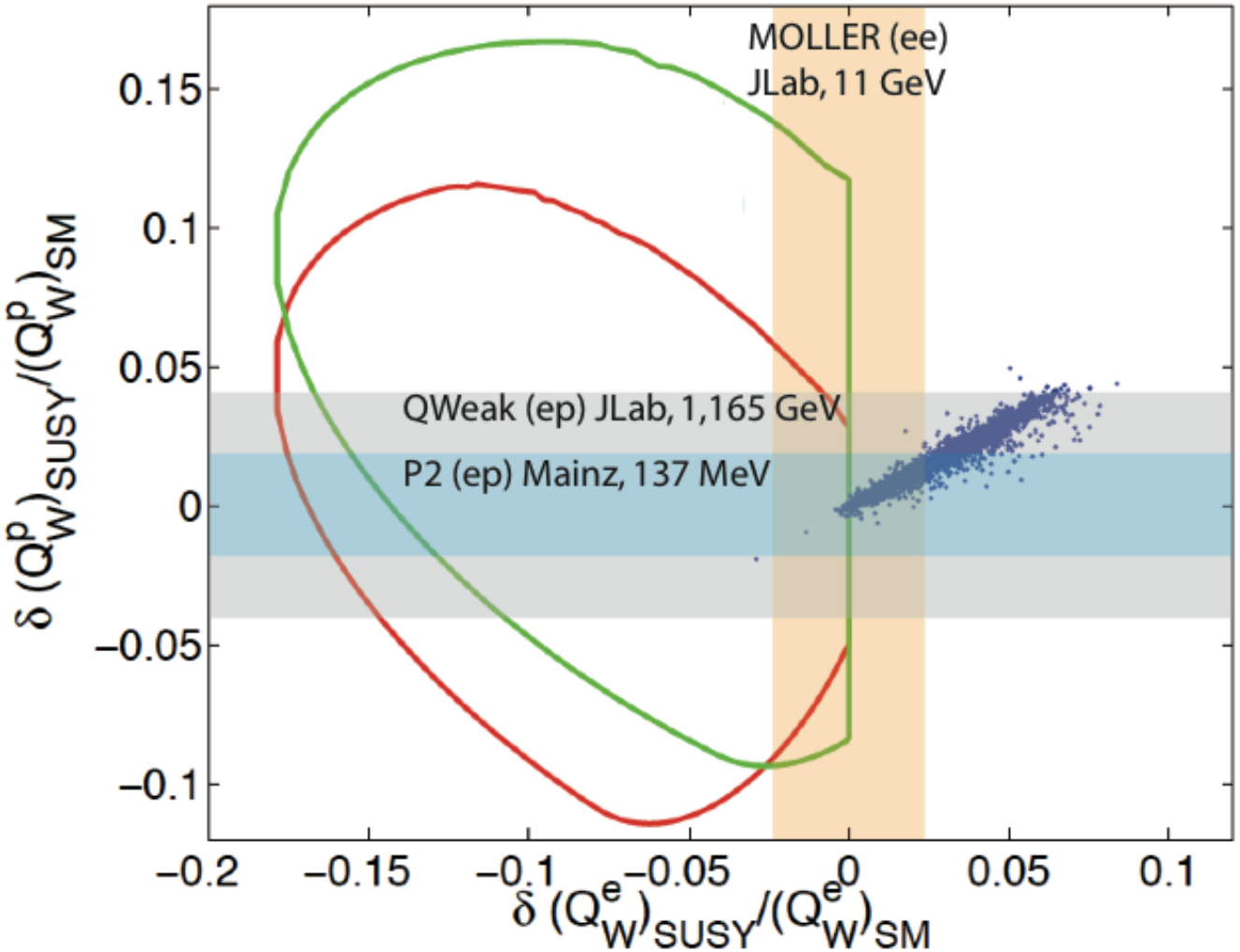

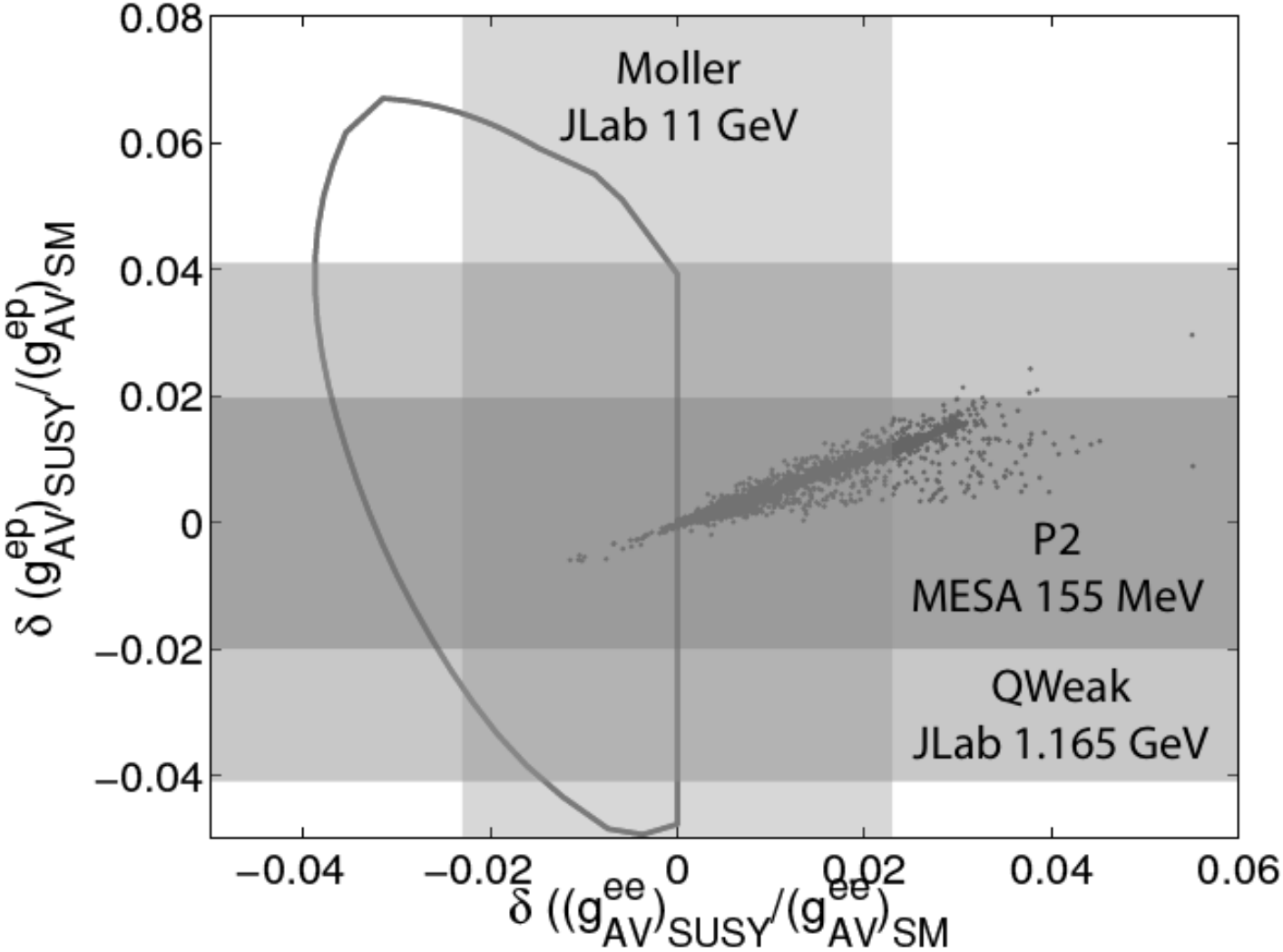
Moller
JLab 11 GeV
P2
MESA 155 MeV
QWeak
JLab 1.165 GeV
0.08
0.06
0.04
0.02
0
−0.02
−0.04
−0.04
−0.02
0
0.02
0.04
0.06
$\delta\,(g_{AV}^{ep})_{SUSY}/(g_{AV}^{ep})_{SM}$
$\delta\,((g_{AV}^{ee})_{SUSY}/(g_{AV}^{ee})_{SM}$

Ramsey-Musolf and Su, ***Phys. Rep. 456 (2008)***

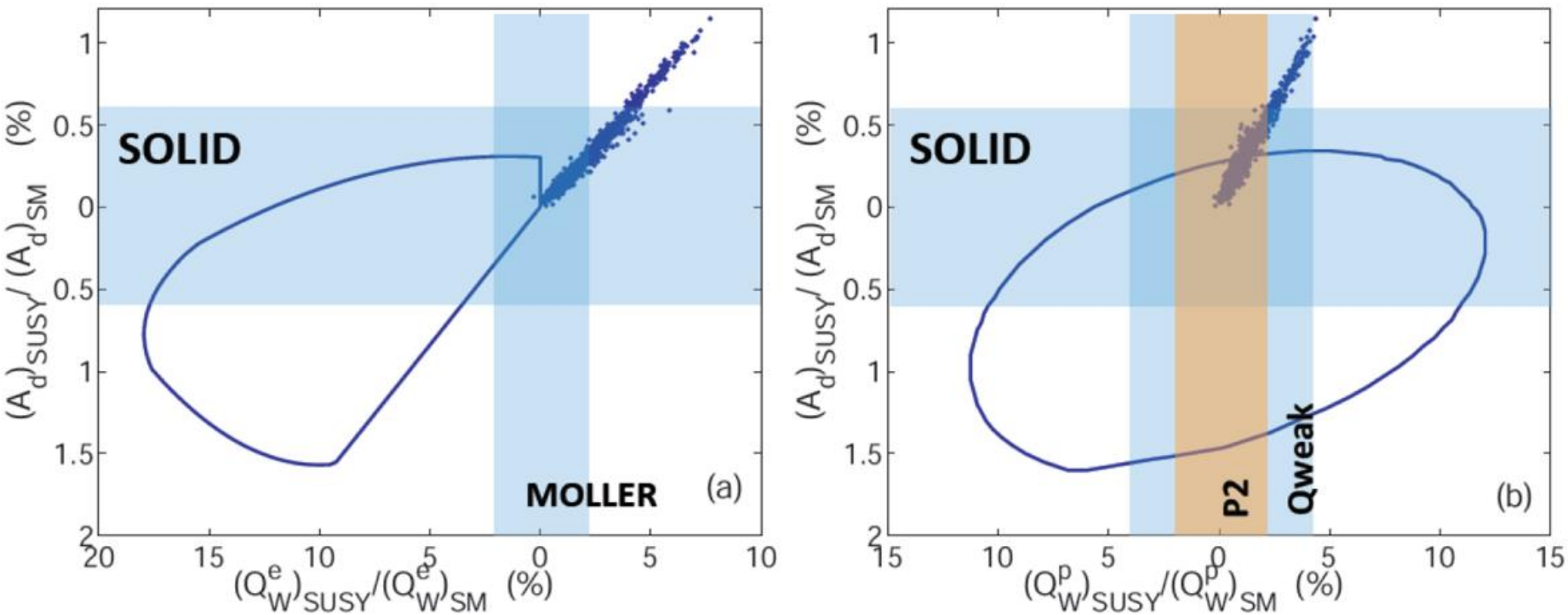

Physics sensitivity from contact interaction (LEP2 convention, $g^2 = 4pi$)

	precision	$\Delta \sin^2\overline{\theta}_W(0)$	Λ_{new} (expected)
APV Cs	0.58 %	0.0019	32.3 TeV
E158	14 %	0.0013	17.0 TeV
Qweak I	19 %	0.0030	17.0 TeV
Qweak final	4.5 %	0.0008	33 TeV
PVDIS	4.5 %	0.0050	7.6 TeV
SoLID	0.6 %	0.00057	22 TeV
MOLLER	2.3 %	0.00026	39 TeV
P2	2.0 %	0.00036	49 TeV
PVES ^{12}C	0.3 %	0.0007	49 TeV

ATLAS

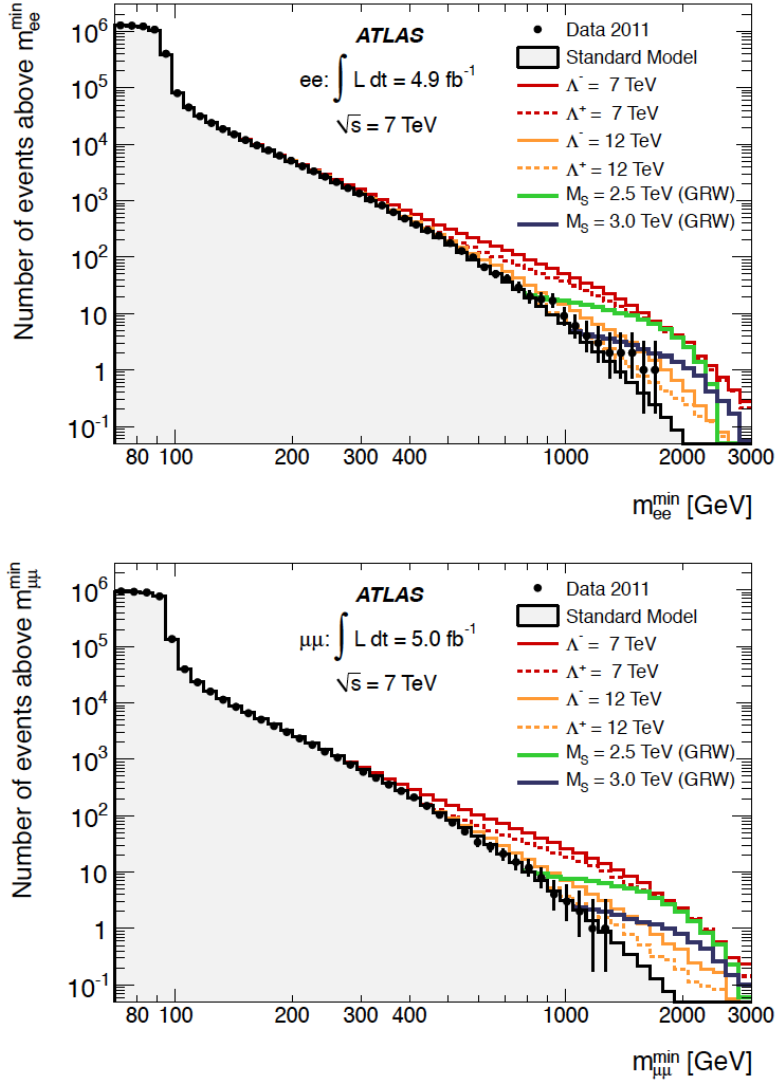

FIG. 3. Distribution of the number of events with dilepton mass above $m_{\ell\ell}^{\min}$ for data (points) and SM prediction from Monte Carlo simulation (filled histograms, shaded gray) in the dielectron channel (top panel) and dimuon channel (bottom panel). The open solid and dashed histograms correspond to the expected distributions in the presence of contact interactions or large extra dimensions for several model parameters. The bin width is constant in $\log(m_{\ell\ell}^{\min})$.

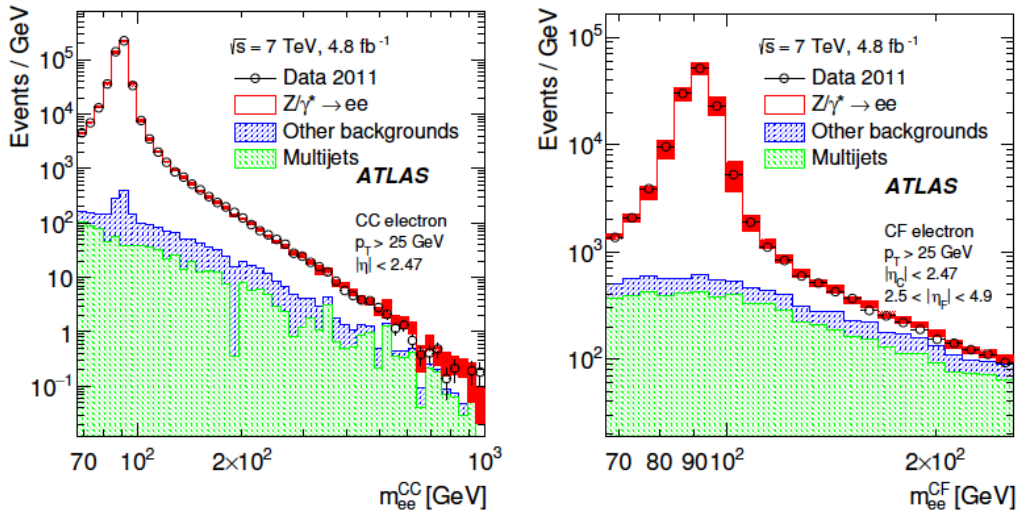

(a) (b)

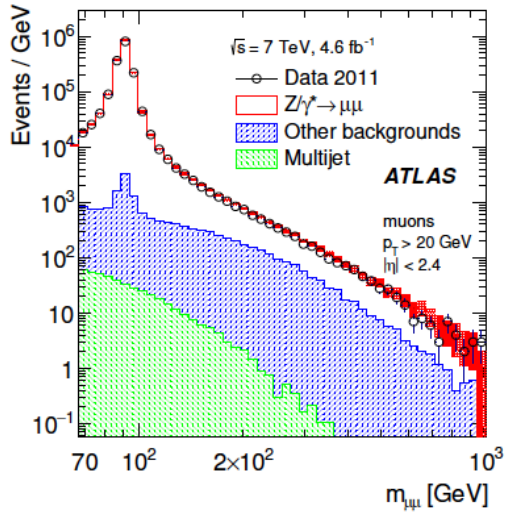

(c)

Figure 1: Dilepton invariant mass distributions obtained from the event selections described in the text, for the (a) CC electron, (b) CF electron and (c) muon channels. Data are shown by open circles and the total expectation is shown as a line with a band representing the total uncertainty (statistical and systematic added in quadrature). The data-driven estimate for the multi-jet background and the simulation-based estimates for all other backgrounds are shown by the shaded areas.

	$\sin^2\theta_{\mathrm{eff}}^{\mathrm{lept}}$
CC electron	$0.2302 \pm 0.0009(\mathrm{stat.}) \pm 0.0008(\mathrm{syst.}) \pm 0.0010(\mathrm{PDF}) = 0.2302 \pm 0.0016$
CF electron	$0.2312 \pm 0.0007(\mathrm{stat.}) \pm 0.0008(\mathrm{syst.}) \pm 0.0010(\mathrm{PDF}) = 0.2312 \pm 0.0014$
Muon	$0.2307 \pm 0.0009(\mathrm{stat.}) \pm 0.0008(\mathrm{syst.}) \pm 0.0009(\mathrm{PDF}) = 0.2307 \pm 0.0015$
El. combined	$0.2308 \pm 0.0006(\mathrm{stat.}) \pm 0.0007(\mathrm{syst.}) \pm 0.0010(\mathrm{PDF}) = 0.2308 \pm 0.0013$
Combined	$0.2308 \pm 0.0005(\mathrm{stat.}) \pm 0.0006(\mathrm{syst.}) \pm 0.0009(\mathrm{PDF}) = 0.2308 \pm 0.0012$

Table 2: The $\sin^2\theta_{\mathrm{eff}}^{\mathrm{lept}}$ measurement results in each of the three studied channels: electron central-central, electron central-forward and muon. Results of the statistical combination of both electron channels and all three channels are shown as well.

Uncertainty source	CC electrons [10^{-4}]	CF electrons [10^{-4}]	Muons [10^{-4}]	Combined [10^{-4}]
PDF	10	10	9	9
MC statistics	5	2	5	2
Electron energy scale	4	6	–	3
Electron energy resolution	4	5	–	2
Muon energy scale	–	–	5	2
Higher-order corrections	3	1	3	2
Other sources	1	1	2	2

Table 3: Contributions to the systematic uncertainties on the $\sin^2\theta_{\mathrm{eff}}^{\mathrm{lept}}$ values extracted from the three analysis channels and on the combined result. Null entries (denoted by "–") correspond to uncertainties that do not apply to a specific channel. Higher-order corrections include NLO QCD and NLO EWK contributions. Other sources include the effect of pileup, background uncertainties, lepton trigger/reconstruction/identification efficiency uncertainties, muon momentum resolution and effects of detector misalignment.

Three
PV experiments

Weak Charge Of Proton: Qweak (Jlab), P2 (MESA)

Weak Charge Of Electron: MOELLER (JLAB)

Weak Charge Of Quarks: SOLID (PVDIS) (JLAB)

- Complementary access by weak charges of proton and electron

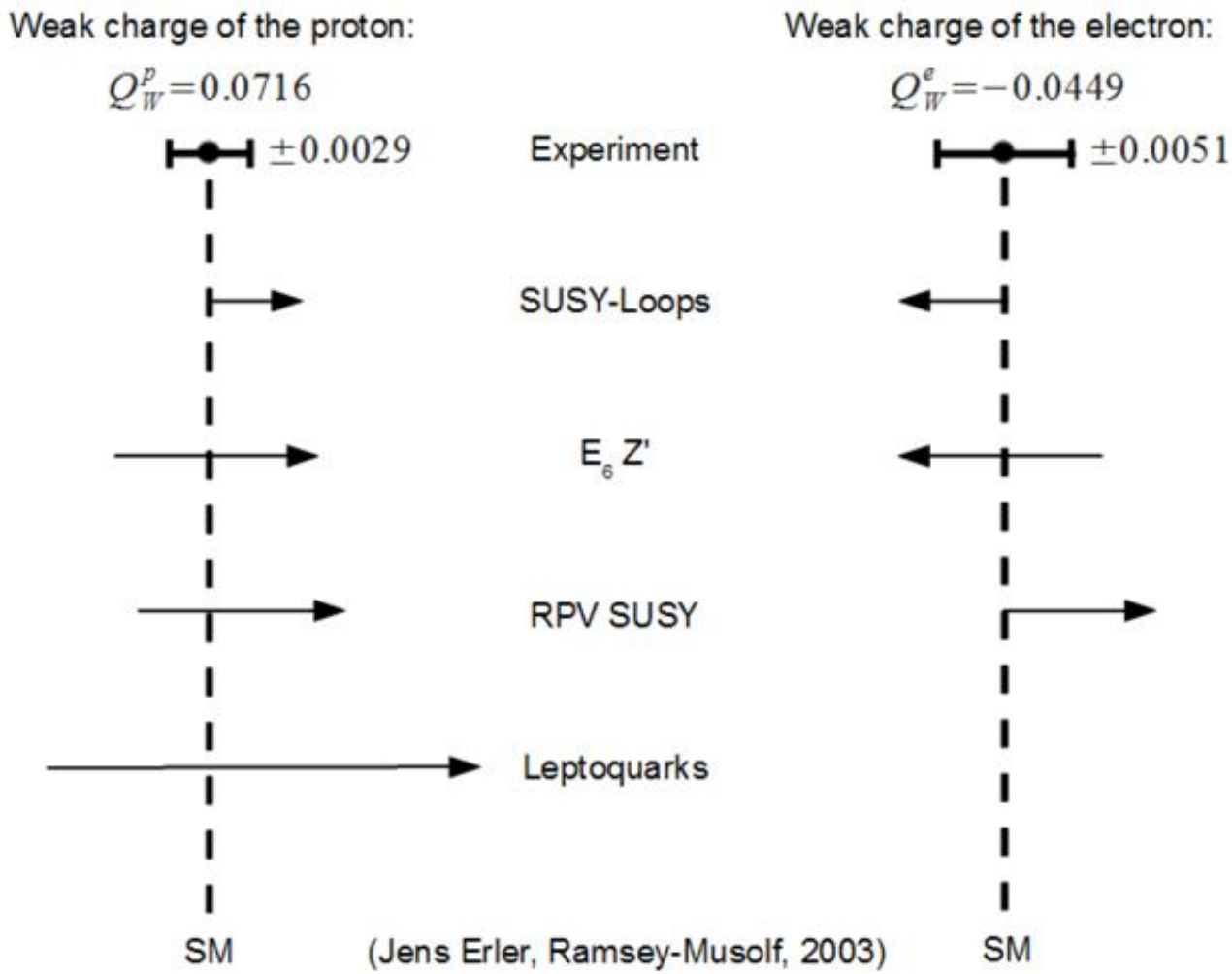

(Jens Erler, Ramsey-Musolf, 2003)

Parity violating electron scattering

Parity Violating Asymmetry in elastic electron proton scattering

$\sigma \approx$

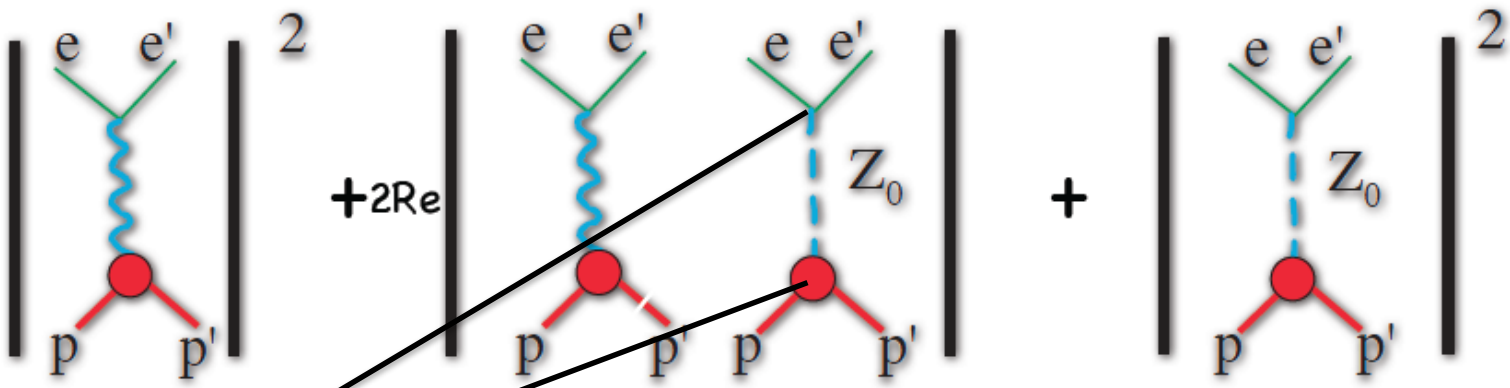

$(V\text{-}A)_e(V\text{-}A)_p$

$A_eV_p+V_eA_p$

V-A coupling:
parity-violating
cross section asymmetry A_{LR}
longitudinally pol. electrons
unpolarised protons

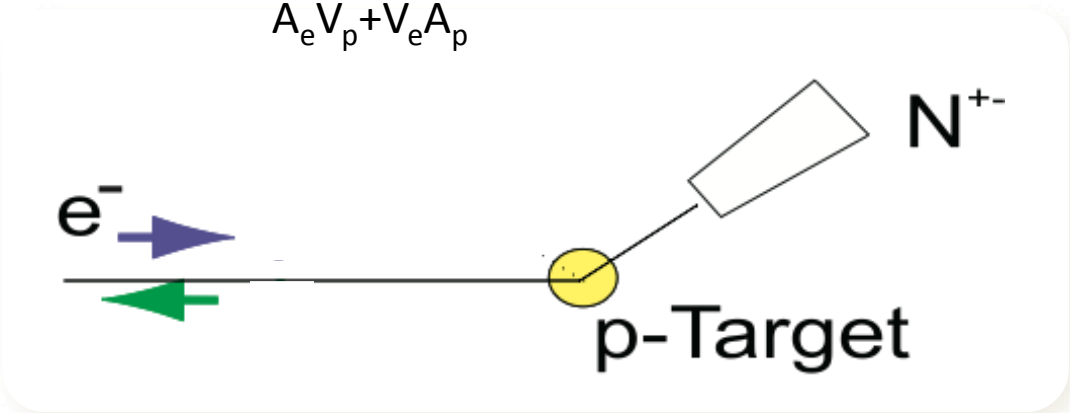

Parity violating cross section asymmetry

$$A_{ep} = \left[\frac{G_F\, Q^2}{4\pi\alpha\sqrt{2}}\right] \frac{\epsilon G_E^{\gamma} G_E^{Z} + \tau G_M^{\gamma} G_M^{Z} - (1-4\sin^2\theta_W)\epsilon' G_M^{\gamma} G_A^{Z}}{\varepsilon (G_E^{\gamma})^2 + \tau (G_M^{\gamma})^2}$$

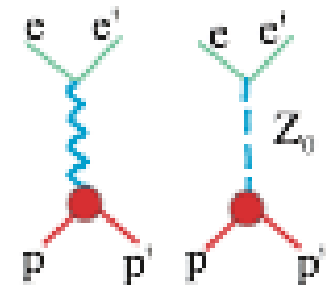

$$A_{RL} = \underbrace{A_V + A_A}_{= A_0} + A_S \begin{cases} A_V = -a\rho'_{eq}\left[(1-4\sin^2\theta_W) - \dfrac{\epsilon G_E^p G_E^n + \tau G_M^p G_M^n}{\epsilon (G_E^p)^2 + \tau (G_M^p)^2}\right] \\ A_A = a\dfrac{(1-4\sin^2\theta_W)\sqrt{1-\epsilon^2}\sqrt{\tau(1+\tau)}G_M^p \tilde{G}_A^p}{\epsilon (G_E^p)^2 + \tau (G_M^p)^2} \\ A_S = a\rho'_{eq}\dfrac{\epsilon G_E^p G_E^s + \tau G_M^p G_M^s}{\epsilon (G_E^p)^2 + \tau (G_M^p)^2} \end{cases}$$

$$a = -G_F q^2/4\pi\alpha\sqrt{2}, \quad \tau = -q^2/4M_p^2, \quad \epsilon = [1 + 2(1+\tau)\tan^2\theta/2]^{-1}$$

Parity violating cross section asymmetry

weak charge

$$A_{LR} = \frac{\sigma(e\uparrow) - \sigma(e\downarrow)}{\sigma(e\uparrow) + \sigma(e\downarrow)} = -\frac{G_F Q^2}{4\sqrt{2}\pi\alpha}(Q_W - F(Q^2))$$

$$Q_W = 1 - 4\sin^2\theta_W(\mu)$$

hadron structure

$$F(Q^2) = F_{EM}(Q^2) + F_{Axial}(Q^2) + F_{Strange}(Q^2)$$

Sensitivity

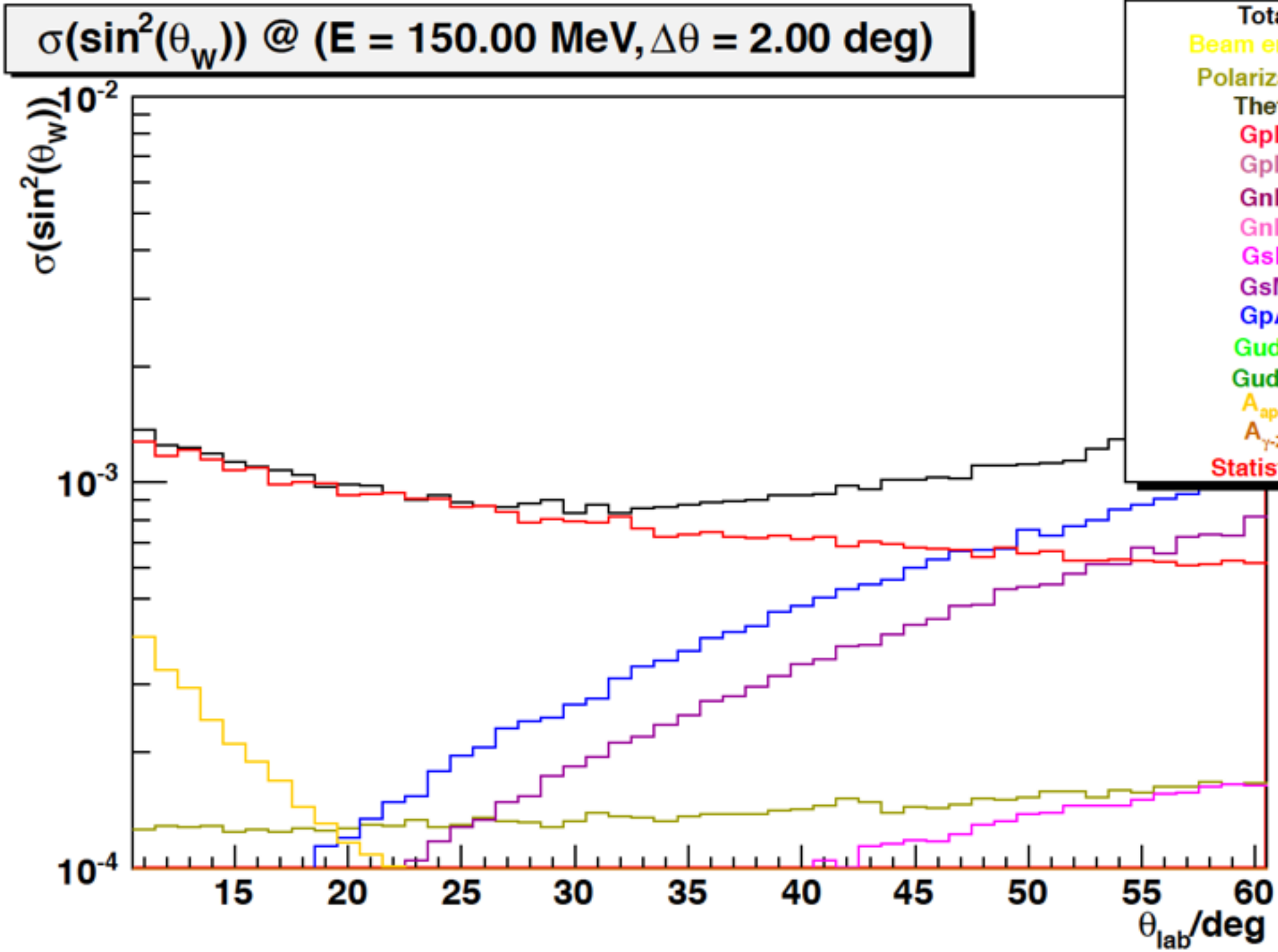
σ(sin²(θw)) @ (E = 150.00 MeV, Δθ = 2.00 deg)
σ(sin²(θw))
10⁻²
10⁻³
10⁻⁴
15
20
25
30
35
40
45
50
55
60
θlab/deg
Tota
Beam e
Polariz
The
Gpl
Gpl
Gnl
Gnl
Gsl
Gsl
Gpl
Gud
Gud
Statis

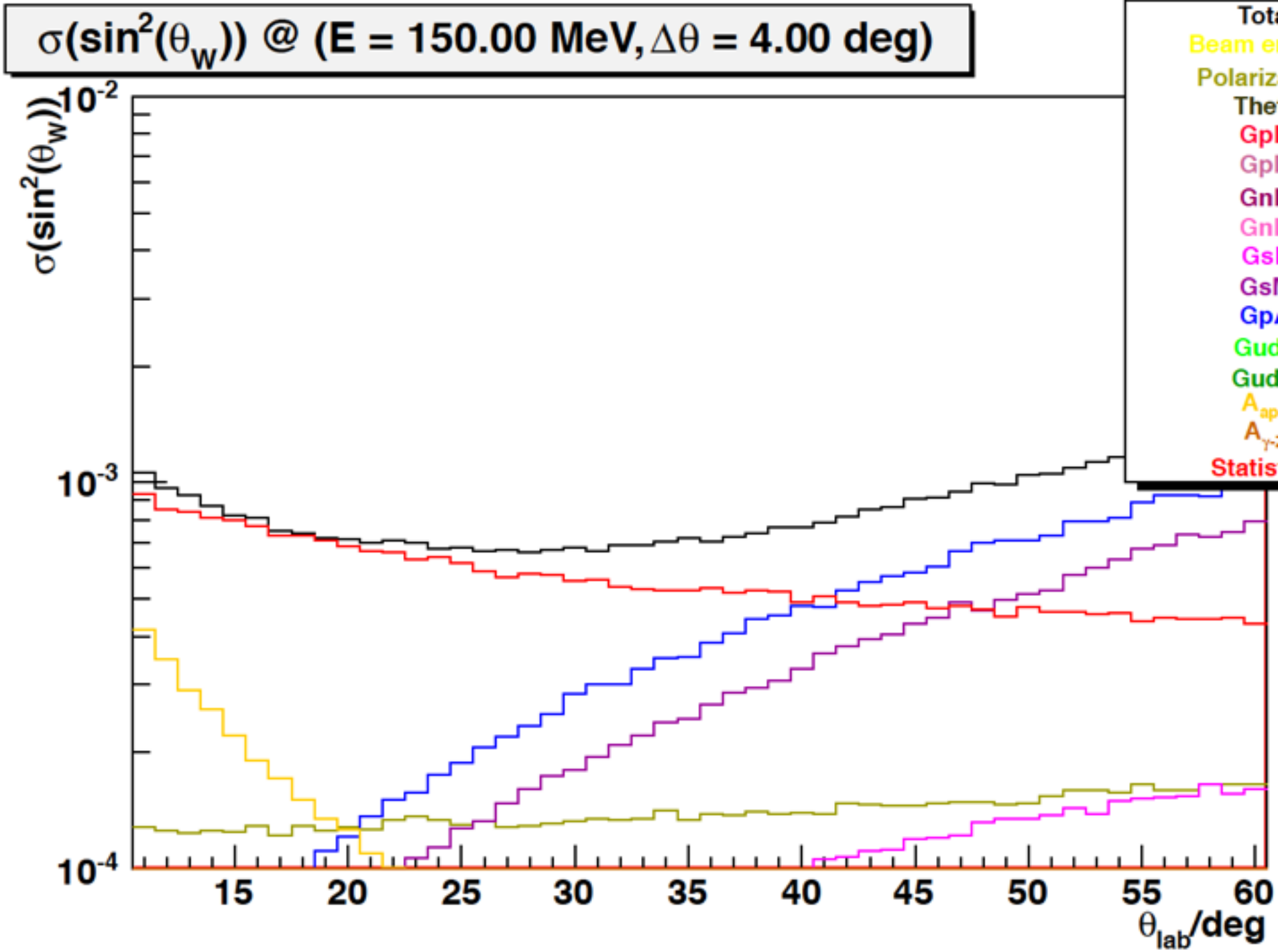
σ(sin²(θw)) @ (E = 150.00 MeV, Δθ = 4.00 deg)
σ(sin²(θw))
10⁻²
10⁻³
10⁻⁴
15
20
25
30
35
40
45
50
55
60
θlab/deg
Tota
Beam e
Polariz
The
Gpl
Gpl
Gnl
Gnl
Gsl
Gsl
Gpa
Gud
Gud
Aap
Aγ-
Statis

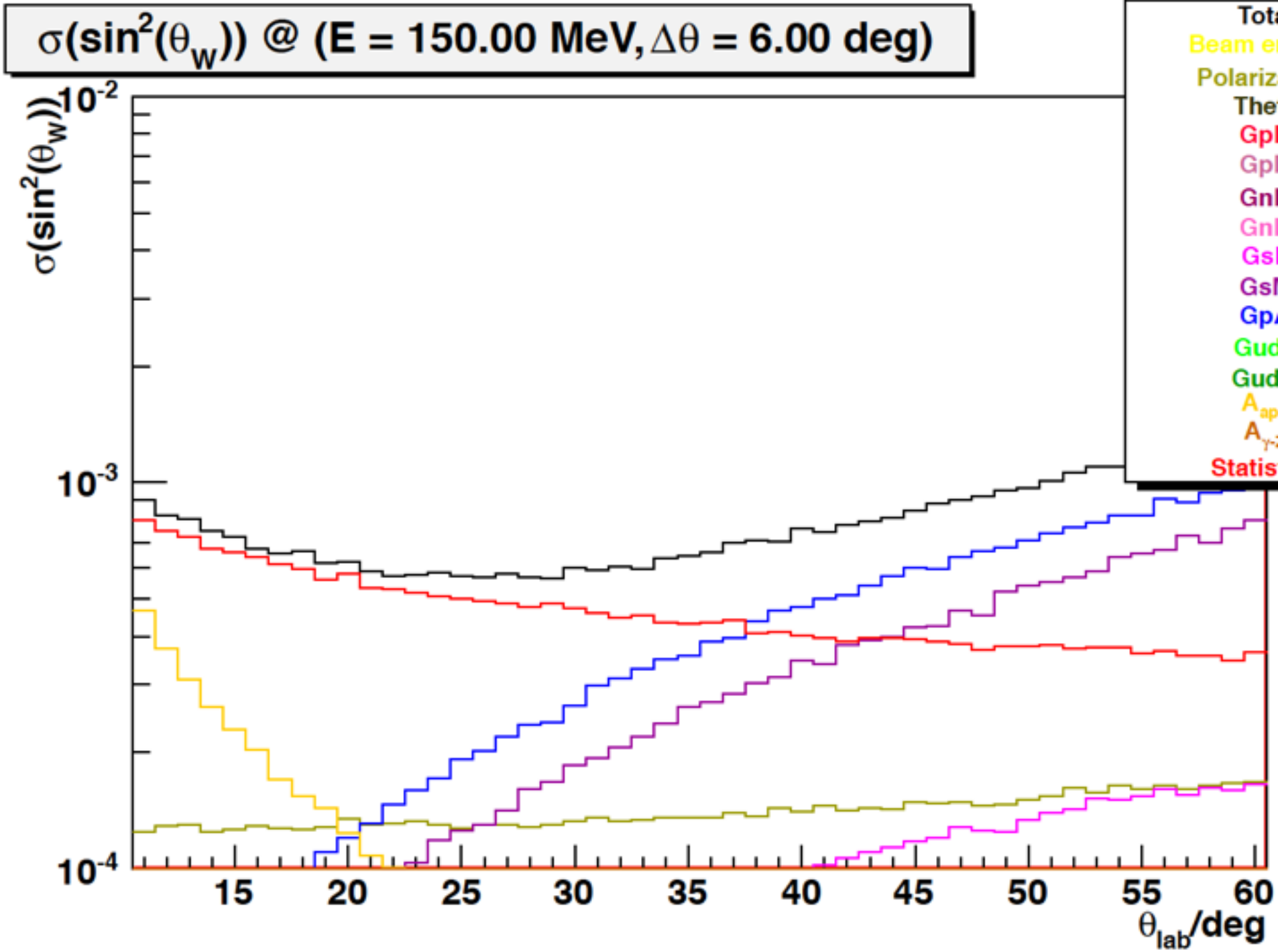
σ(sin²(θw)) @ (E = 150.00 MeV, Δθ = 6.00 deg)
σ(sin²(θw))
10⁻²
10⁻³
10⁻⁴
15
20
25
30
35
40
45
50
55
60
θlab/deg
Tota
Beam en
Polariz
The
Gpl
Gpl
Gnl
Gnl
Gsl
Gsl
Gpl
Gud
Gud
Statis

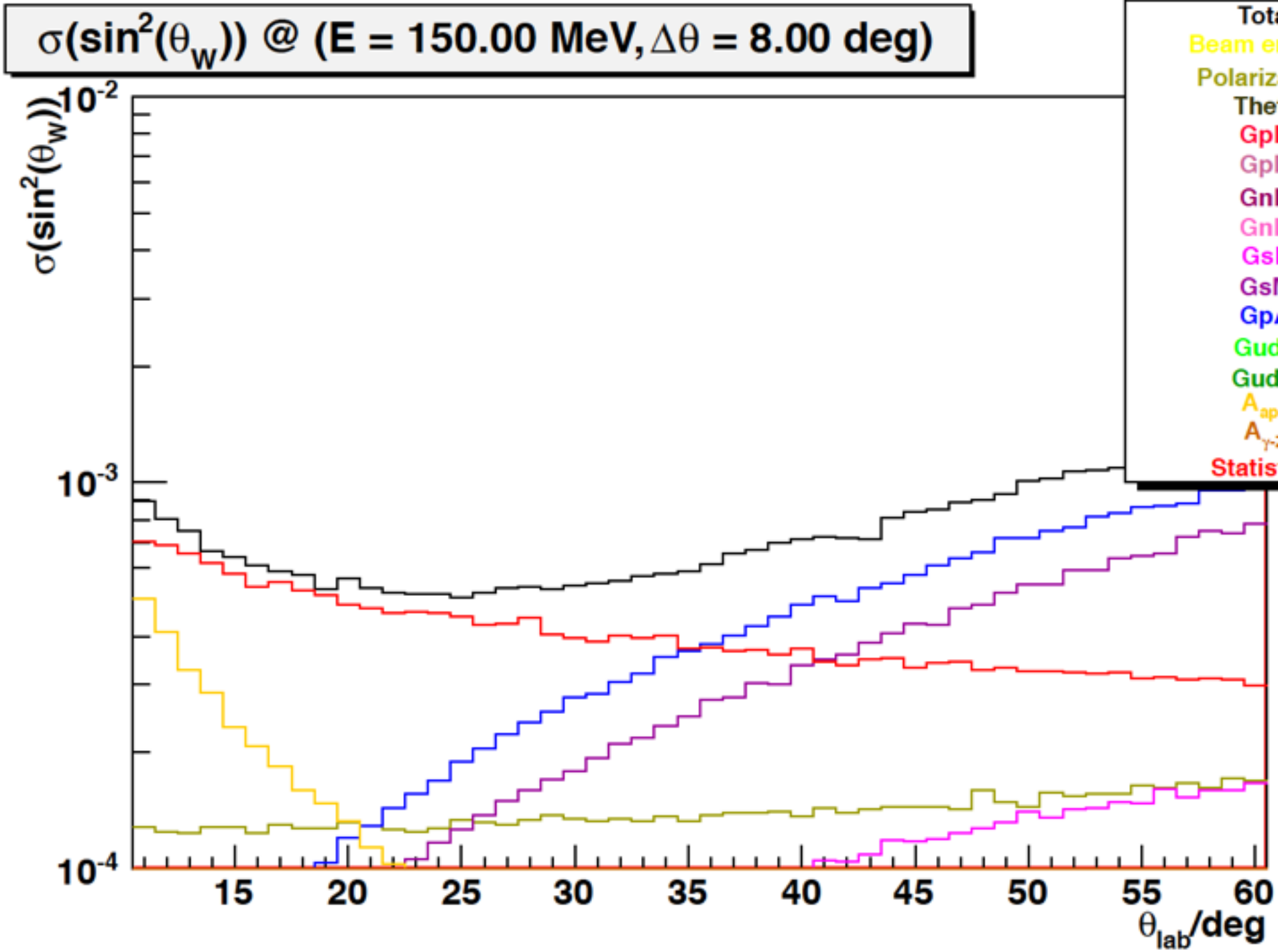
σ(sin²(θw)) @ (E = 150.00 MeV, Δθ = 8.00 deg)
σ(sin²(θw))
10⁻²
10⁻³
10⁻⁴
15
20
25
30
35
40
45
50
55
60
θlab/deg
Tota
Beam e
Polariz
The
Gpl
Gpl
Gnl
Gnl
Gsl
Gsl
Gpl
Gud
Gud
Statis

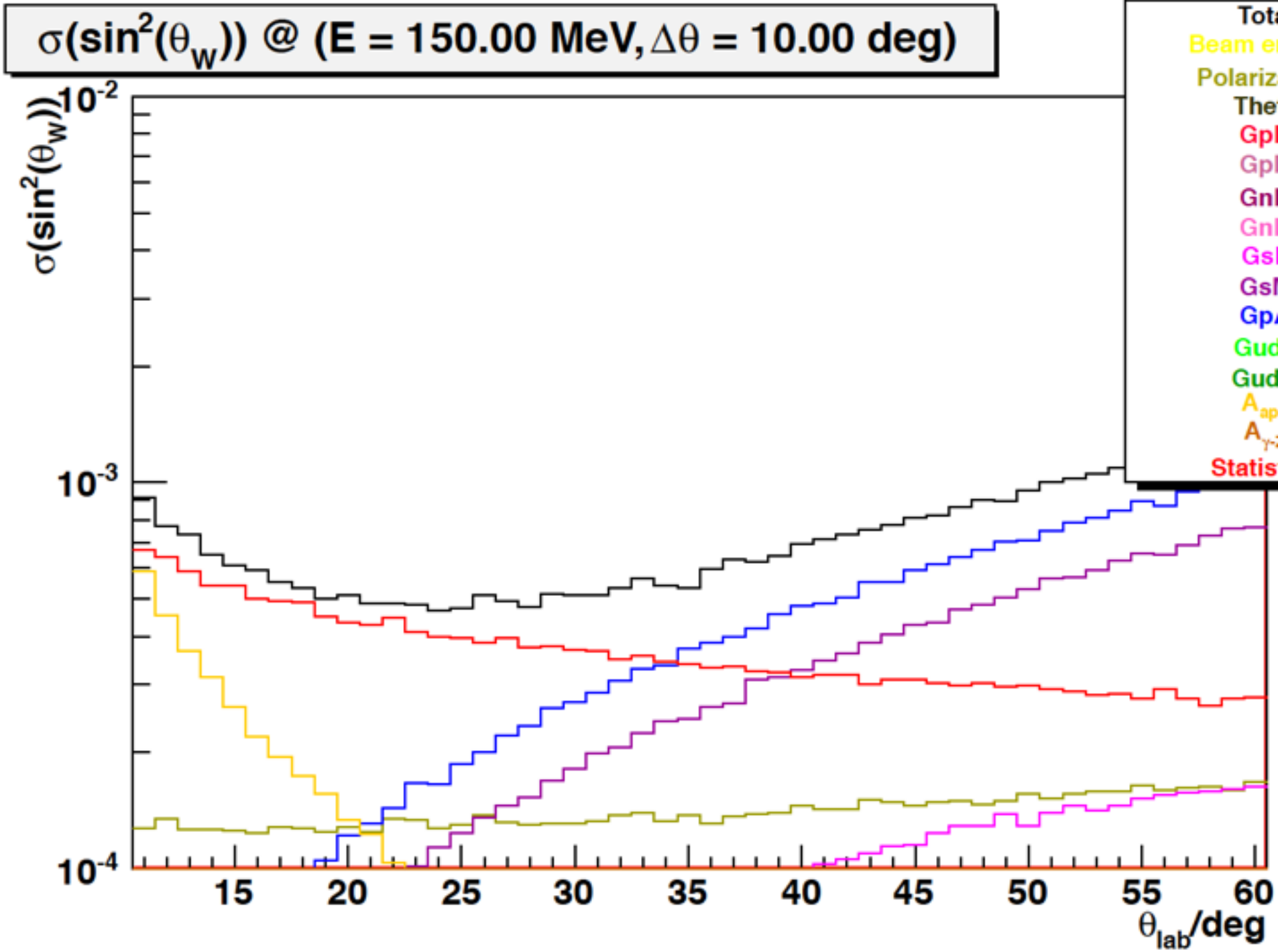
σ(sin²(θw)) @ (E = 150.00 MeV, Δθ = 10.00 deg)
σ(sin²(θw))
10⁻²
10⁻³
10⁻⁴
15
20
25
30
35
40
45
50
55
60
θlab/deg
Tota
Beam e
Polariz
The
Gpl
Gpl
Gnl
Gnl
Gsl
Gsl
Gpa
Gud
Gud
Aap
Statis

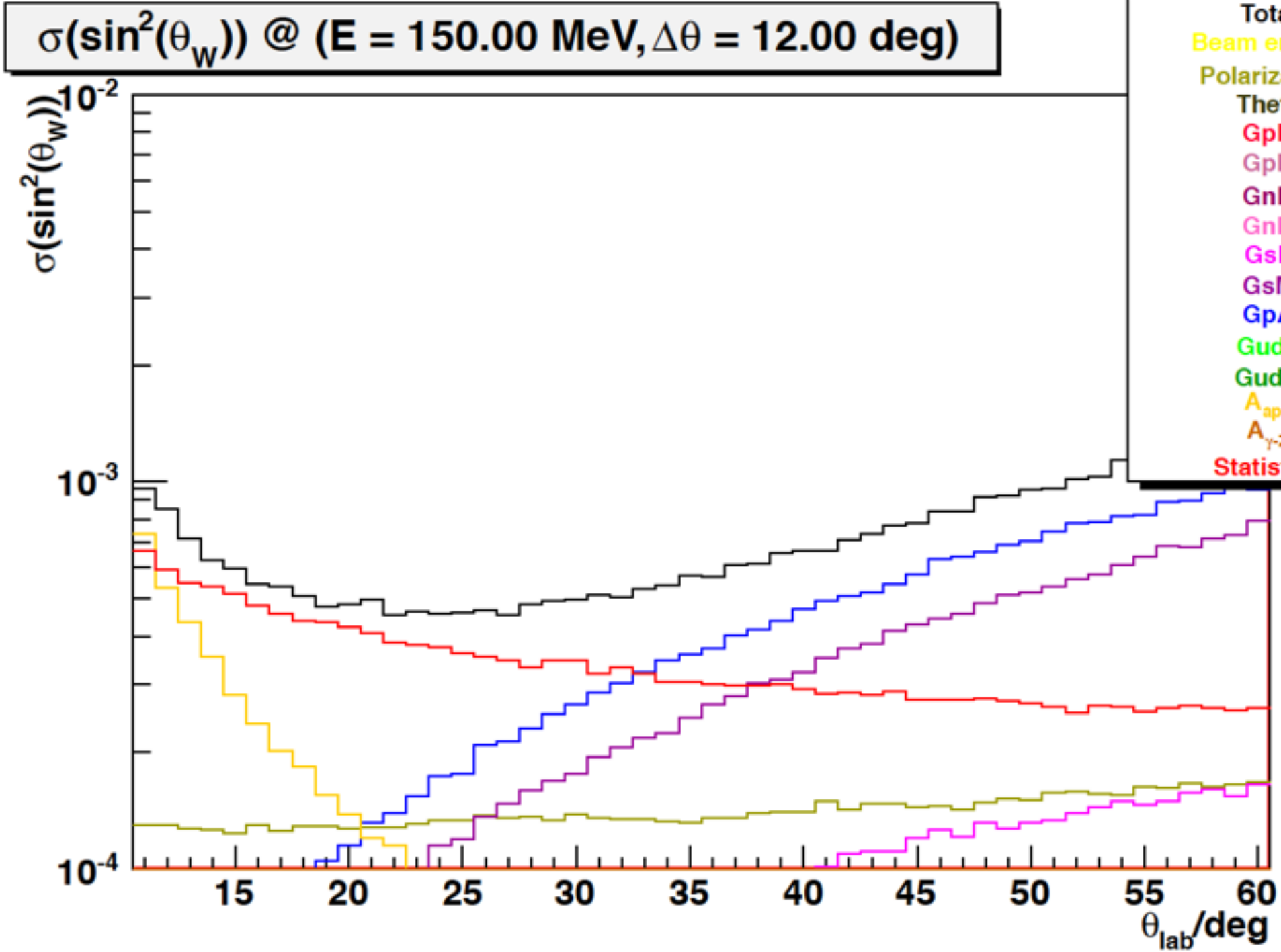
σ(sin²(θW)) @ (E = 150.00 MeV, Δθ = 12.00 deg)
σ(sin²(θW))
10⁻²
10⁻³
10⁻⁴
15
20
25
30
35
40
45
50
55
60
θlab/deg
Tota
Beam e
Polariz
The
Gpl
Gpl
Gnl
Gnl
Gsl
Gsl
GpA
Gud
Gud
Aap
Statis

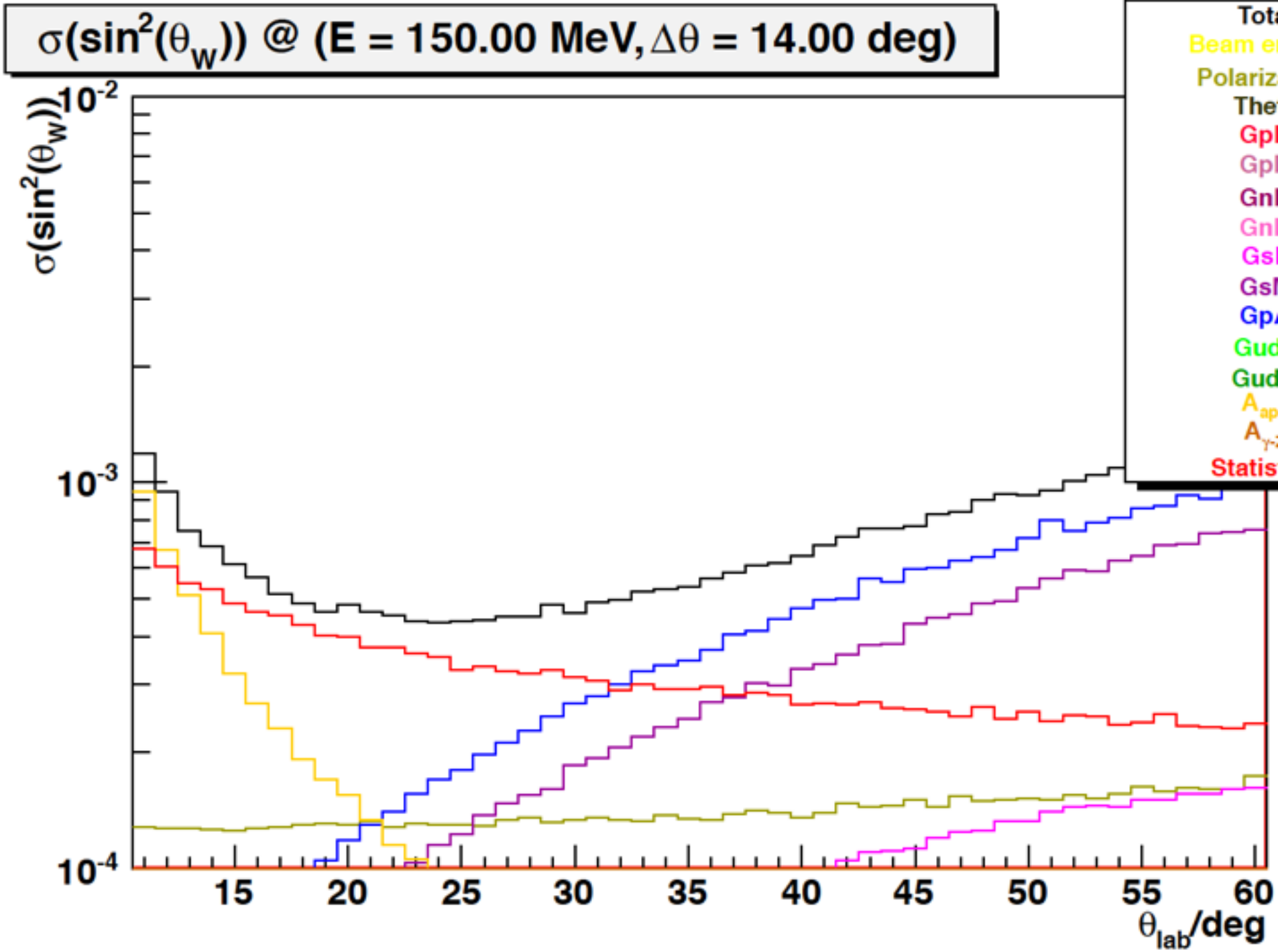
σ(sin²(θw)) @ (E = 150.00 MeV, Δθ = 14.00 deg)
σ(sin²(θw))
10⁻²
10⁻³
10⁻⁴
15
20
25
30
35
40
45
50
55
60
θlab/deg
Tota
Beam e
Polariz
The
Gpl
Gpl
Gnl
Gnl
Gsl
Gsl
Gpl
Gud
Gud
Aap
Statis

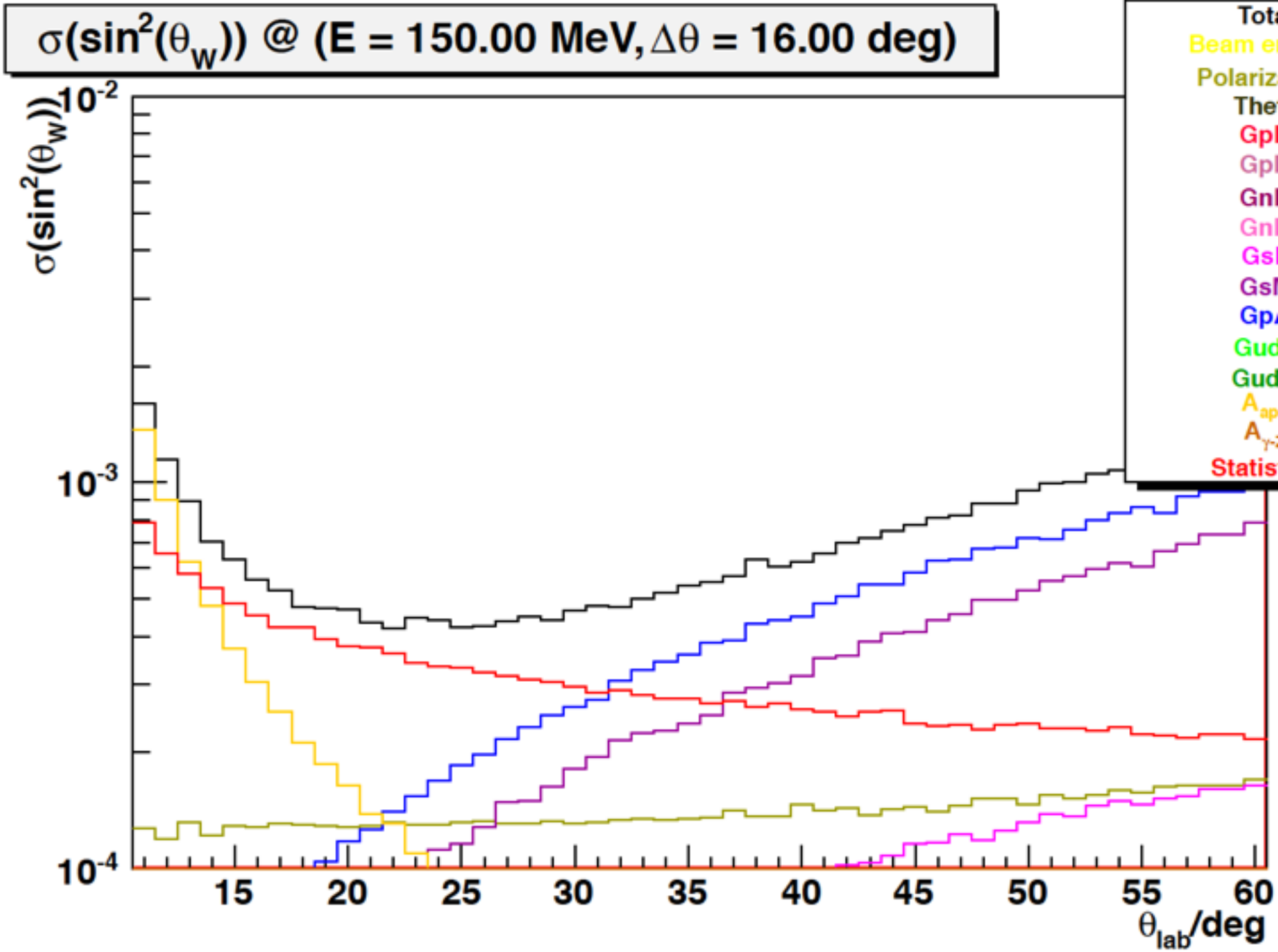
σ(sin²(θw)) @ (E = 150.00 MeV, Δθ = 16.00 deg)
σ(sin²(θw))
10⁻²
10⁻³
10⁻⁴
15
20
25
30
35
40
45
50
55
60
θlab/deg
Tota
Beam e
Polariz
The
Gpl
Gpl
Gnl
Gnl
Gsl
Gsl
Gpl
Gud
Gud
Aap
Statis

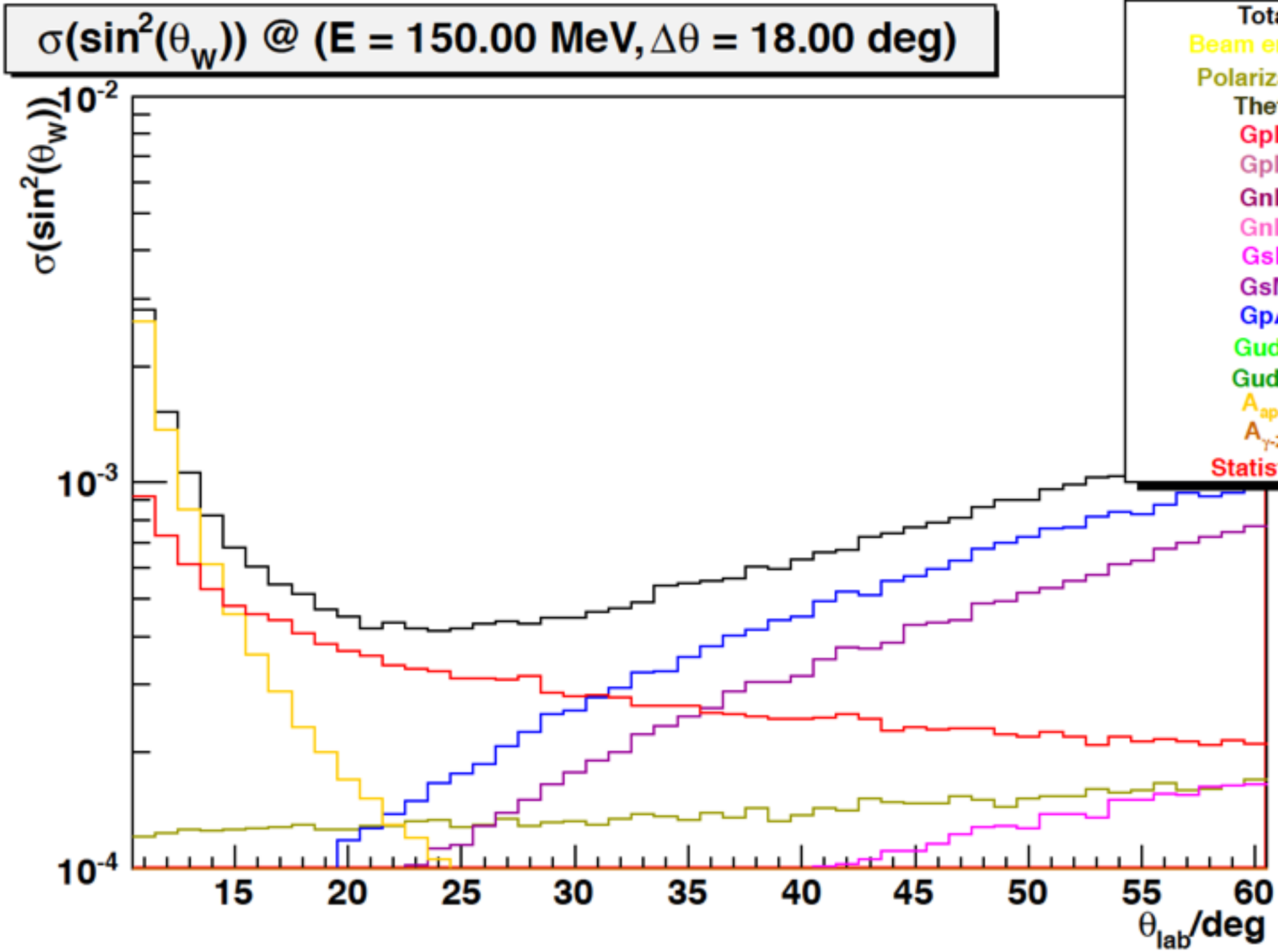
σ(sin²(θw)) @ (E = 150.00 MeV, Δθ = 18.00 deg)
σ(sin²(θw))
10⁻²
10⁻³
10⁻⁴
15
20
25
30
35
40
45
50
55
60
θlab/deg
Tota
Beam e
Polariz
The
Gpl
Gpl
Gnl
Gnl
Gsl
Gsl
Gpl
Gud
Gud
Aap
Statis

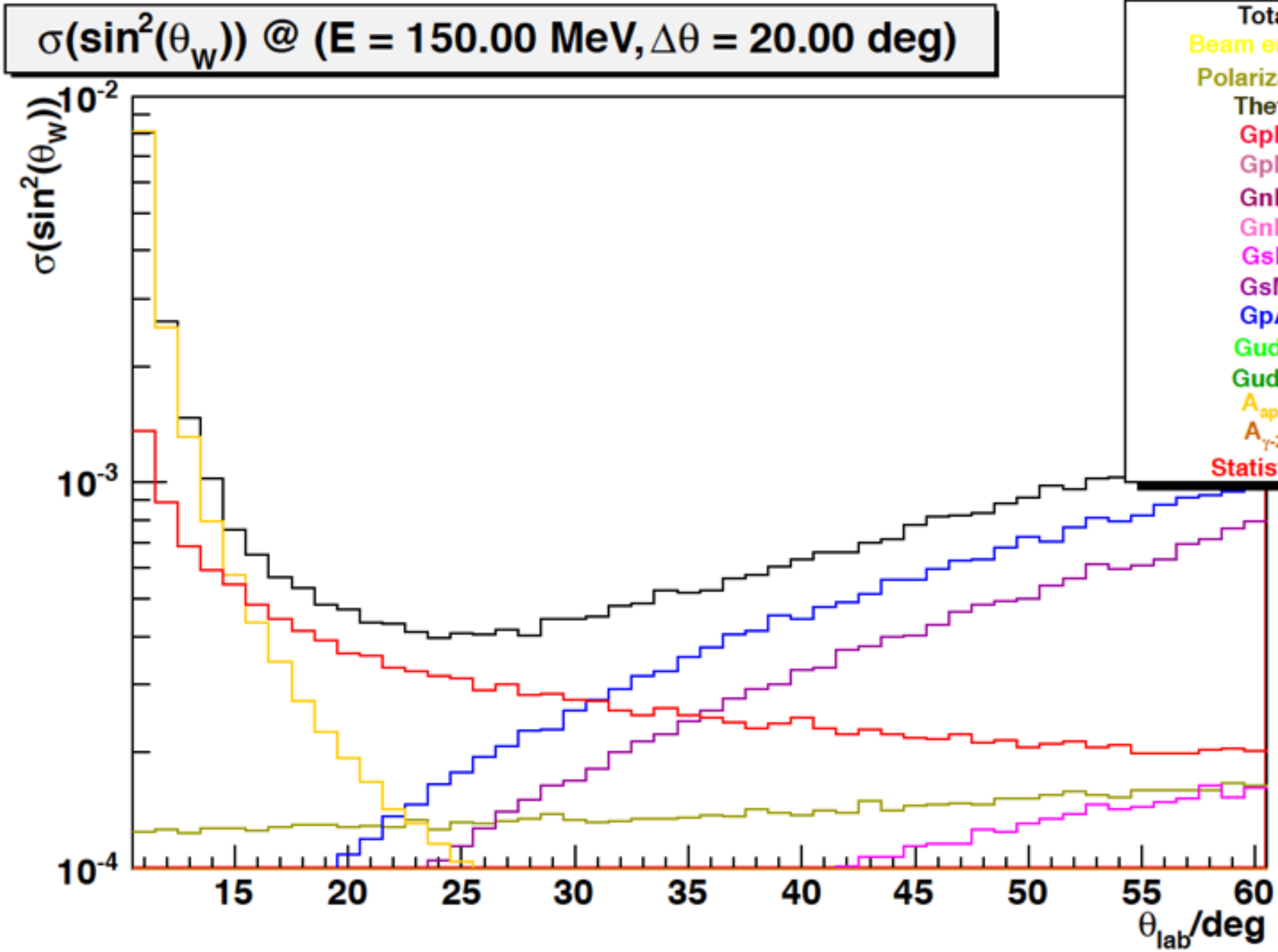
σ(sin²(θw)) @ (E = 150.00 MeV, Δθ = 20.00 deg)
σ(sin²(θw))
10⁻²
10⁻³
10⁻⁴
15
20
25
30
35
40
45
50
55
60
θlab/deg
Tota
Beam e
Polariz
The
Gpl
Gpl
Gnl
Gnl
Gsl
Gsl
Gpl
Gud
Gud
Statis

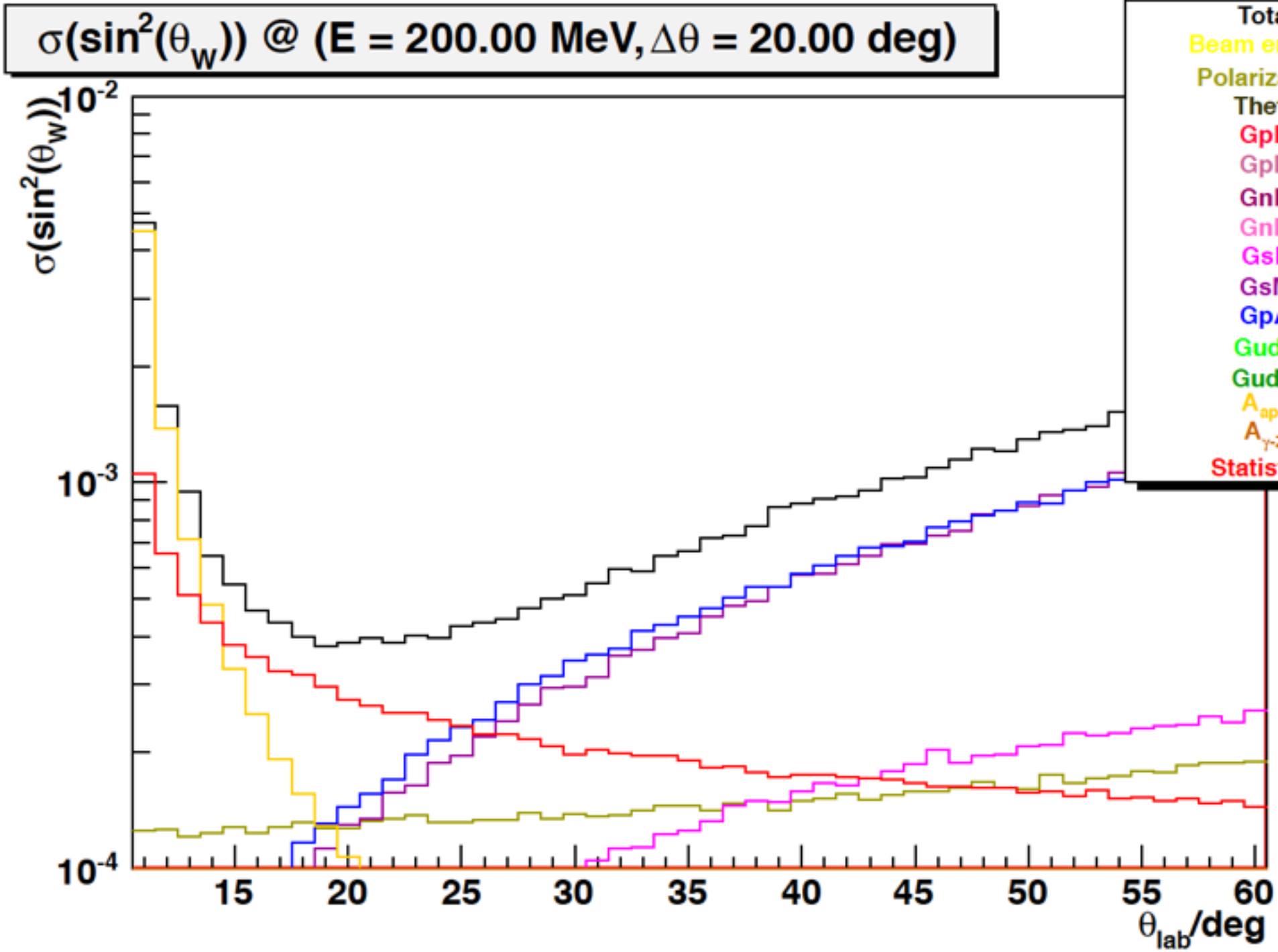
σ(sin²(θw)) @ (E = 200.00 MeV, Δθ = 20.00 deg)
σ(sin²(θw))
10⁻²
10⁻³
10⁻⁴
15
20
25
30
35
40
45
50
55
60
θlab/deg
Tota
Beam e
Polariz
The
Gpl
Gpl
Gnl
Gnl
Gsl
Gsl
Gpl
Gud
Gud
Aap
Aγ-
Statis

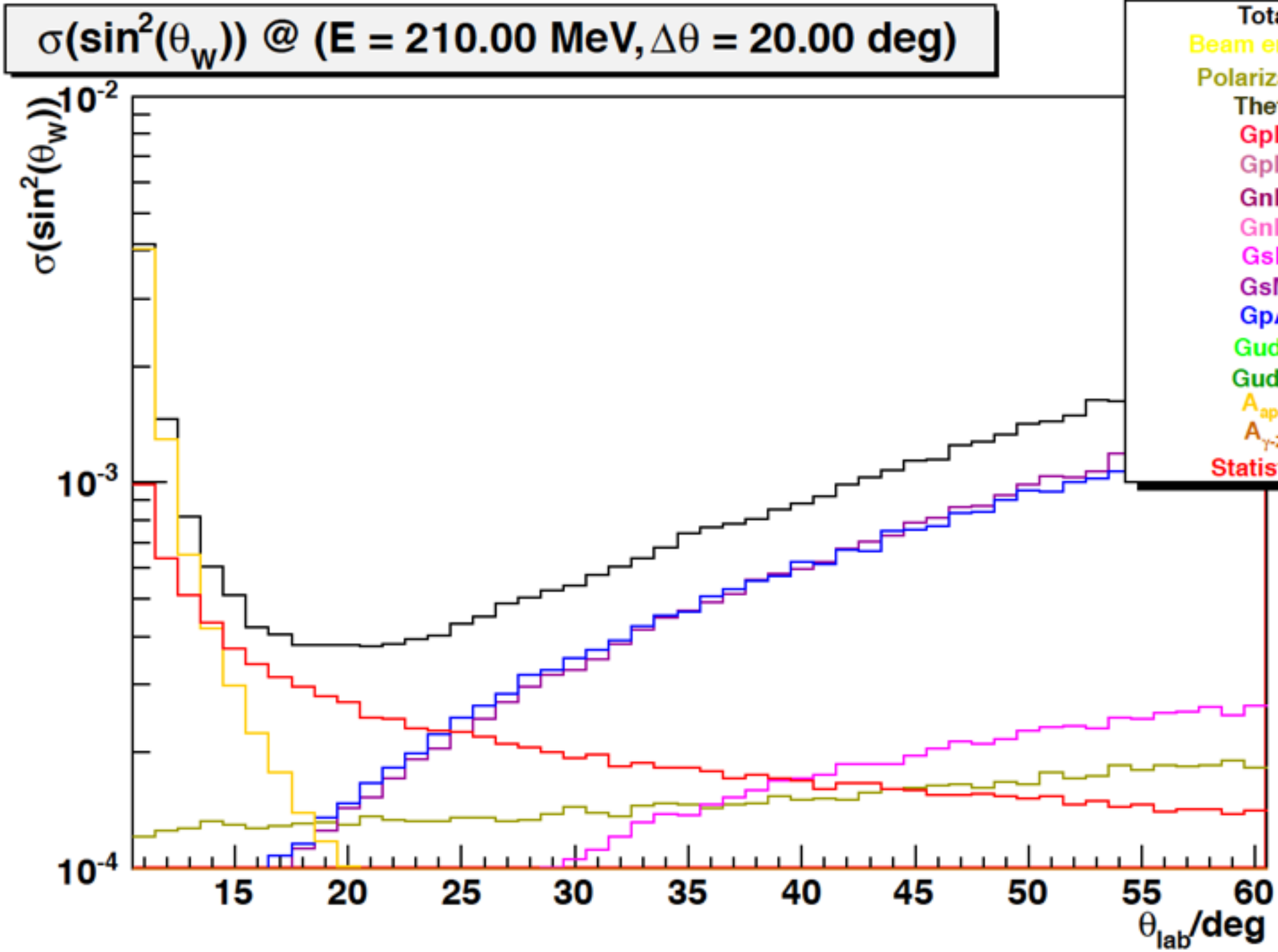
σ(sin²(θw)) @ (E = 210.00 MeV, Δθ = 20.00 deg)
σ(sin²(θw))
10⁻²
10⁻³
10⁻⁴
15
20
25
30
35
40
45
50
55
60
θlab/deg
Tota
Beam en
Polariz
The
Gpl
Gpl
Gnl
Gnl
Gsl
Gsl
GpA
Gud
Gud
Aap
Statis

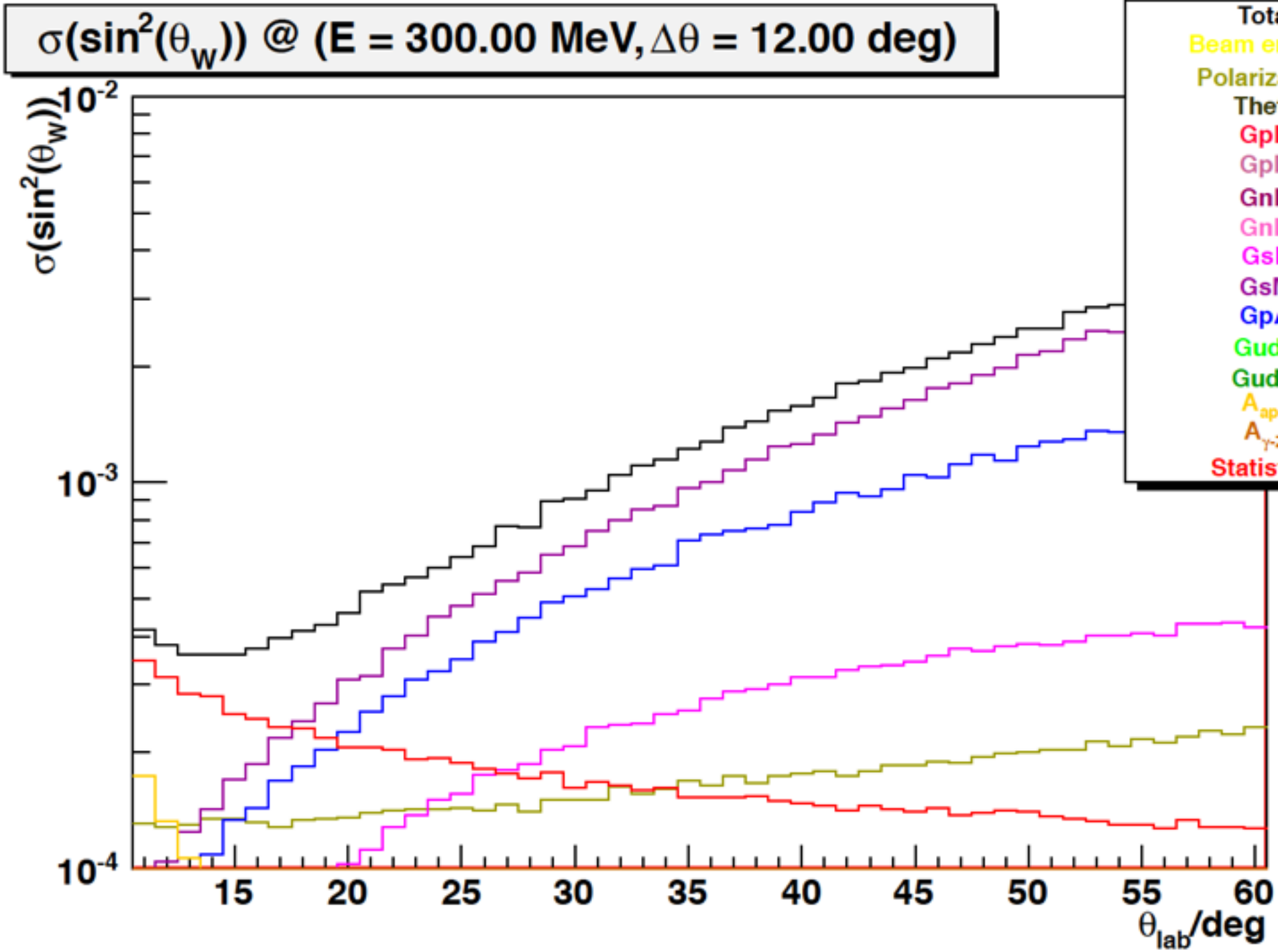
σ(sin²(θw)) @ (E = 300.00 MeV, Δθ = 12.00 deg)
σ(sin²(θw))
10⁻²
10⁻³
10⁻⁴
15
20
25
30
35
40
45
50
55
60
θlab/deg
Tota
Beam en
Polariz
The
Gpl
Gpl
Gnl
Gnl
Gsl
Gsl
Gpl
Gud
Gud
Statis

Carbon/Lead

EXPERIMENTAL REALIZATION

MESA:
- 150µA
- 150MeV-200MeV
- Polarimetry

Enhanced sensitivity
To new physics

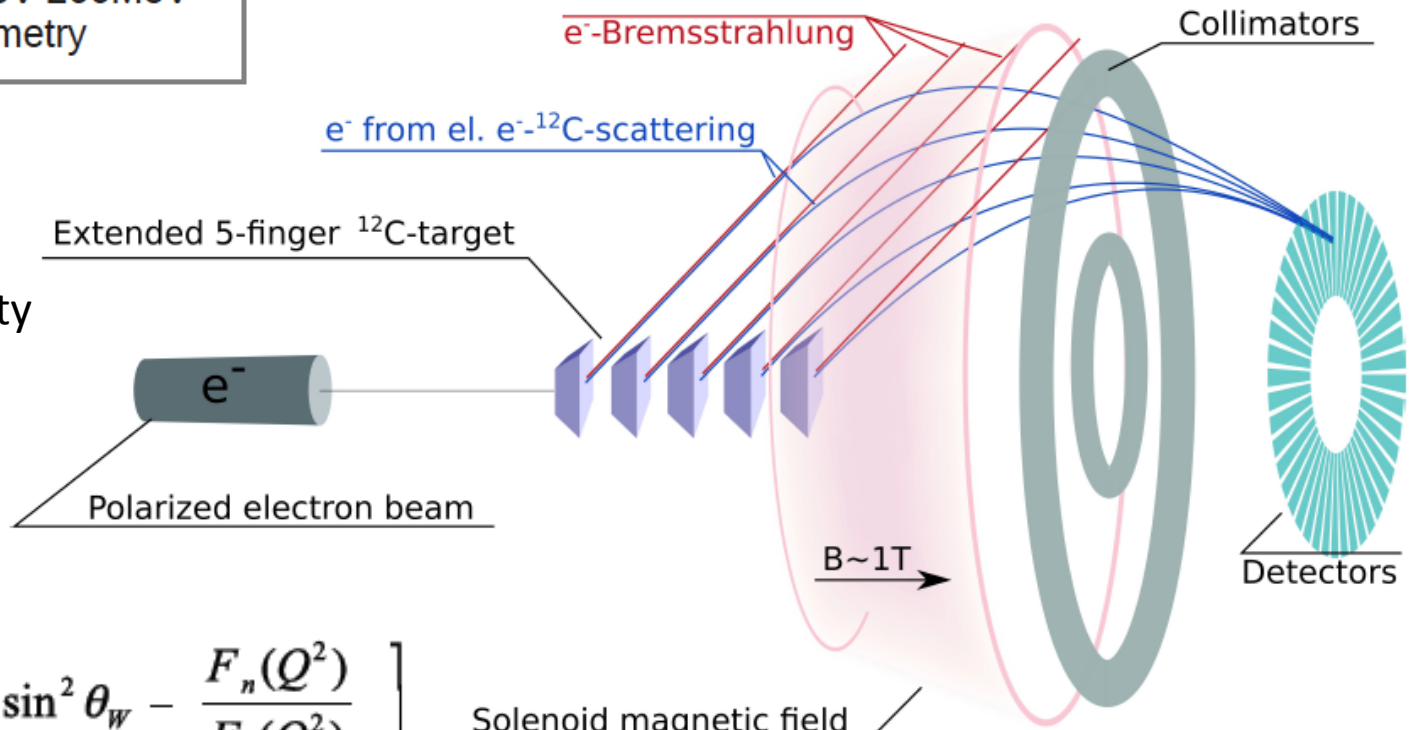

$$-N = \frac{G_F Q^2}{2\pi\alpha\sqrt{2}}\left[\underbrace{\sin^2\theta_W}_{\approx 0} - \frac{F_n(Q^2)}{F_p(Q^2)}\right]$$

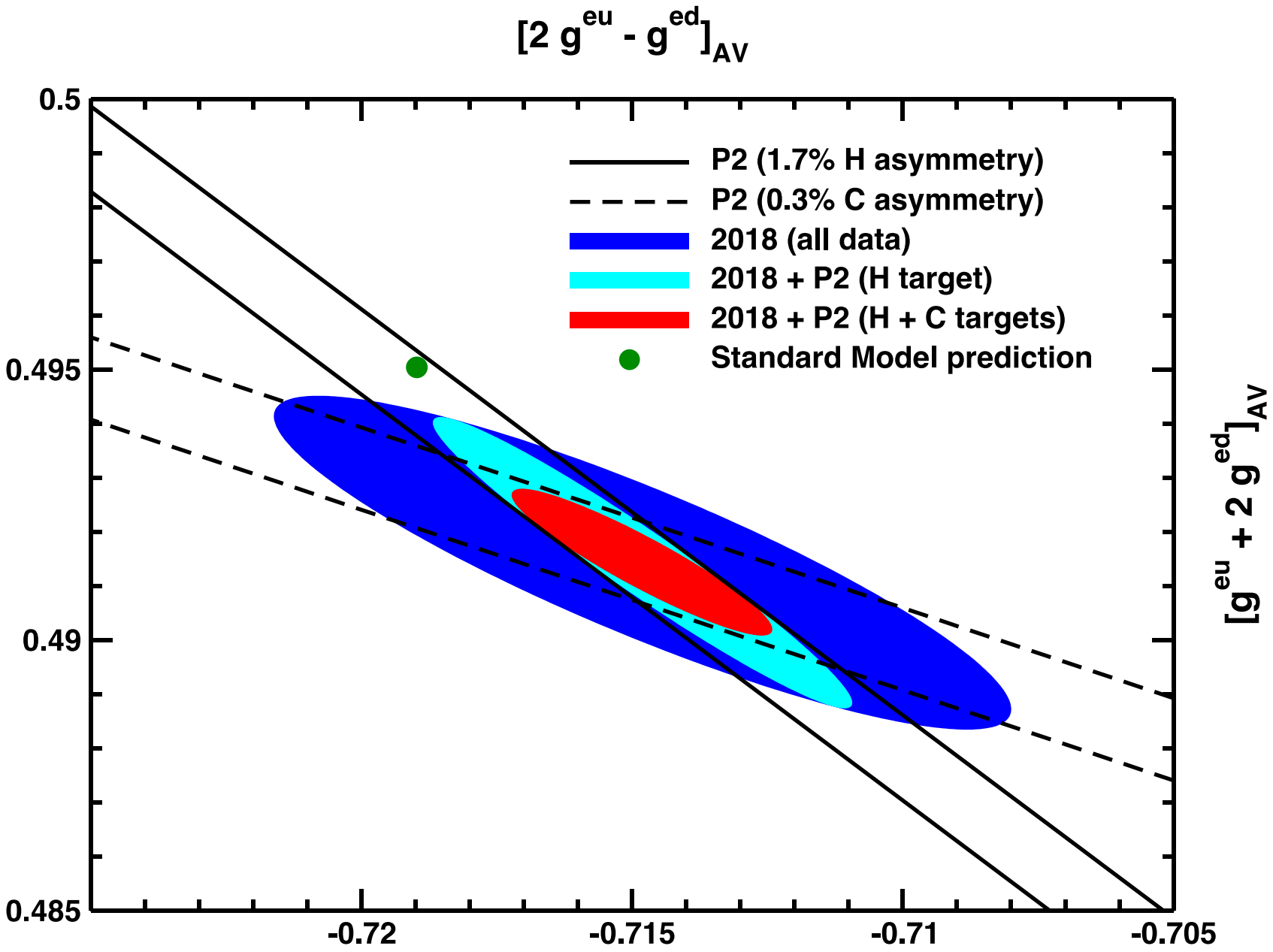
$[2\,g^{eu} - g^{ed}]_{AV}$
$[g^{eu} + 2\,g^{ed}]_{AV}$
0.5
0.495
0.49
0.485
-0.72
-0.715
-0.71
-0.705
P2 (1.7% H asymmetry)
P2 (0.3% C asymmetry)
2018 (all data)
2018 + P2 (H target)
2018 + P2 (H + C targets)
Standard Model prediction

Neutron Skin for beginner

Where do the neutrons go?

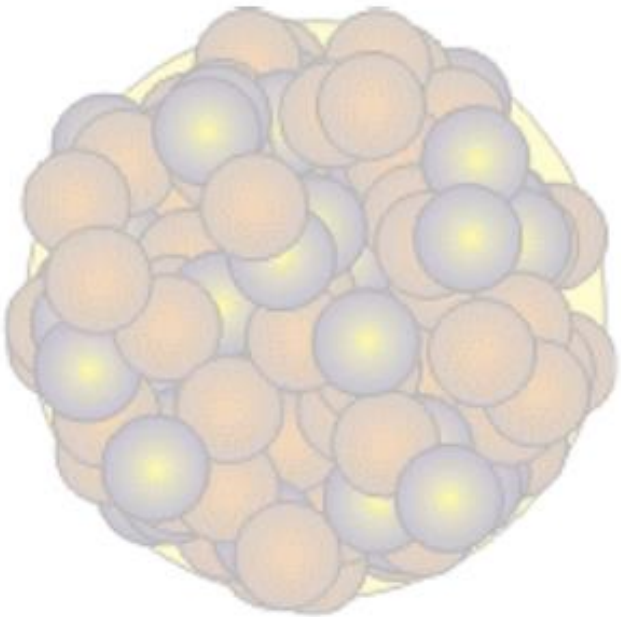

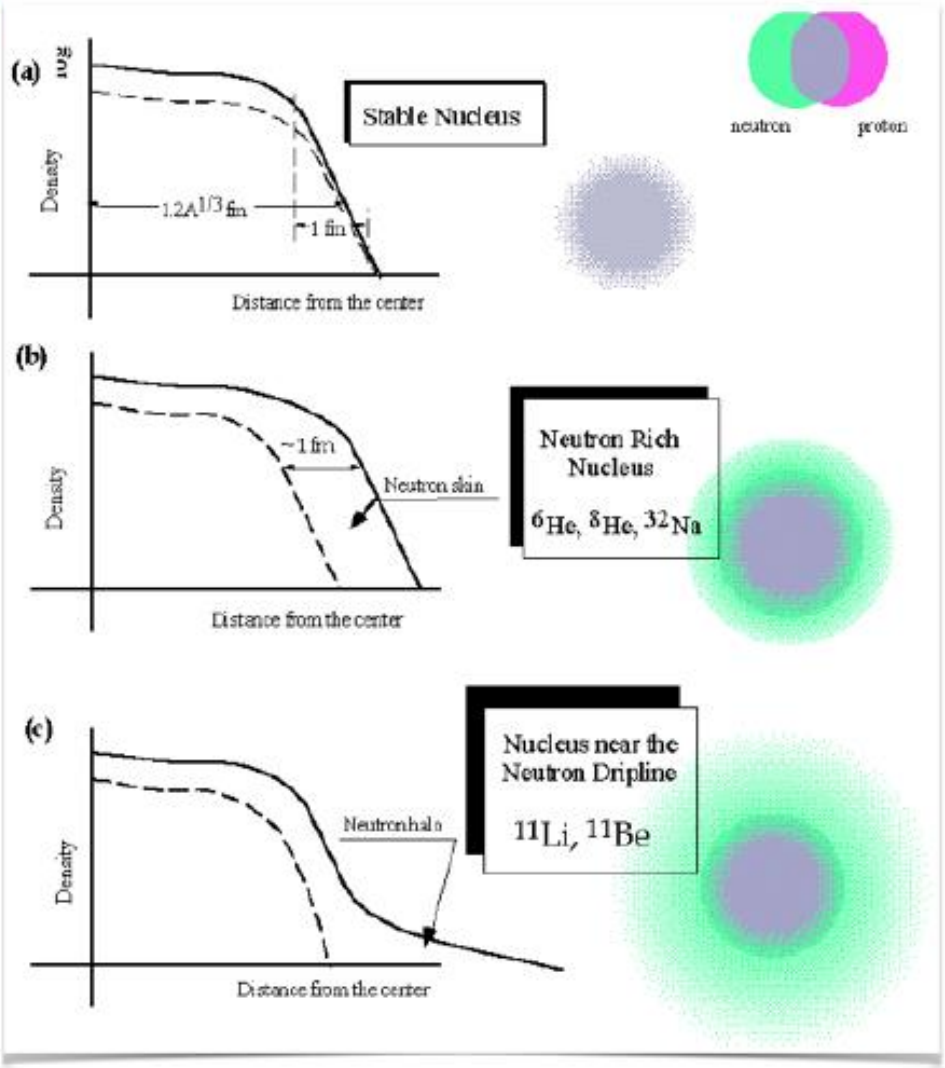

Pressure forces neutrons out against surface tension

→ **EOS**

Neutron Skin for beginner

Where do the neutrons go?

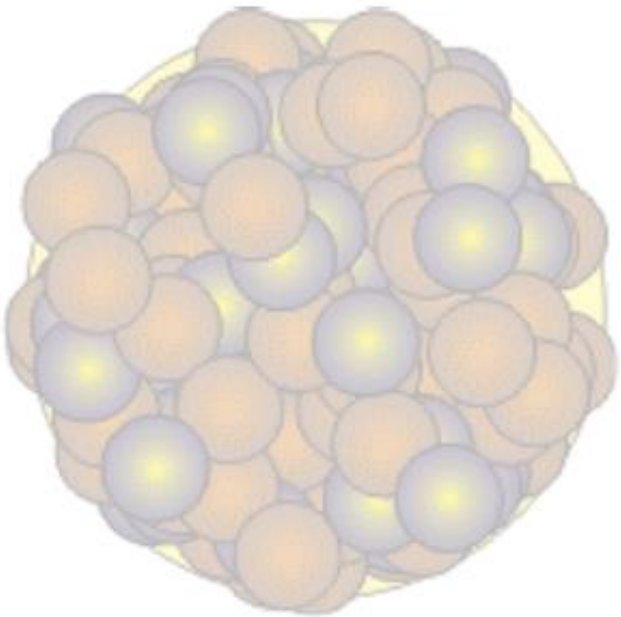

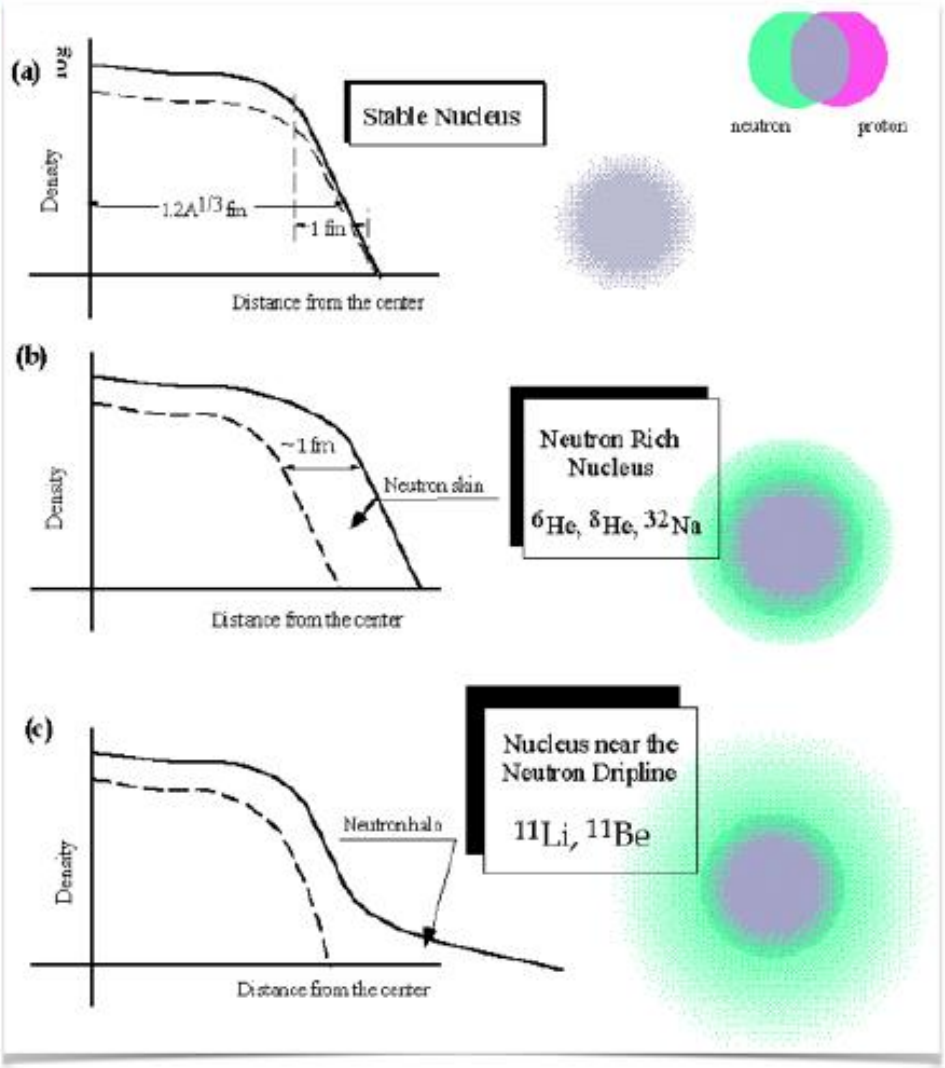

Pressure forces neutrons out against surface tension

→ **EOS**

Detector geometry

Detector

- Quartz dimensions: 300 x 70 x 10-15 mm3 – 5-10mm
- PMTs at 45º
- PMTs to be used? Hamamatsu or ElectronTubes
- Ring Inner and Outer diameter? 450-900-quartz longer
- Quartz angles?

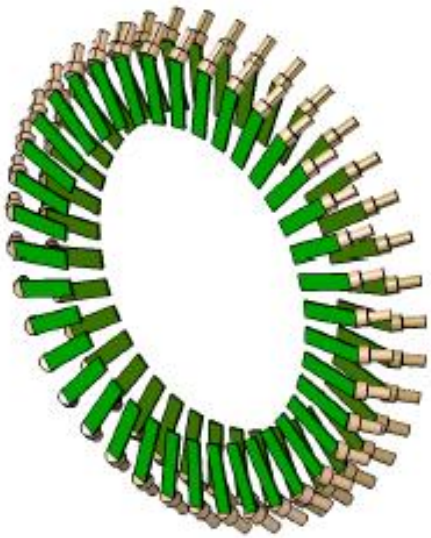

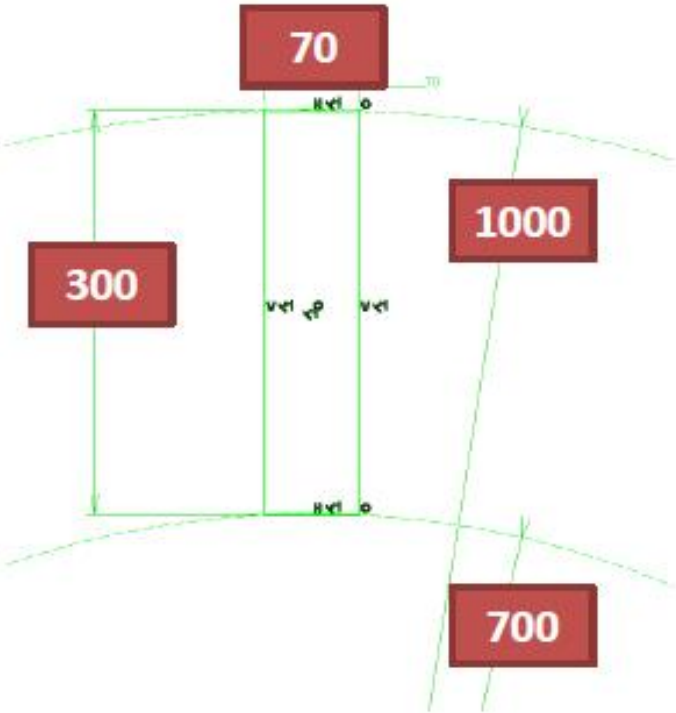

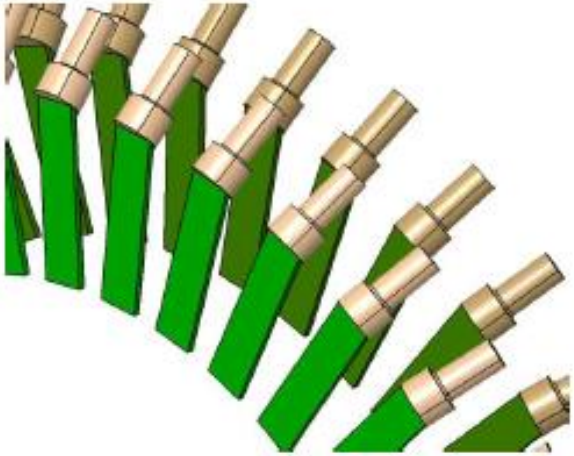

Detector

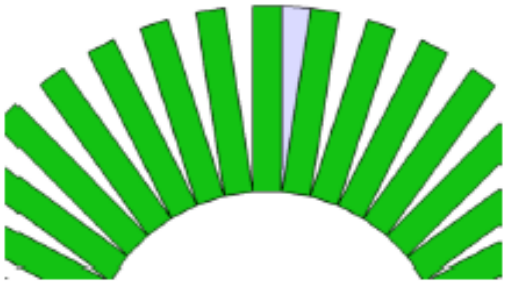

Case 1

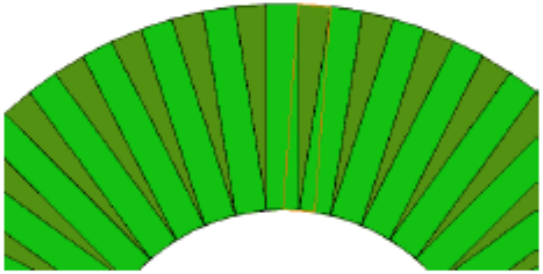

Case 2

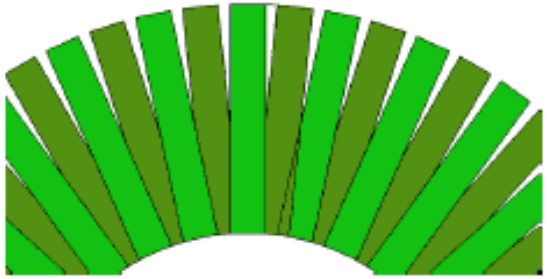

Case 3

Case 4

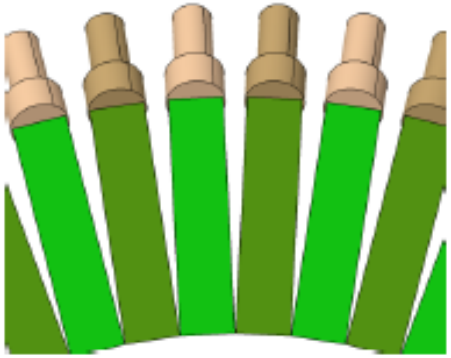

Case 5

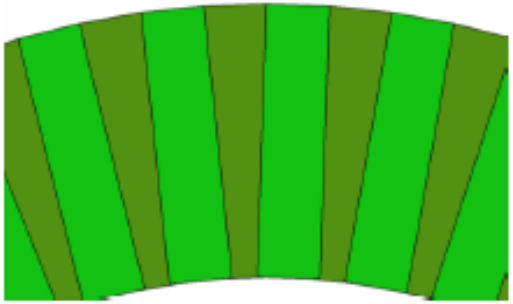

Case 6

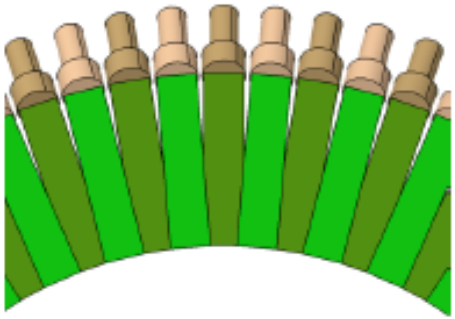

Case 7

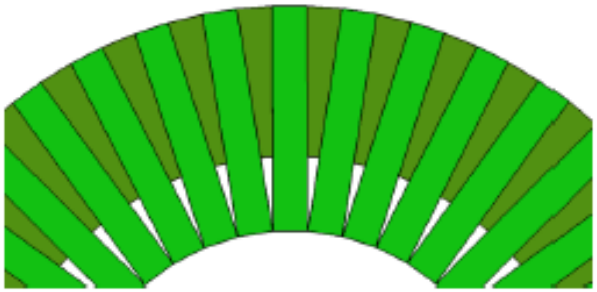

Ri: 450
Qh: 450

Ri: 700
Qh: 300

Lead Shield

	Z	Dist to 0	Ri	Ro	Weight	
Front	100	970	250	530	730	
Inner Cylinder	1929	1070	380	480	5910	
“Teeth”	2000	1070	480	530	1770	100 mm/tooth
Outer Cylinder	101	2899	1000	1300	2480	

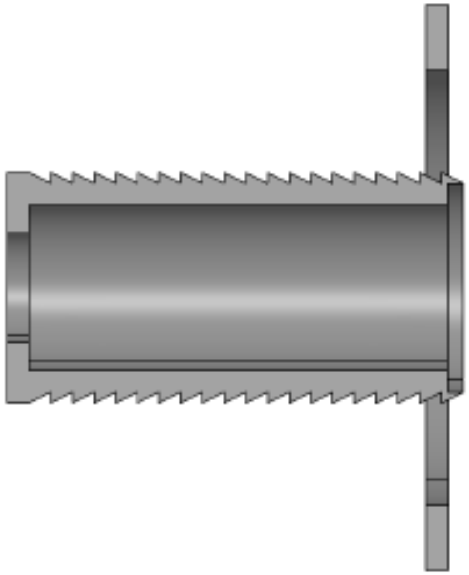

~11 tons

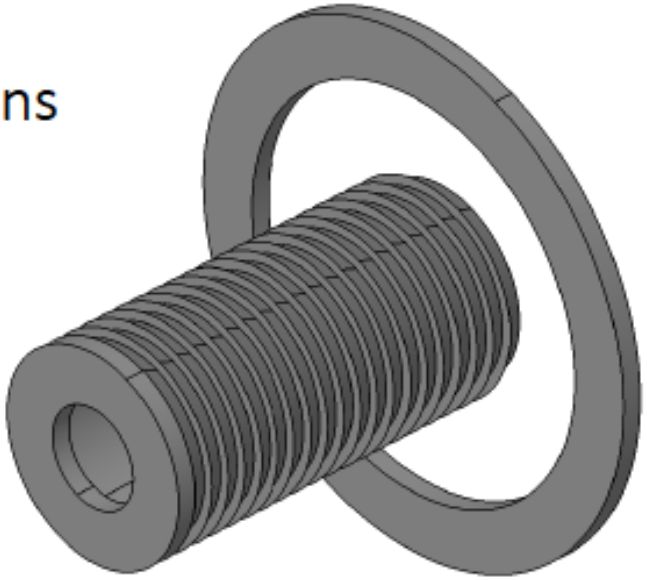

Lead Shield Support

- Geometry? Inner cylinder
- Material? ~~Steel,~~ Aluminum? nothing magnetic
- Space in the hall? -Juergen
- Impact on the magnetic field
- Impact of the magnetic field on the support

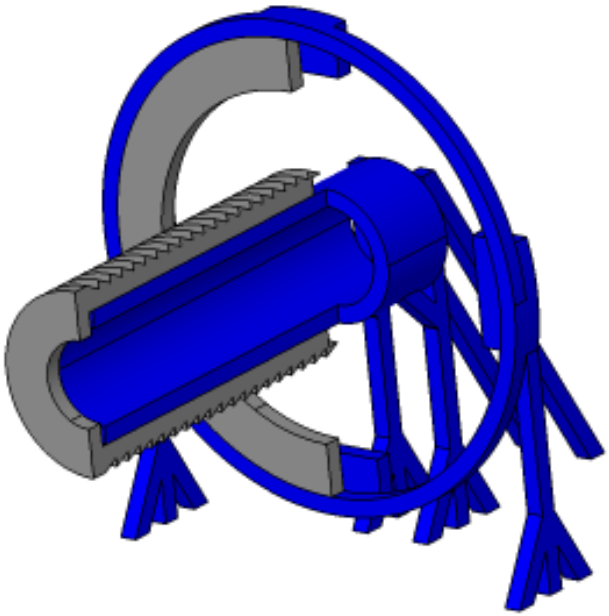

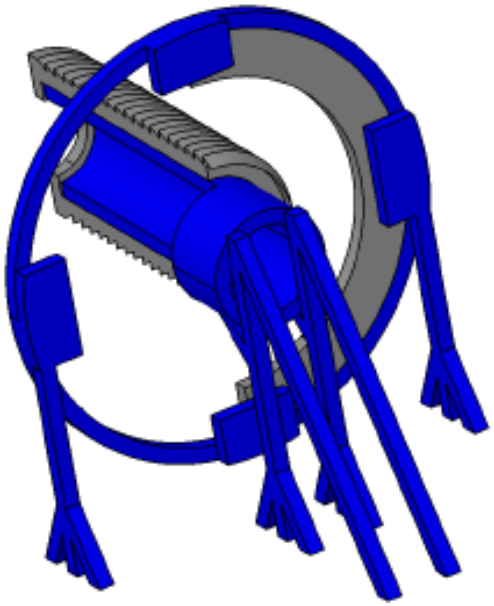

Lead Shield Support

- Aluminium
  - Safey factor: 3
  - Displacement: 3mm

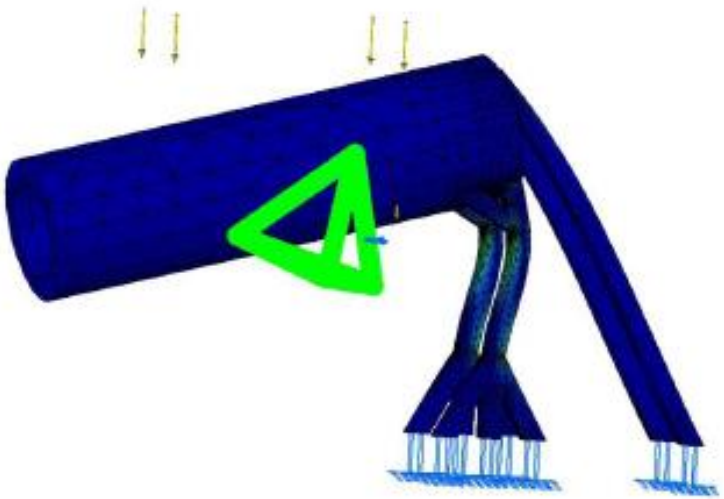

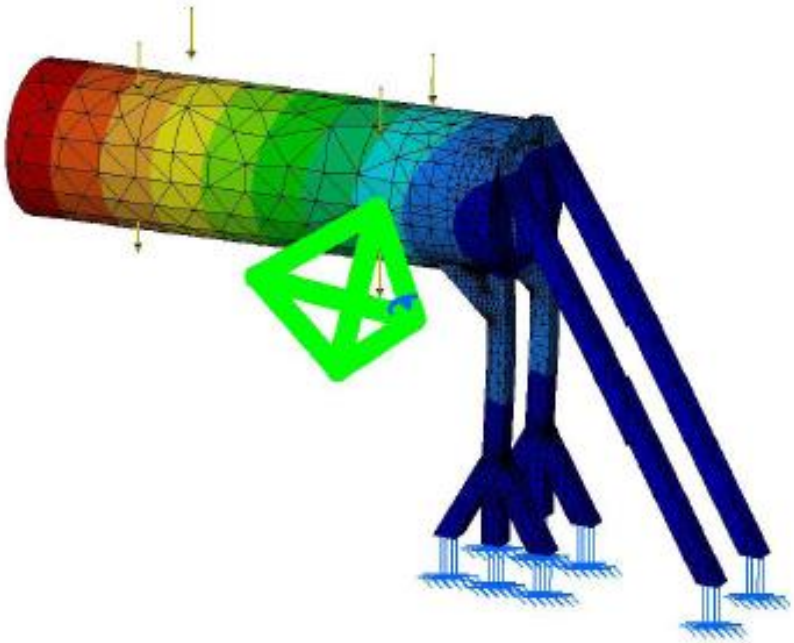

Solenoid

- FOPI Solenoid
  - Length: 3.8m
  - Inner diameter: 2.4m
  - Weight: 108.7 tn – Juergen, floor?

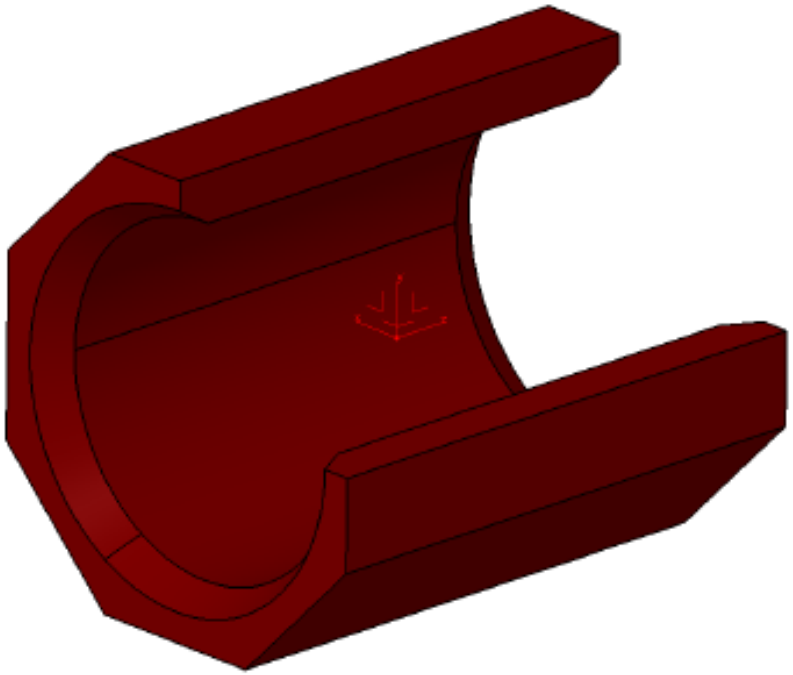

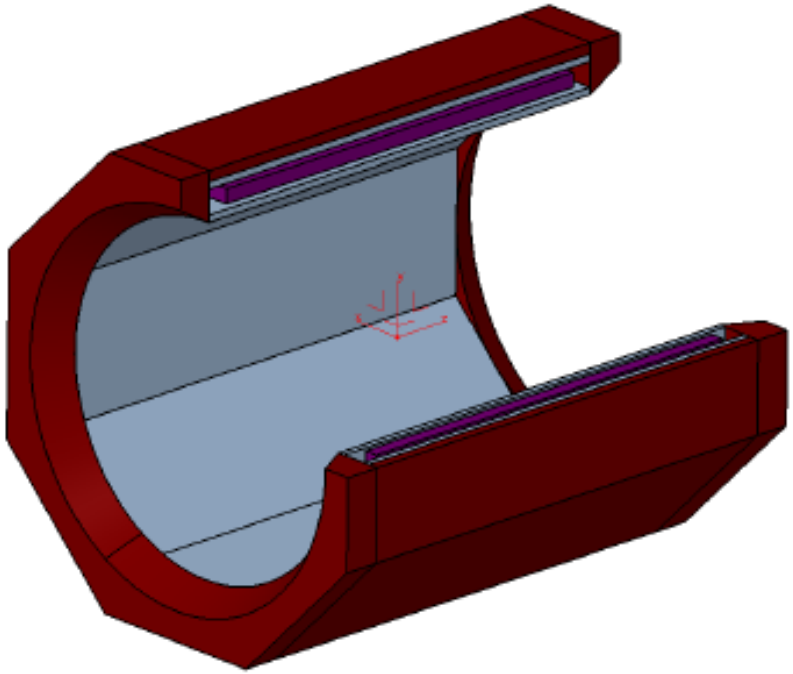

Solenoid

- Field Map available
- Waiting for
  - Drawings
  - Coil specifications

Solenoid

- Simulations for
  - Impact in the magnetic field
  - Impact by the magnetic field
- CST Software

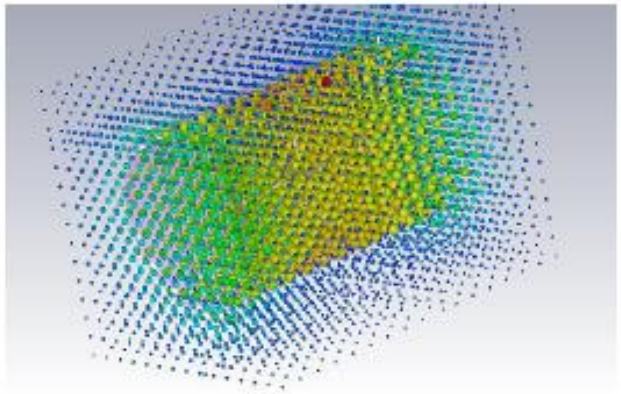

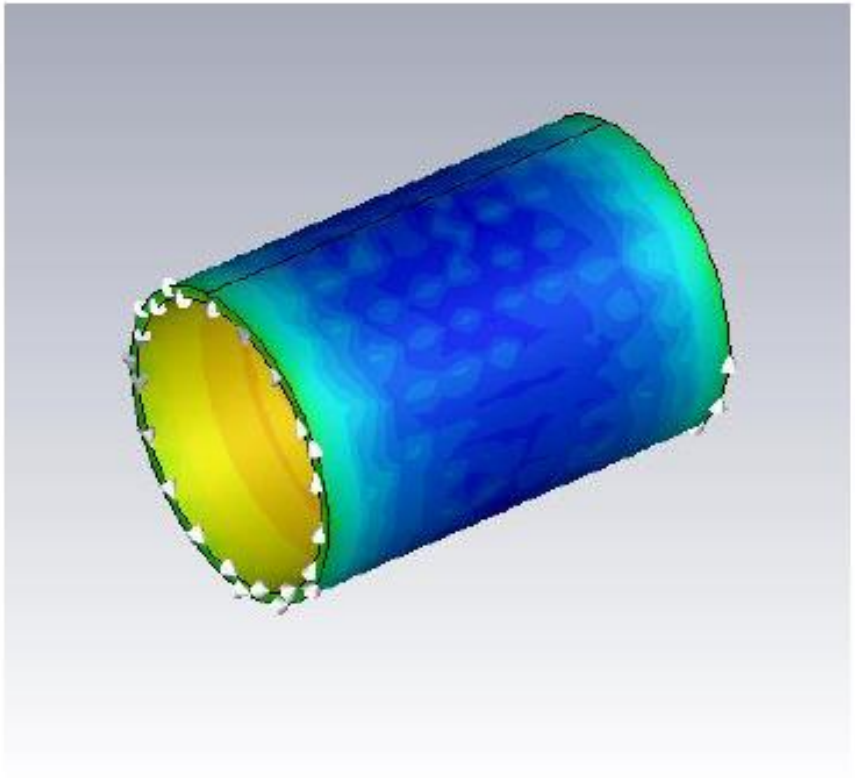

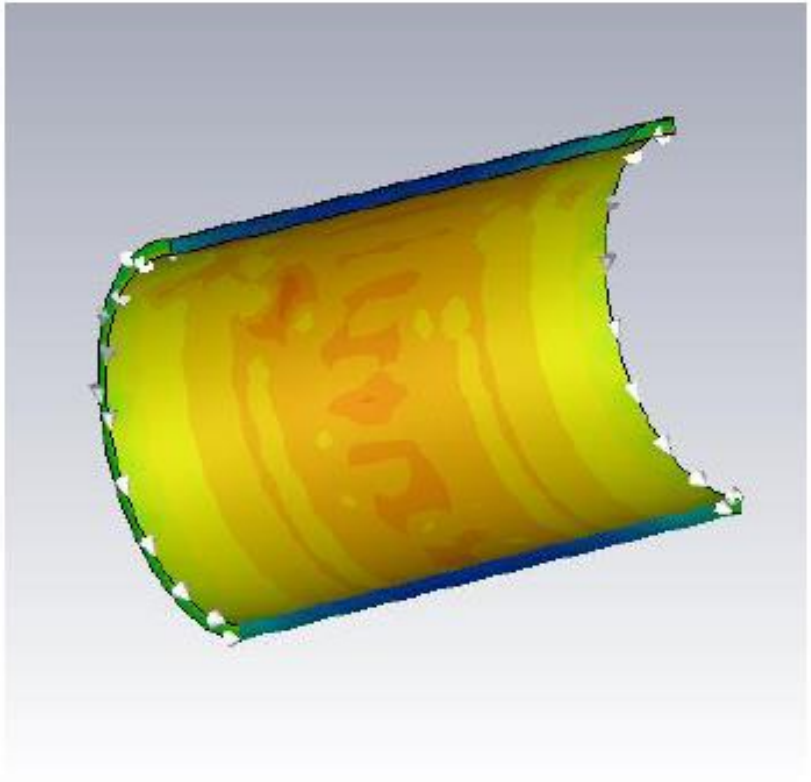

Complete Setup

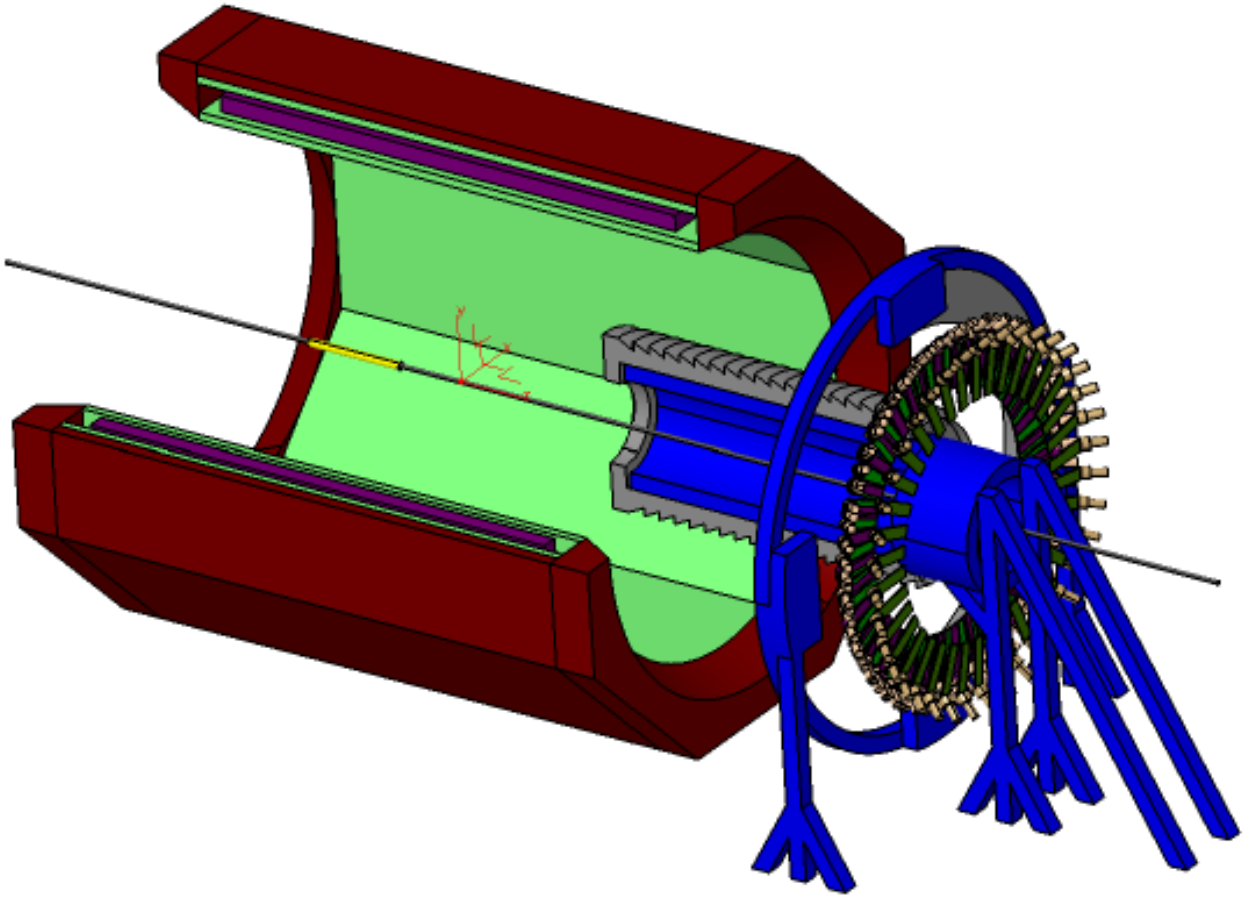

Change colours
No axis system
Highlight the Quartzes
3D PDF

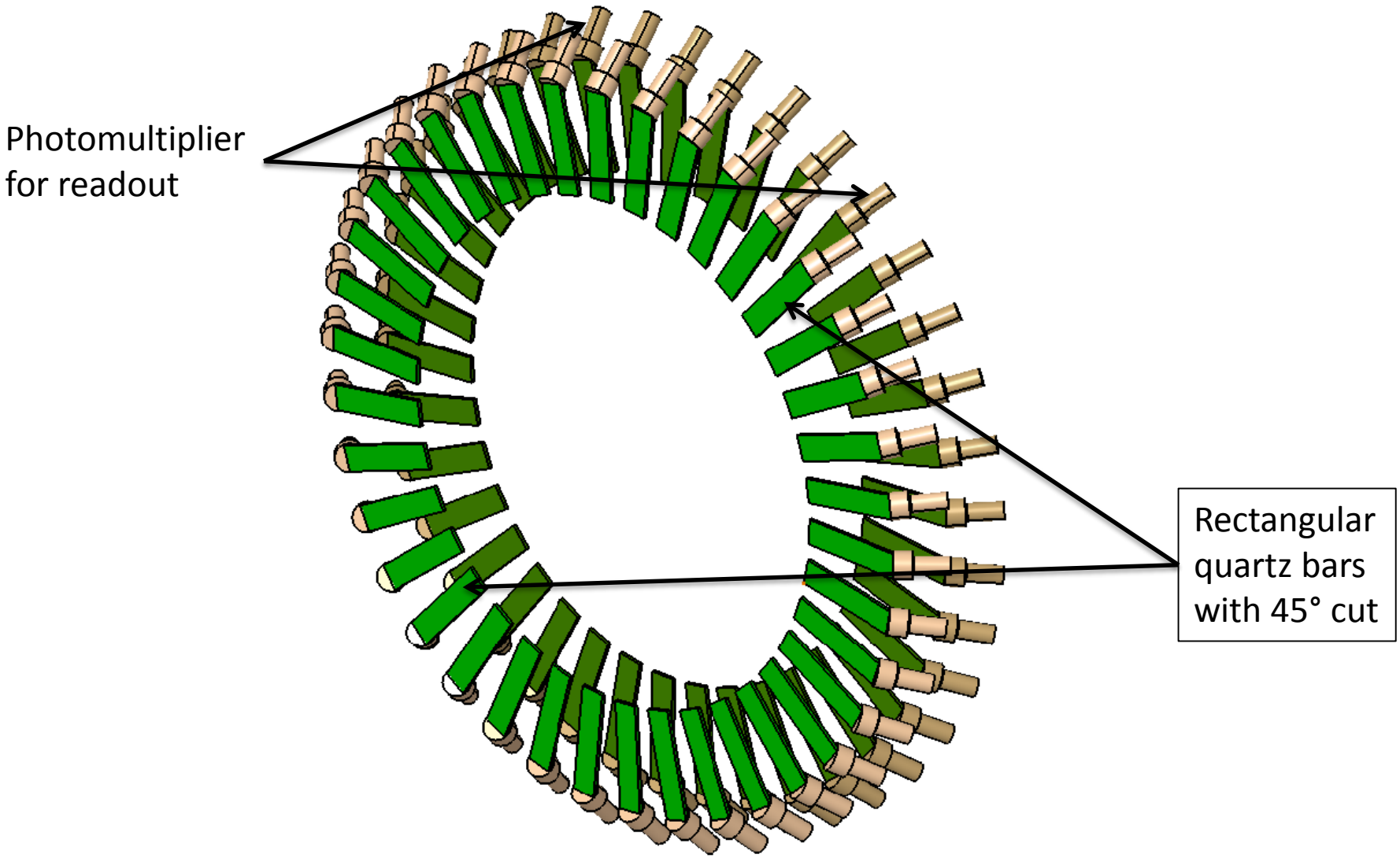
Photomultiplier
for readout
Rectangular
quartz bars
with 45° cut

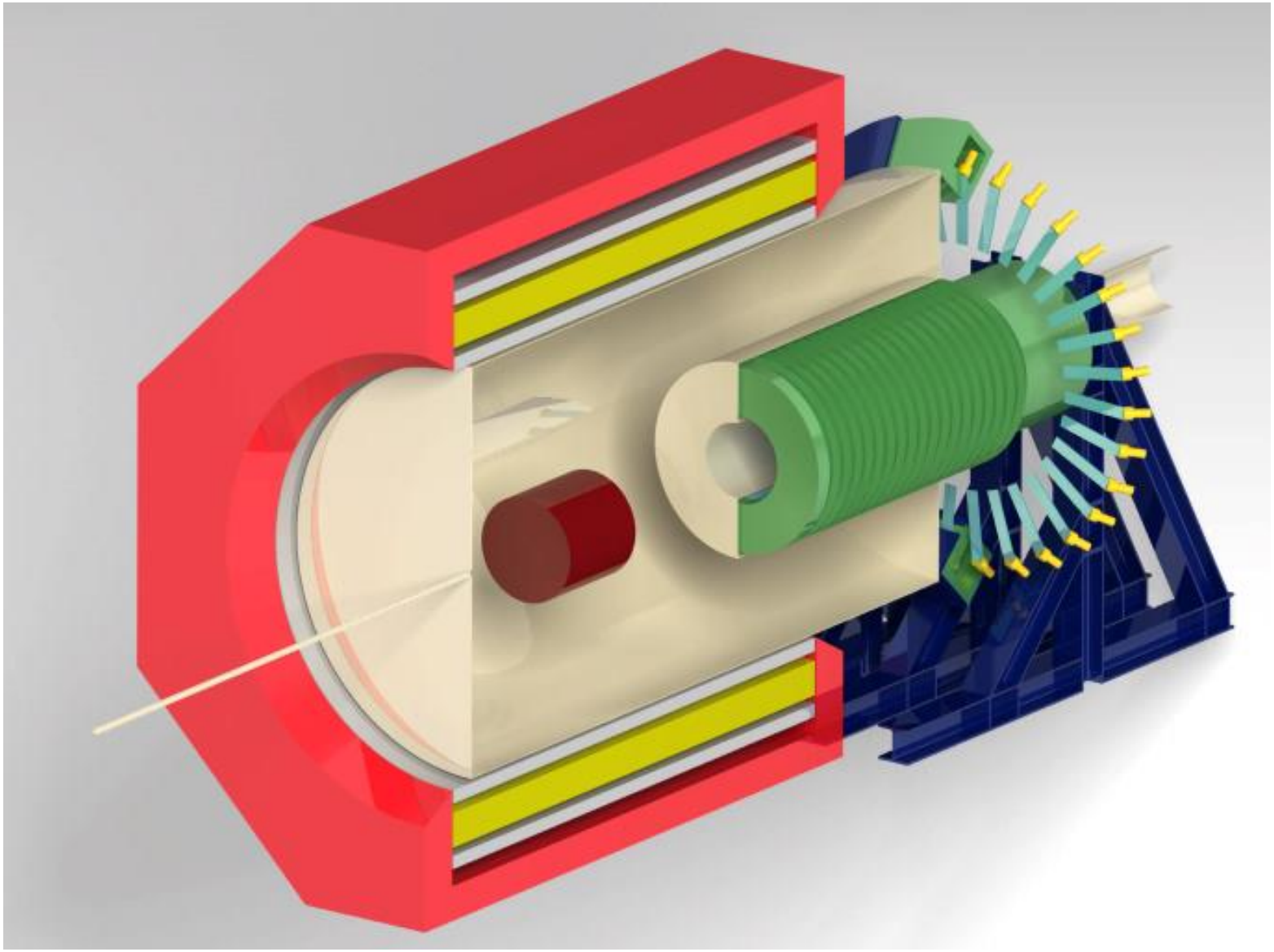

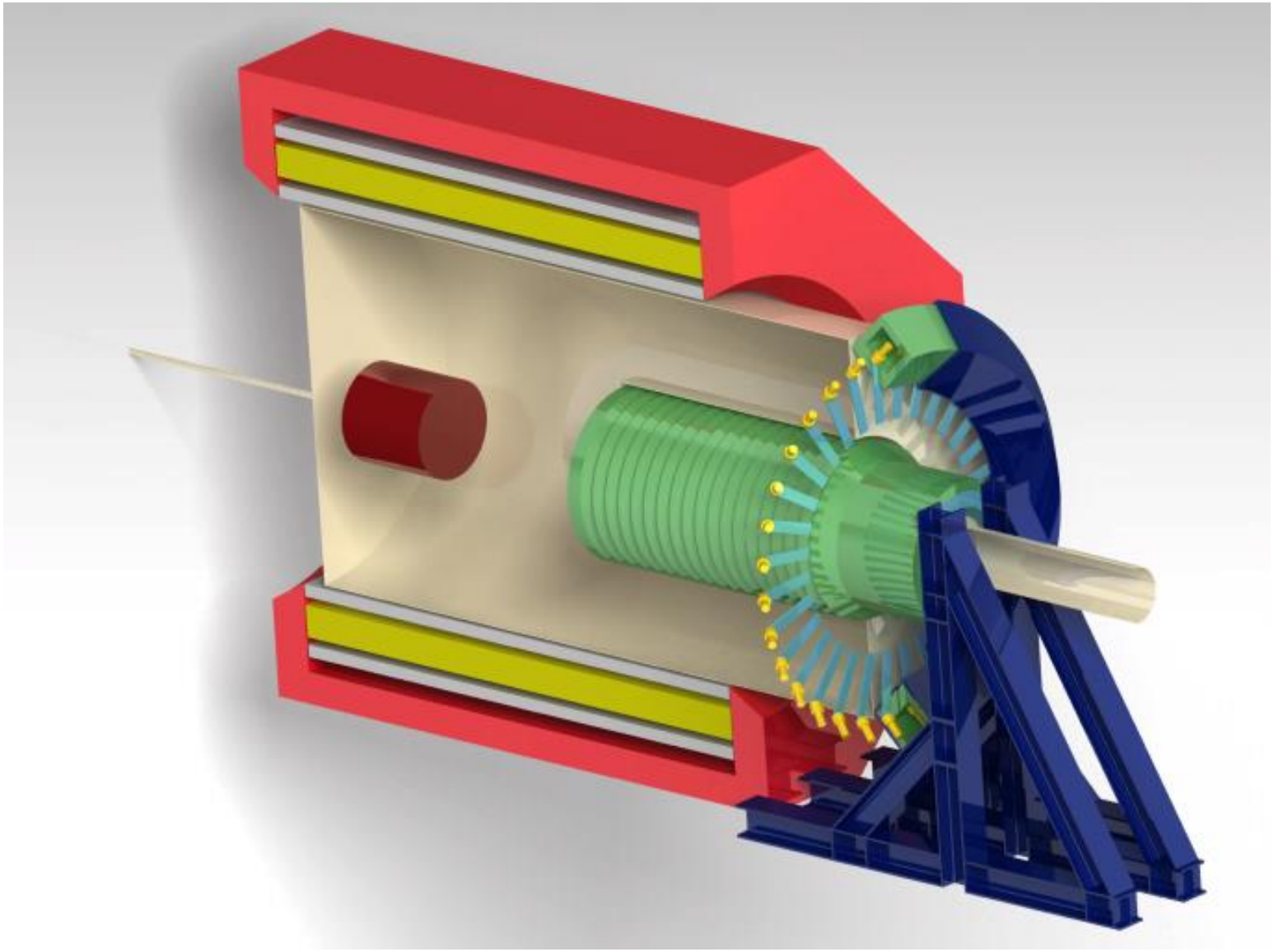

Solenoid

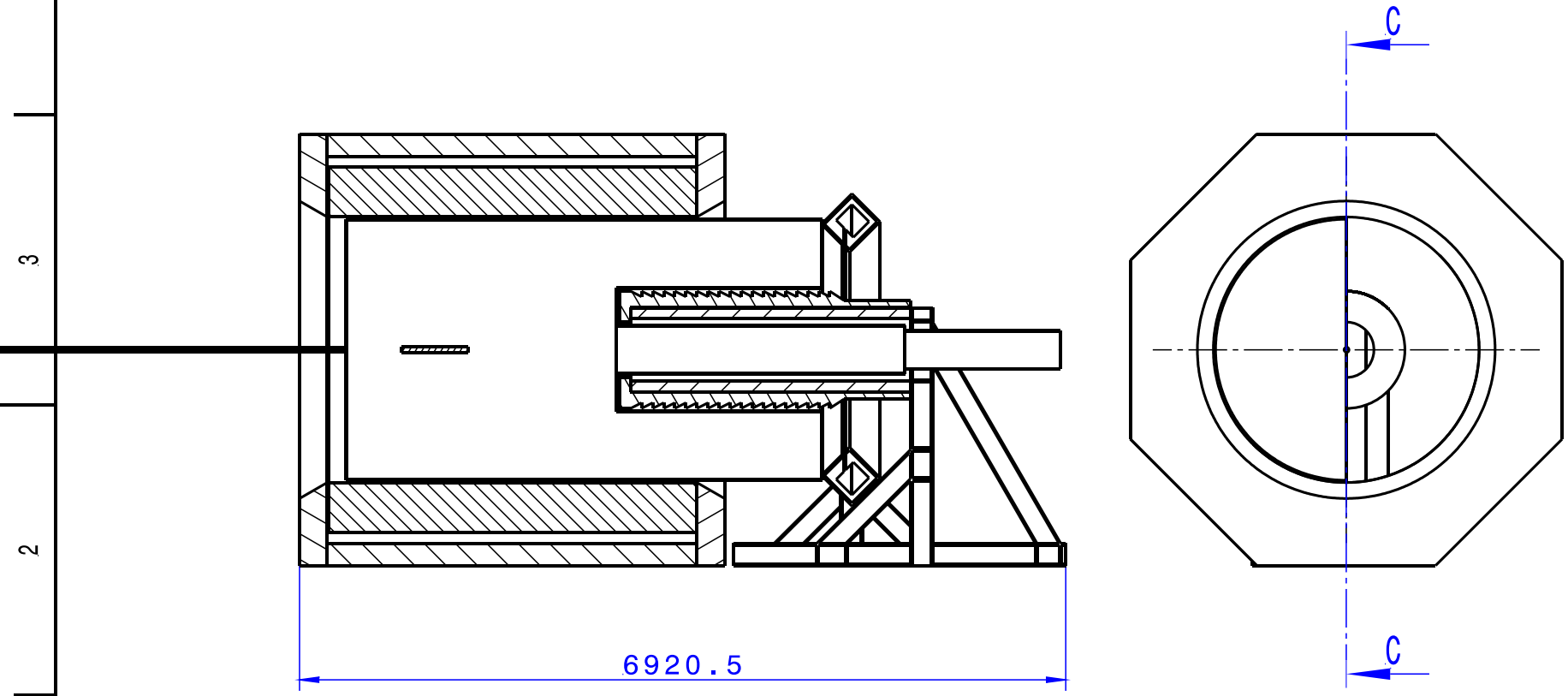

Assembly
1:50

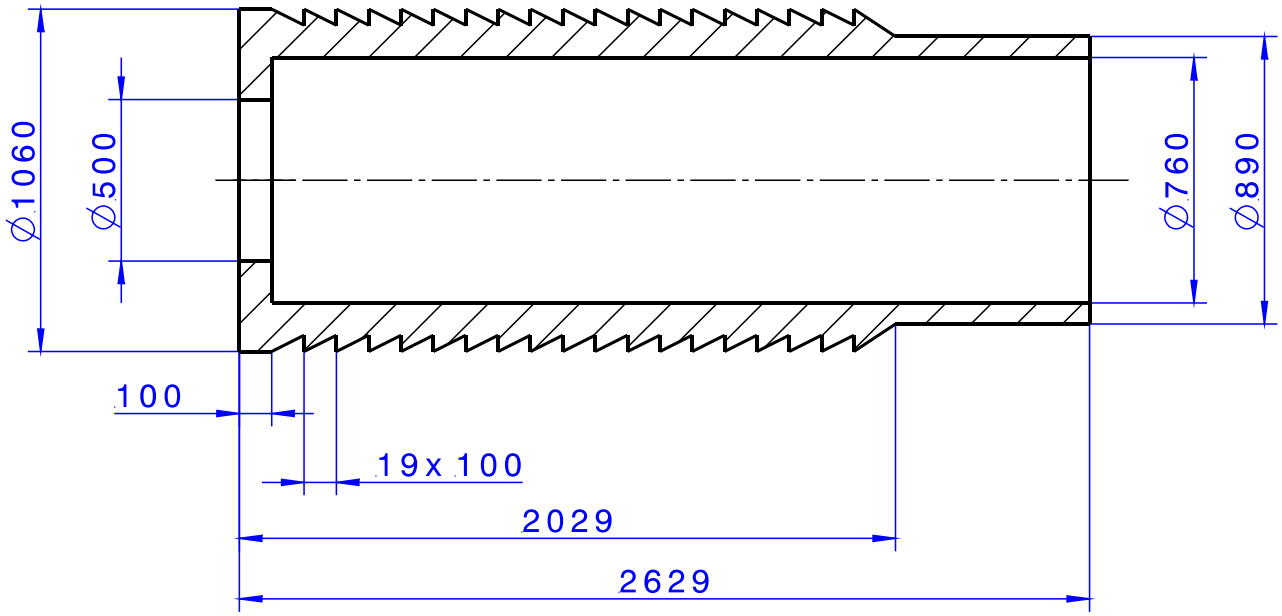

Barrel Shielding

1:20

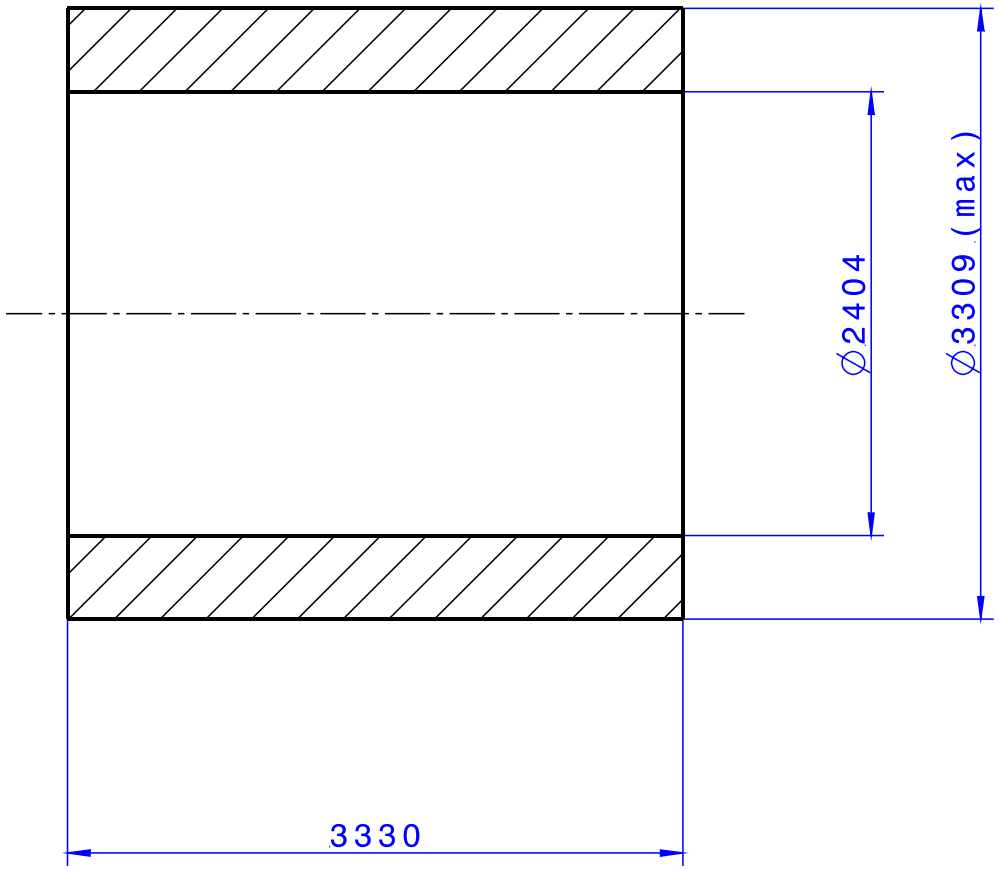

Coil
1:35

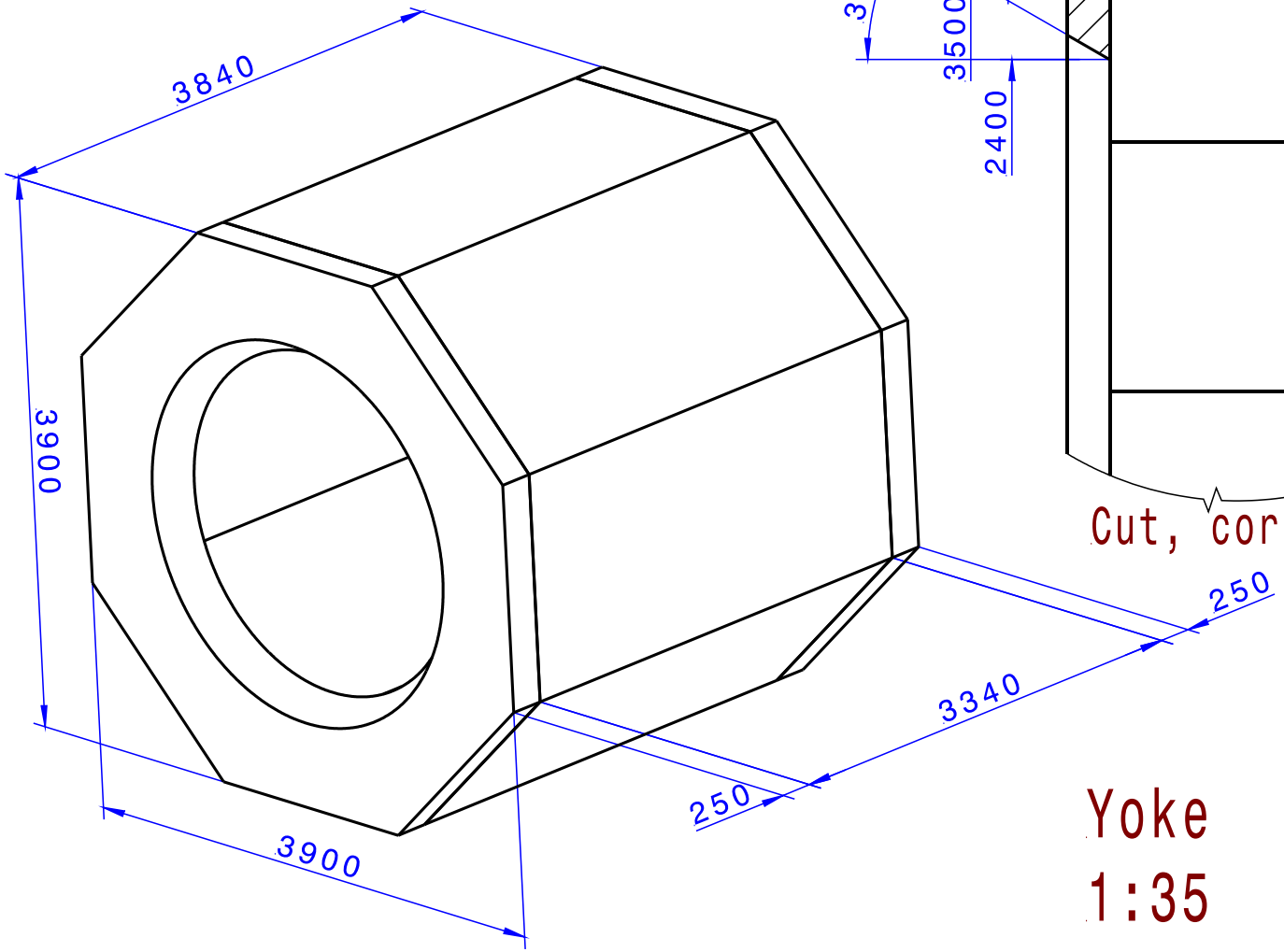

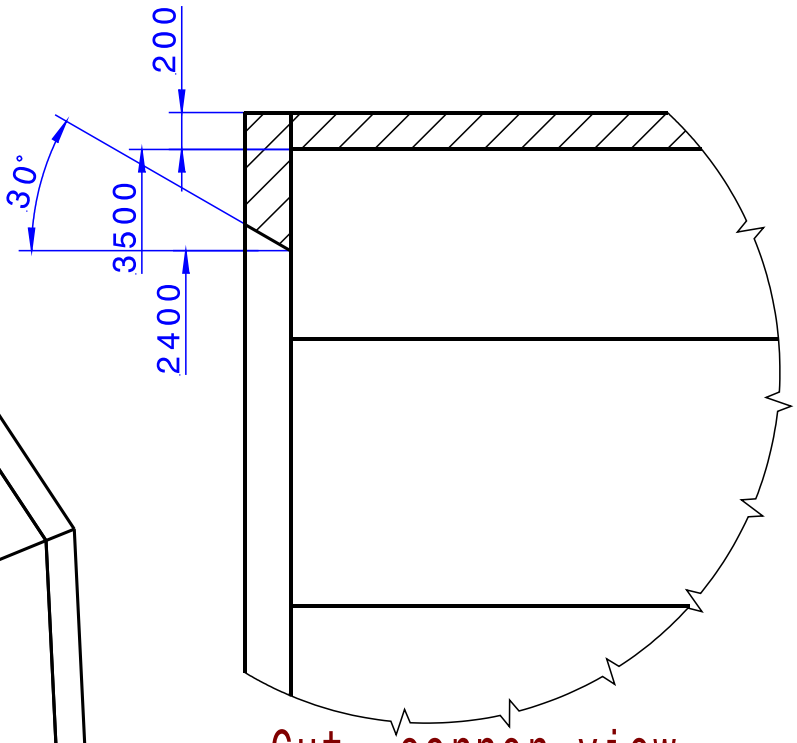

Cut, corner view

Yoke

1:35

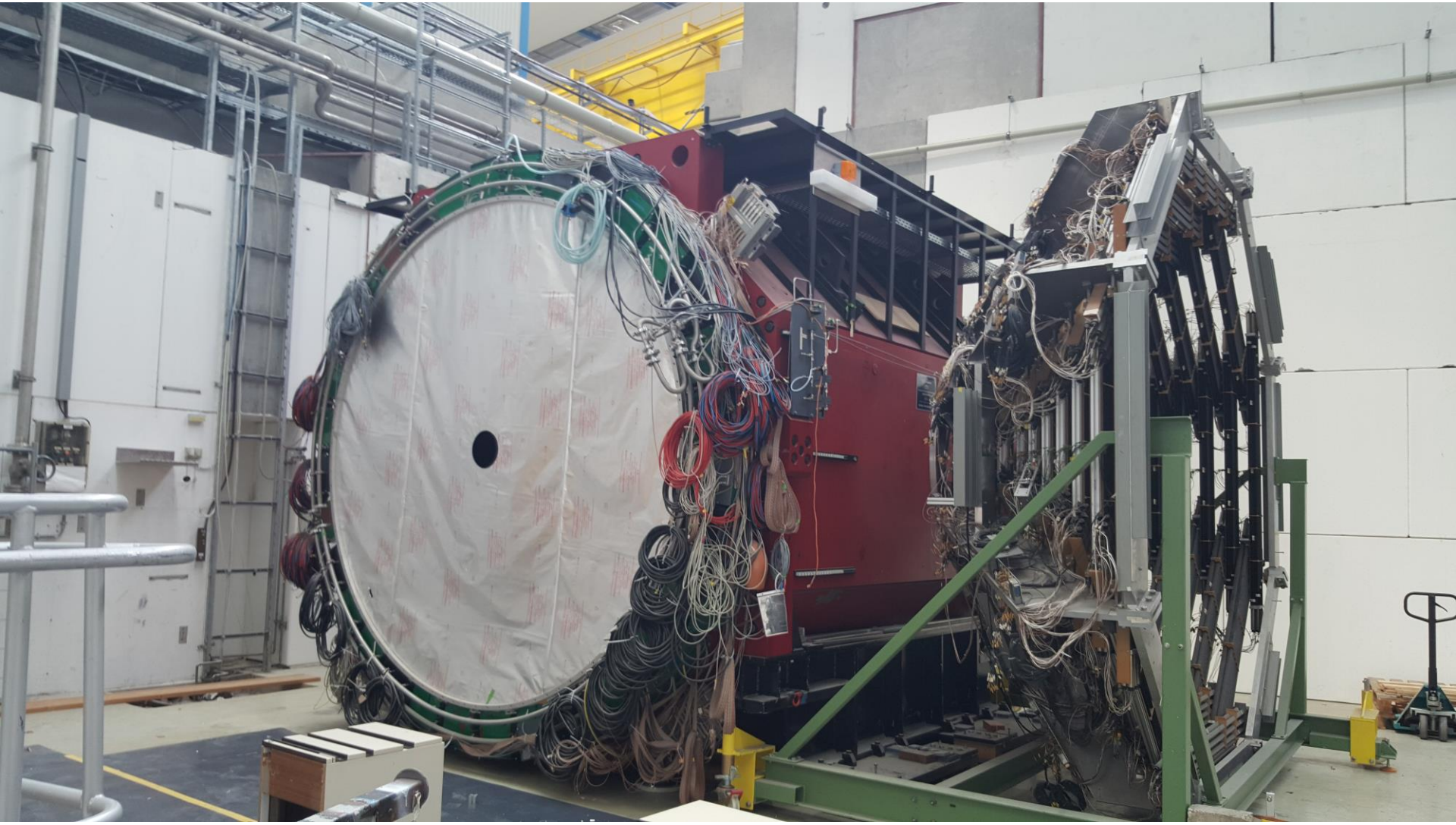

Field component along beam axis

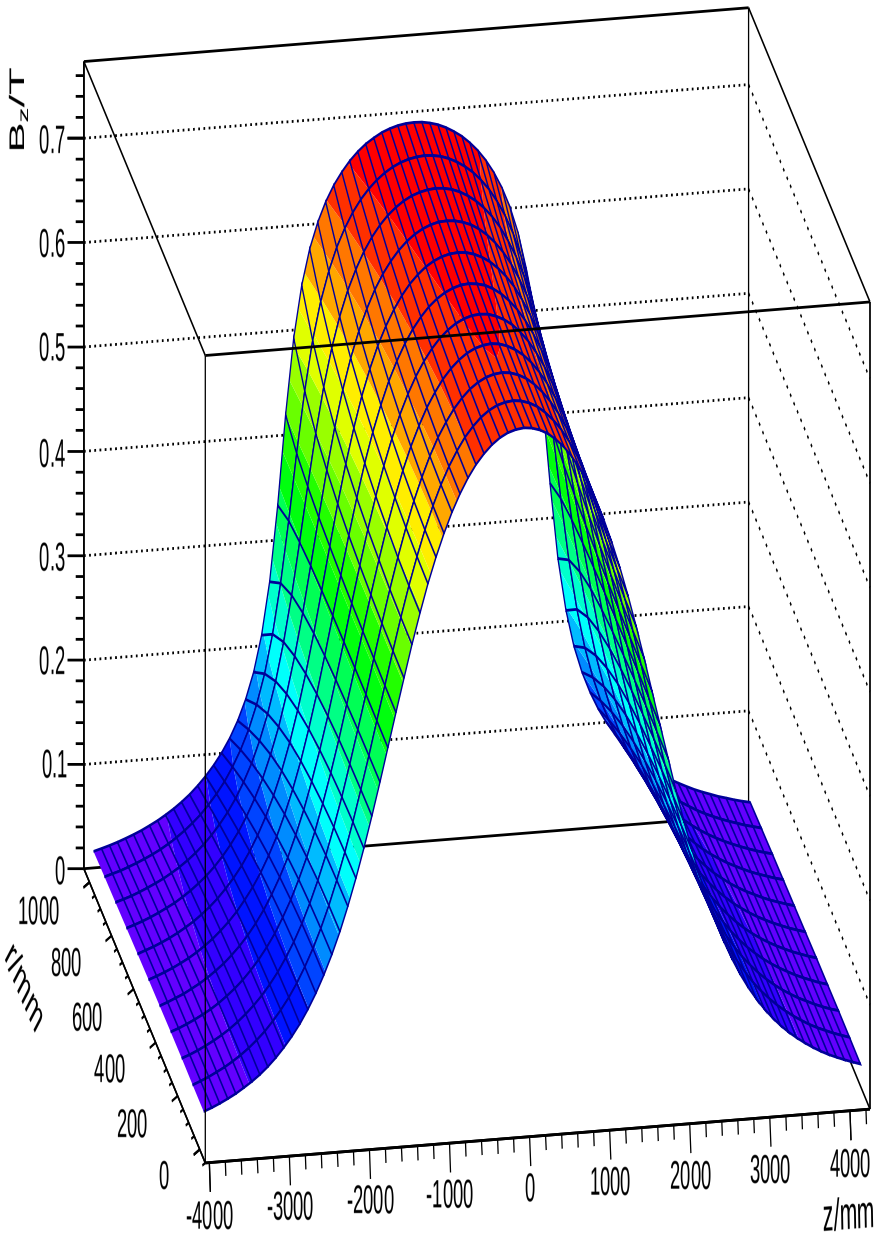

Radial field component

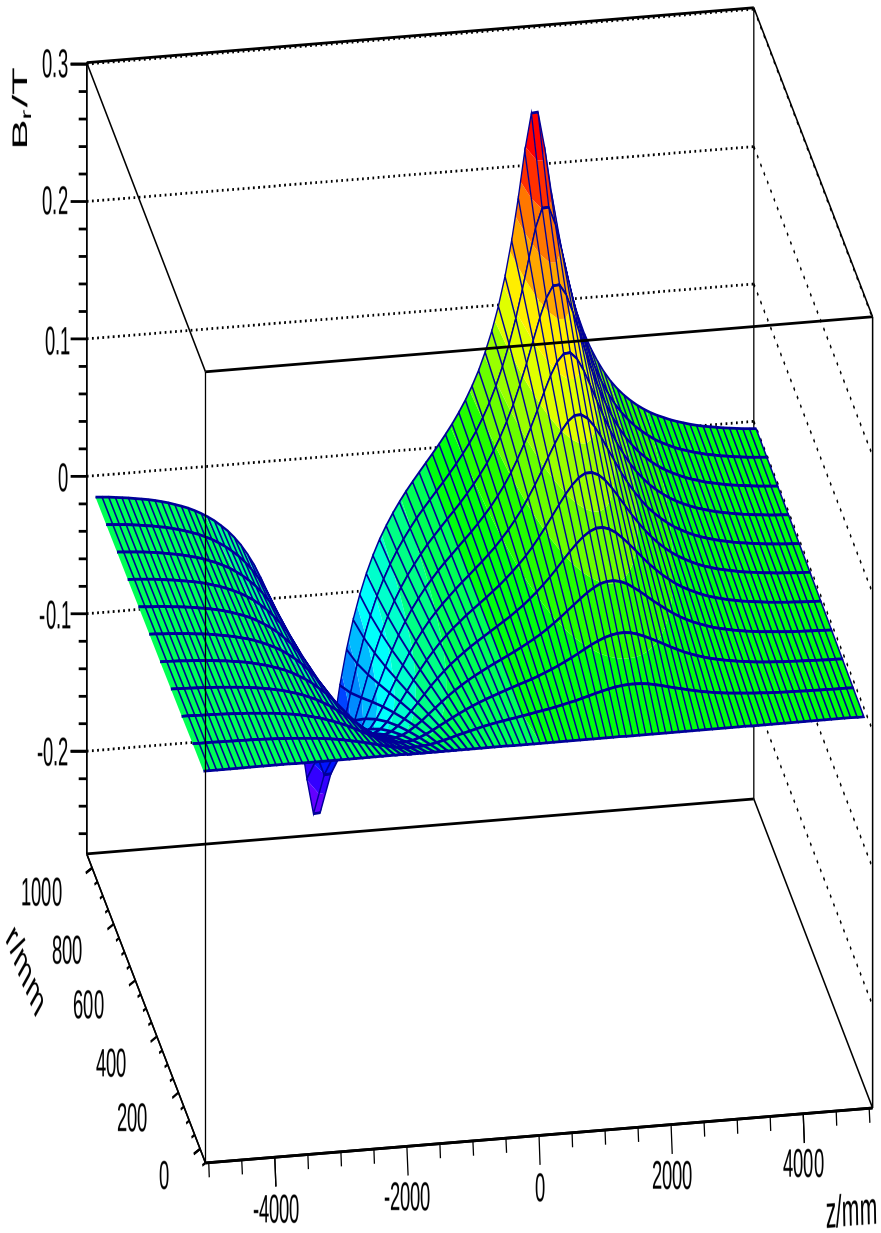

PMT position

PMTs far fr

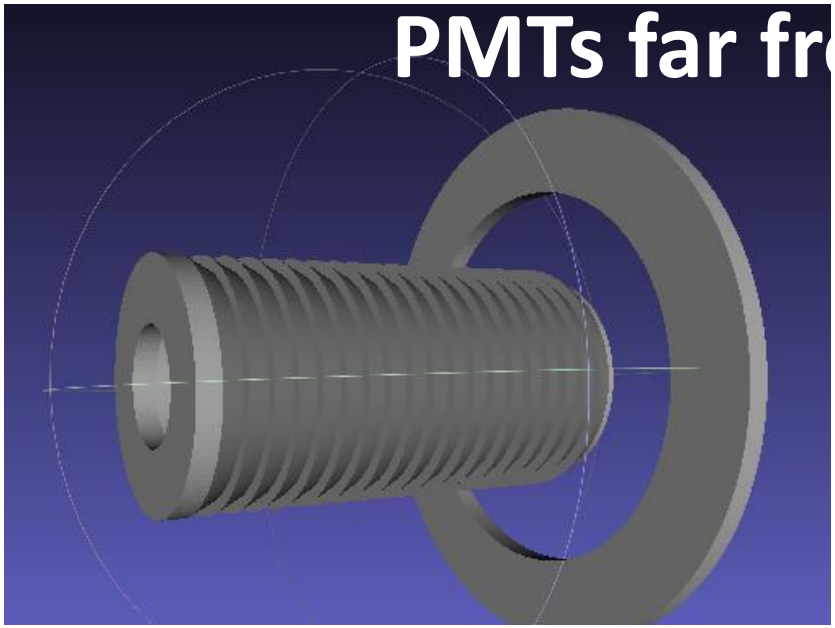

Event rate distribution @ z = 3000.00 mm

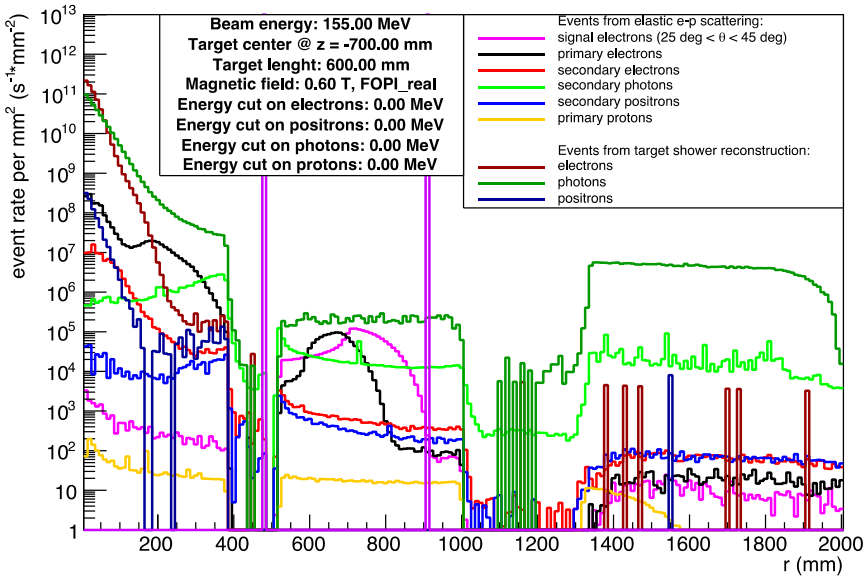

Photo electron rate distribution @ z = 3000.00 mm

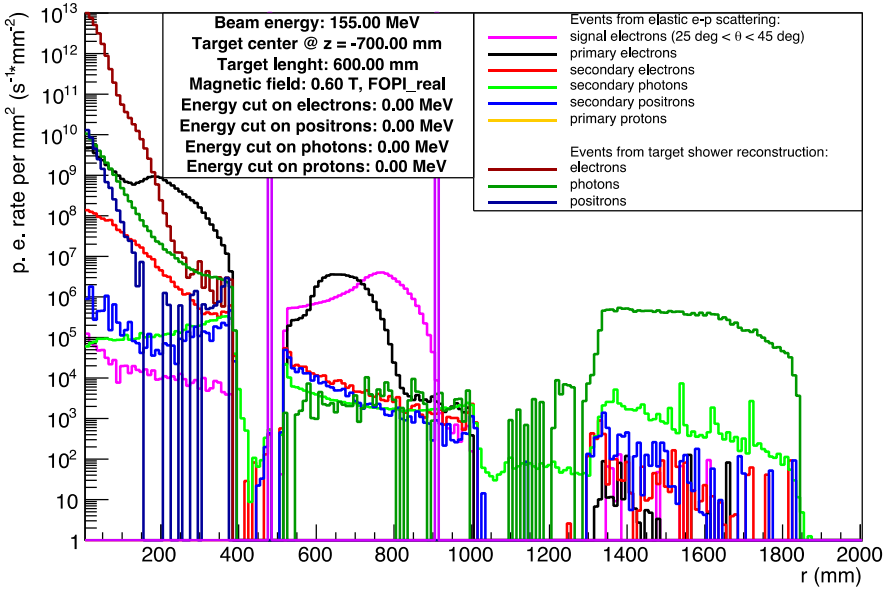

PMTs near bea

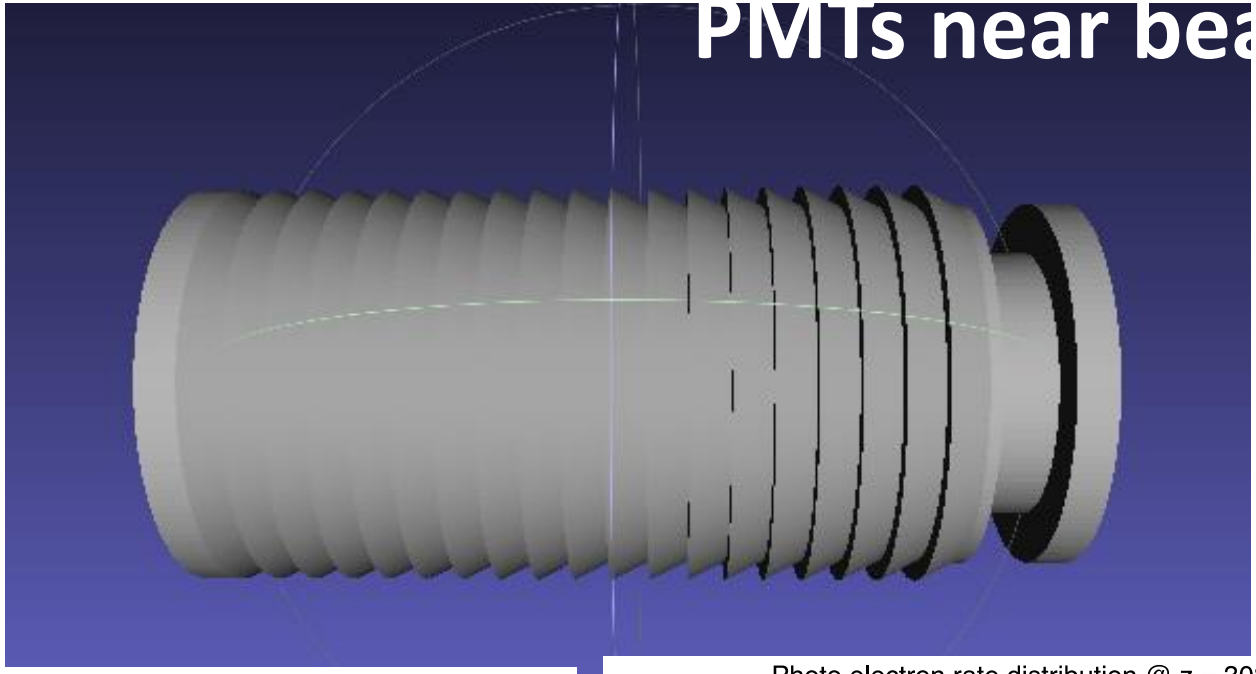

Event rate distribution @ z = 3085.00 mm

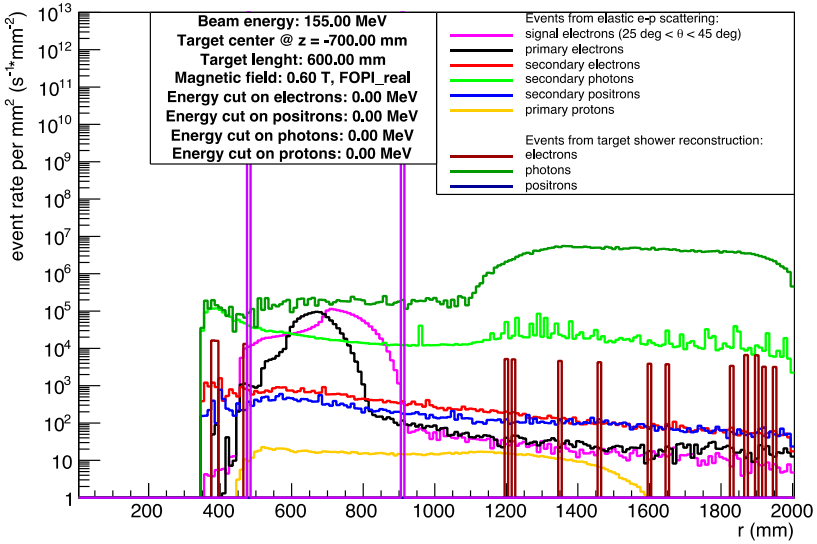

Photo electron rate distribution @ z = 3085.00 mm

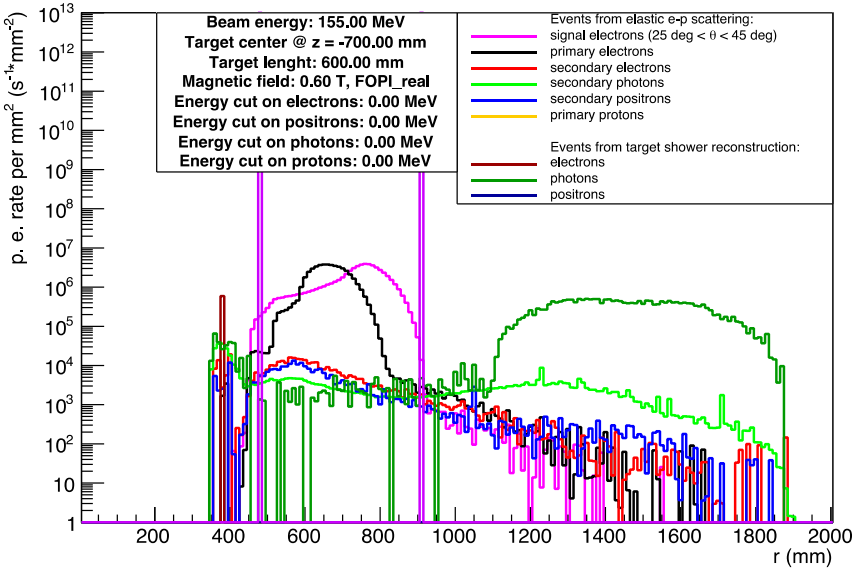

Ray traces

Raytrace simulations in the magnetic field

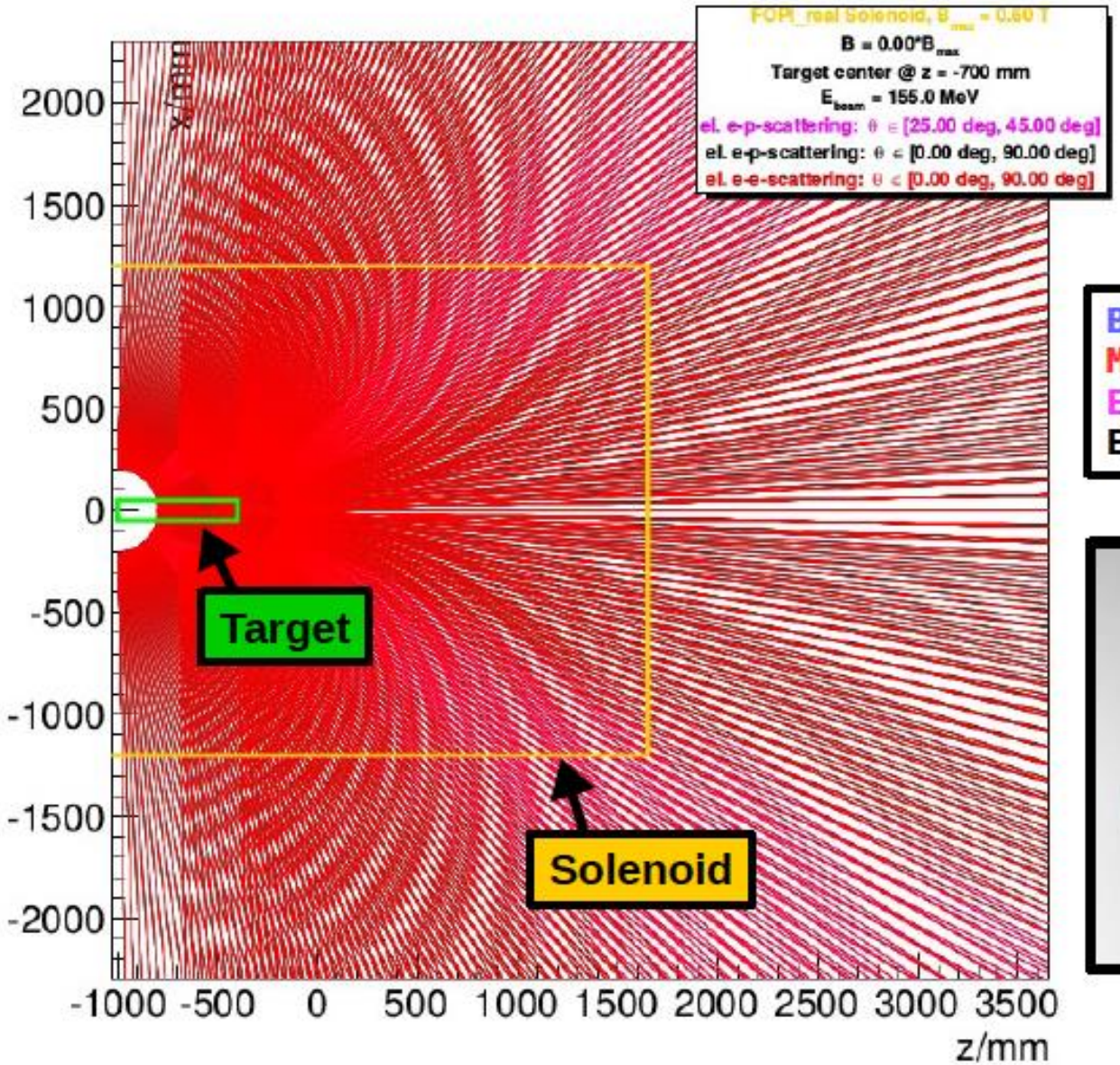

Magnetic field:
OFF

Beam energy = 155 MeV
Moller, θ ∈ [0°, 90°]
Elastic e-p, θ ∈ [25°, 45°]
Elastic e-p, θ ∈ [0°, 90°]

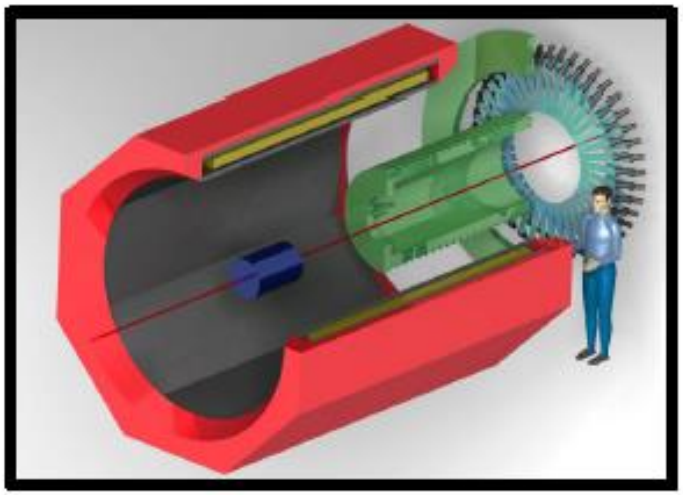

Raytrace simulations in the magnetic field

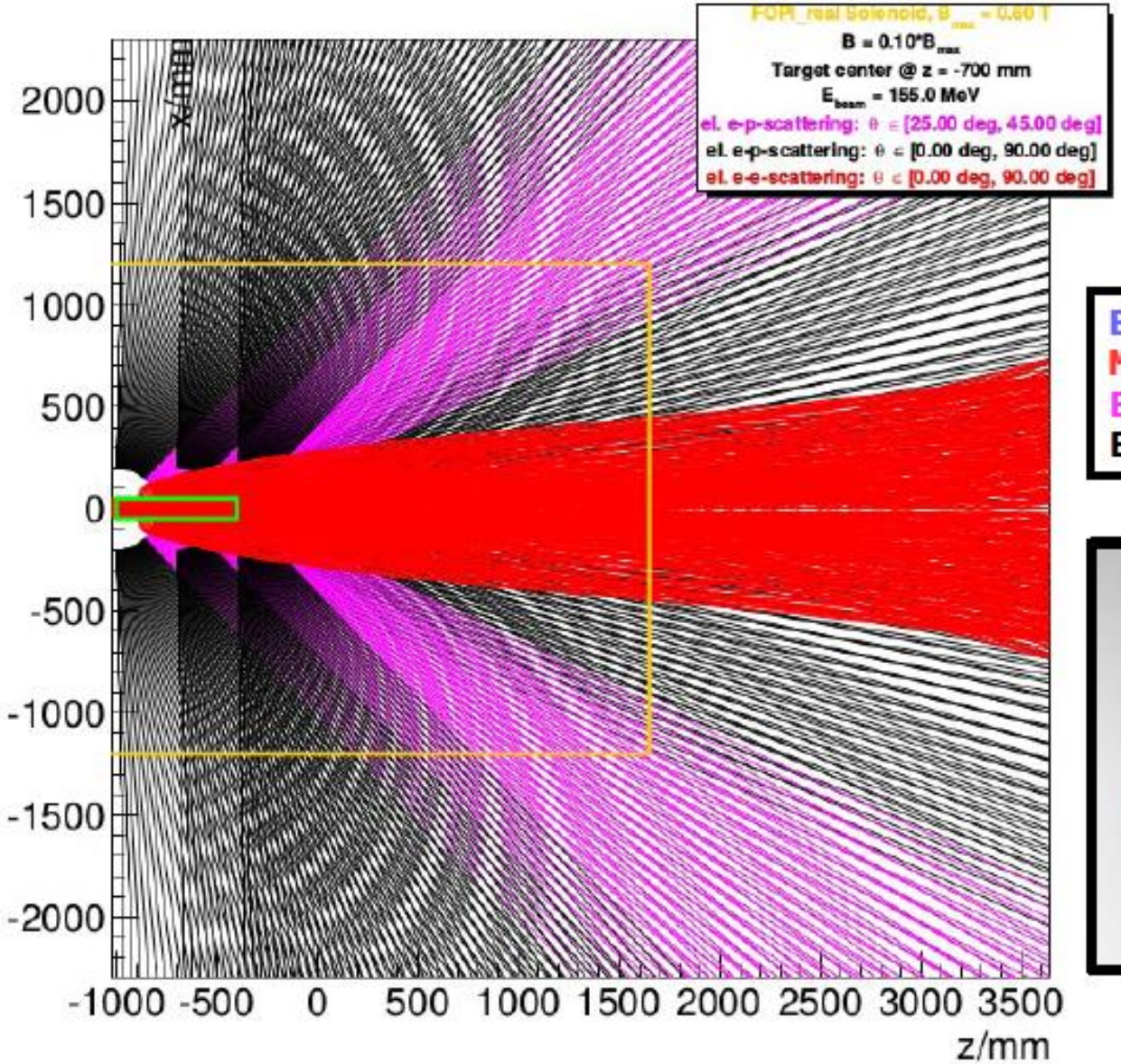

Magnetic field:
0.06 T

Beam energy = 155 MeV
Moller, θ ∈ [0°, 90°]
Elastic e-p, θ ∈ [25°, 45°]
Elastic e-p, θ ∈ [0°, 90°]

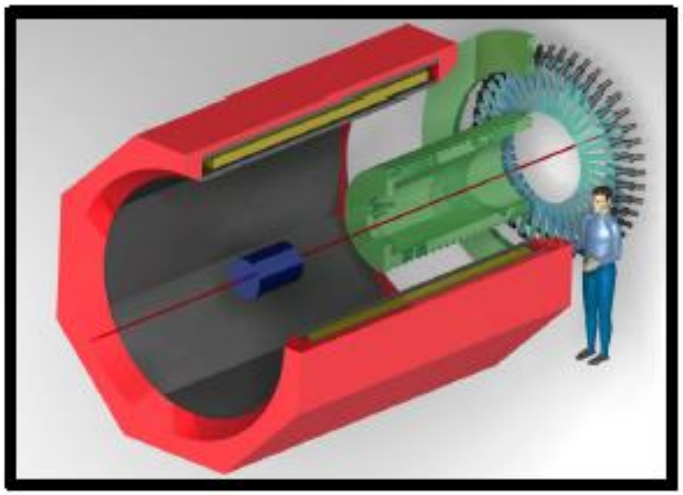

Raytrace simulations in the magnetic field

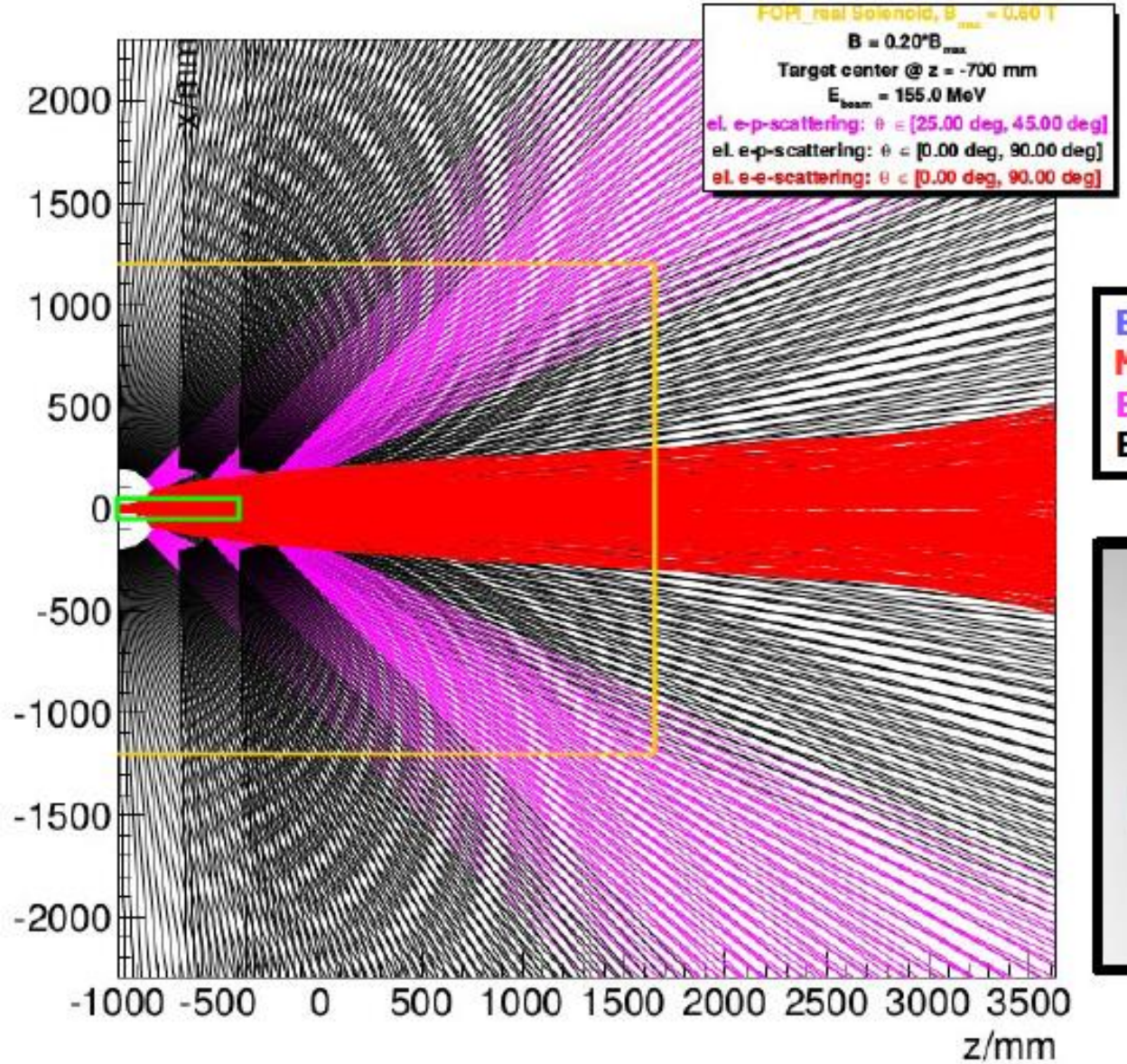

Magnetic field:
0.12 T

Beam energy = 155 MeV
Moller, θ ∈ [0°, 90°]
Elastic e-p, θ ∈ [25°, 45°]
Elastic e-p, θ ∈ [0°, 90°]

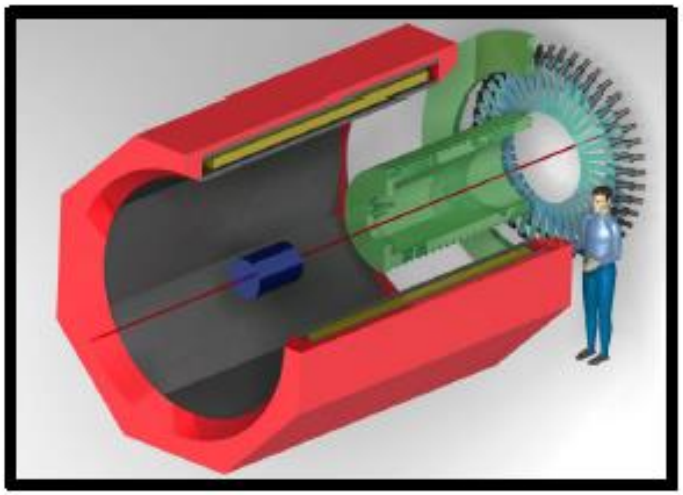

Raytrace simulations in the magnetic field

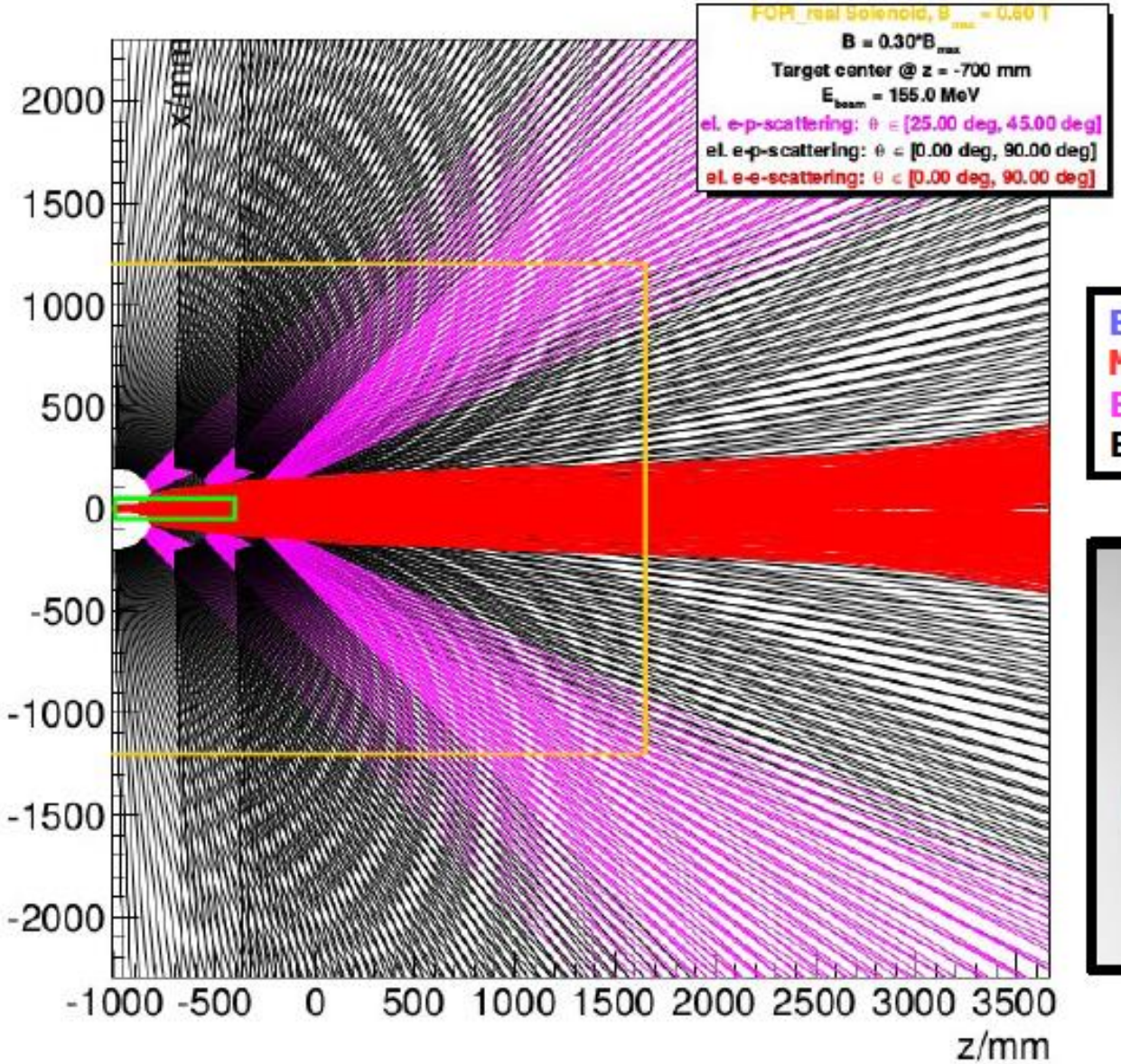

Magnetic field:
0.18 T

Beam energy = 155 MeV
Moller, θ ∈ [0°, 90°]
Elastic e-p, θ ∈ [25°, 45°]
Elastic e-p, θ ∈ [0°, 90°]

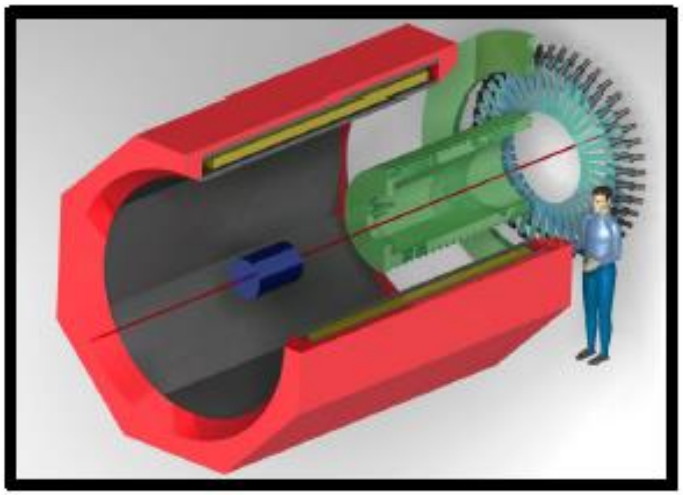

Raytrace simulations in the magnetic field

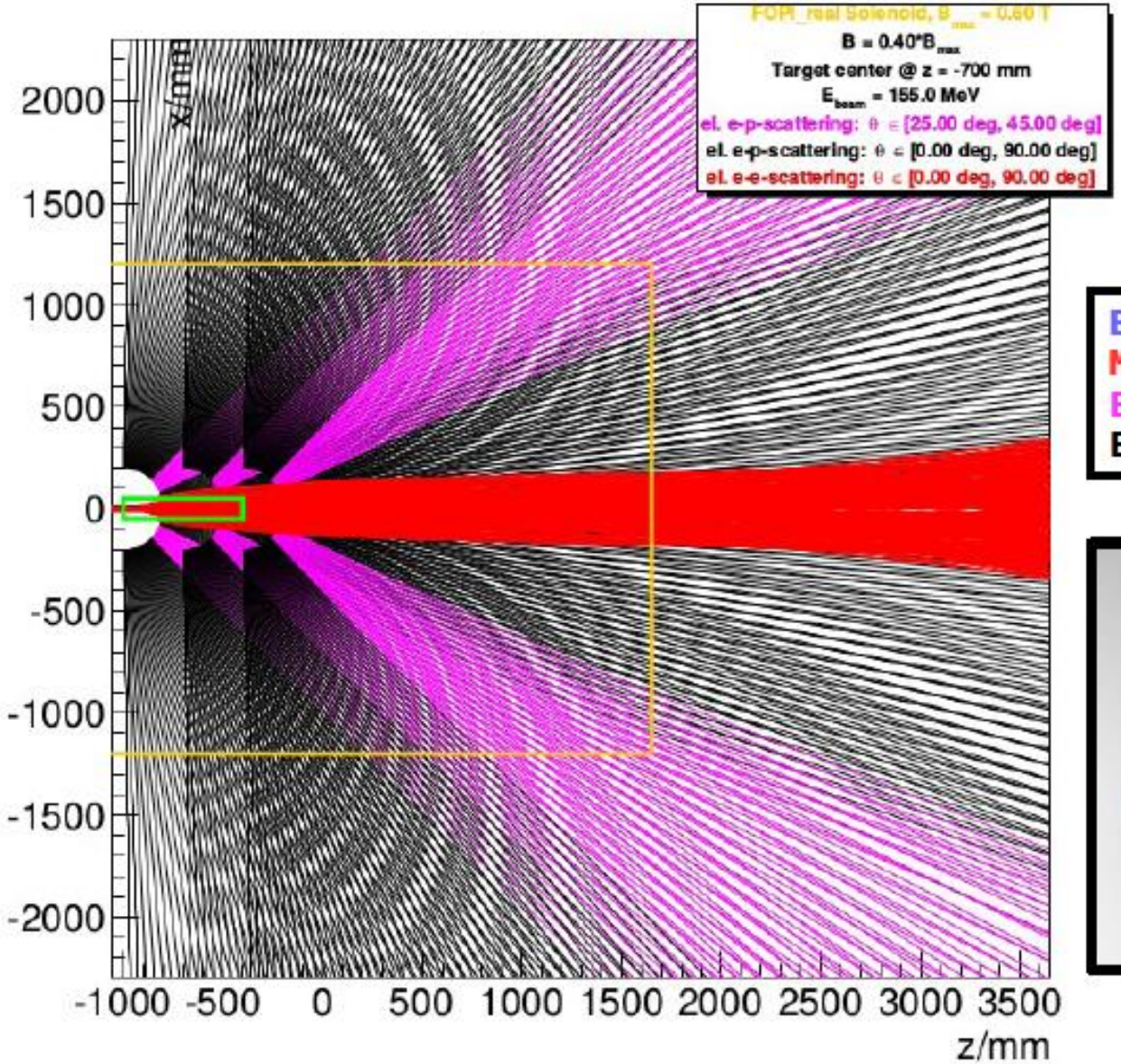

Magnetic field:
0.24 T

Beam energy = 155 MeV
Moller, θ ∈ [0°, 90°]
Elastic e-p, θ ∈ [25°, 45°]
Elastic e-p, θ ∈ [0°, 90°]

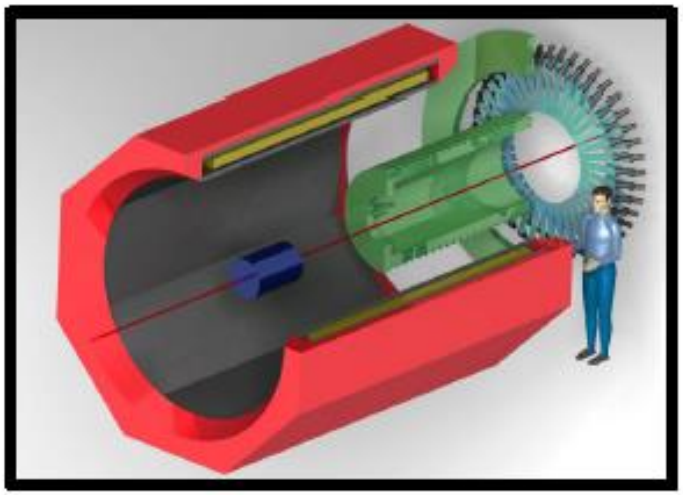

Raytrace simulations in the magnetic field

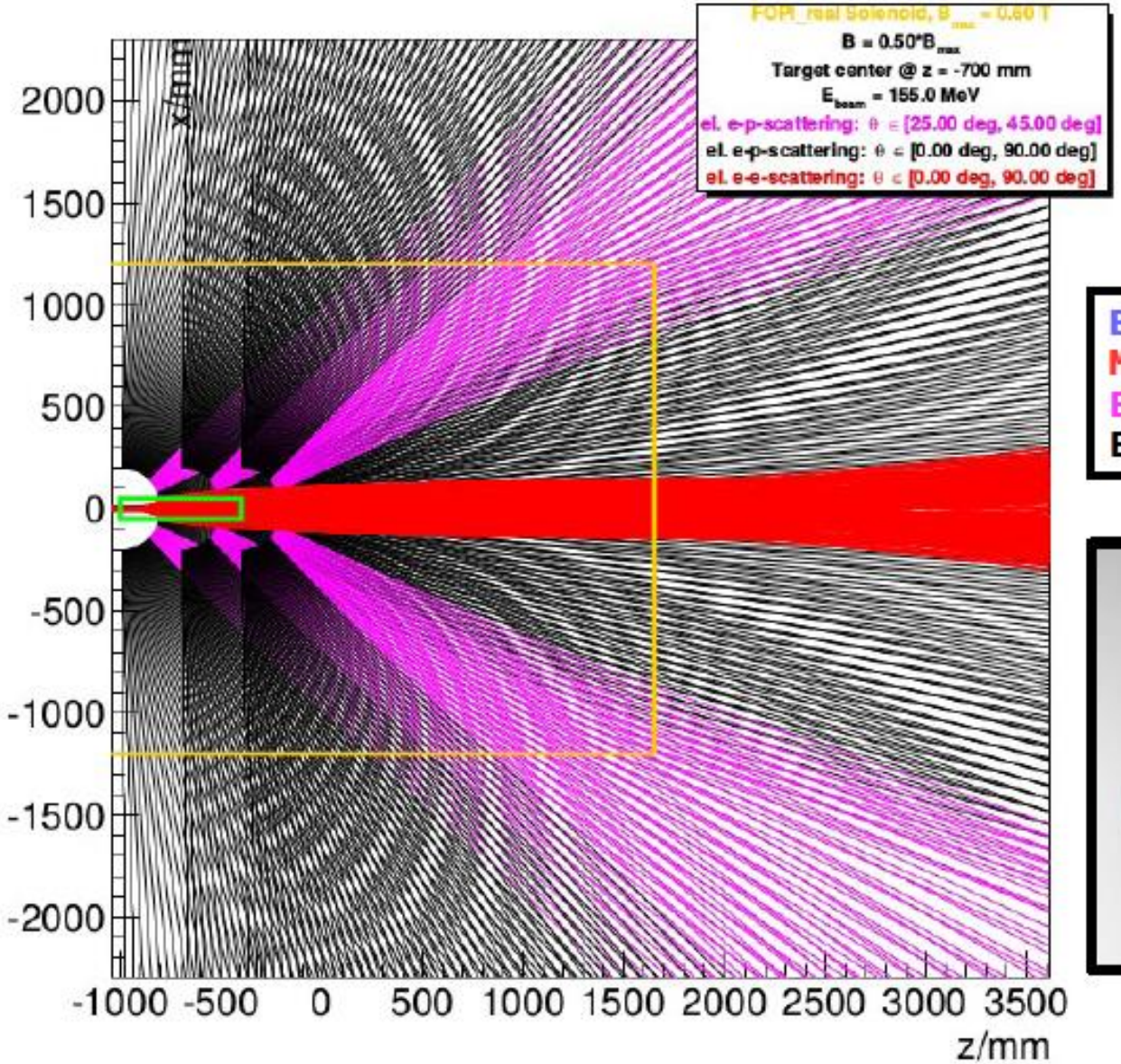

Magnetic field:
0.3 T

Beam energy = 155 MeV
Moller, θ ∈ [0°, 90°]
Elastic e-p, θ ∈ [25°, 45°]
Elastic e-p, θ ∈ [0°, 90°]

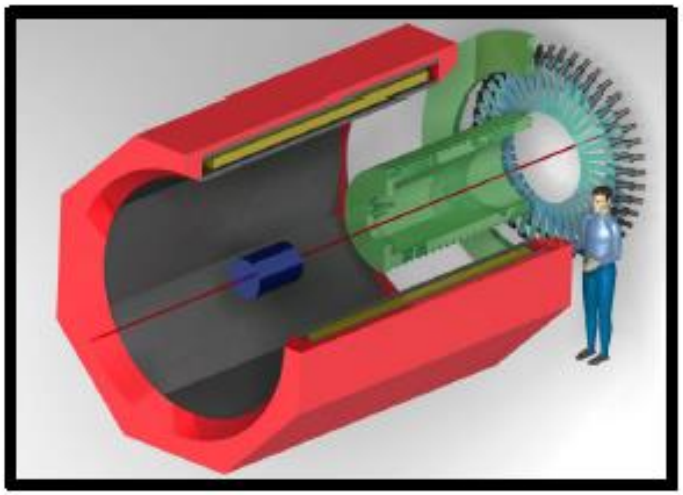

Raytrace simulations in the magnetic field

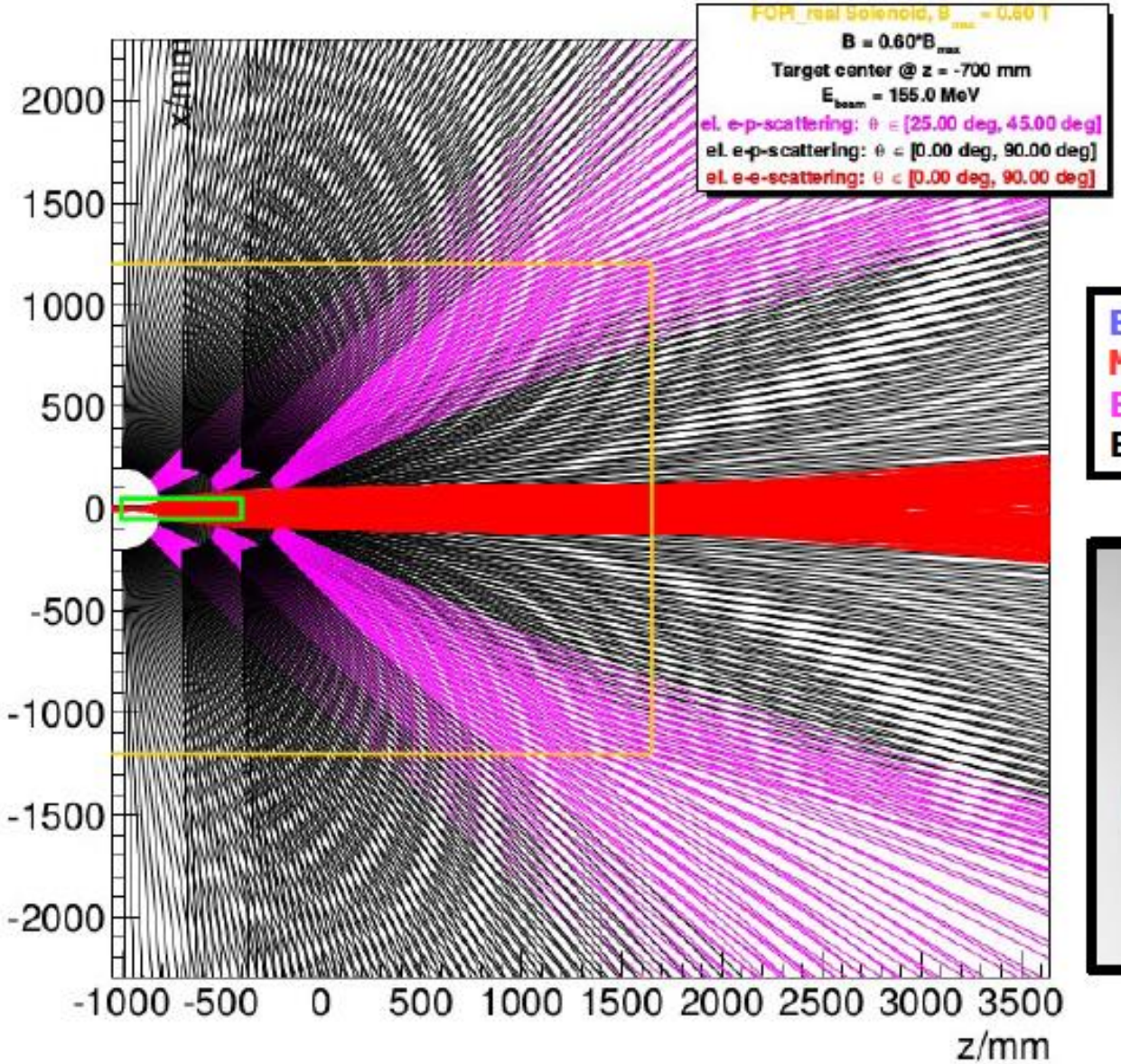

Magnetic field:
0.36 T

Beam energy = 155 MeV
Moller, θ ∈ [0°, 90°]
Elastic e-p, θ ∈ [25°, 45°]
Elastic e-p, θ ∈ [0°, 90°]

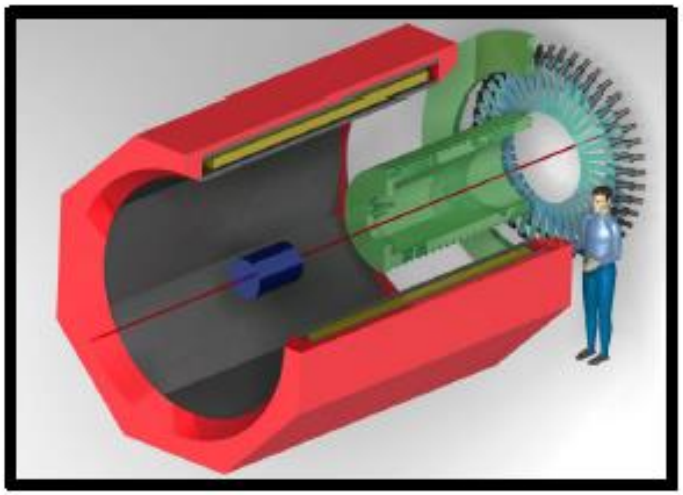

Raytrace simulations in the magnetic field

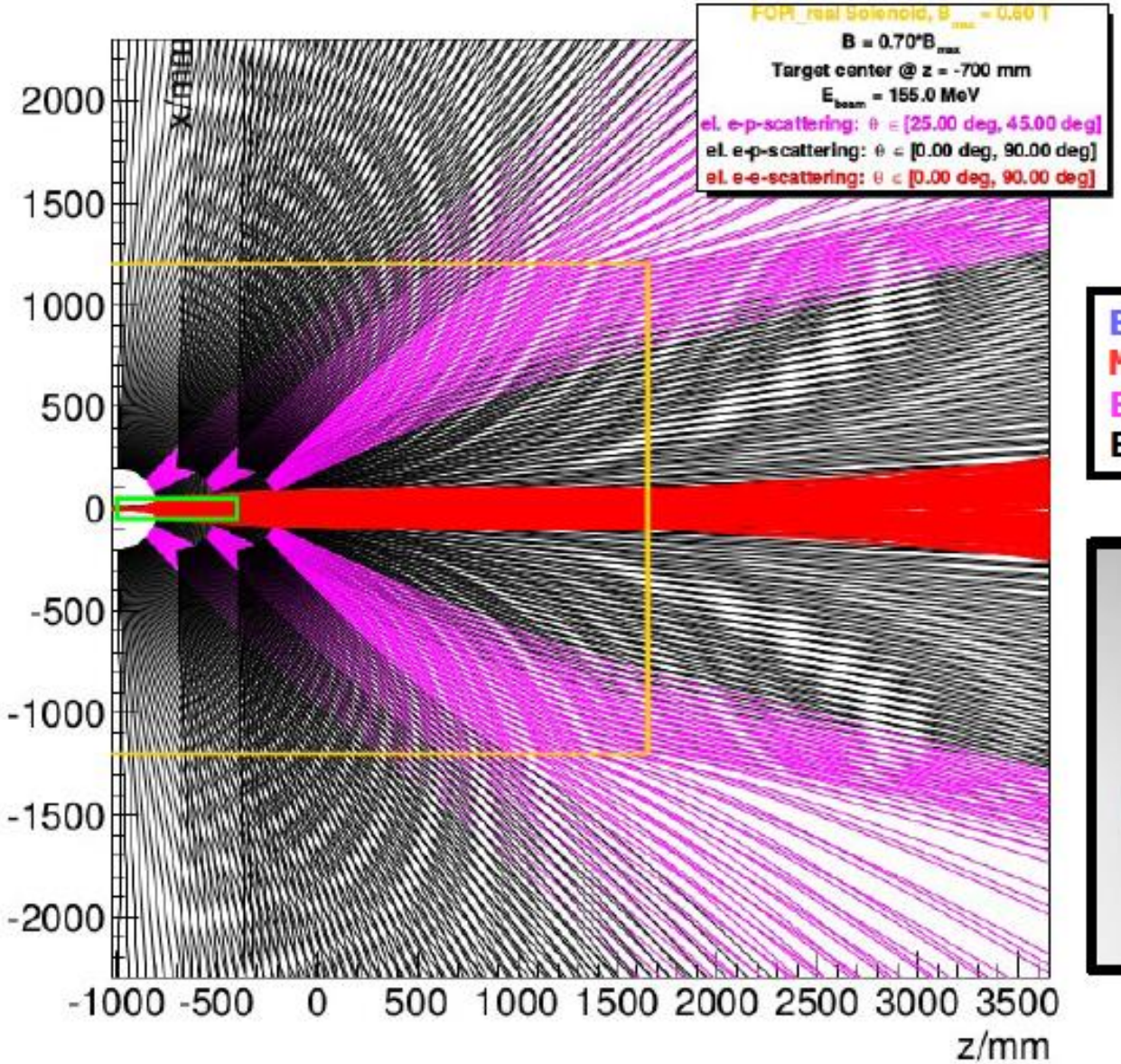

Magnetic field:
0.42 T

Beam energy = 155 MeV
Moller, θ ∈ [0°, 90°]
Elastic e-p, θ ∈ [25°, 45°]
Elastic e-p, θ ∈ [0°, 90°]

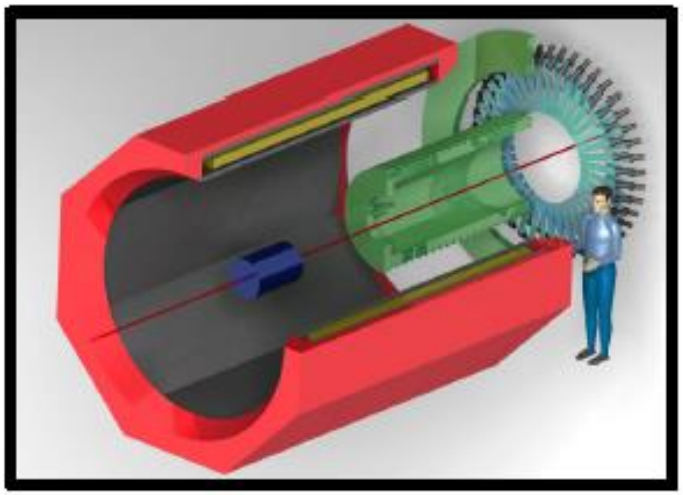

Raytrace simulations in the magnetic field

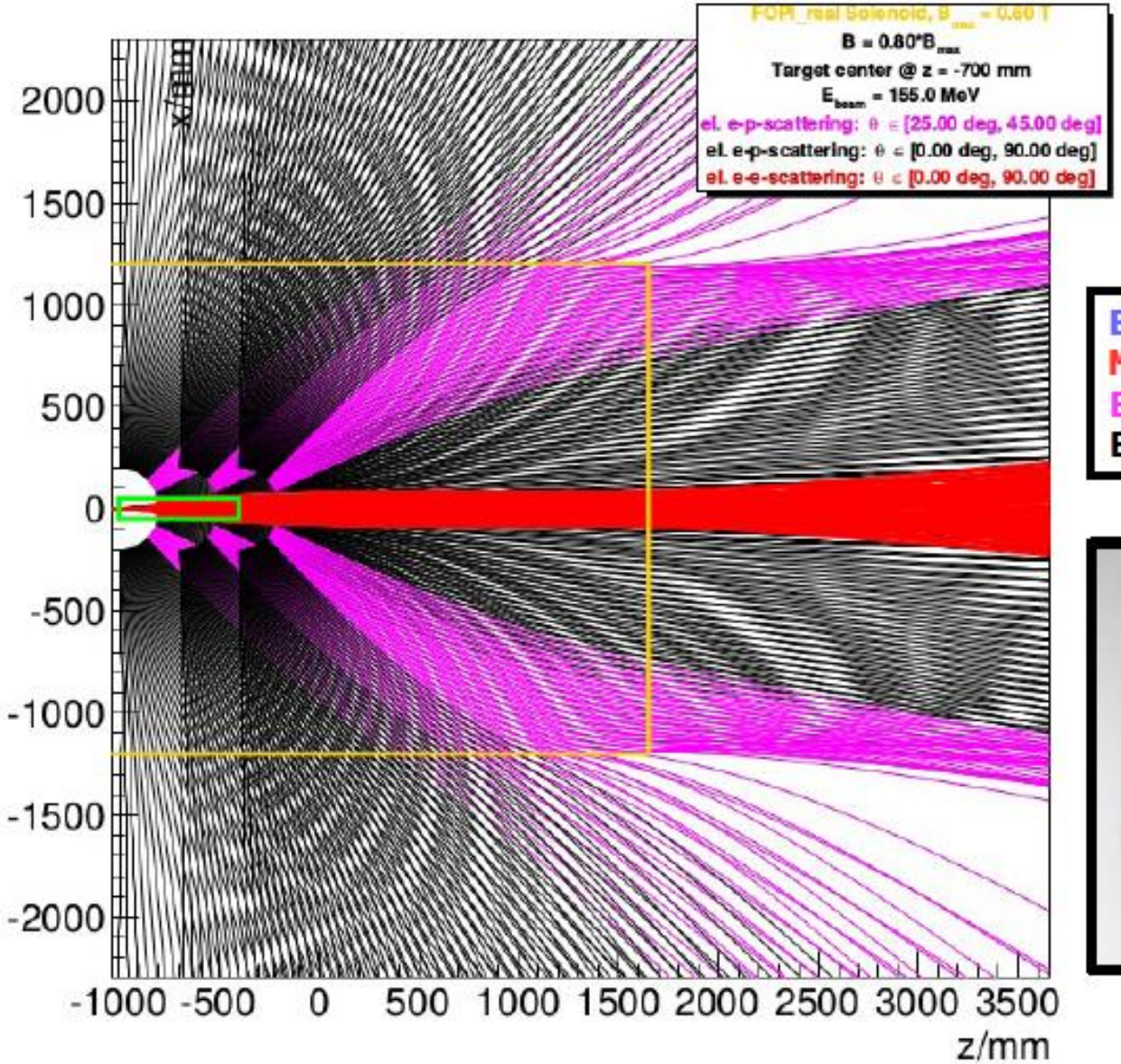

Magnetic field:
0.48 T

Beam energy = 155 MeV
Moller, θ ϵ [0°, 90°]
Elastic e-p, θ ϵ [25°, 45°]
Elastic e-p, θ ϵ [0°, 90°]

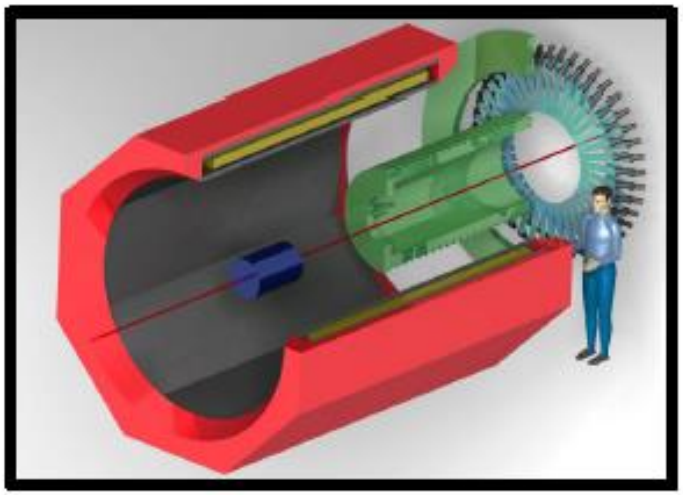

Raytrace simulations in the magnetic field

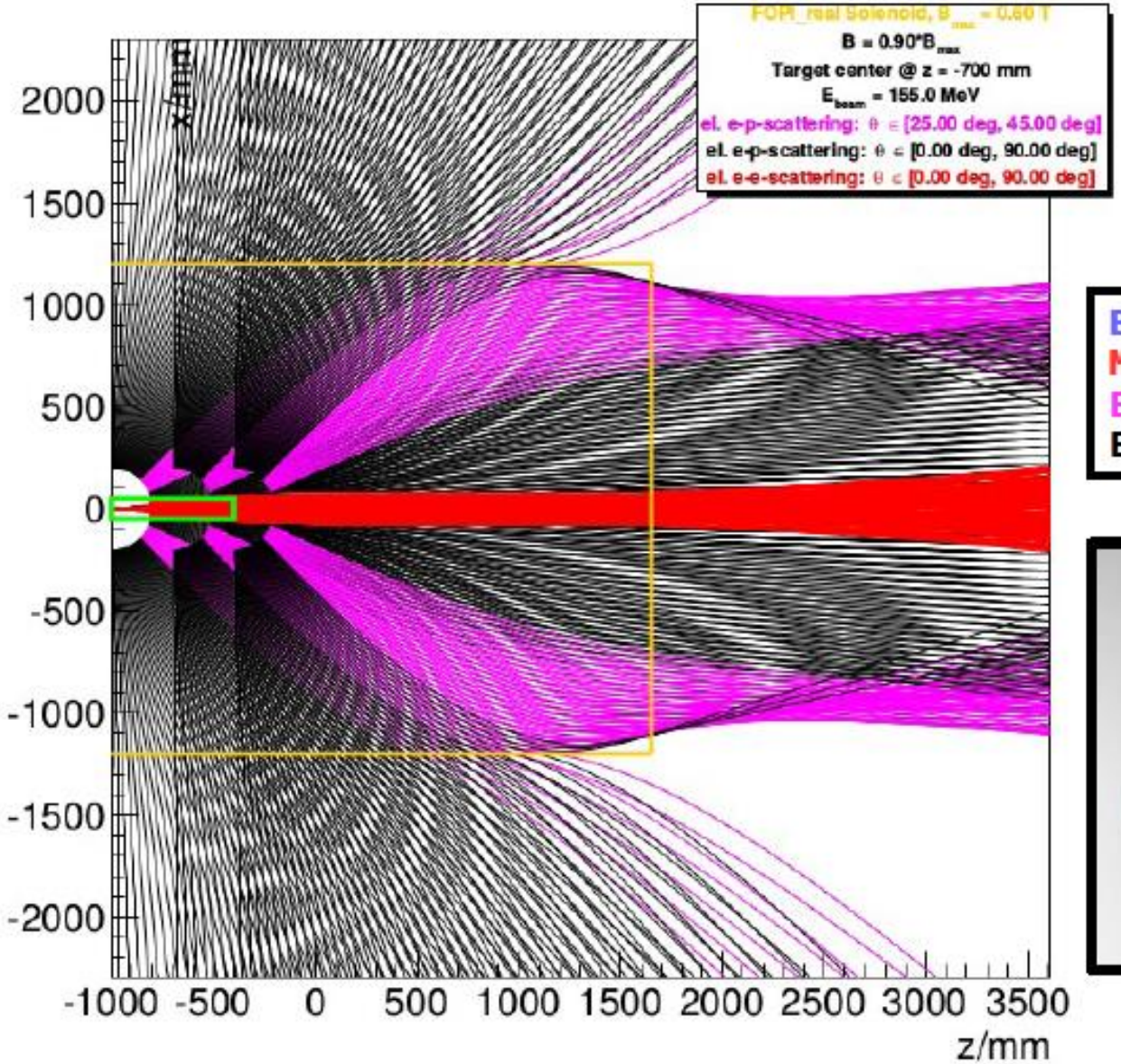

Magnetic field:
0.54 T

Beam energy = 155 MeV
Moller, θ ϵ [0°, 90°]
Elastic e-p, θ ϵ [25°, 45°]
Elastic e-p, θ ϵ [0°, 90°]

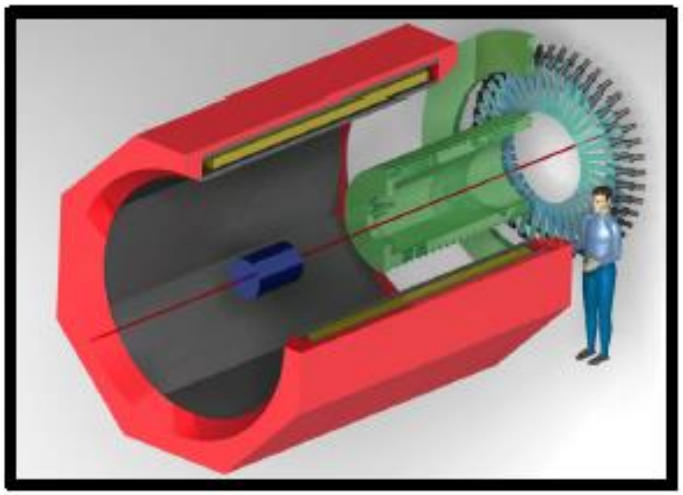

Raytrace simulations in the magnetic field

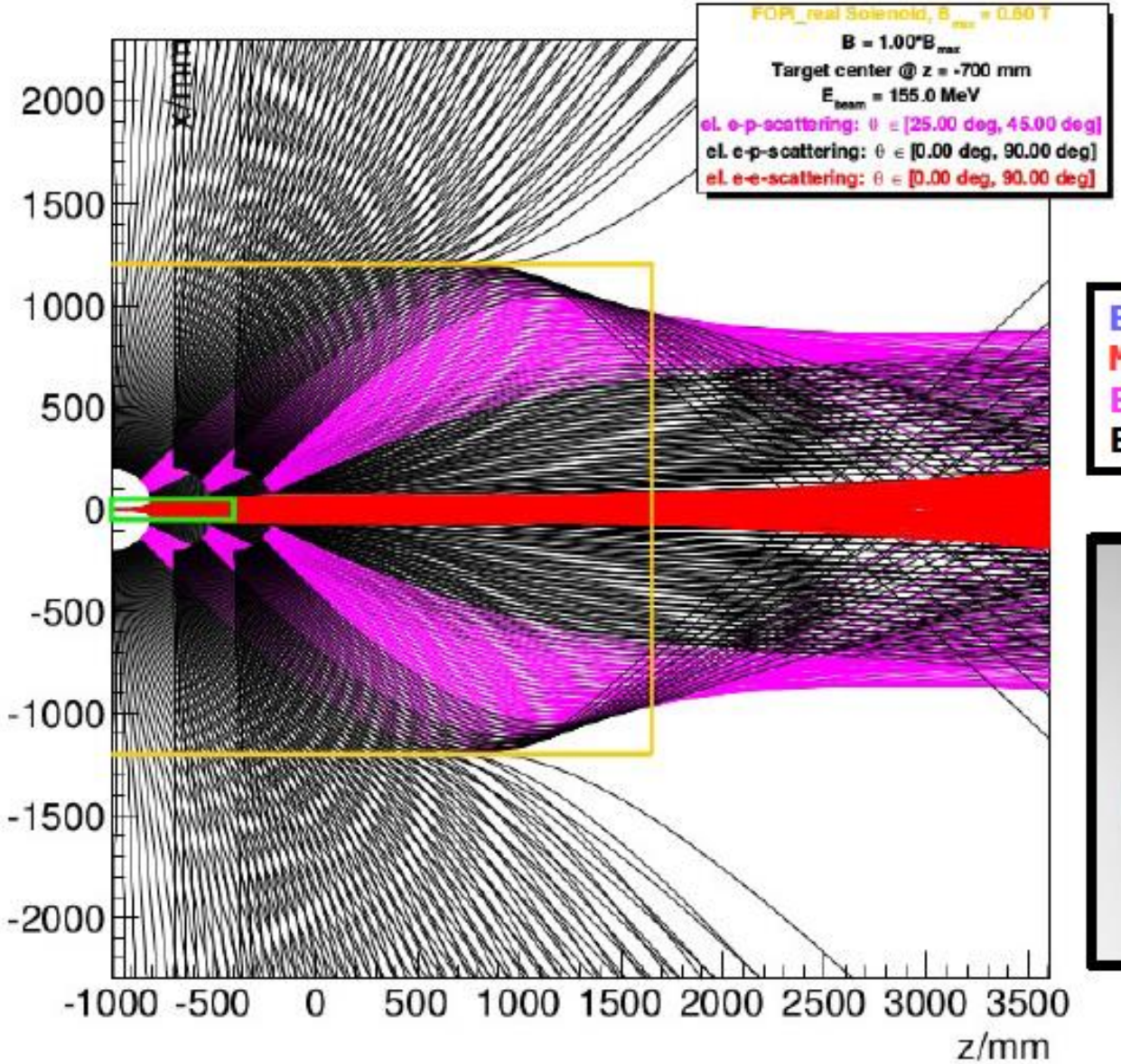

Magnetic field:
0.6 T

Beam energy = 155 MeV
Moller, θ ϵ [0°, 90°]
Elastic e-p, θ ϵ [25°, 45°]
Elastic e-p, θ ϵ [0°, 90°]

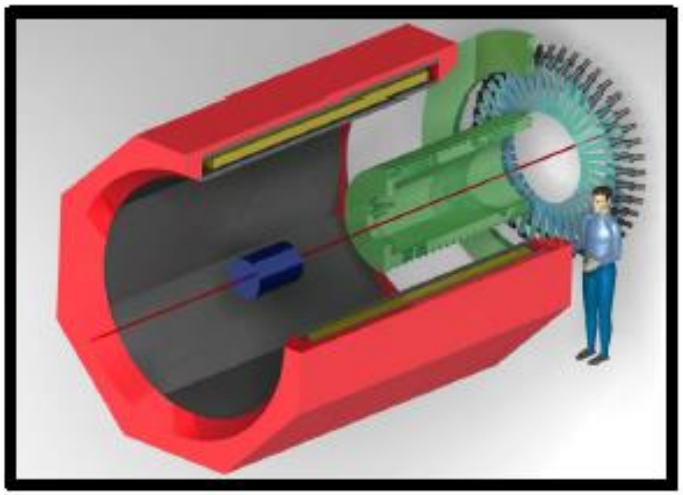

Raytrace simulations in the magnetic field

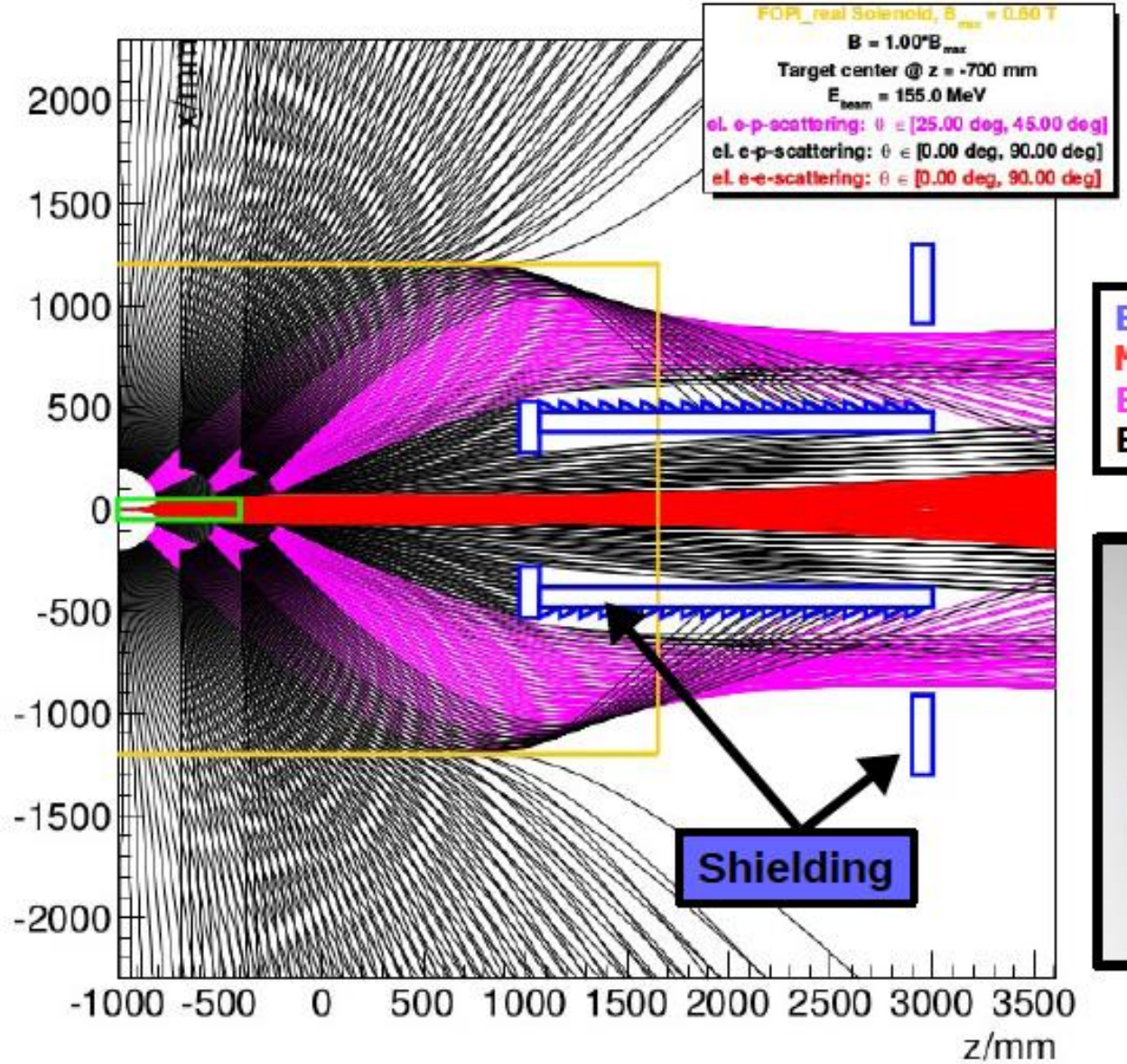

Magnetic field:
0.6 T

Beam energy = 155 MeV
Moller, θ ϵ [0°, 90°]
Elastic e-p, θ ϵ [25°, 45°]
Elastic e-p, θ ϵ [0°, 90°]

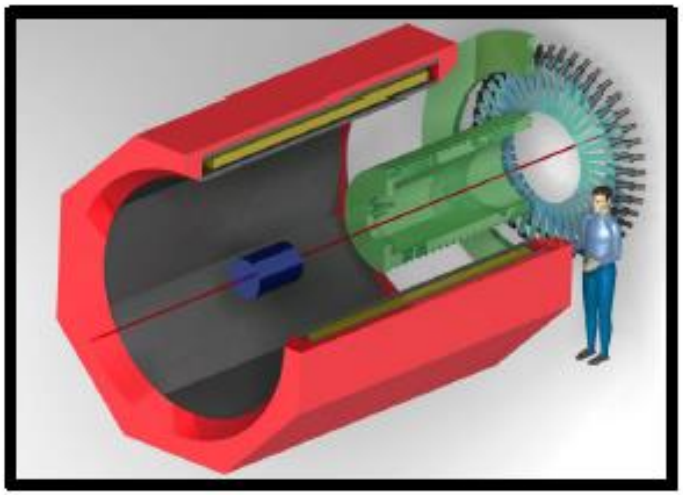

Raytrace simulations in the magnetic field

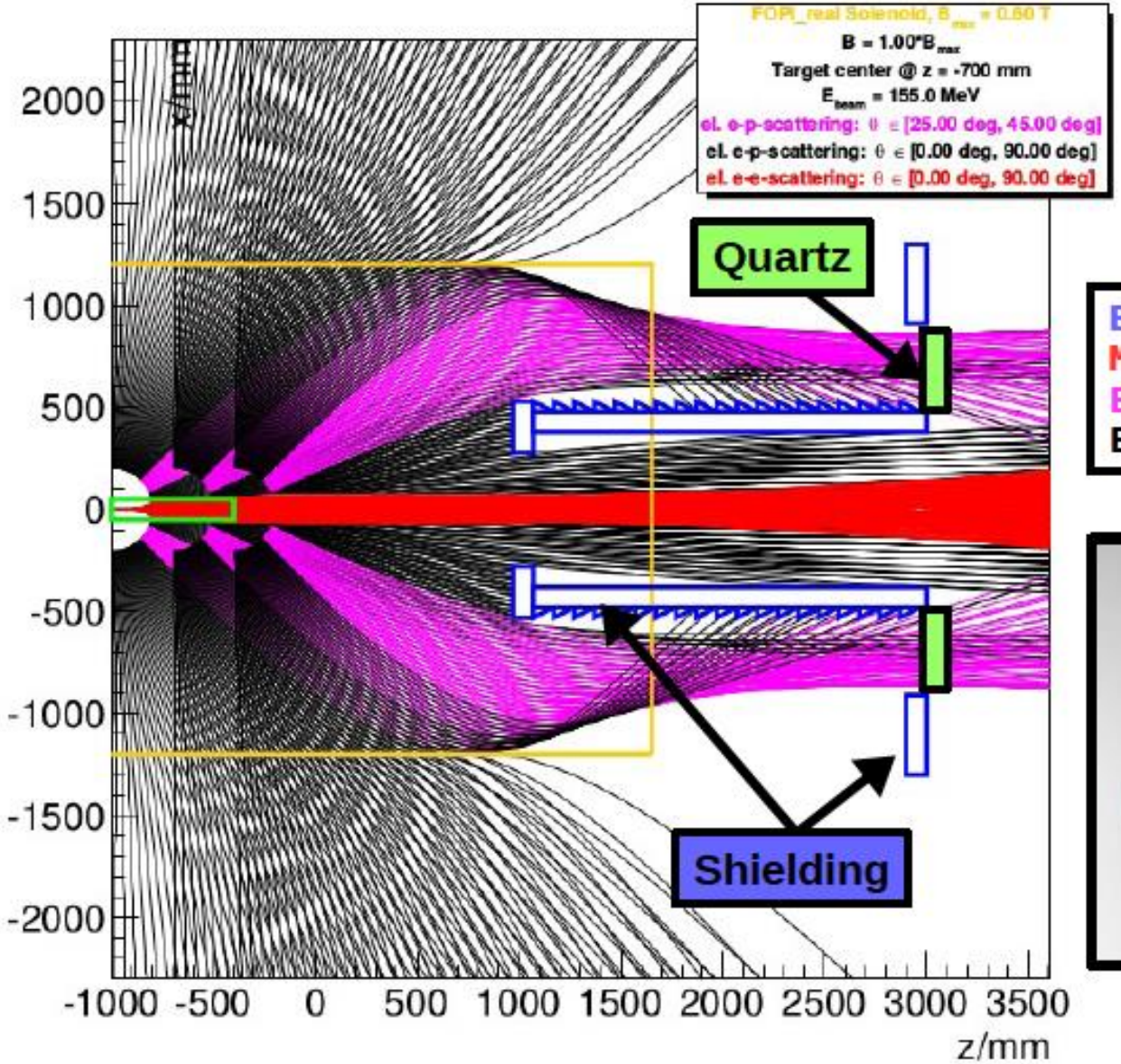

Magnetic field:
0.6 T

Beam energy = 155 MeV
Moller, θ ϵ [0°, 90°]
Elastic e-p, θ ϵ [25°, 45°]
Elastic e-p, θ ϵ [0°, 90°]

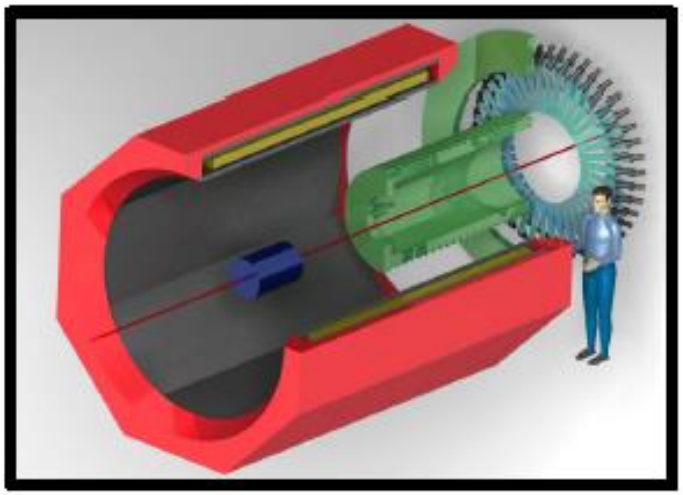

Geant4 Simulation of detector module response

Tracking of optical photons in detector module

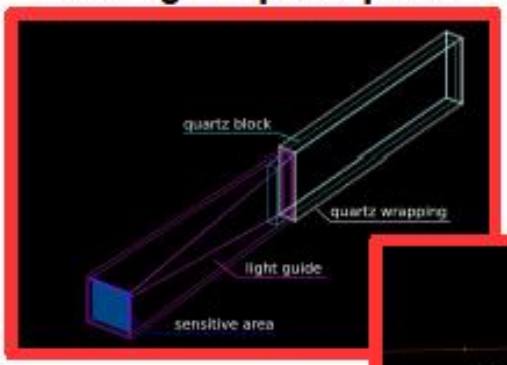

(K. Gerz)

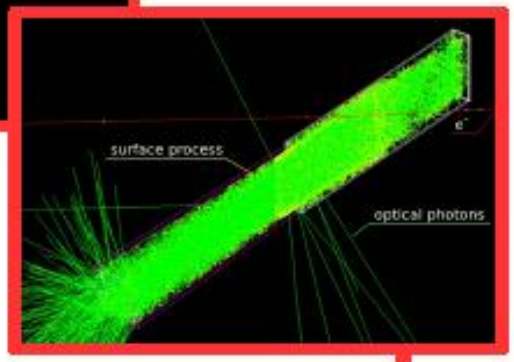

Photo electron yield distribution, E = 155 MeV

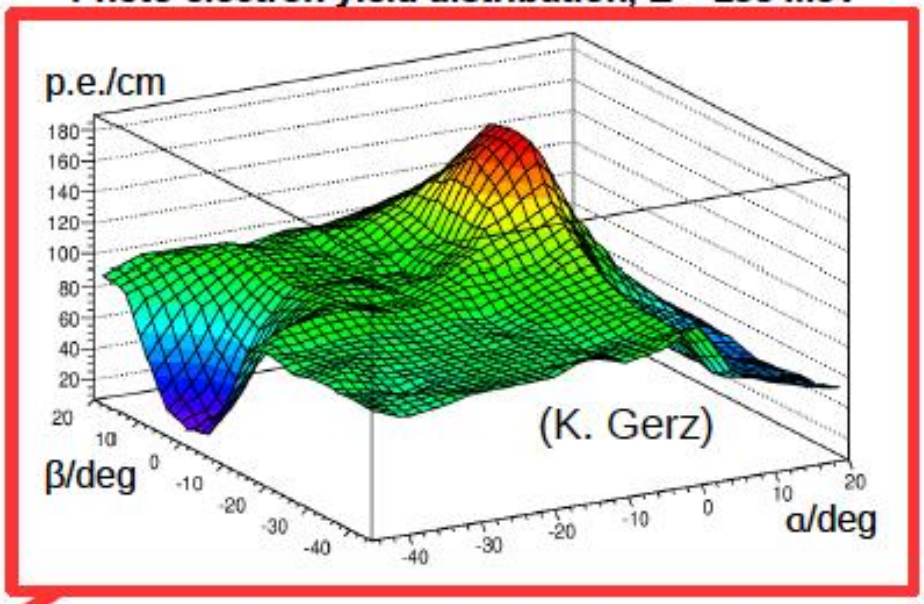

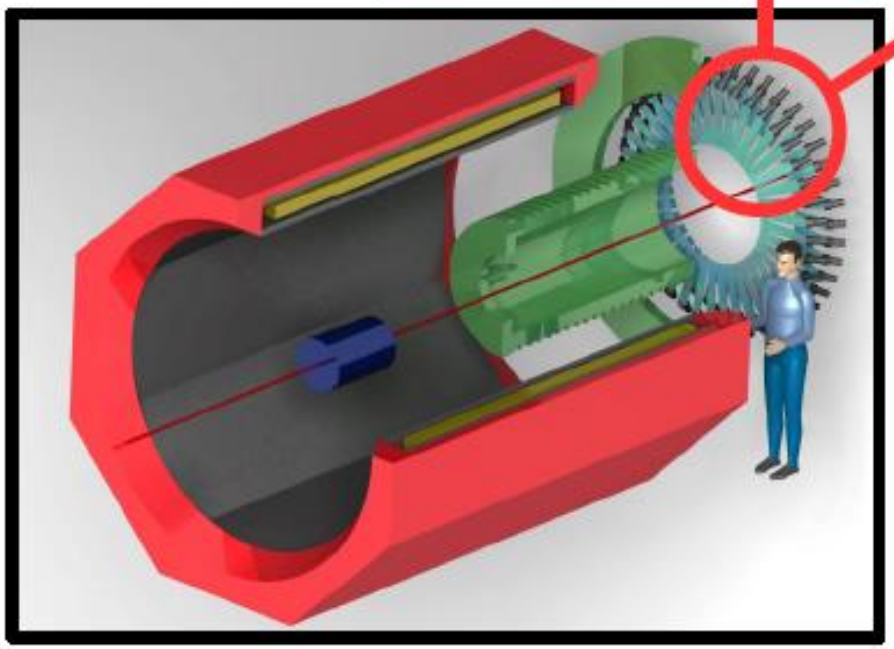

Create parametrization of photo electron yield for different

- Active materials
- Geometries
- Particle types
- Particle energies
- Impact angles

Particle rates

Overview of Particle rate- and asymmetry contributions:

Contribution	rate/s^{-1}	(rate*asymmetry)/(total rate)/ppb
pp total	9.81e+10	-46.25
mc total	5.06e+11	-13.67
mc signal_electrons_elep	7.92e+10	-7.20
mc primary_electrons_elep	4.59e+10	-2.18
mc secondary_electrons_elep	1.13e+09	-0.14
mc secondary_photons_elep	3.32e+10	-4.06
mc secondary_positrons_elep	6.61e+08	-0.08
mc primary_protons_elep	1.14e+07	-0.01
mc secondary_electrons_target_shower	2.34e+08	0.00
mc secondary_photons_target_shower	3.46e+11	0.00
mc secondary_positrons_target_shower	0.00e+00	0.00

Overview of Photoelectron rate- and asymmetry contributions:

Contribution	rate/s^{-1}	(rate*asymmetry)/(total rate)/ppb	
pp total	9.81e+10	-46.25	
mc total	4.80e+12	-34.90	
mc signal_electrons_elep	2.74e+12	-24.75	mean of 34 P.E. per e-
mc primary_electrons_elep	2.03e+12	-9.87	amplification by factor 34
mc secondary_electrons_elep	1.22e+10	-0.13	
mc secondary_photons_elep	5.20e+09	-0.06	suppression by factor 6
mc secondary_positrons_elep	8.87e+09	-0.10	
mc primary_protons_elep	0.00e+00	0.00	
mc secondary_electrons_target_shower	0.00e+00	0.00	
mc secondary_photons_target_shower	4.30e+09	0.00	
mc secondary_positrons_target_shower	0.00e+00	0.00	

total suppression of photons by a factor 204

dilution by photons 10^{-3}

Simulations spectra

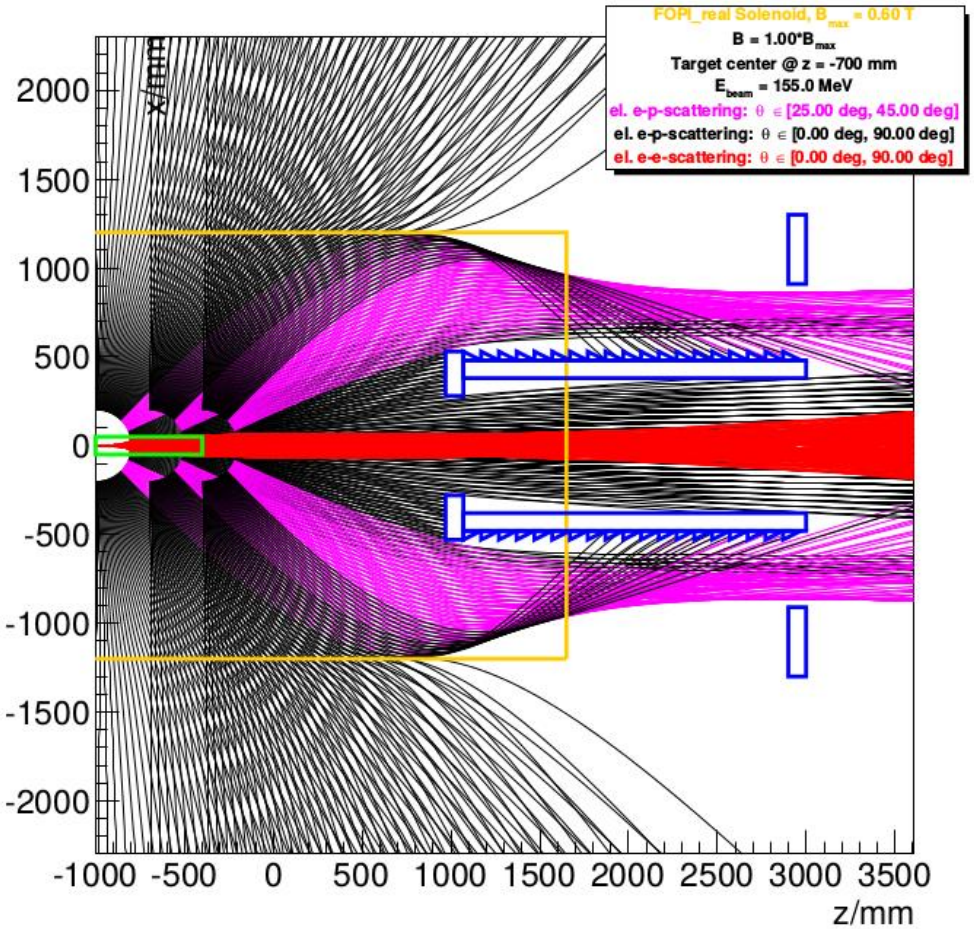
FOPI_real Solenoid, B_max = 0.60 T
B = 1.00*B_max
Target center @ z = -700 mm
E_beam = 155.0 MeV
el. e-p-scattering: θ ∈ [25.00 deg, 45.00 deg]
el. e-p-scattering: θ ∈ [0.00 deg, 90.00 deg]
el. e-e-scattering: θ ∈ [0.00 deg, 90.00 deg]
x/mm
2000
1500
1000
500
0
-500
-1000
-1500
-2000
-1000 -500 0 500 1000 1500 2000 2500 3000 3500
z/mm

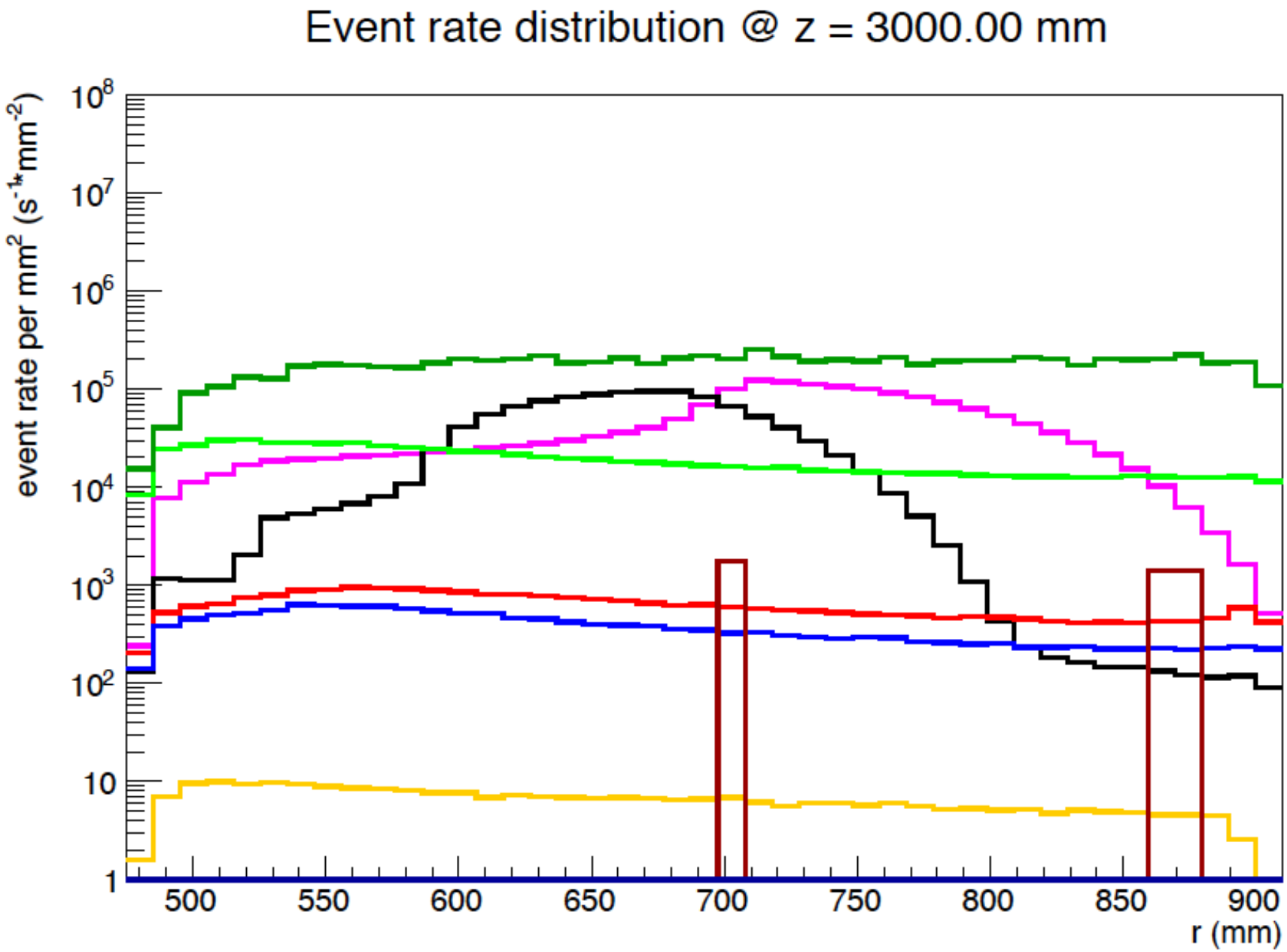
Event rate distribution @ z = 3000.00 mm
event rate per mm^2 (s^{-1}*mm^{-2})
10^8
10^7
10^6
10^5
10^4
10^3
10^2
10
1
500
550
600
650
700
750
800
850
900
r (mm)

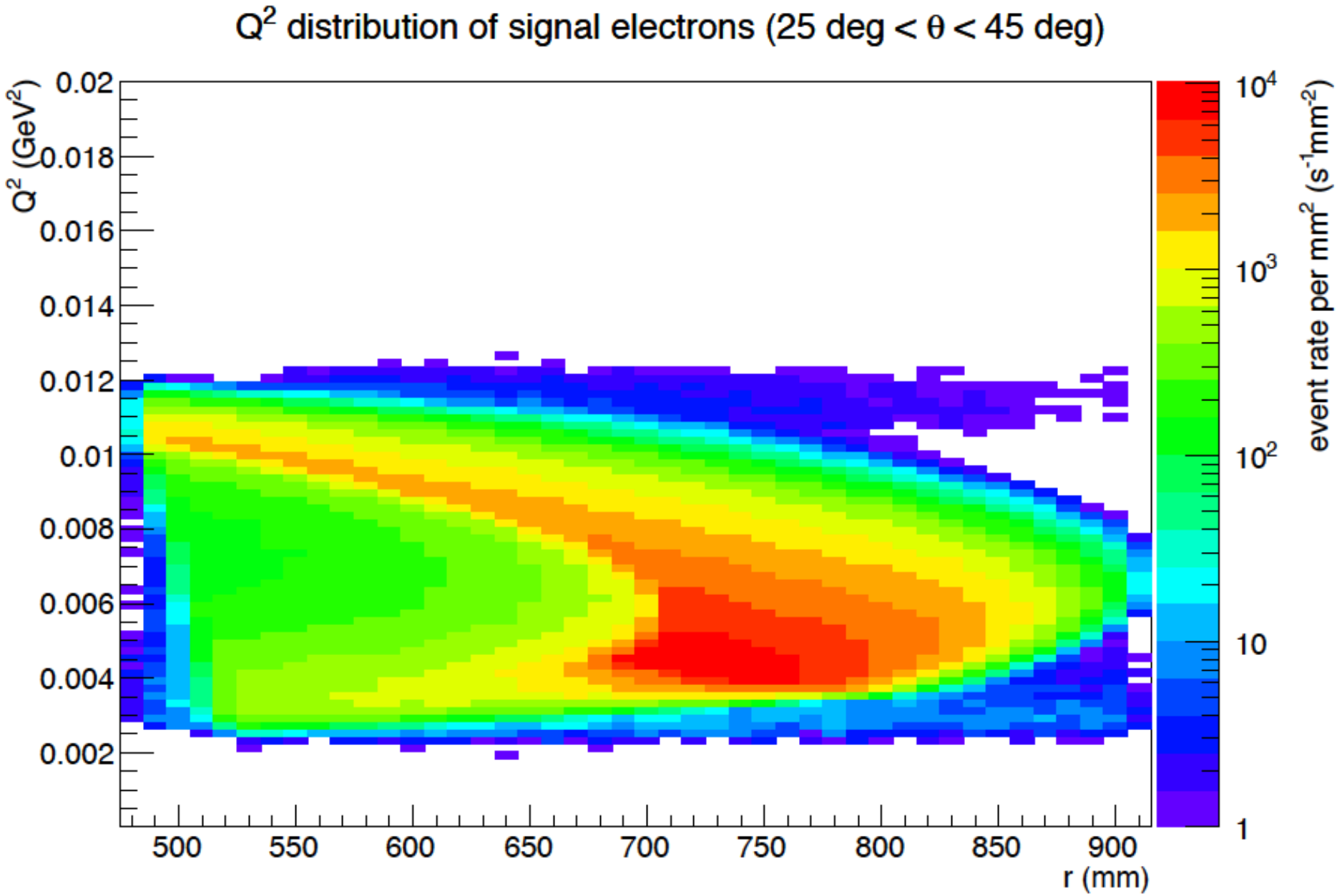
Q² distribution of signal electrons (25 deg < θ < 45 deg)
Q² (GeV²)
0.02
0.018
0.016
0.014
0.012
0.01
0.008
0.006
0.004
0.002
500
550
600
650
700
750
800
850
900
r (mm)
event rate per mm² (s⁻¹mm⁻²)
10⁴
10³
10²
10
1

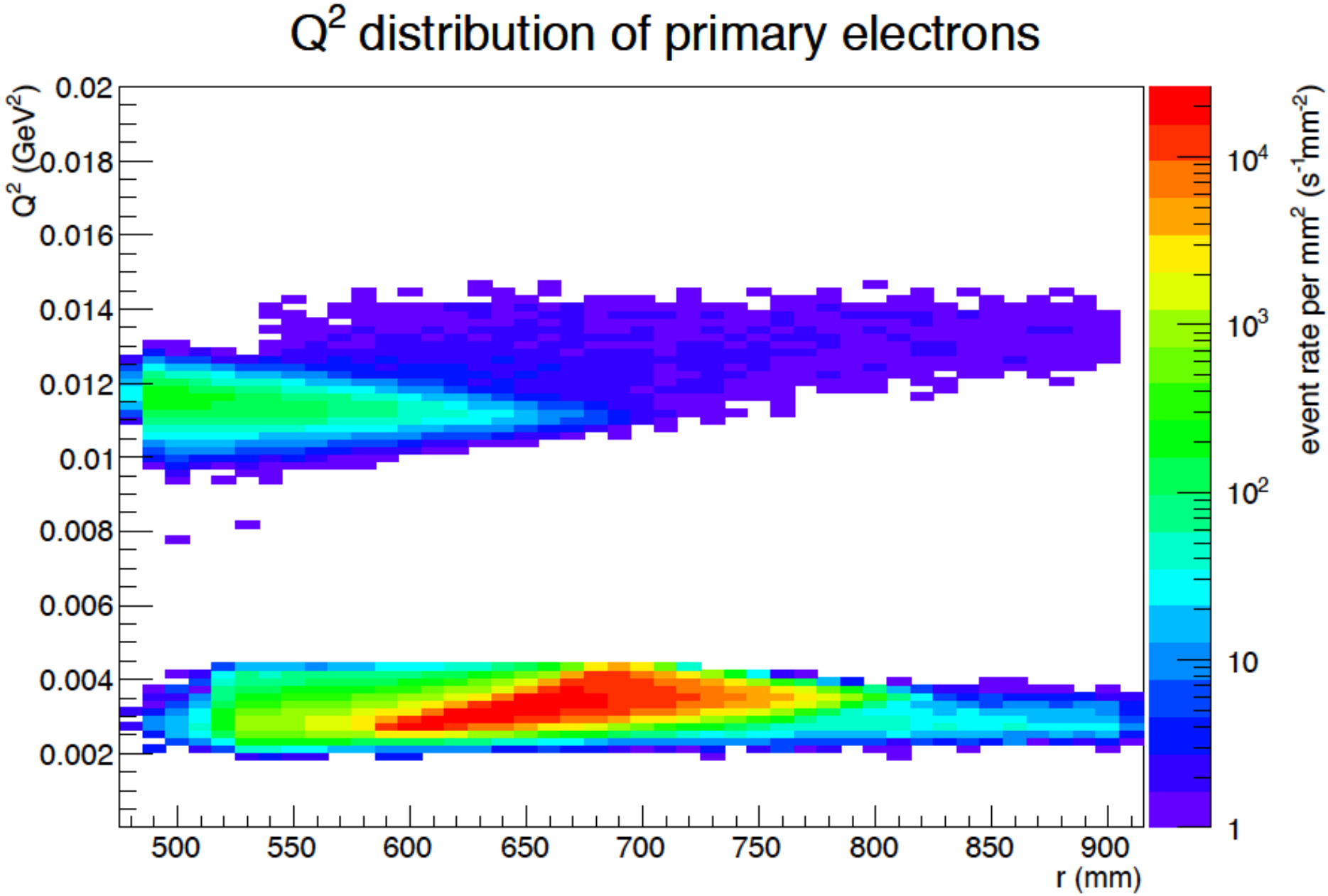
Q2 distribution of primary electrons
Q2 (GeV2)
0.02
0.018
0.016
0.014
0.012
0.01
0.008
0.006
0.004
0.002
500
550
600
650
700
750
800
850
900
r (mm)
event rate per mm2 (s-1mm-2)
104
103
102
10
1

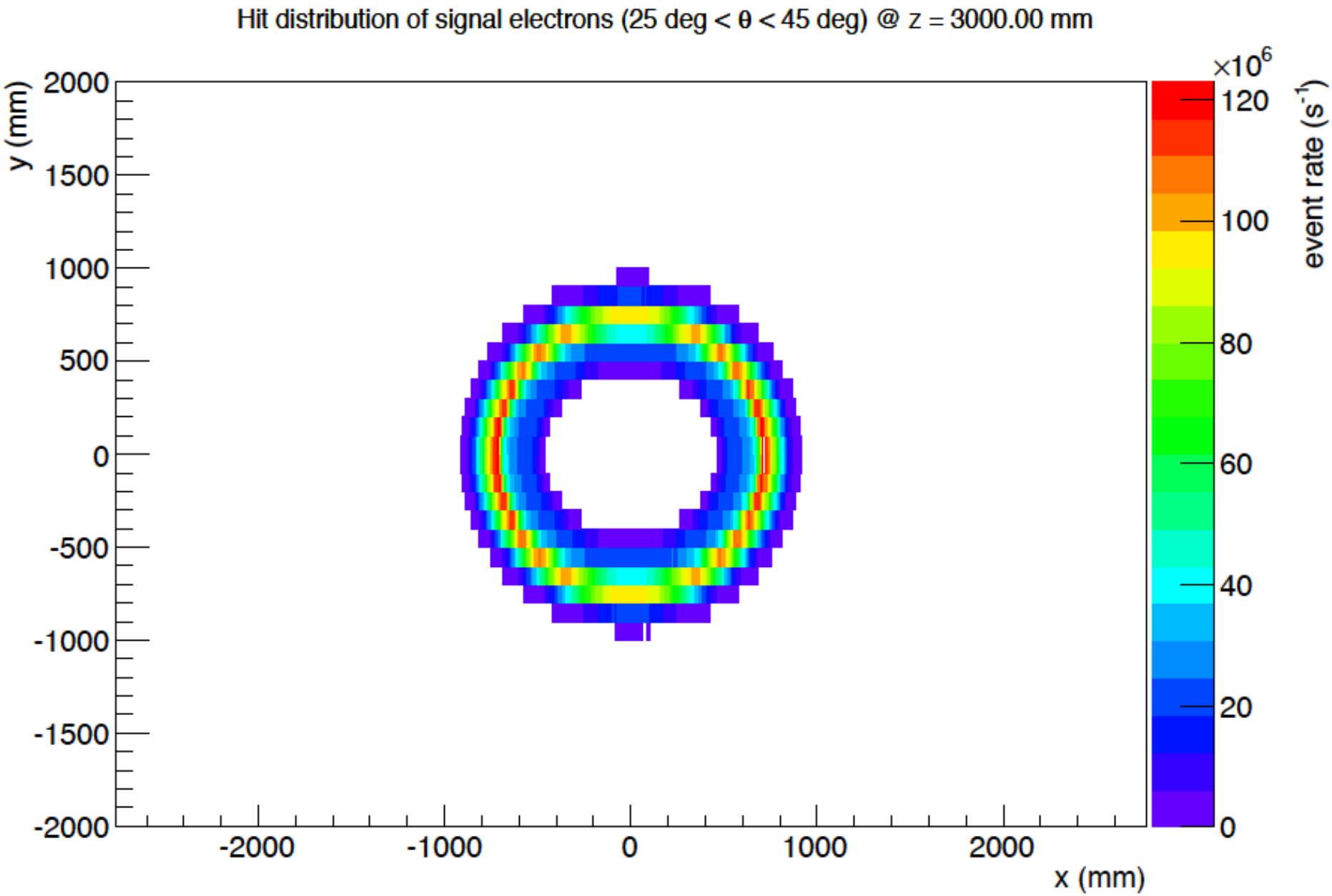
Hit distribution of signal electrons (25 deg < θ < 45 deg) @ z = 3000.00 mm
y (mm)
2000
1500
1000
500
0
-500
-1000
-1500
-2000
-2000
-1000
0
1000
2000
x (mm)
×10^6
120
100
80
60
40
20
0
event rate (s^-1)

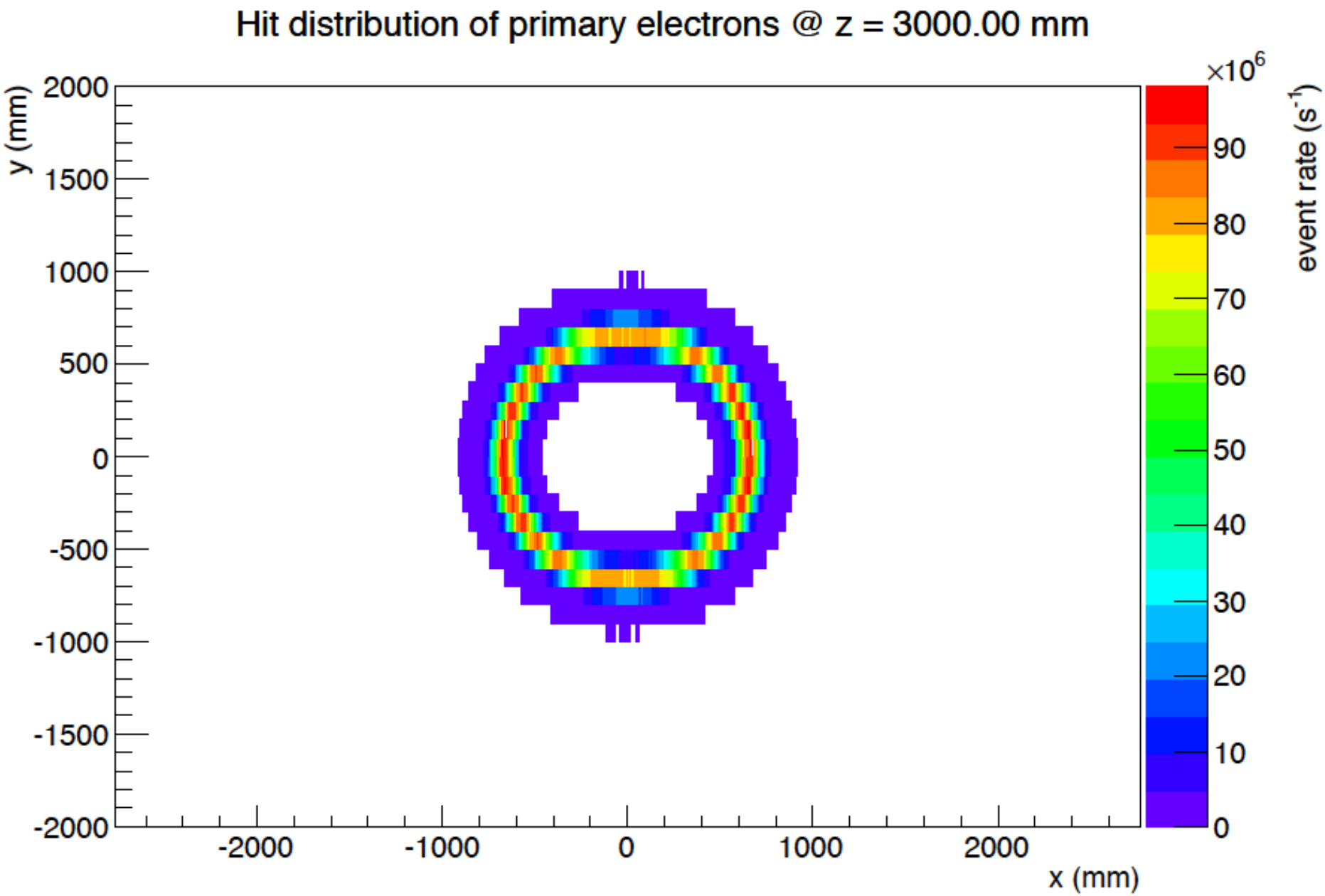
Hit distribution of primary electrons @ z = 3000.00 mm
y (mm)
2000
1500
1000
500
0
-500
-1000
-1500
-2000
-2000
-1000
0
1000
2000
x (mm)
×10^6
90
80
70
60
50
40
30
20
10
0
event rate (s^-1)

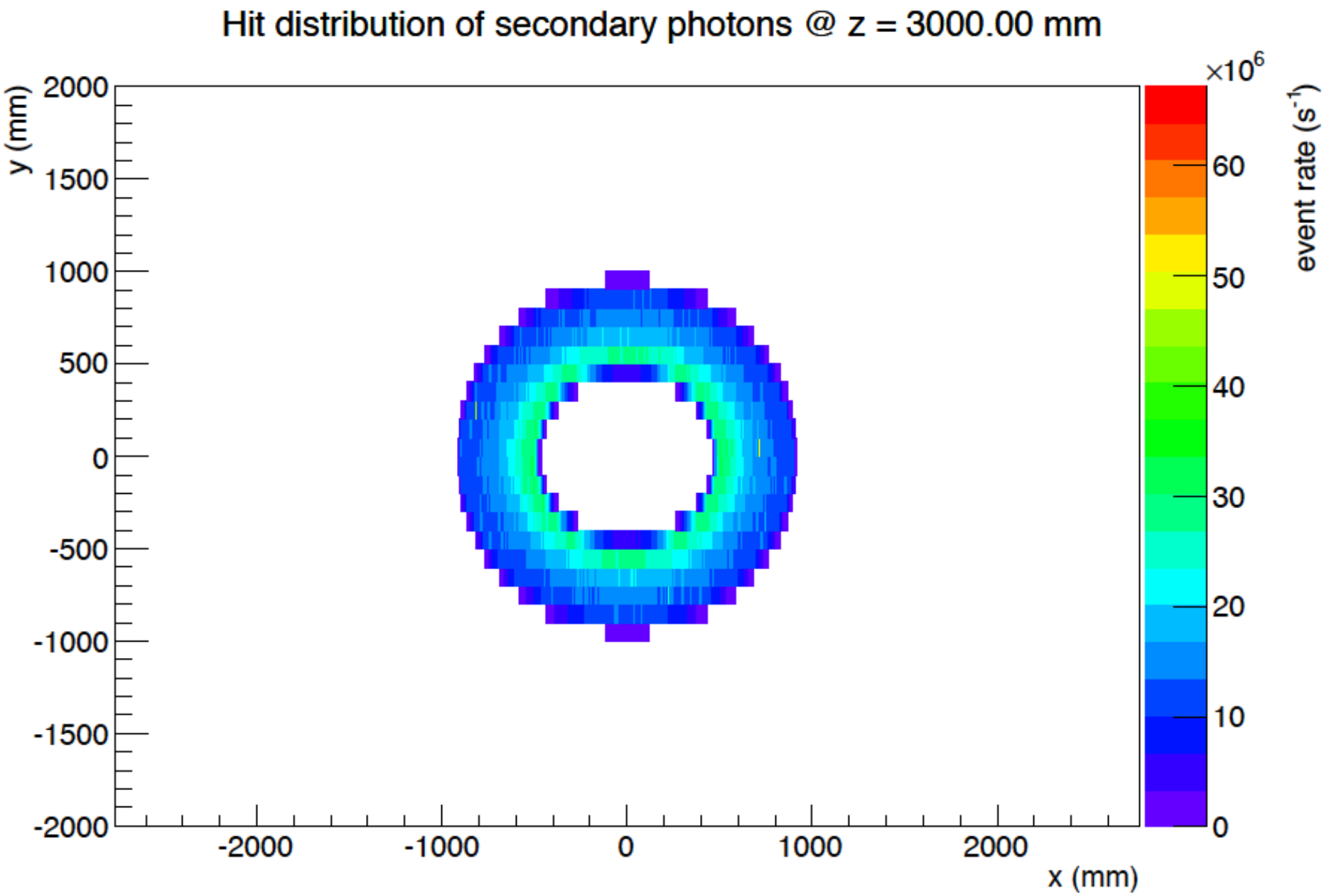
Hit distribution of secondary photons @ z = 3000.00 mm
y (mm)
2000
1500
1000
500
0
-500
-1000
-1500
-2000
-2000
-1000
0
1000
2000
x (mm)
×10^6
60
50
40
30
20
10
0
event rate (s^-1)

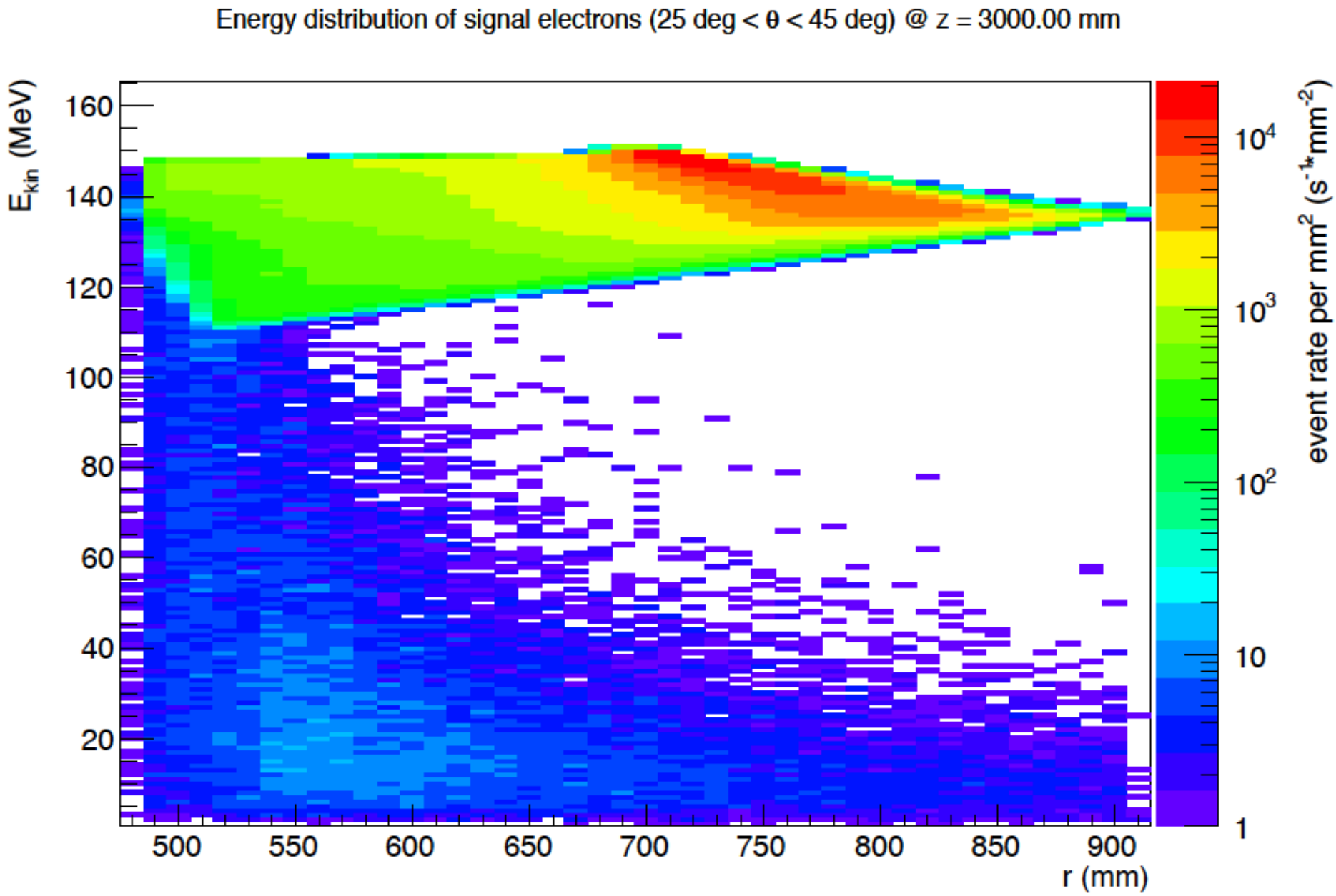
Energy distribution of signal electrons (25 deg < θ < 45 deg) @ z = 3000.00 mm
E_kin (MeV)
160
140
120
100
80
60
40
20
500
550
600
650
700
750
800
850
900
r (mm)
event rate per mm² (s⁻¹*mm⁻²)
10⁴
10³
10²
10
1

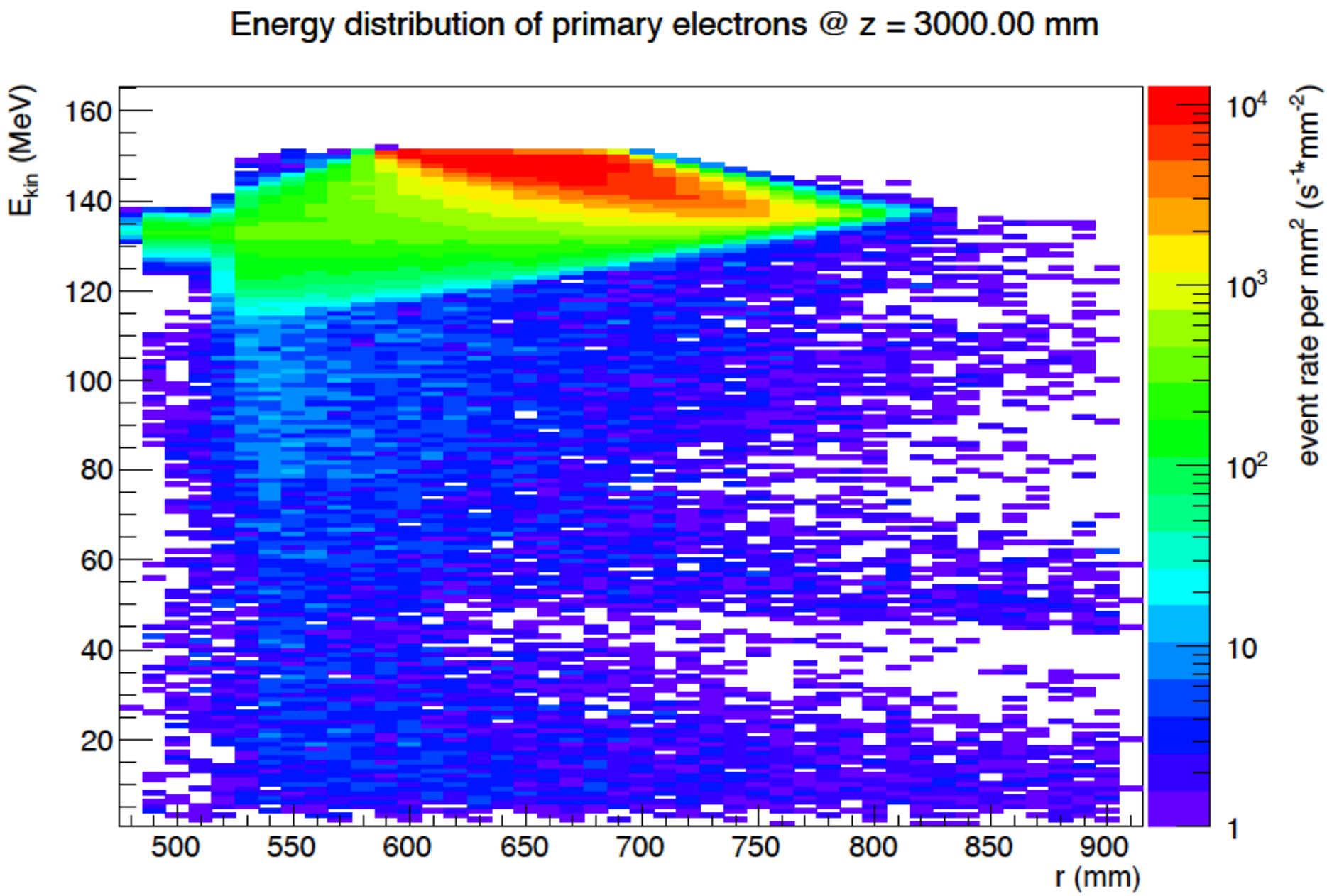
Energy distribution of primary electrons @ z = 3000.00 mm
E_{kin} (MeV)
160
140
120
100
80
60
40
20
500
550
600
650
700
750
800
850
900
r (mm)
10^4
10^3
10^2
10
1
event rate per mm^2 ($s^{-1}*mm^{-2}$)

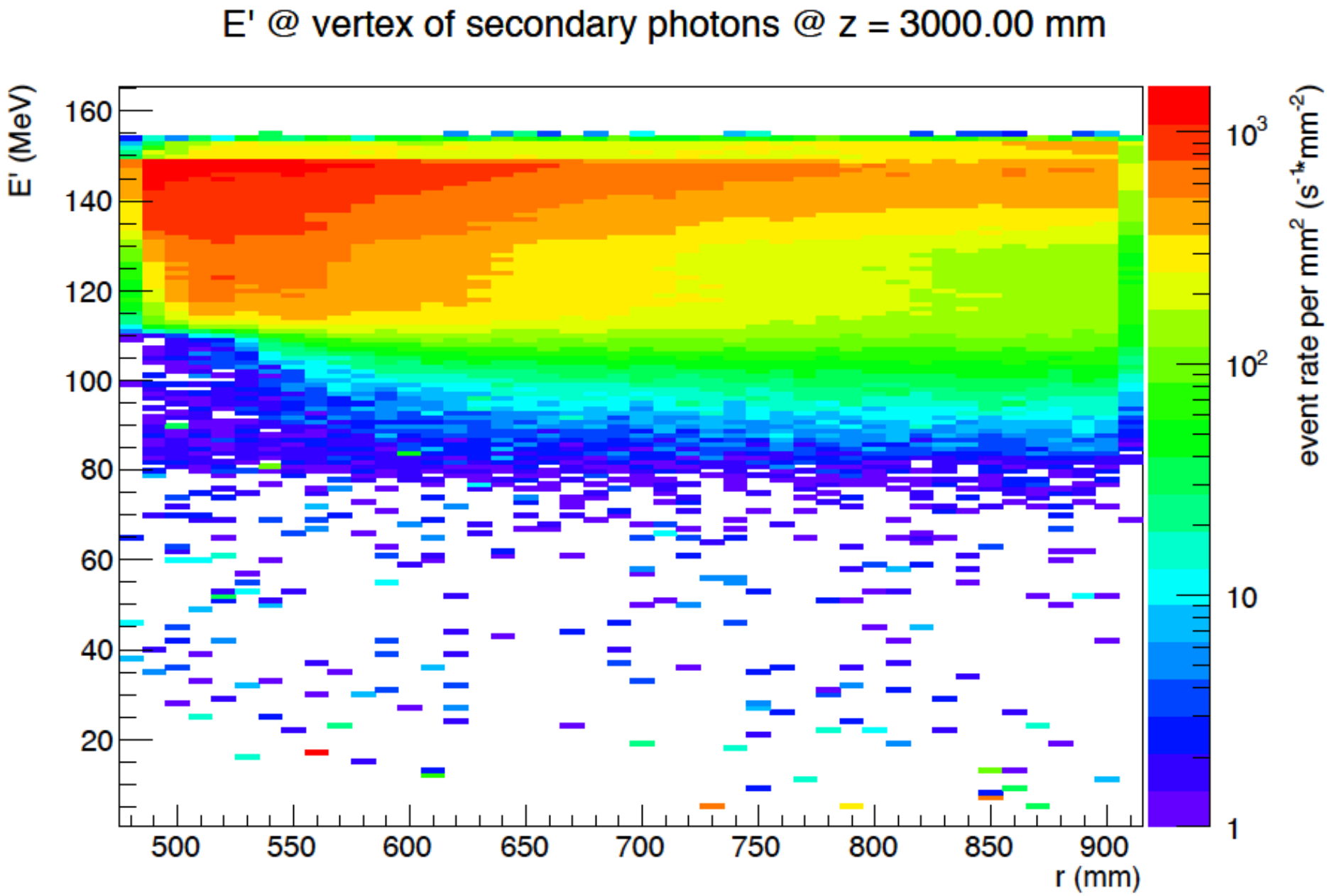
E' @ vertex of secondary photons @ z = 3000.00 mm
E' (MeV)
160
140
120
100
80
60
40
20
500
550
600
650
700
750
800
850
900
r (mm)
10^3
10^2
10
1
event rate per mm^2 (s^{-1}*mm^{-2})

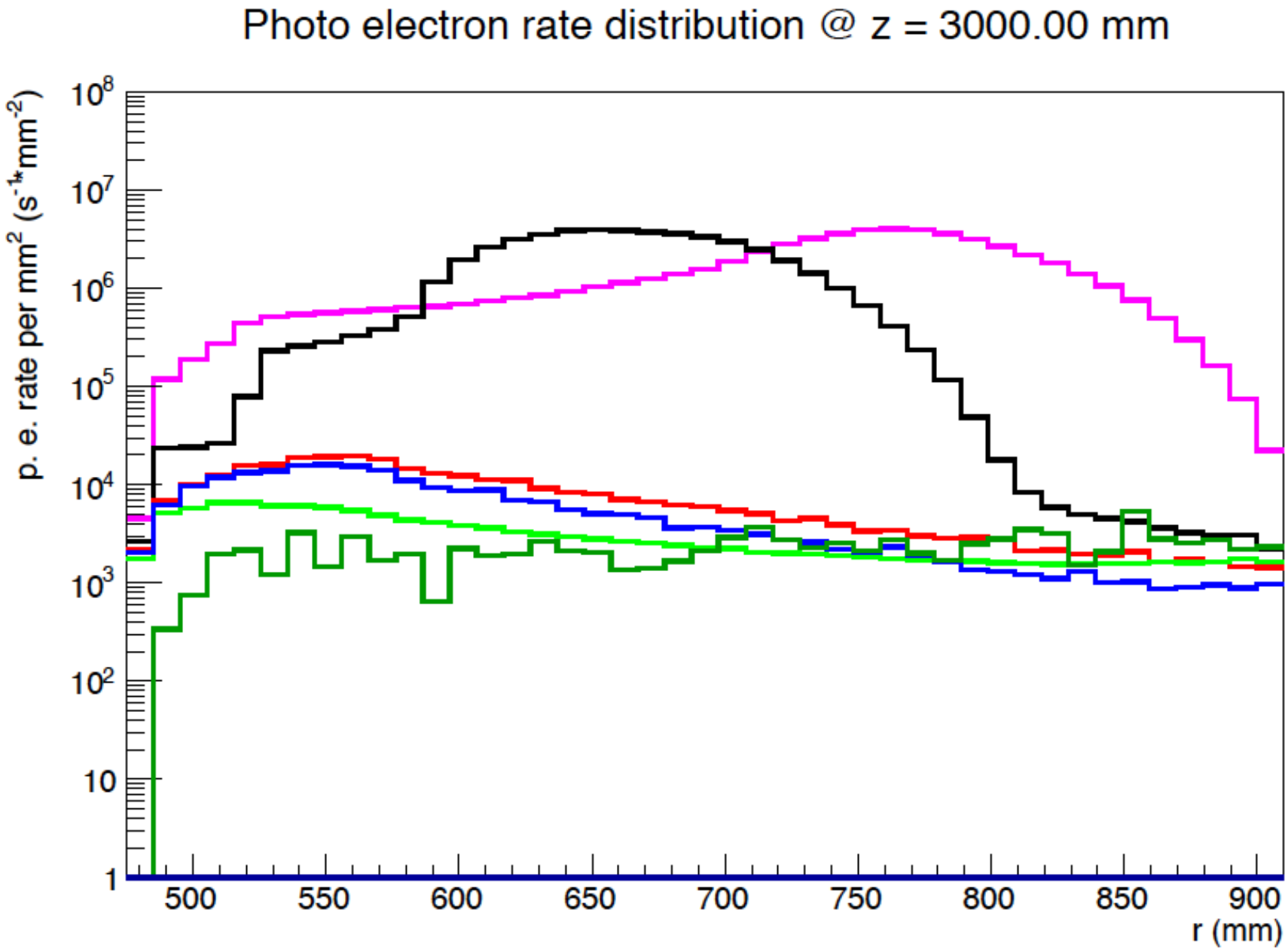
Photo electron rate distribution @ z = 3000.00 mm
p. e. rate per mm^2 (s^{-1}*mm^{-2})
10^8
10^7
10^6
10^5
10^4
10^3
10^2
10
1
500
550
600
650
700
750
800
850
900
r (mm)

Spin angle on detectors

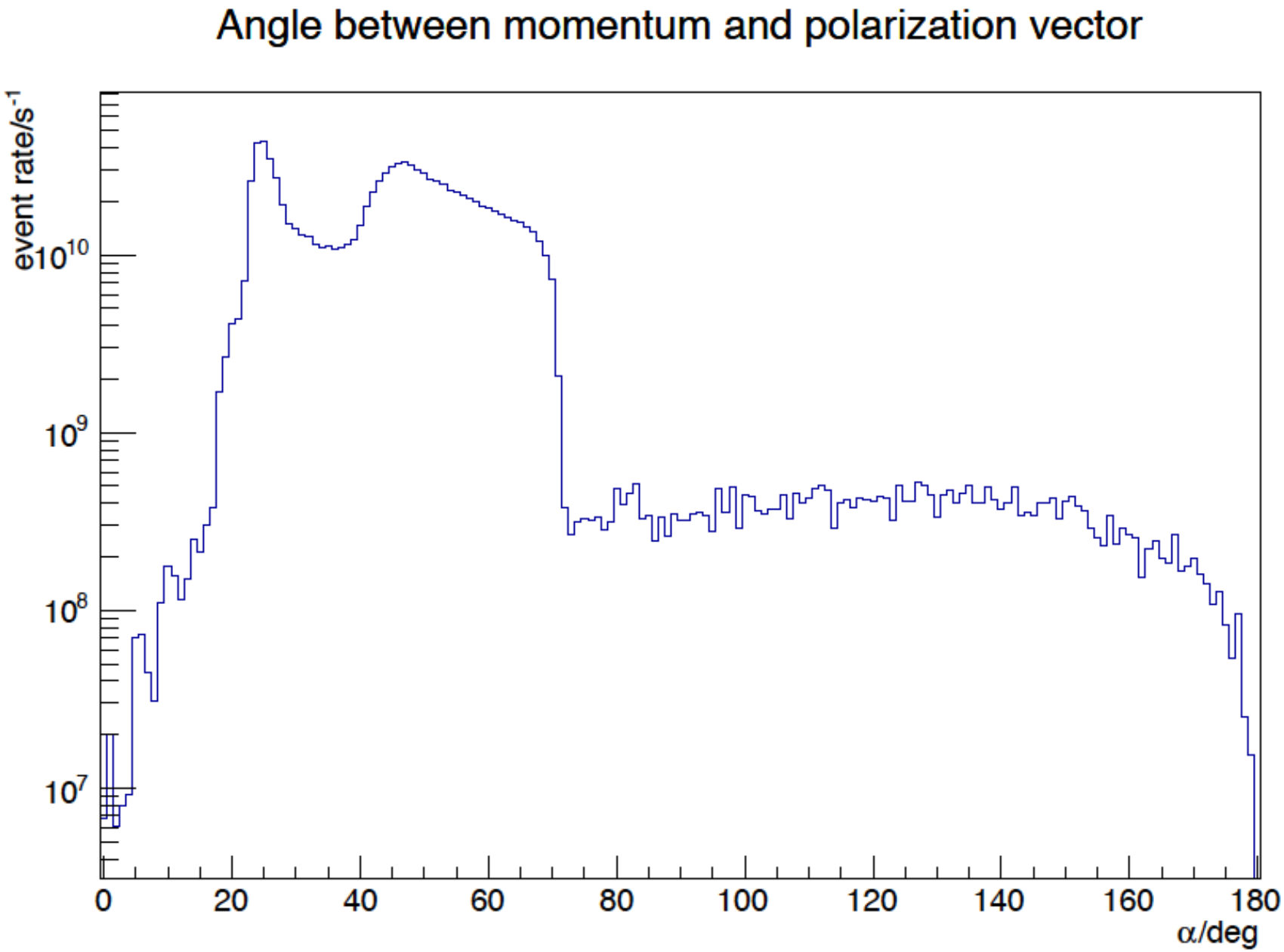
Angle between momentum and polarization vector
event rate/s^{-1}
10^{10}
10^{9}
10^{8}
10^{7}
0
20
40
60
80
100
120
140
160
180
α/deg

Impact angle on detectors

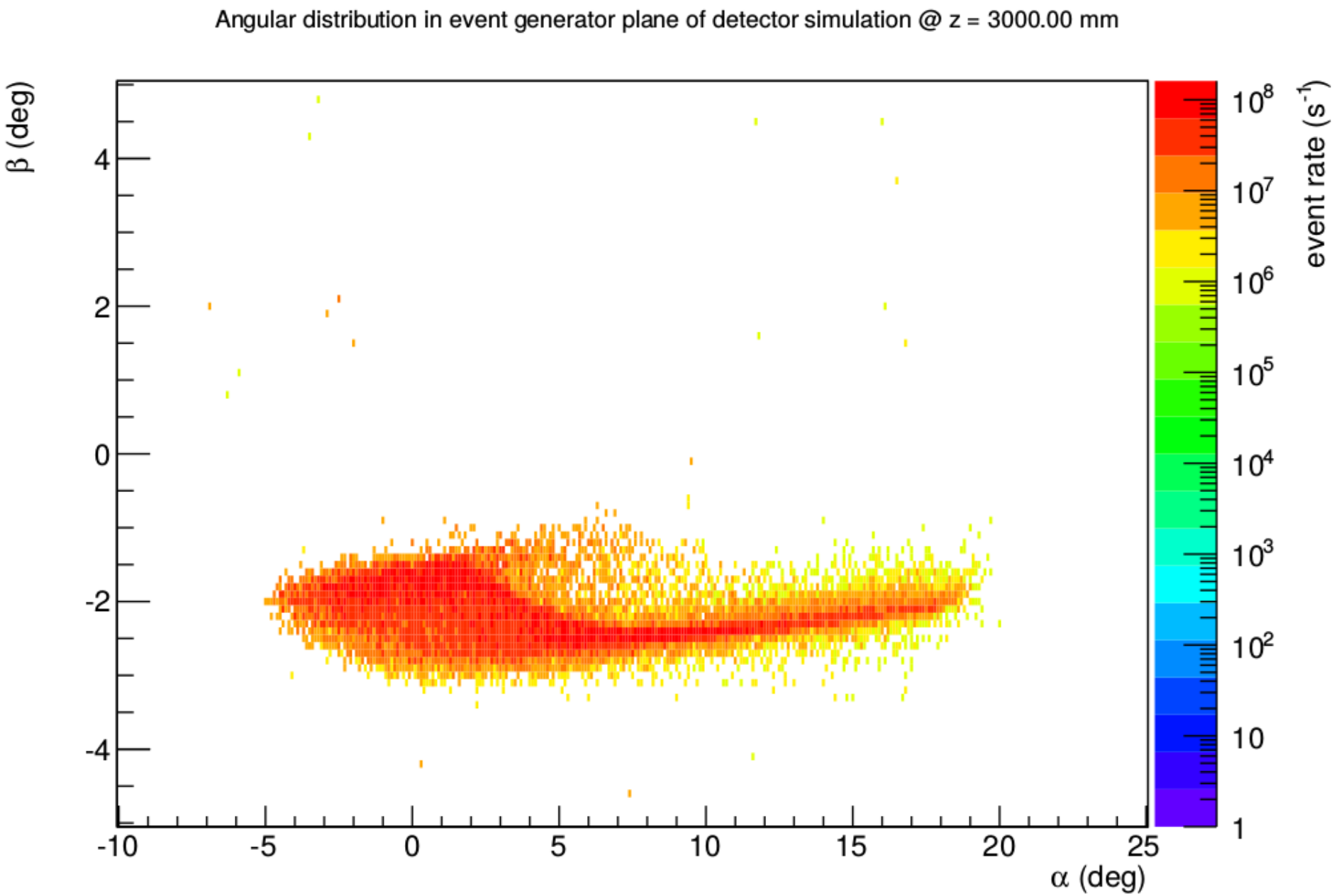
Angular distribution in event generator plane of detector simulation @ z = 3000.00 mm
β (deg)
4
2
0
-2
-4
-10
-5
0
5
10
15
20
25
α (deg)
event rate (s^{-1})
10^8
10^7
10^6
10^5
10^4
10^3
10^2
10
1

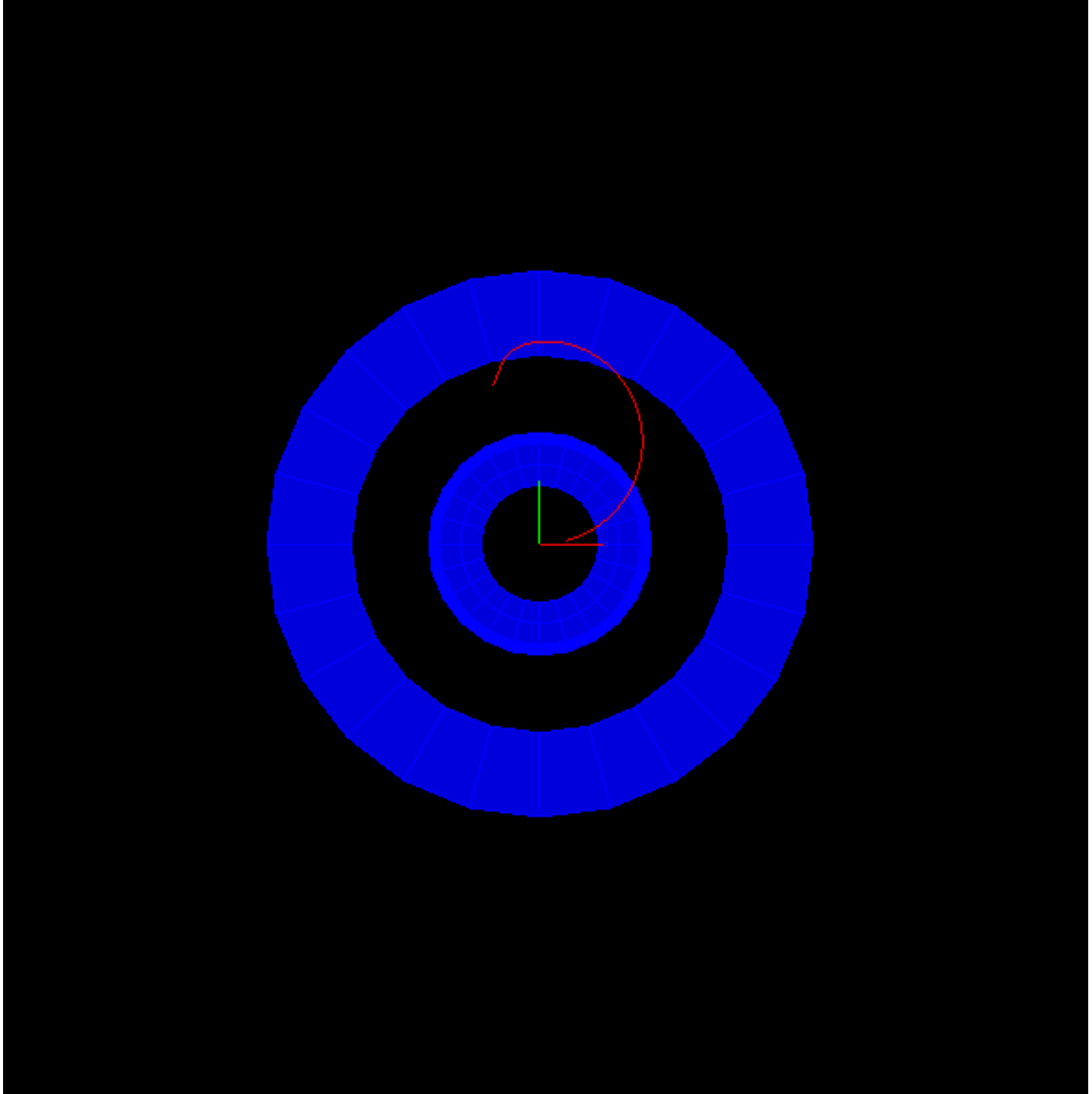

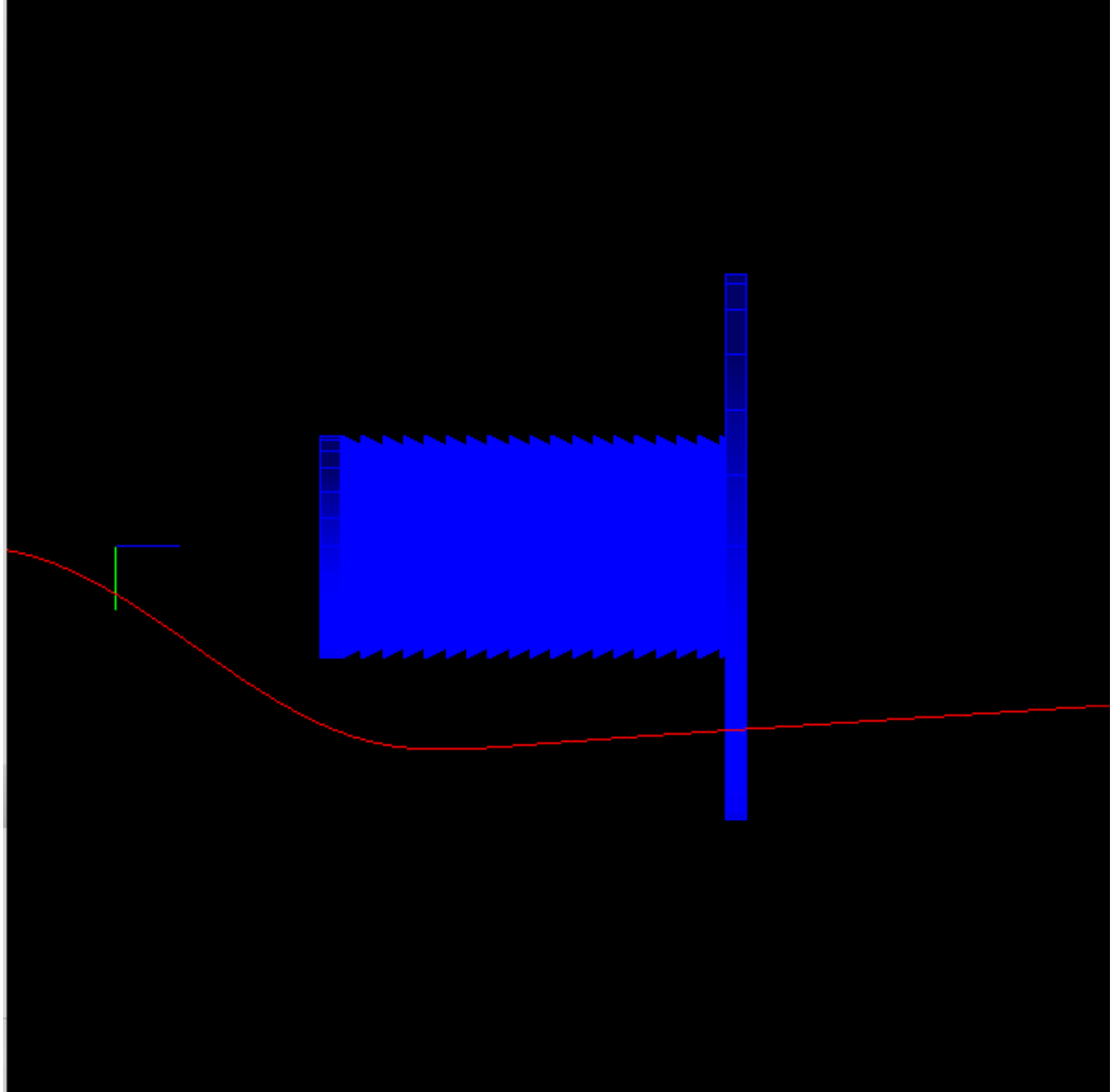

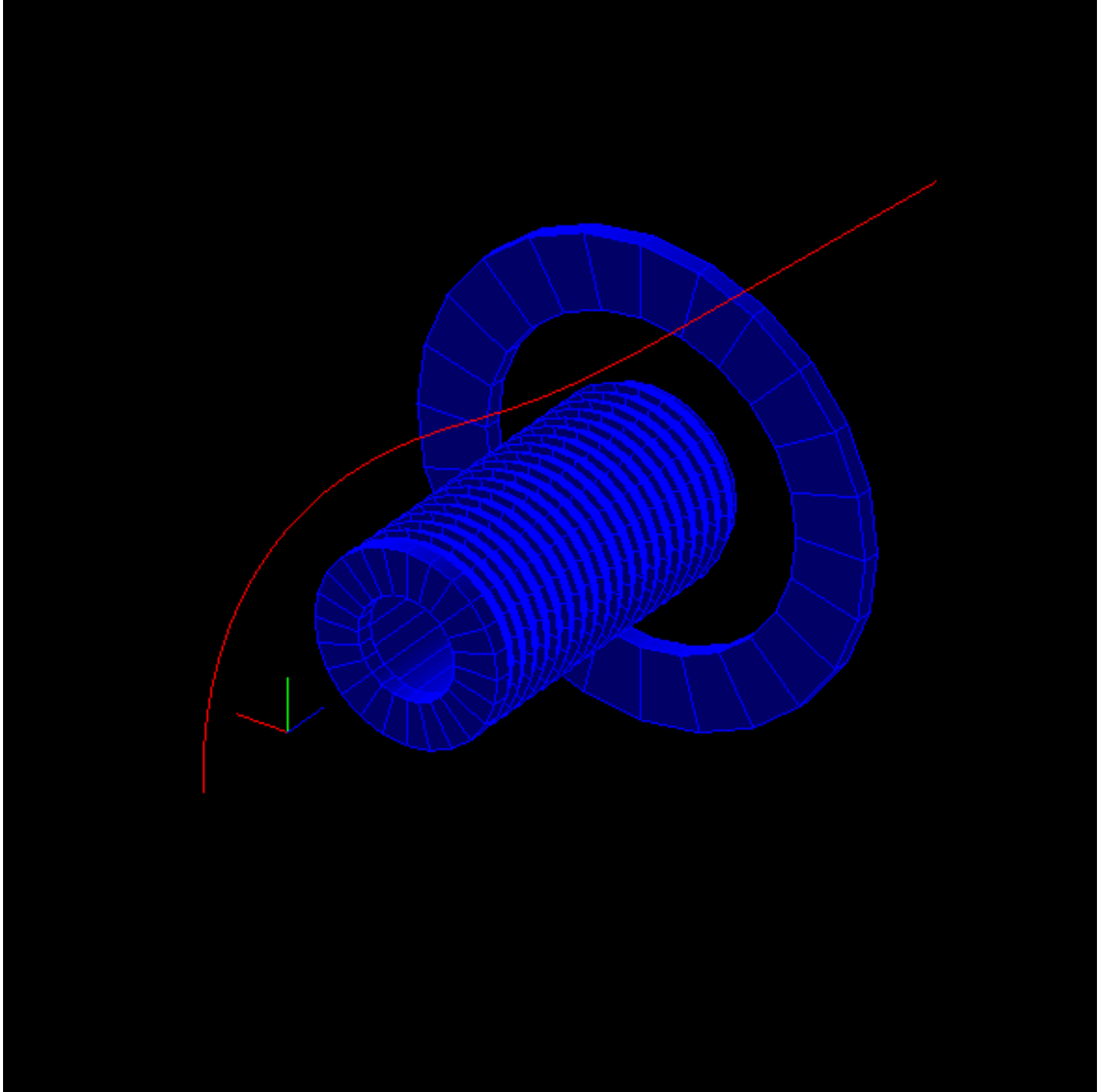

Tracking system

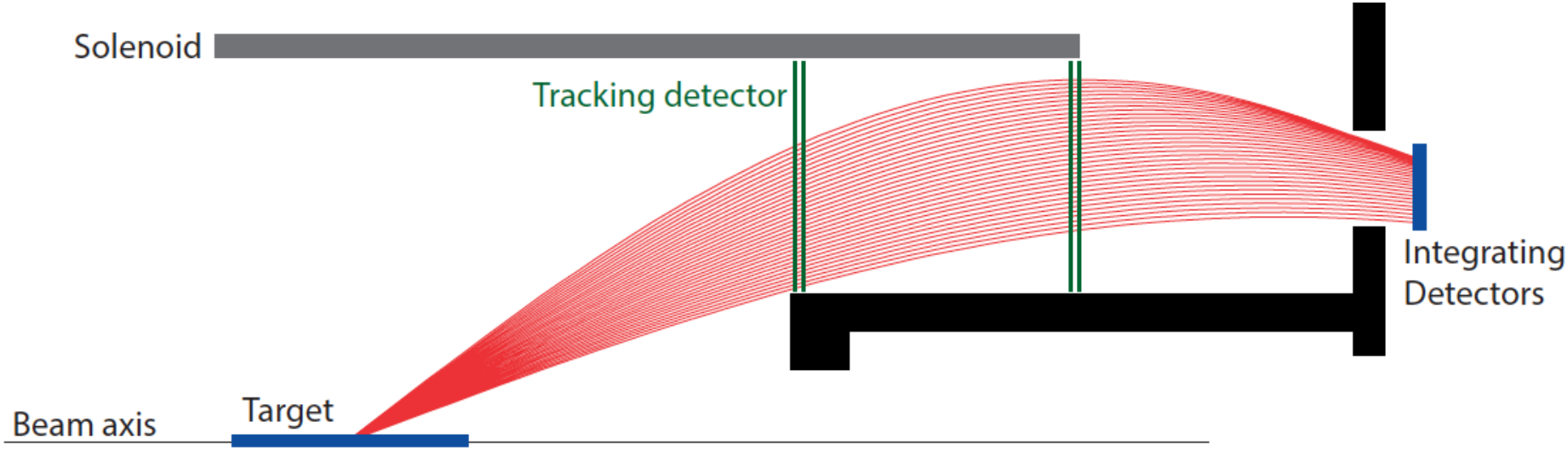

P2:
About 3m^2 active area
4 sectors of 20° each
Each sector 4 layers
About 2-3 €/m^2

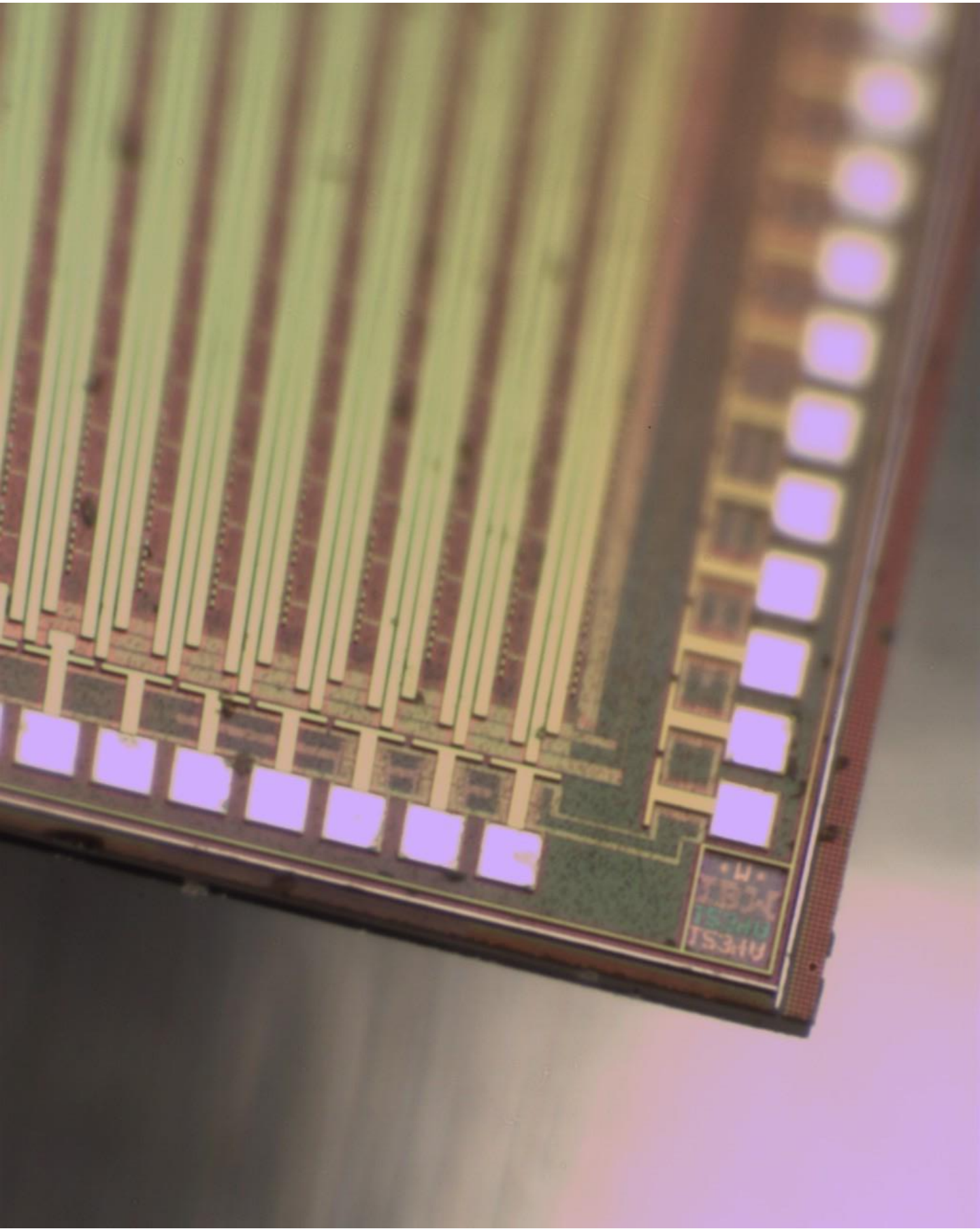

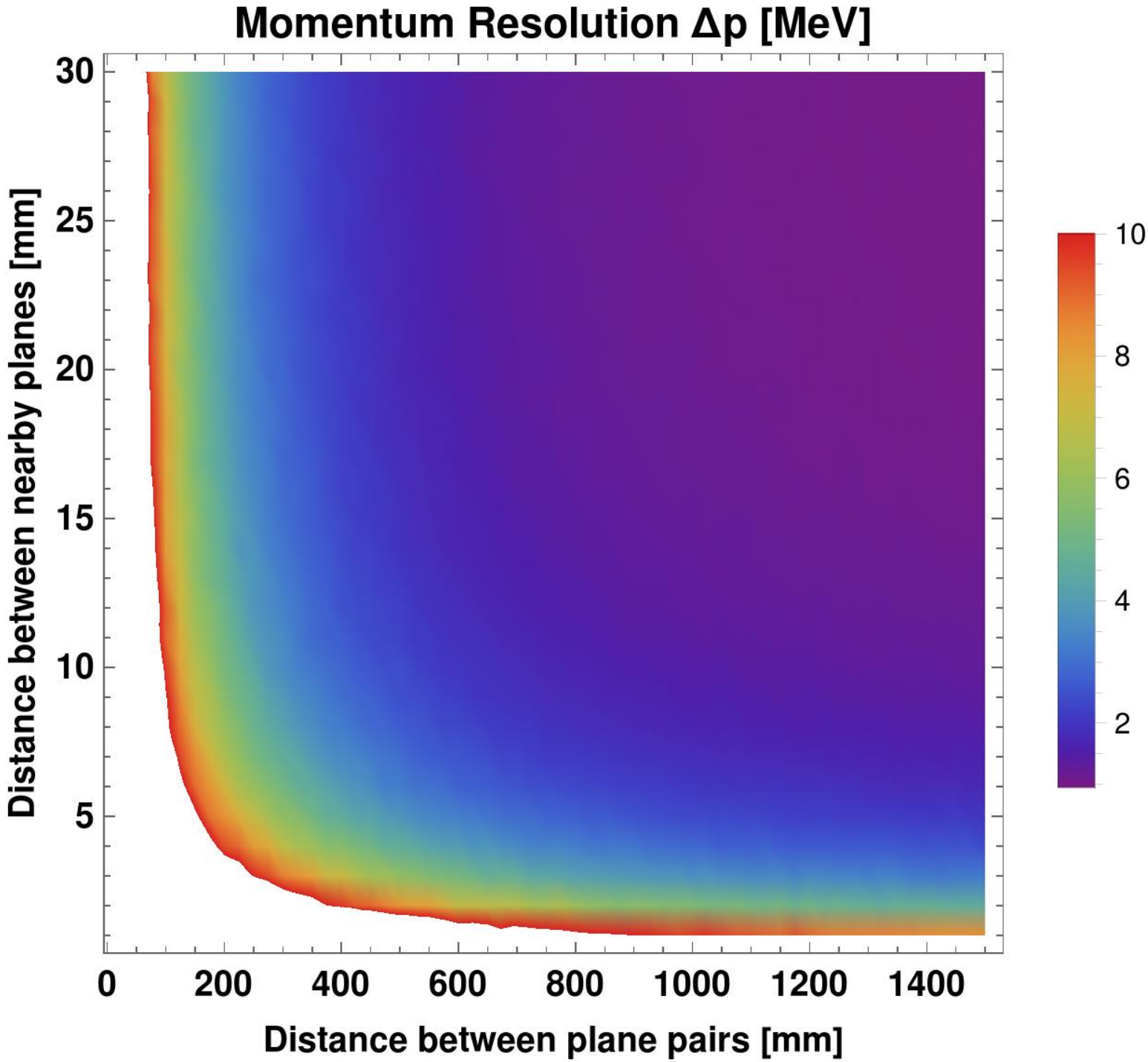
Momentum Resolution Δp [MeV]
Distance between nearby planes [mm]
30
25
20
15
10
5
0
200
400
600
800
1000
1200
1400
Distance between plane pairs [mm]
10
8
6
4
2

Weak mixing angle measurement requires determination of momentum transfer Q^2

- Tracking detector in solenoid field
- Valuable for systematic studies
- Challenging high-rate, low momentum environment:
  Use High-Voltage Monolithic Active Pixel Sensors (HV-MAPS), in two double planes

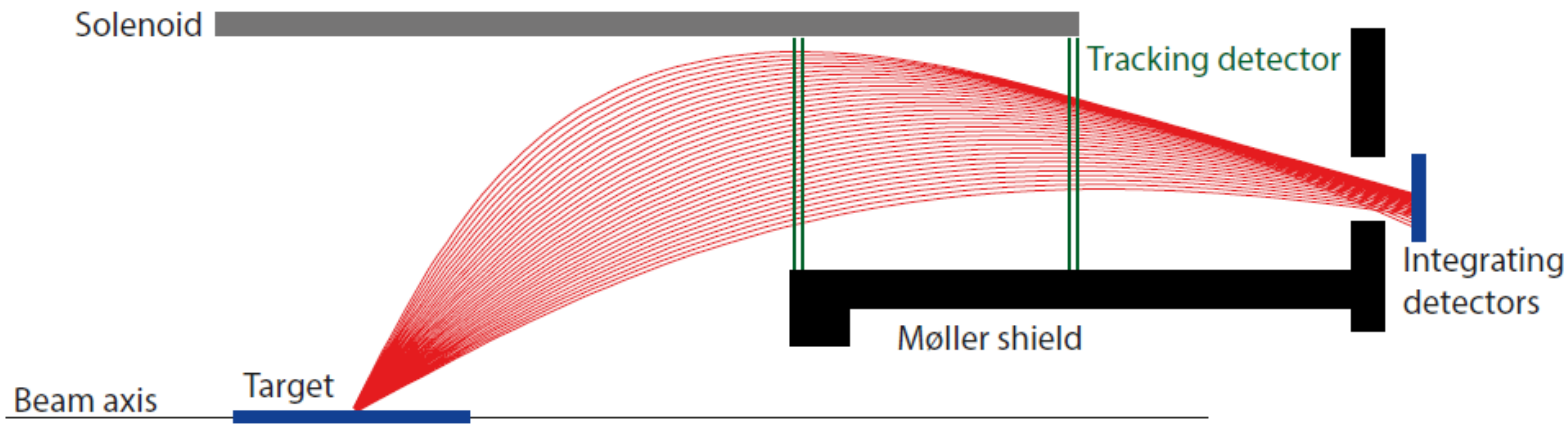

- High Voltage Monolithic Active Pixel Sensors (HV-MAPS)
- Developed jointly with the Mu3e Collaboration
- First Large Prototype (Mupix 8, 2 cm x 1 cm) fulfils specifications (30 MHz hits per chip, 99.9% efficiency
- Excellent time resolution (< 6 ns)
- Readout over ultra-thin Kapton/Aluminium flexprints working
- 2 cm by 2 cm chip being designed

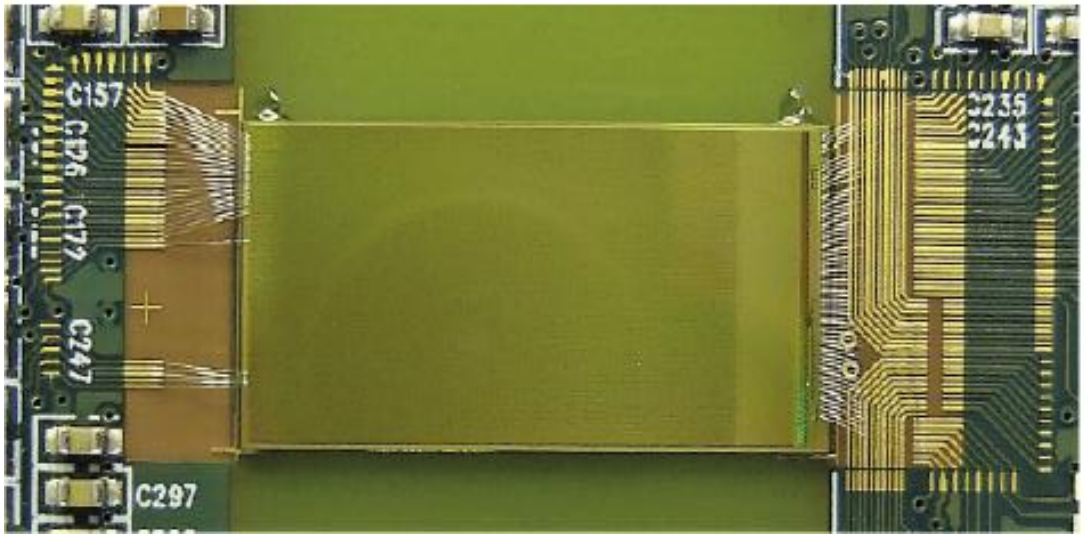

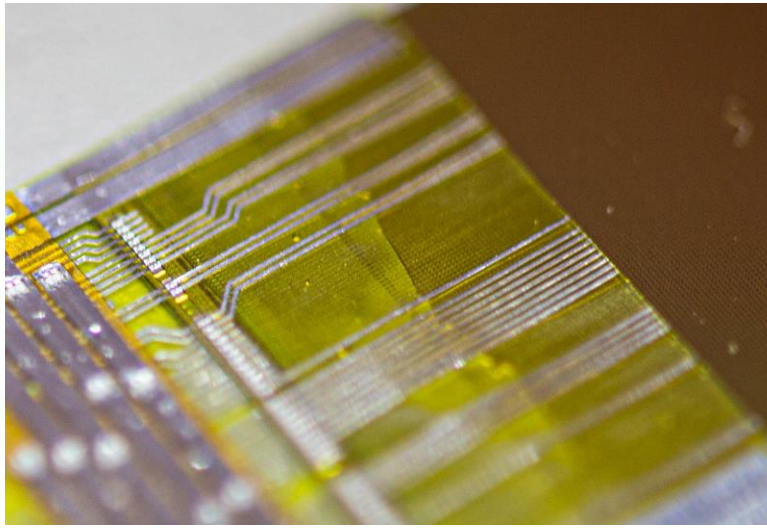

- Detailed CAD design
- Includes helium gas cooling channels and readout and powering PCBs

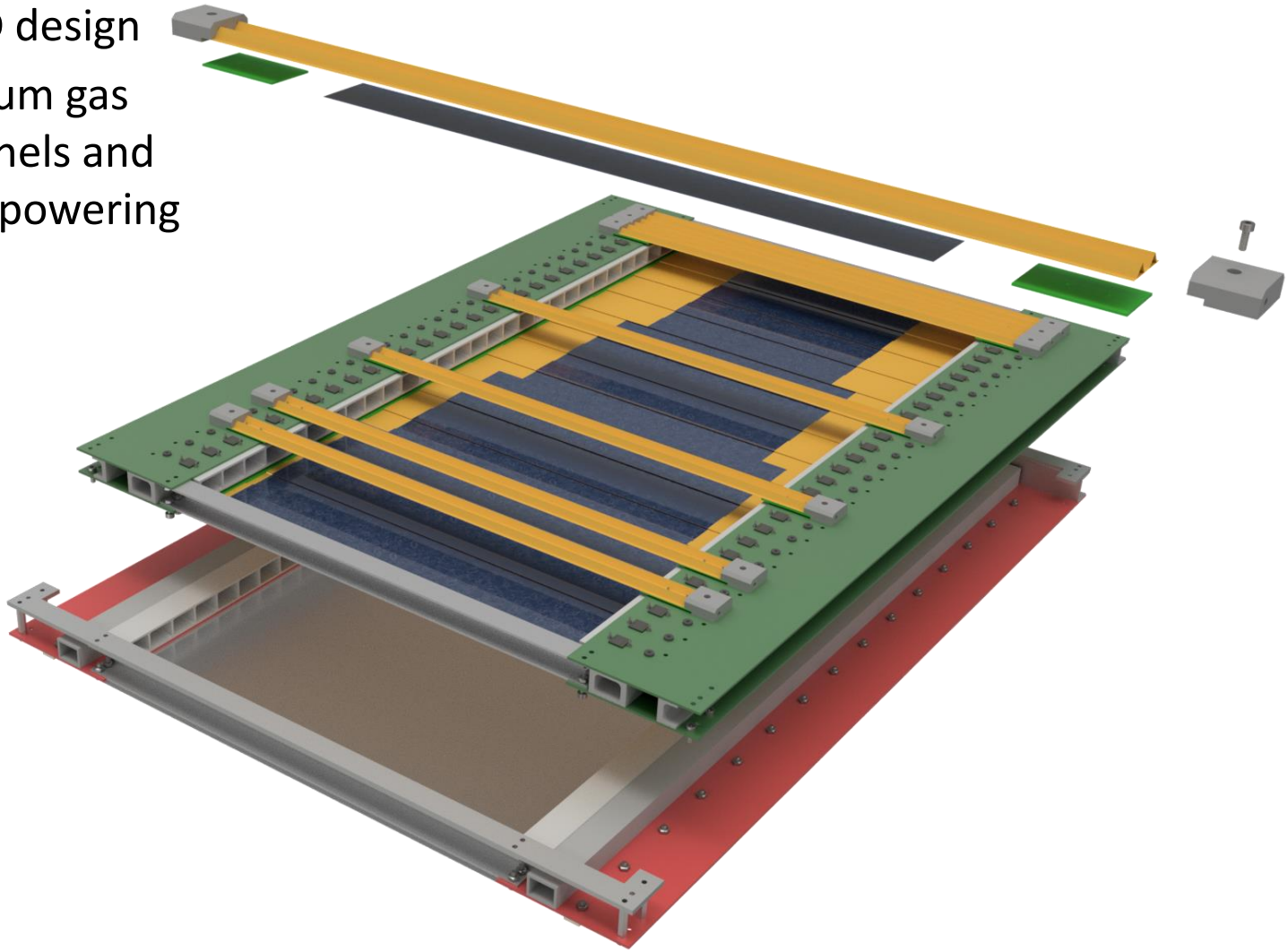

- CFD simulation of helium gas cooling
- Can keep temperatures at a safe level for the sensors
- Large gradients

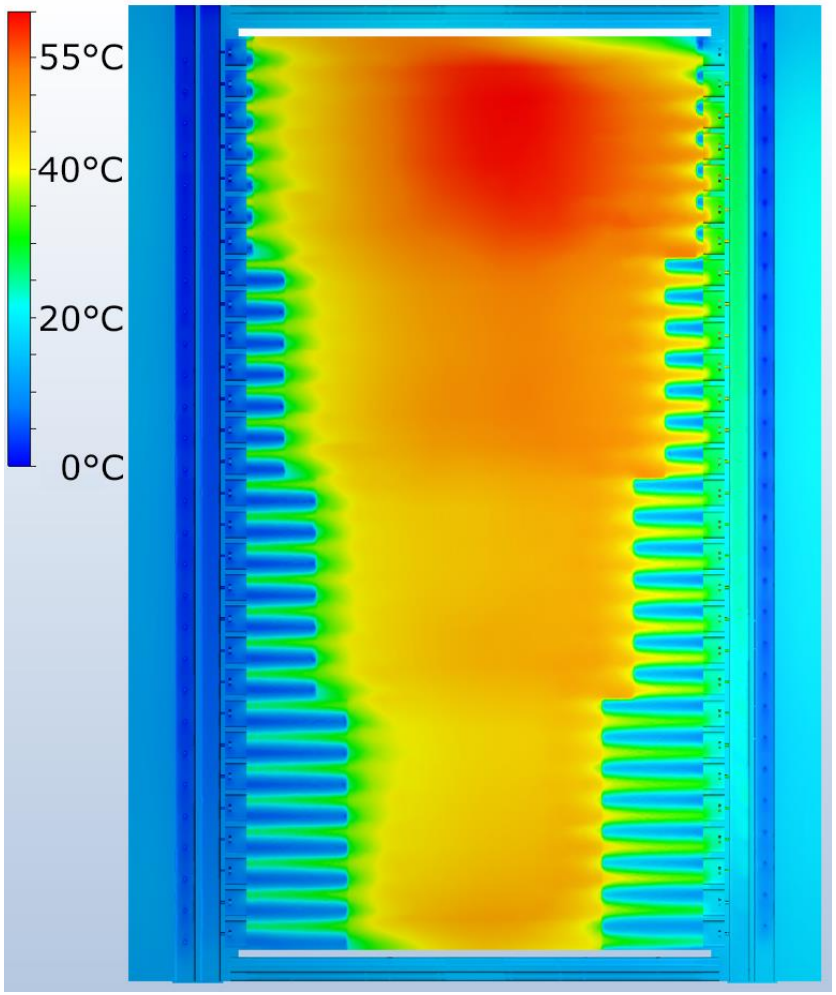

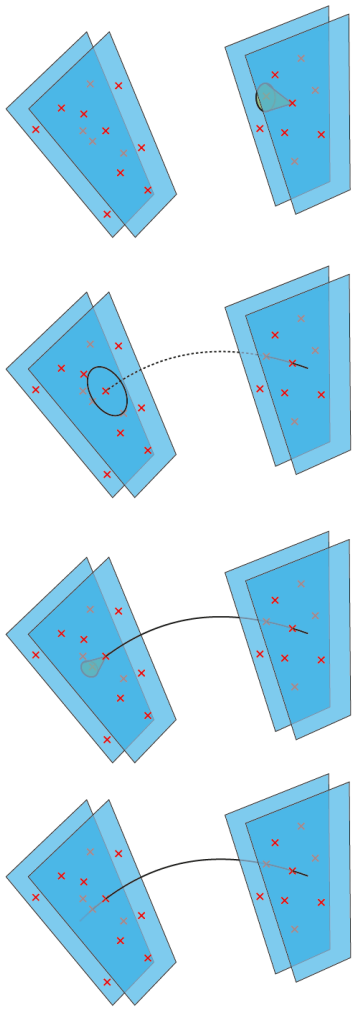

- Parametrization-based track finding
- Robust up to nominal electron rate

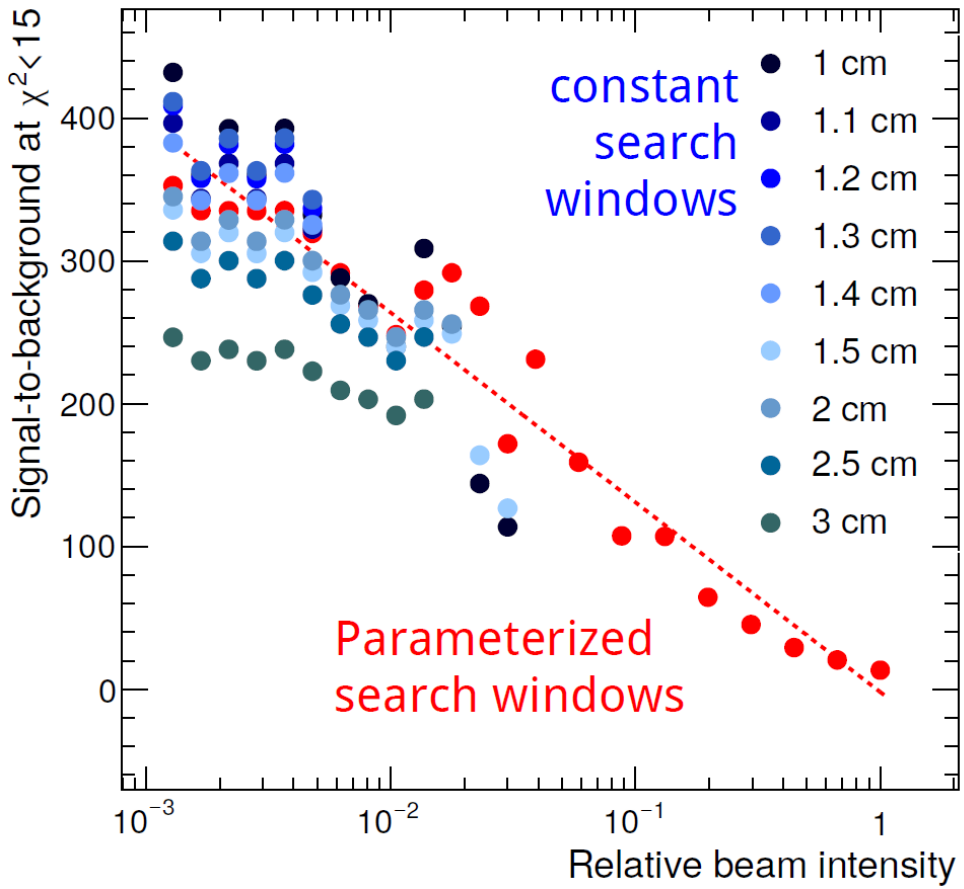

- Complicated by inhomogeneous magnetic field in tracker region
- Use a general broken lines algorithm with a Rung-Kutta-Nyström propagator
- Resolution well sufficient for a good Q^2 reconstruction

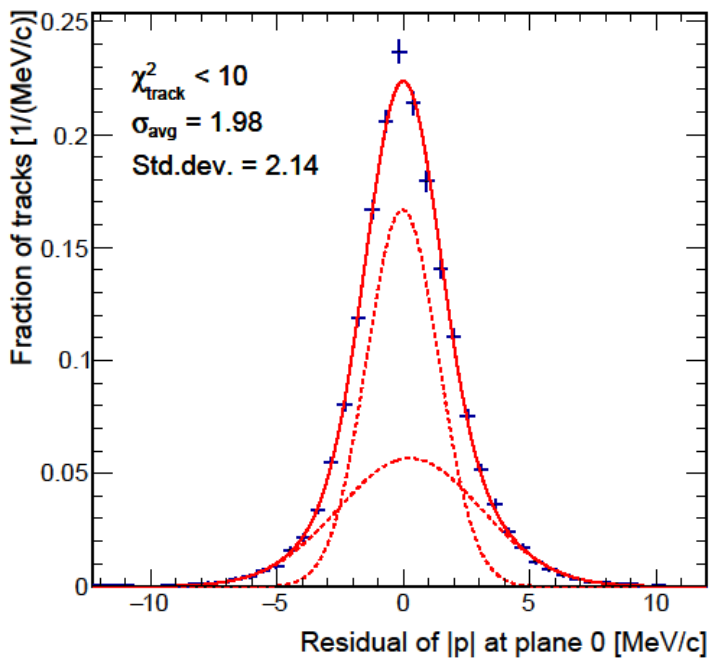

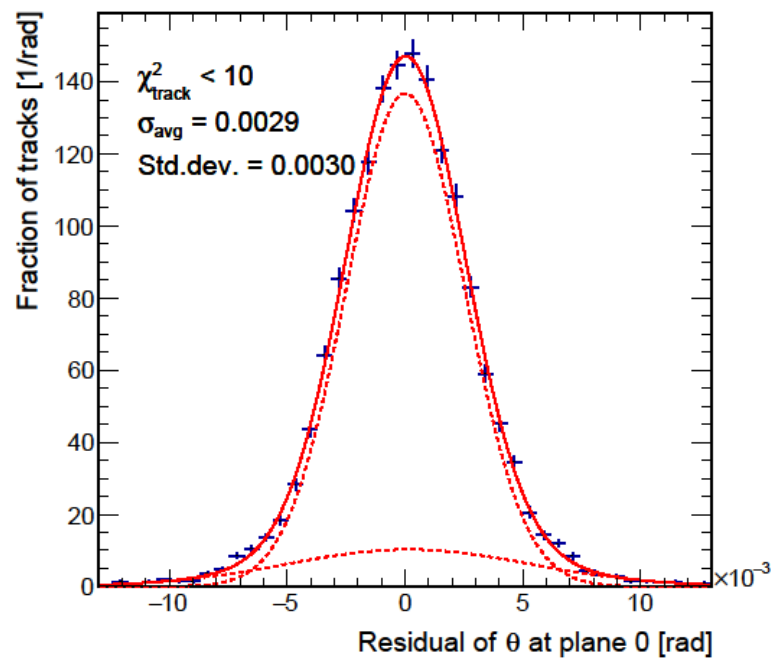

- Heatable single-strip prototype with temperature sensors
- Measurements in good agreement with CFD simulation

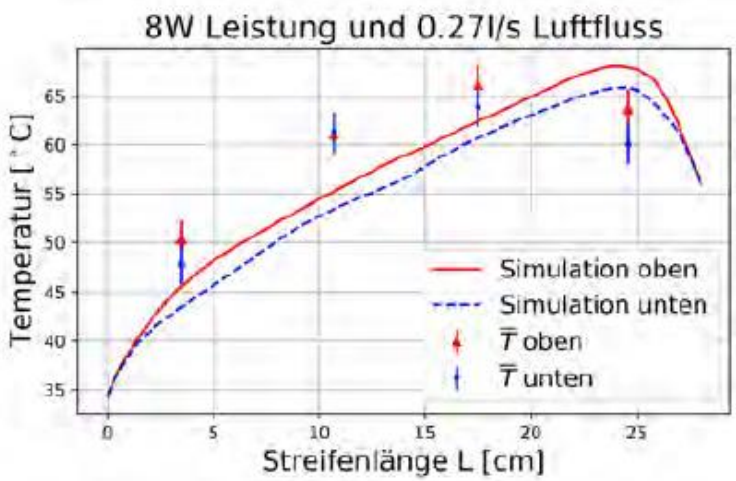

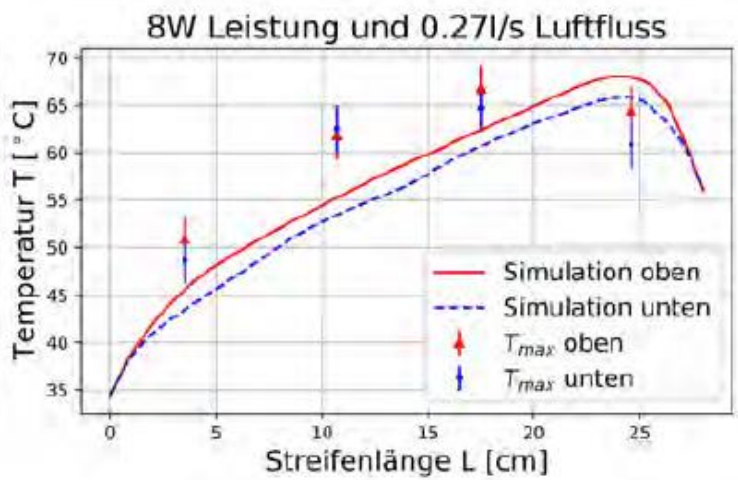

- Full-scale heatable tracker module
- Helium box
- Currently under test

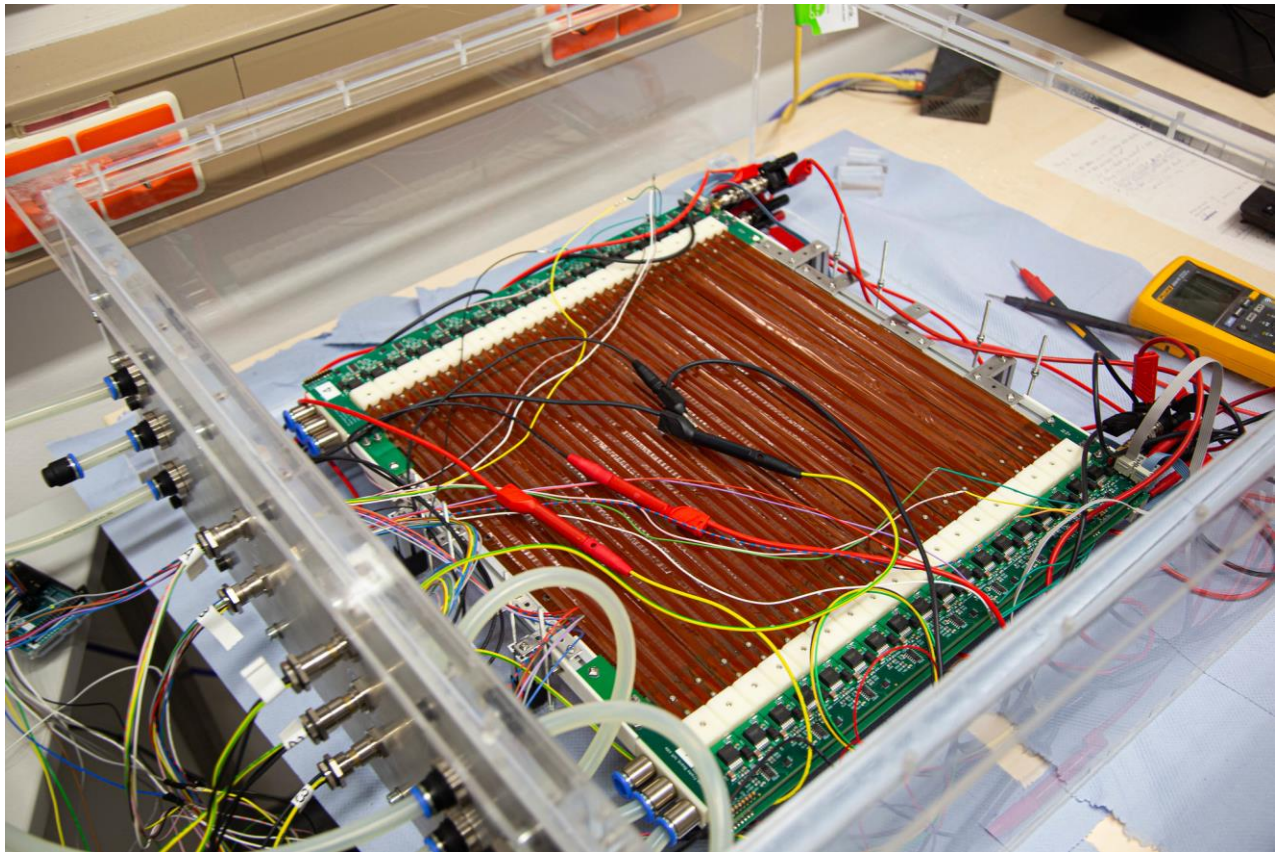

- Reconstructed Q^2 is strongly affected by effects in target:
- Effects need to be well modelled
- Radiative corrections to hard scattering: Incorporate theory calculations
- Multiple Coulomb scattering in hydrogen: various models in GEANT4 to be evaluated against data
- Unfolding of the resulting distribution: develop algorithm

- Transport data out of the detector
- Sort in time and space
- Find tracks online
- Based largely on the experience in the Mu3e experiment

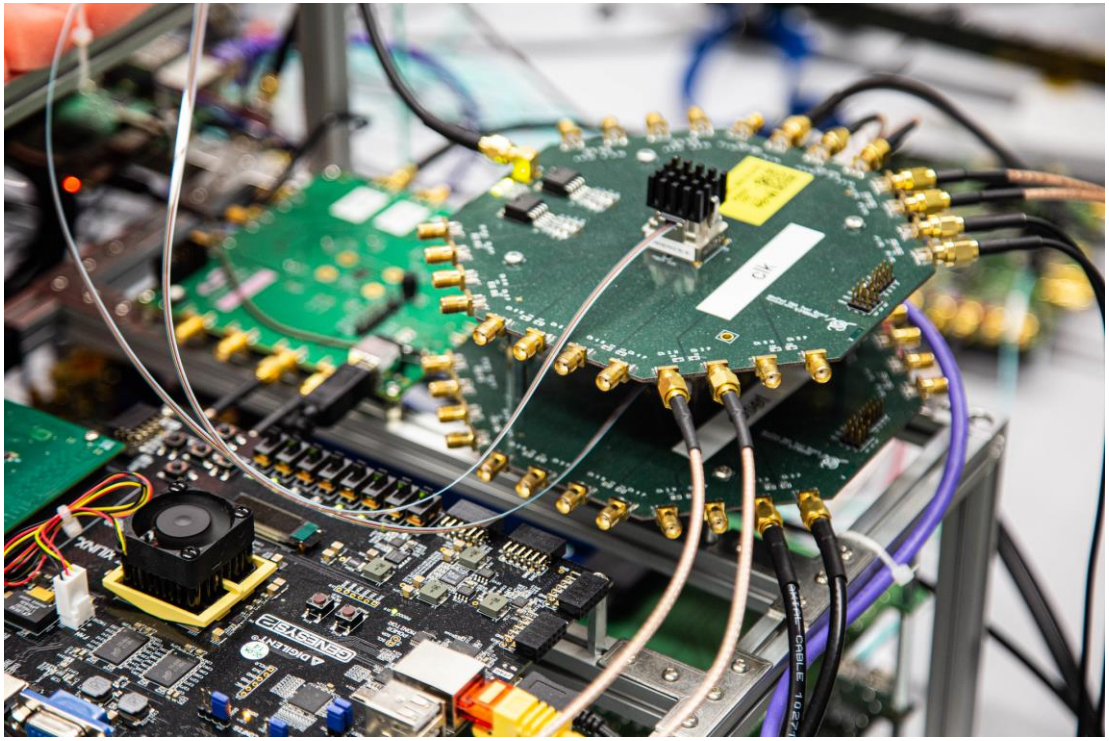

False asymmetries

Apparative (false) asymmetries:

Extreme good control of beam and target

Flip Helicity fast

Extra spin flip

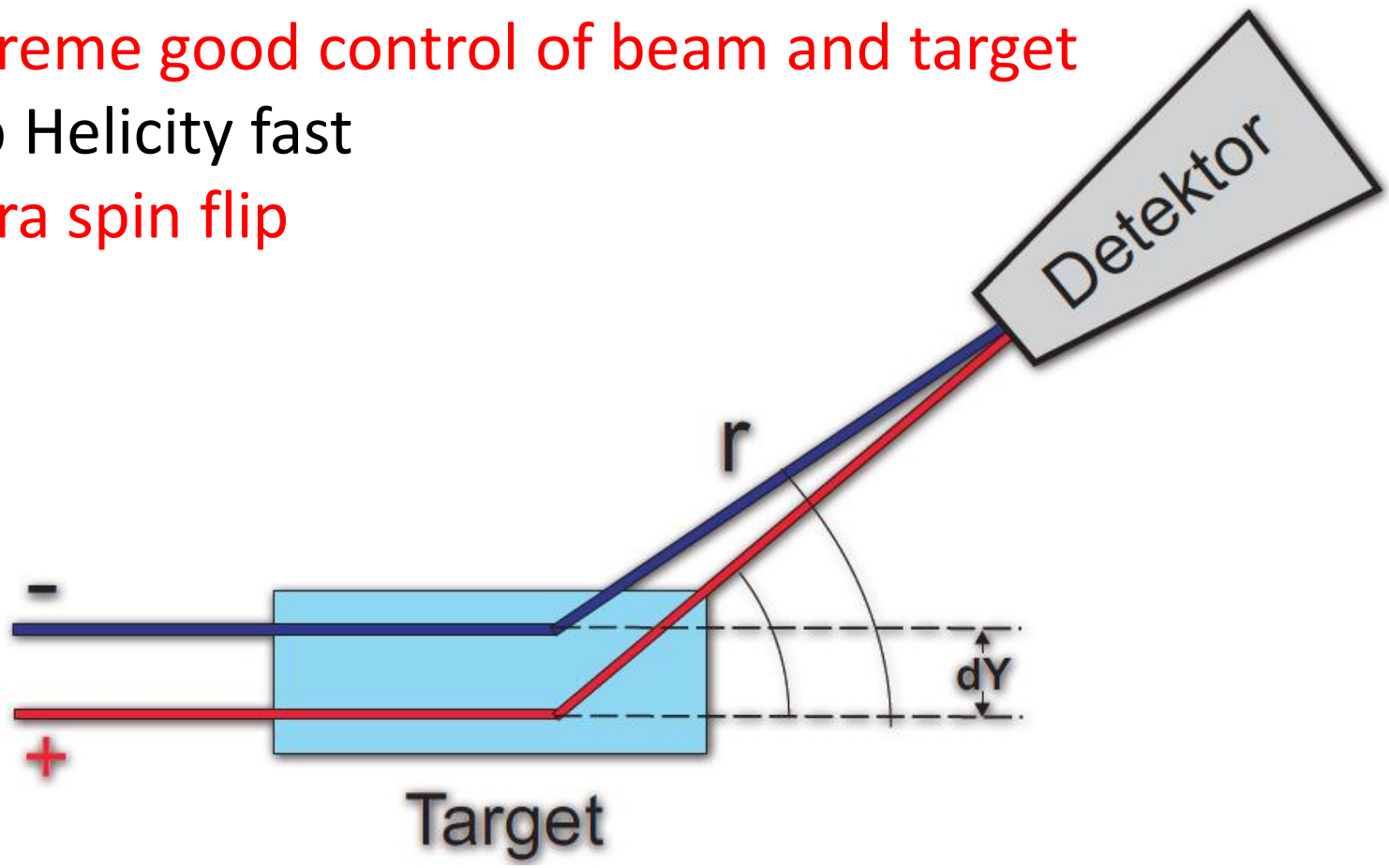

- >10 years of experience of beam delivery to a parity violation experiment

Systematics of A4 @210MeV, extrapolated to 10000h of data taking:

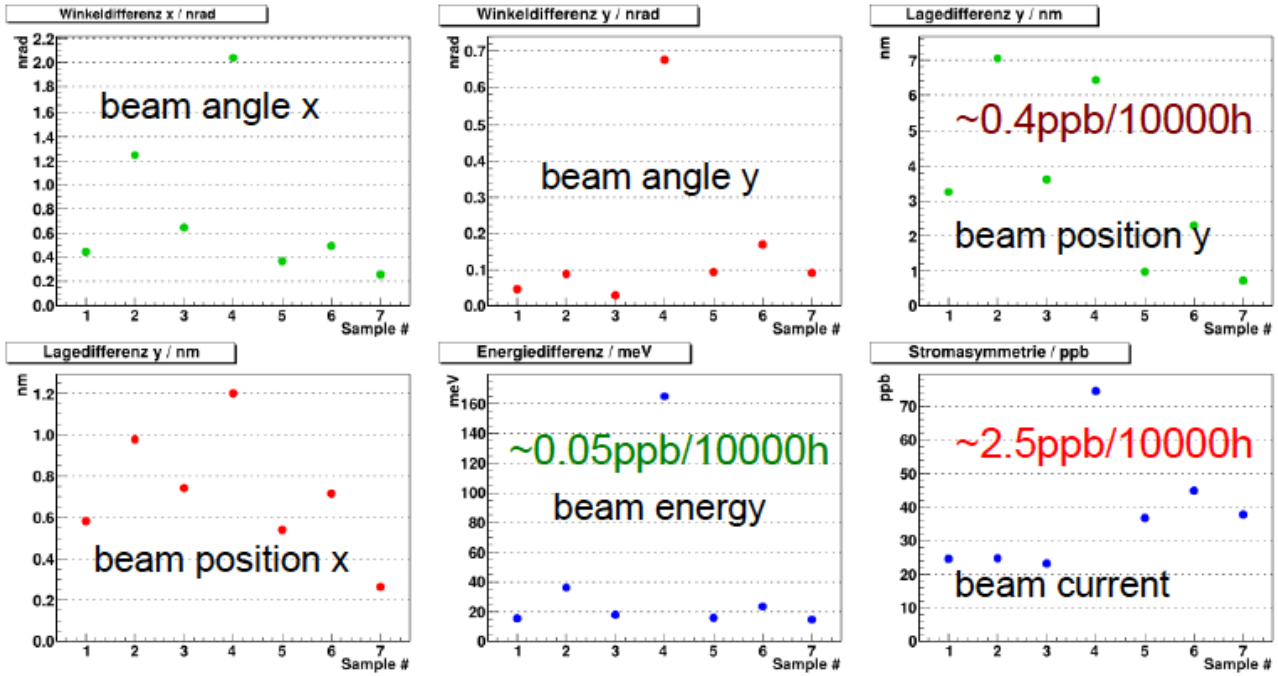

Need to improve by factors of 10 ~ 100, in total *max. 0.1ppb*!

dedicated simulations for P2 in preparation

- cavity monitors measure beam position (XYMOs)
- steering magnets correct beam direction (WEDLs)

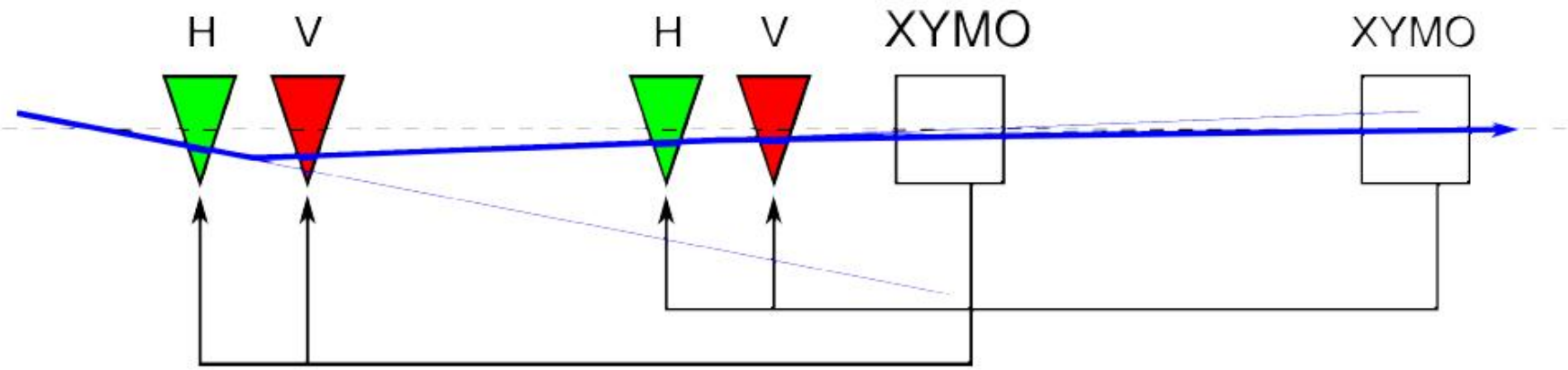

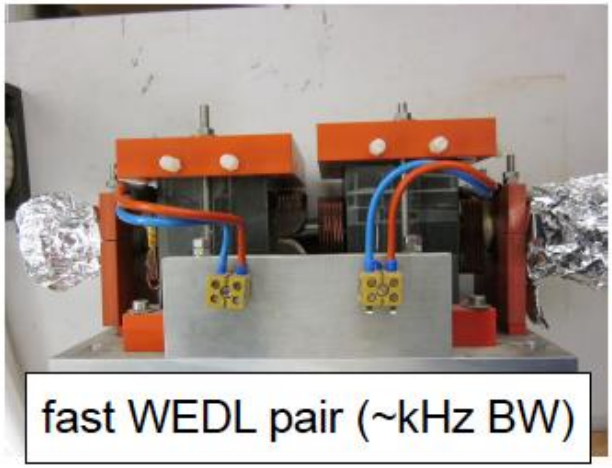
fast WEDL pair (~kHz BW)


slow WEDL pair (~Hz BW)


XYMO (sub-μm resolution)

For suppression of helicity correlations (ppb level!):

- measure helicity correlations (stabs off) → feed forward parameters
- turn on feed-forward (suppress correlations) → $A_i \rightarrow 0$
- turn on feed-back (reduce uncorrelated noise) → $\Delta A_i \rightarrow 0$

First demonstration using outdated FPGA evaluation board:

- fast WEDLs can do at least ±24μrad in <10μs @150MeV
- need to test this with beam!

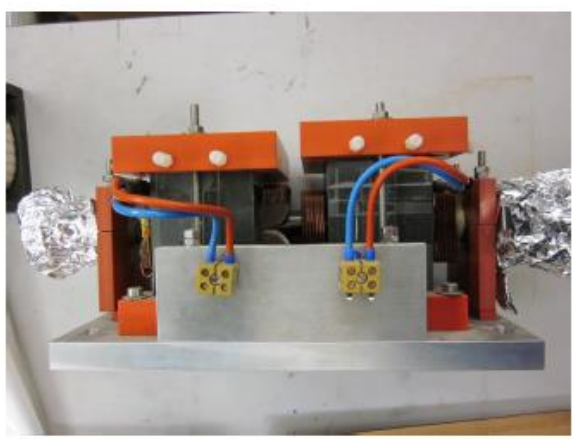

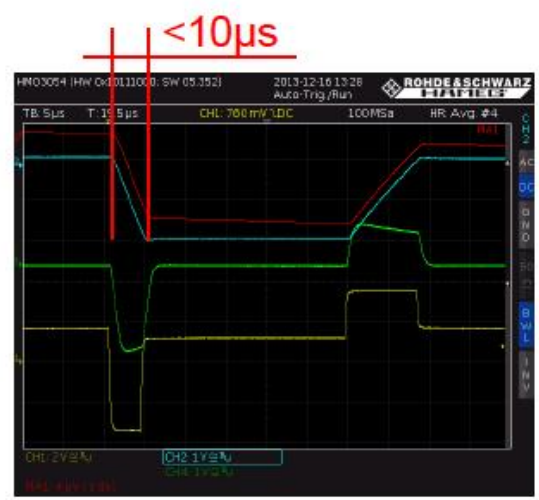

PCs for runcontrol, electronic logbook (ELOG), and data storage

embedded PC (stabtrig) Spartan-6 FPGA board with IP cores for i2c and trigger

Zynq7000-based DAQ boards
2 ADCs, 2 DACs each, all 125 MSa/s

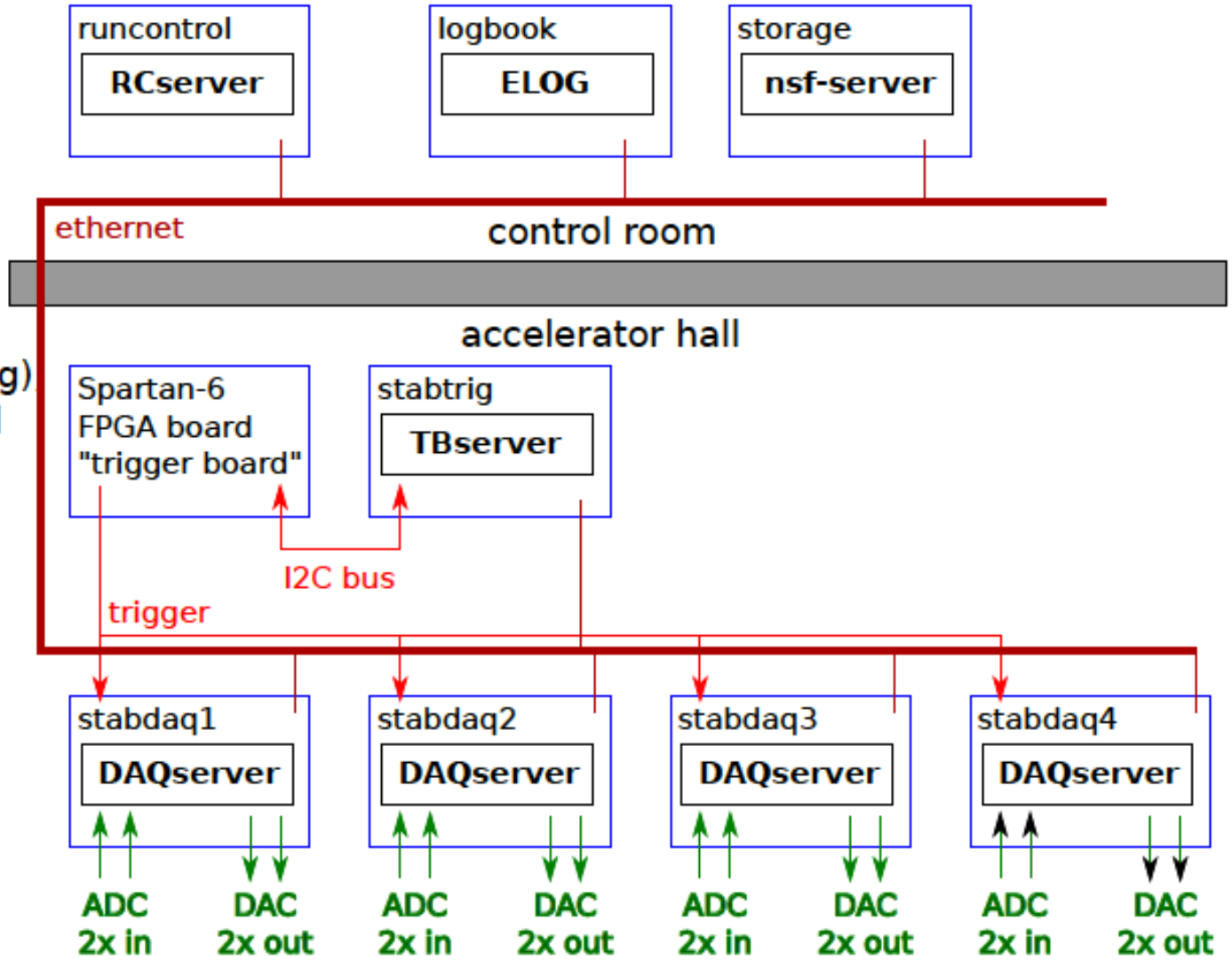

ADCs and DACs for readout and control of beamline elements: XYMOs (beam position monitors), fast steerers

- gain experience steering <200 MeV beam through s.c. solenoid
- operate beam position / angle stabilization “across” solenoid – modifications to control loop?
- prob. use 3Tmax. s.c. solenoid (fallback solution: 5T from A2)
- most realistic test of polarimetry+beam stablization for P2 possible before MESA put into operation

5 T max. (in use in A2 experiment)

3 T max. (available)

First digital beam stabilization tests for P2 with 180MeV@MAMI

- using RedPitaya internal PID blocks (used only PI)!
- not yet optimized transfer functions!

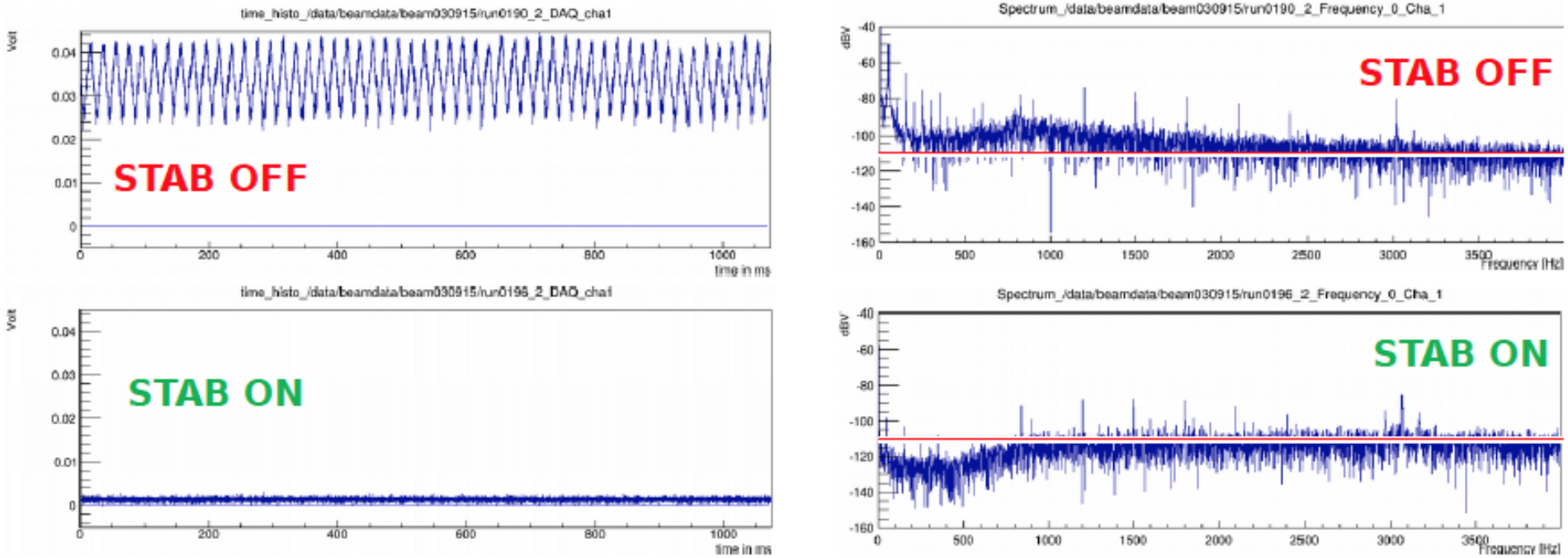

- **-50dB @50Hz, -50 dB @100Hz, -20dB @1000Hz**
  (A4/MAMI: -40dB@50Hz)

PhD thesis Ruth Herbertz

Planned Setup Beam Control in MESA

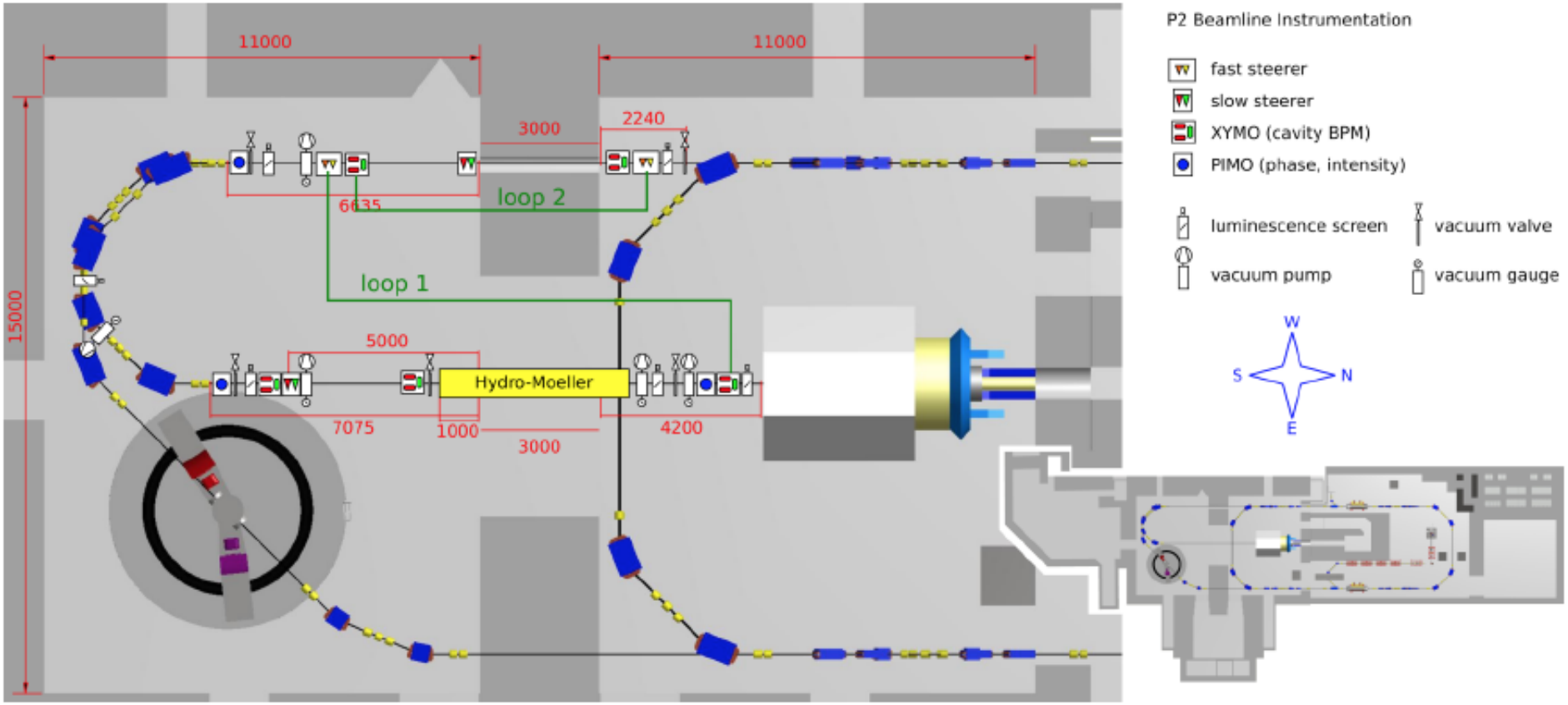

Asymmetry Uncertainties Results

JOHANNES GUTENBERG UNIVERSITÄT MAINZ

Expected Asymmetry Uncertainties after 10kh measuring time at 150µA

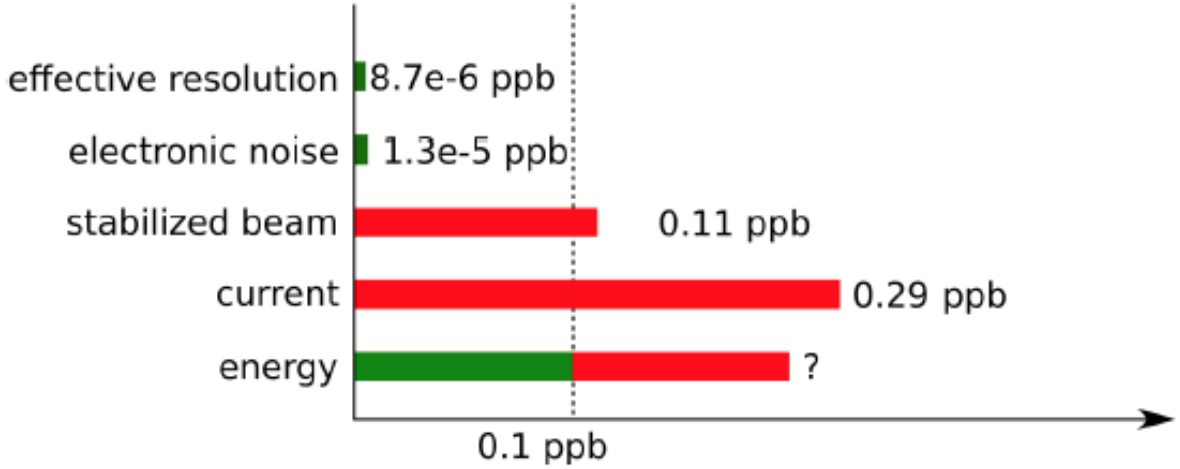

- Position and current based on signal widths measured in Tests at MAMI
- Scaled to 150µA in 10kh and averaged over 8192 samples of 8ns.
- Energy asymmetry is estimated from A4 data. 0.1 ppb feasible but not yet demonstrated. Relative energy width of 10^{-5} needed.

ACCELENCE

Polarimetry

Double scattering polarimeter

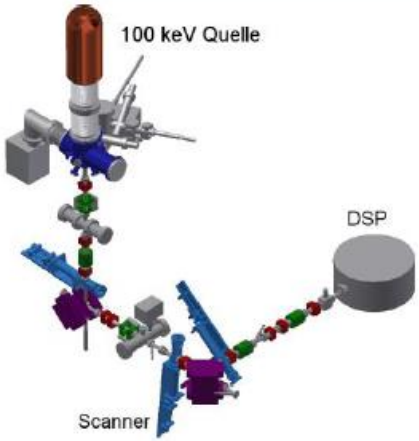

DSP: opened top flange

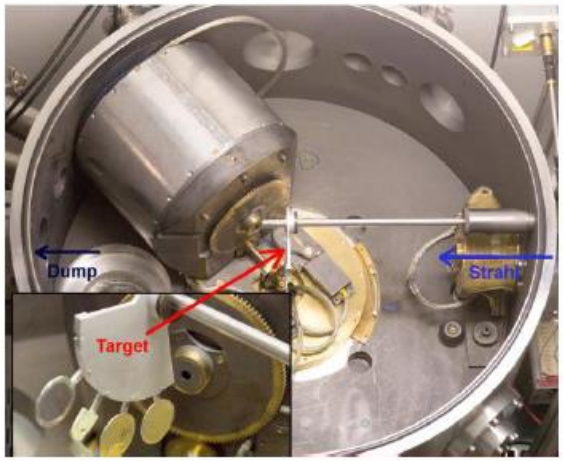

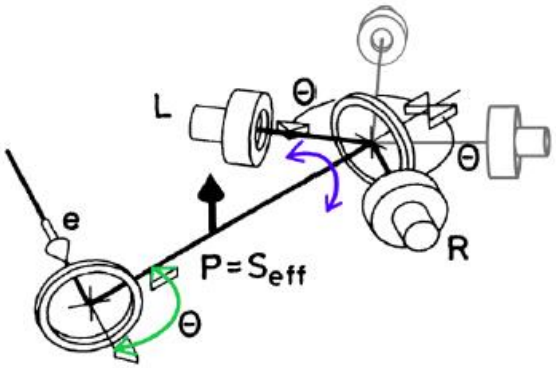

Dicke Targets

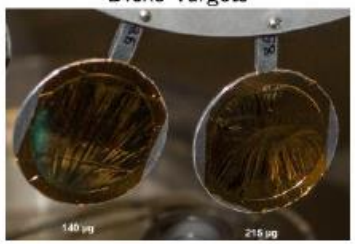

Dünne Targets

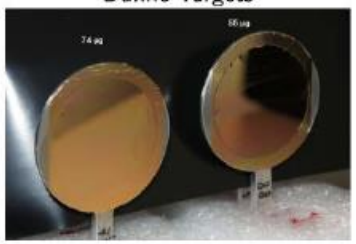

- Für $S_T = S_{eff}$ (unpolarisiert): $A = \frac{N_L - N_R}{N_L + N_R} = S_T S_{eff} = S_{eff}^2$

Double scattering at two foils,
35 nm gold thickness

ca. 1900 measurements a 60 s
~ 164 h measurement time

A = 9,25 +- 0,06 %
dA/A = 0,66 % (statistical error)

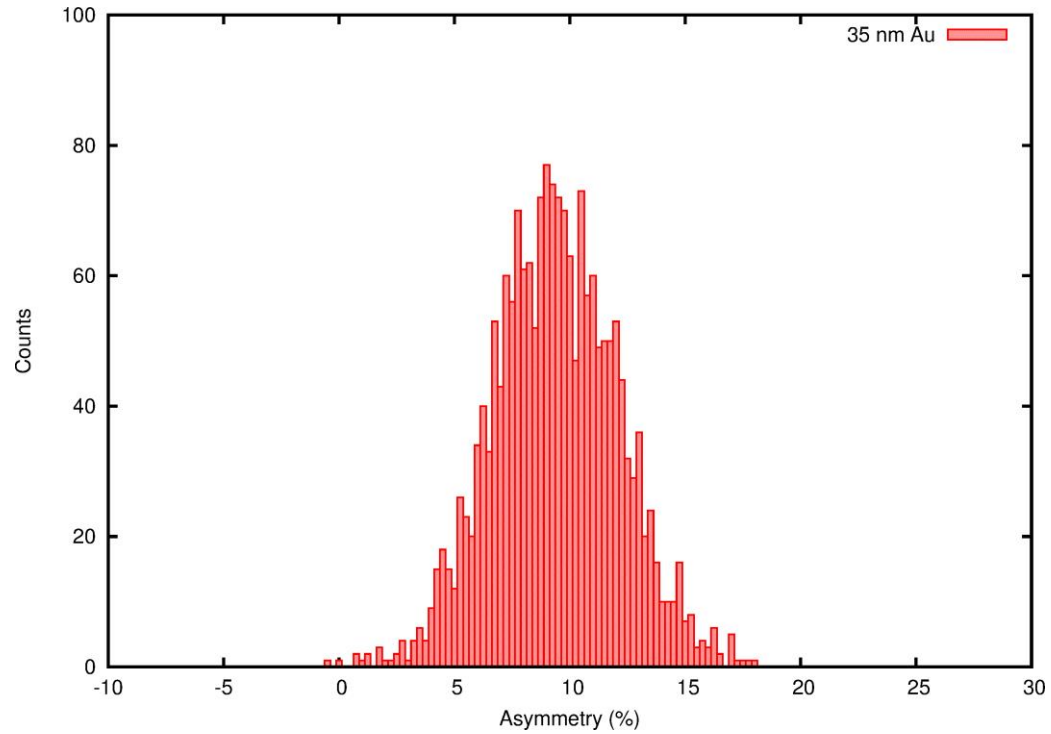

Analyzing power calibration could be feasible at the <1% level (or even better)!
Open questions: Target stability (radiation damage!), reproducibility, consistency checks,

Hydro Moller Polarimeter

The promise:(*)

- **Hydro-Möller: Atomic trap with completely electron-spin polarized Hydrogen**
- **Online capability, high accuracy (<0.5%)**
- **Statistical efficiency approaches 0.5% in 2 hours (Target: $3*10^{-16}$ cm^{-2})**
- **Acceptance similar to conventional Möller**

(*)E. Chudakov, V. Luppov: IEEE Trans. Nucl. Sc. 51, 1533 (2004)

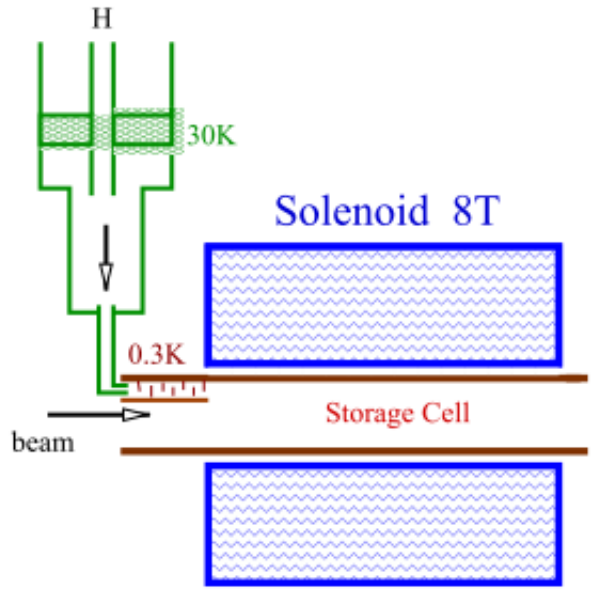

Complete trap with 77mm diam.
Cold bore 7T Solenoid
$\Delta B/B < 10^{-5}$ ($1cm^3$ Volume)(**)

(*): T. Roser et. al. NIM A **301** 42-46 (1990)
(**): W. Kaufmann et. al. NIM A **335** 17-25 (1993)

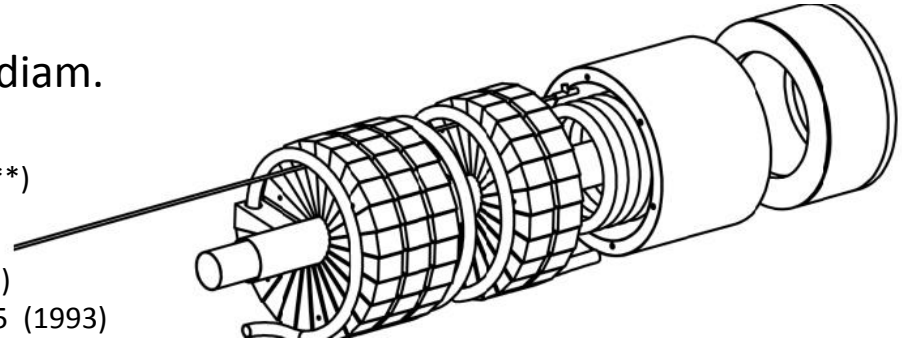

1.1K Stage heat exchangers
Presently in fabrication in KPH Machine shop

Patricia Bartolome, Valerie Tyukine

Module	Ready	Status	Remarks & Problems
Cryostat housing	End 2014	R&D Construction	Con: Using Super-MLI Accurate positioning of solenoid
Stage 1.10 K	End 2014	Development Construction	HT-HE Pre-HE LT–HE Valves
Stage 0.25 K	End 2015	R&D	Final-HE Mixing Chamber Film burners Technologies not yet under control!
Hydrogen feed system	End 2016	R&D	Literature references Transition unit not ready
Super conducting solenoid	End 2014	Test	
Detection system		R&D	Collaboration ?
Pumping system	Summer 2016	Not yet funded	^{3}He Still ^{4}He Evaporator ^{4}He Separator ^{4}He Pre–HE
^{3}He - Filling	End 2016	Not yet funded	Volume = 200 l STP
Target test	End 2017		

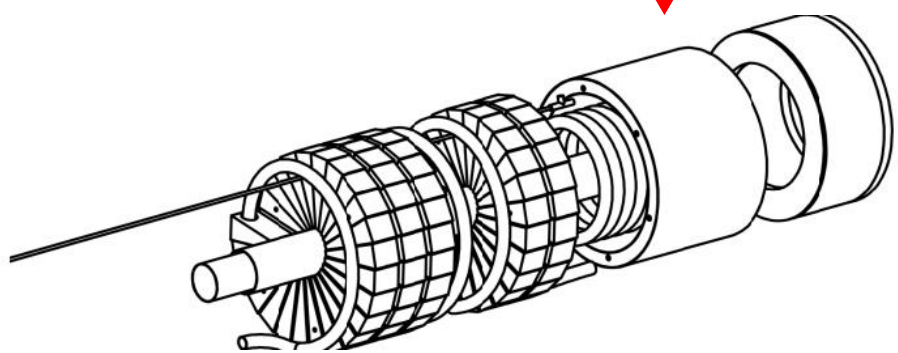

1.1K Stage heat exchangers

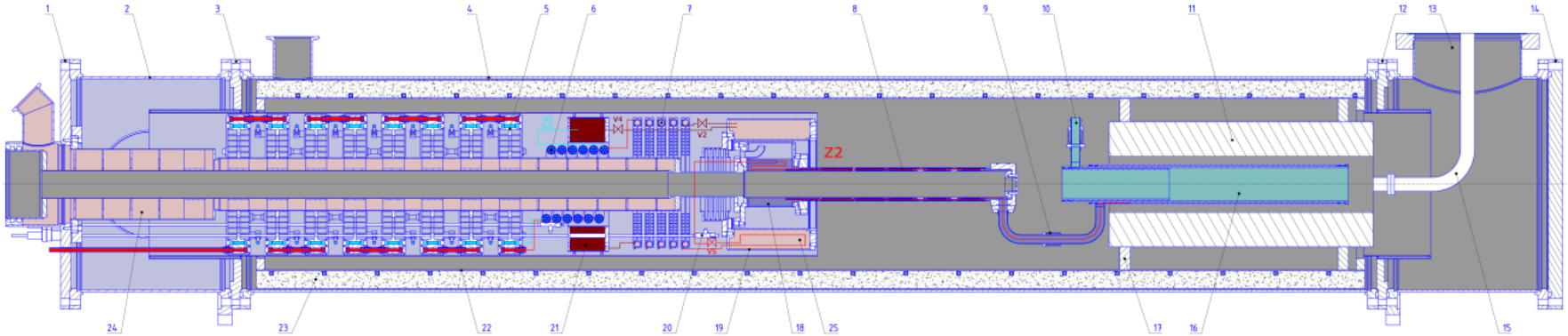

Detail X 90° gedreht

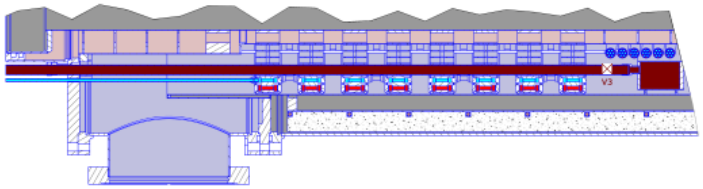

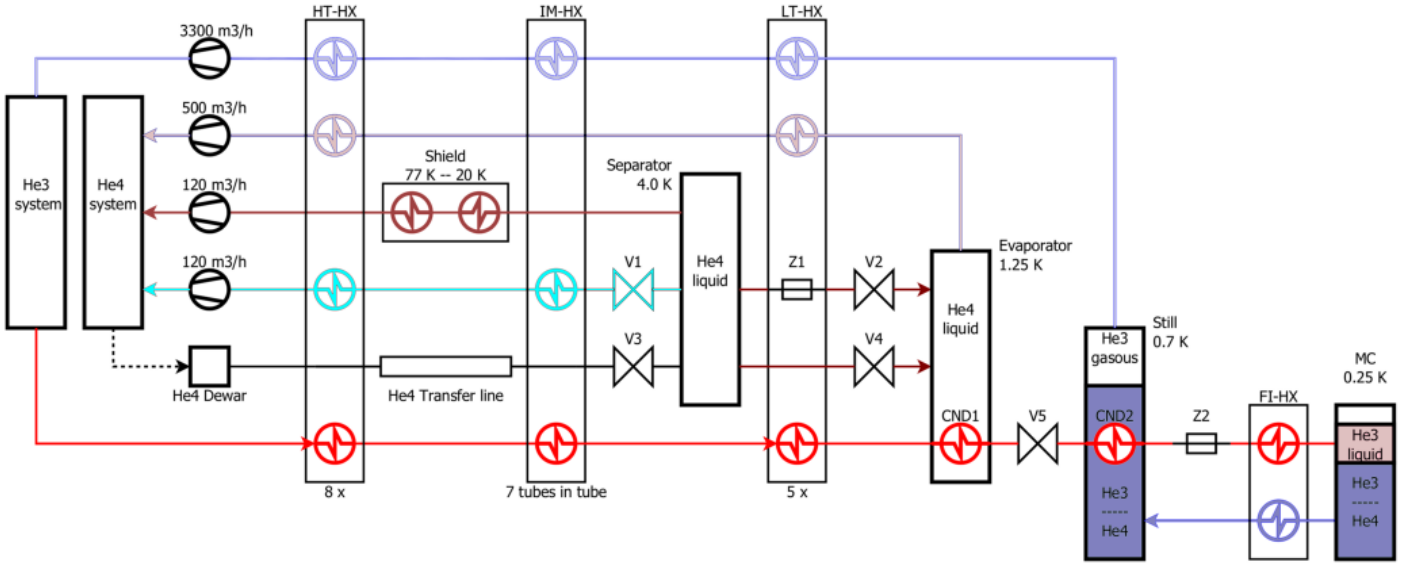

Baugruppenübersicht

Nr.:	Bezeichnung	Z. - Nr.:
1	Mainflansch	
2	Crosspiece	
3	Between flange Cryostat	
4	Case	
5	High Temperature HX	
6	Intermediate HX	
7	Low Temperature HX	
8	Final HX	
9	Flinburner	
10	Double-sided Flinburner	
11	Solenoid	
12	Between flange Solenoid	
13	T - piece	
14	Output flange	
15	He4 - connections	
16	Mixing chamber	
17	Thermally insulated mounting	
18	Still	
19	Evaporator	
20	Needle valve	
21	Seperator	
22	77 Kelvin - Shield	
23	M L I	
24	Evaporator pump line	
25	Condenser	

Maßstab: 1 : 2 | ACAD Version 2000

Nr.: C - 00-00-00-00

Cryostat Flow Diagramm

Stand Juni 2015

Z.-Nr.: 2403 - 0 Flow Diagramm

Double Mott scattering polarimeter (DSP)

- Goal $\Delta P/P = 0.3\%$, offline
- 2nd FP: functionality demonstrated
- several reasons for remaining systematic uncertainties identified
- 3rd FP: installation at MESA in 2020, (enabled by accelerated installation scheme) reduction of remaining uncertainties, and comparison with MP at 5 MeV,

Atomic hydrogen trap (Hydro-Møller)

- Goal $\Delta P/P = 0.5\%$, online
- 2nd FP: He3/He4 dilution cryostat designed, several parts already fabricated
- Accelerator lattice adapted for installation of detection system (chicane)
- 3rd FP: operation cryostat, trapping H-atoms and operation with beam

DSP-Schematic

A. Gellrich et al. Phys. Rev. A 43 (1991) 204

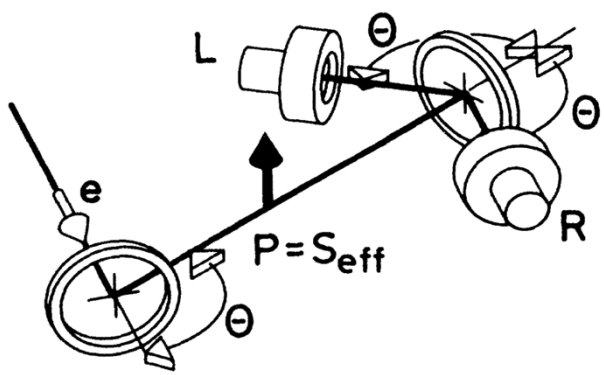

Hydro-Møller- Schematic

E. Chudakov and V. Luppov IEEE Trans. Nucl. Sc. 51 (2004) 1533

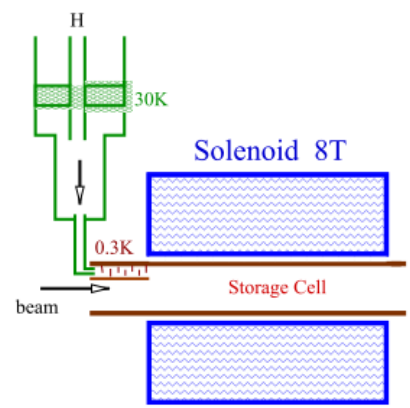

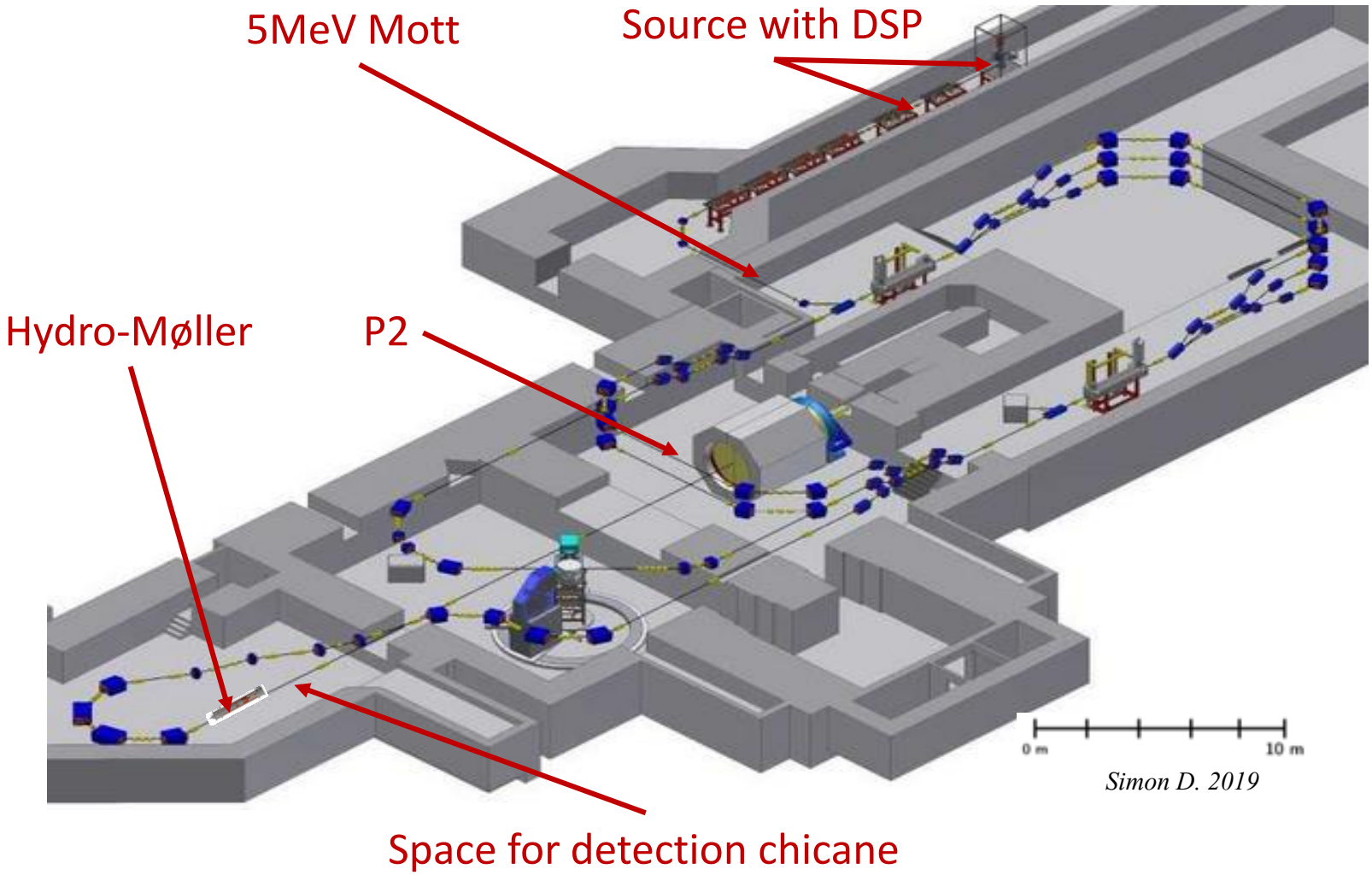
5MeV Mott
Source with DSP
Hydro-Møller
P2
0 m
10 m
Simon D. 2019
Space for detection chicane

DSP at 100ke

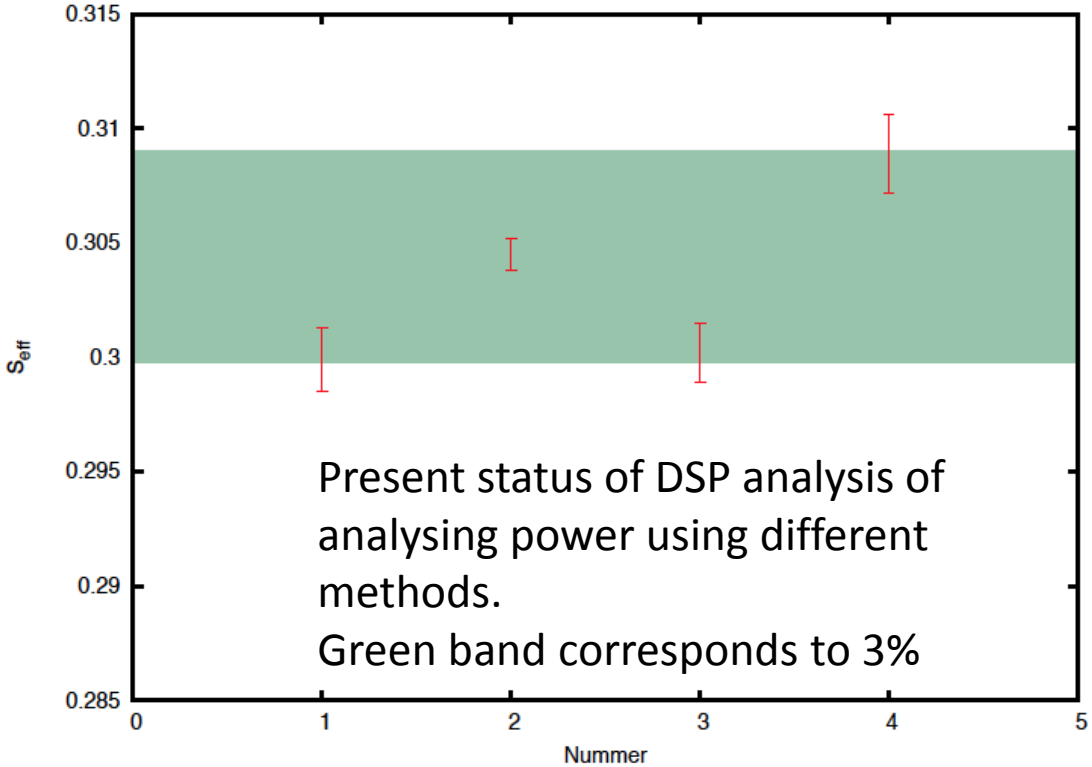

Present status of DSP analysis of analysing power using different methods.
Green band corresponds to 3%

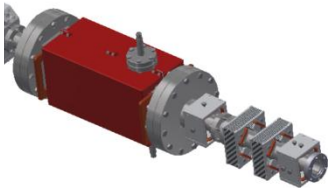

pen flange

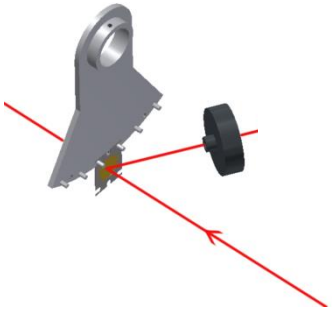

CAD rendering double scattering arrangement

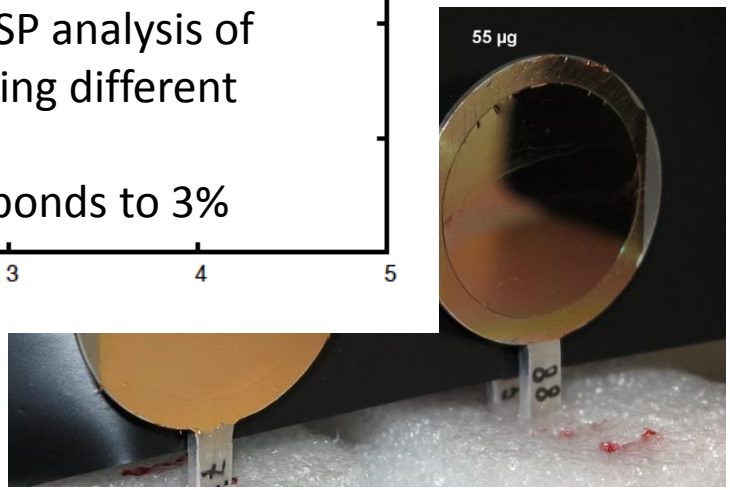

Targets used for calibration

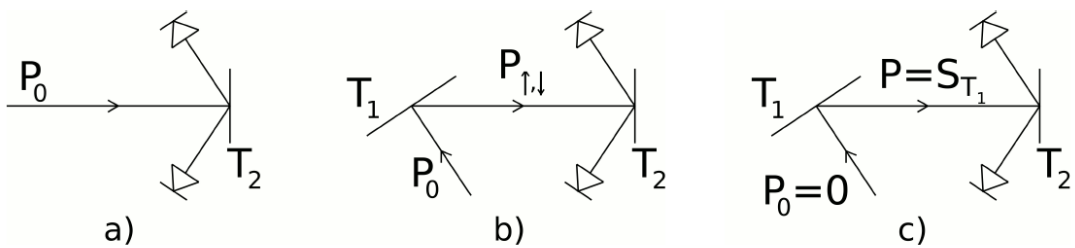

H. Hopster, DL Abraham, Rev. Scient. Instrum. 59 (1988) 49,
S. Mayer st al. Rev. Scient. Instrim 64 (1993) 952

3 arrangements, 4 experiments, 5 Observables, assuming P_0 can be switched to $-P_0$ resulting in $P_\uparrow$ and $P_\downarrow$ after the first scattering

$$A_0 = P_0 S_{eff,2}$$ ***a) Switch-Asym. second Target in pol. beam***

$$A_T = P_0 S_{eff,1}$$ ***b) Switch-Asym. first target in pol. beam***

$$A_\uparrow = P_\uparrow S_{eff,2} = \frac{S_{eff,1}+\alpha P_0}{1+P_0 S_{eff,1}} S_{eff,2}$$ ***b) Double scat. Asym for +P -beam***

$$A_\downarrow = P_\downarrow S_{eff,2} = \frac{S_{eff,1}-\alpha P_0}{1-P_0 S_{eff,1}} S_{eff,2}$$ ***b) Double scat. Asym for –P -beam***

$$A = S_{eff,1} S_{eff,2}$$ ***c) Double scat. Asym for unpol . beam***

α= Depolarisation in Target (only double scattering with pol. incident beam)

Cryostat design with several stages of heat exchangers, 3He/4He mixing circuit, superconducting solenoid and cold hydrogen dissociator

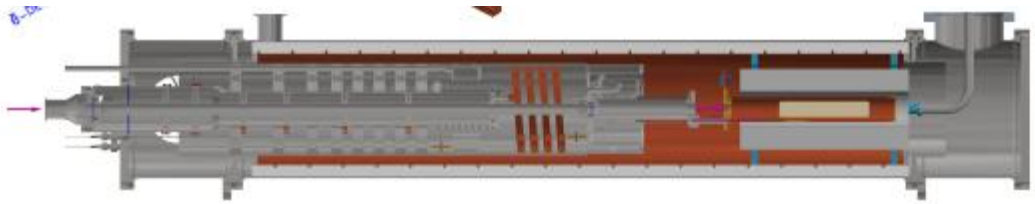

Thanks: N. Borisov, Yu. Usov (JINR), Ch. Keith, M. Lowry, E. Chudakov (JLAB), T. Niinikoski (CERN)

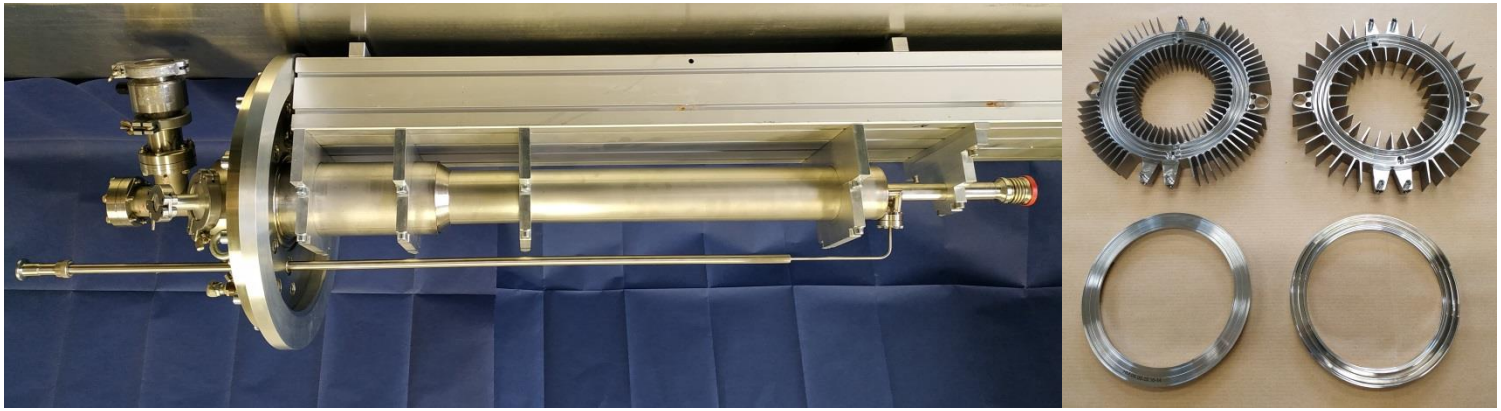

Left: Central piece of cryostat – "evaporator pump line", heat exchanger support . and beam pipe. Right: heat exchangers in "all welded" technology. Fabricated by KPH machine shop supported & several industry suppliers

Some estimations concerning polarization dilution:

Ideally, the trapped gas polarization is nearly 100 % ($\sim 10^{-5}$ contamination).

No Beam

- Hydrogen molecules $\sim 10^{-5}$
- Upper states $|c\rangle$ and $|d\rangle < 10^{-5}$
- Excited states $< 10^{-5}$
- Helium and residual gas $< 0.1\%$ - measurable with the beam

At 100.0 μA e-beam

- Depolarization by beam RF $< 2 \times 10^{-4}$
- Ion, electron contamination $< 10^{-5}$
- Excited states $< 10^{-5}$
- Ionization heating $< 10^{-10}$
- Expected depolarization $< 2 \times 10^{-4}$

Topic E: Polarimetry

Polarized source

Polarized source STEAM in it's operational position in Hall-3

-Standard operation 100kV with higher field as the MAMI operational source for better beam quality at P2 current.
-source high voltage test succesful, 165 kV achieved without problems.
-Beam test expected 12/2017

Topic E: Polarimetry

Double Mott scatterung polarimeter

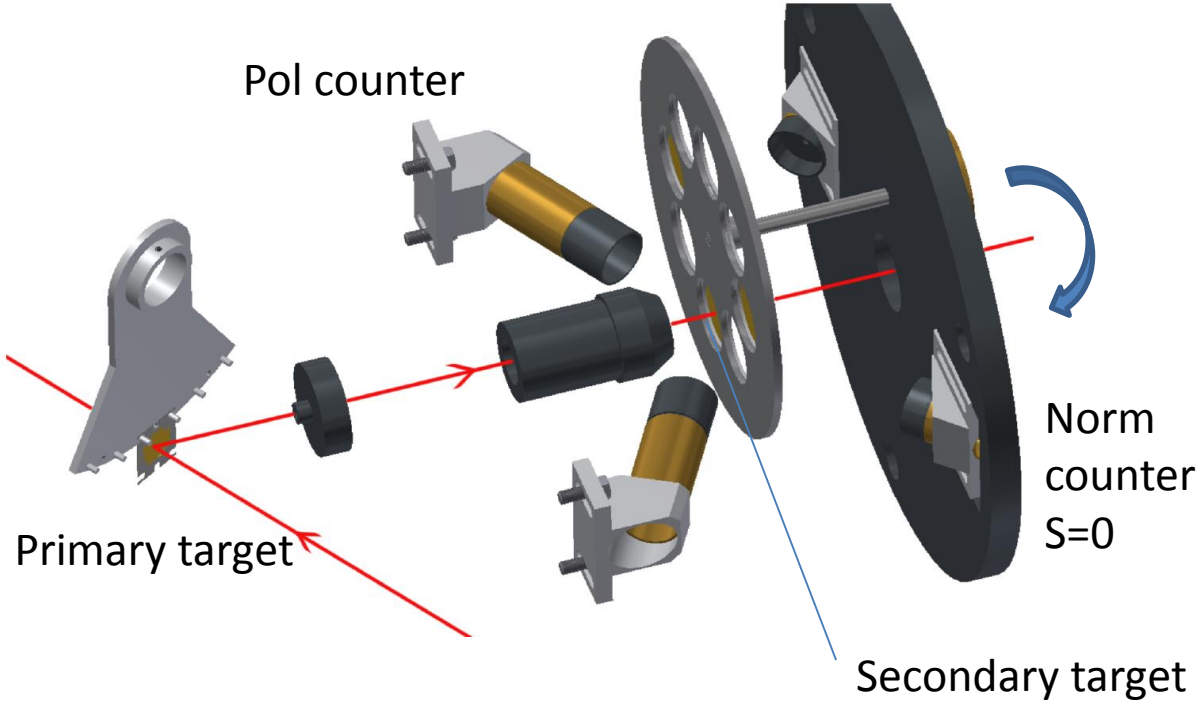

Magnification of double scattering chamber.

-Rotation of two polarization /normalization counters allows to obtain double ratio

- But normalization counters still needed, due to possible misalignment of of rotation axis and scattered beam axis
- Requires correct relative distance of polarization/normalization counters

Topic E: Polarimetry

Double scattering polarimeter - PhD work Matthias Molitor

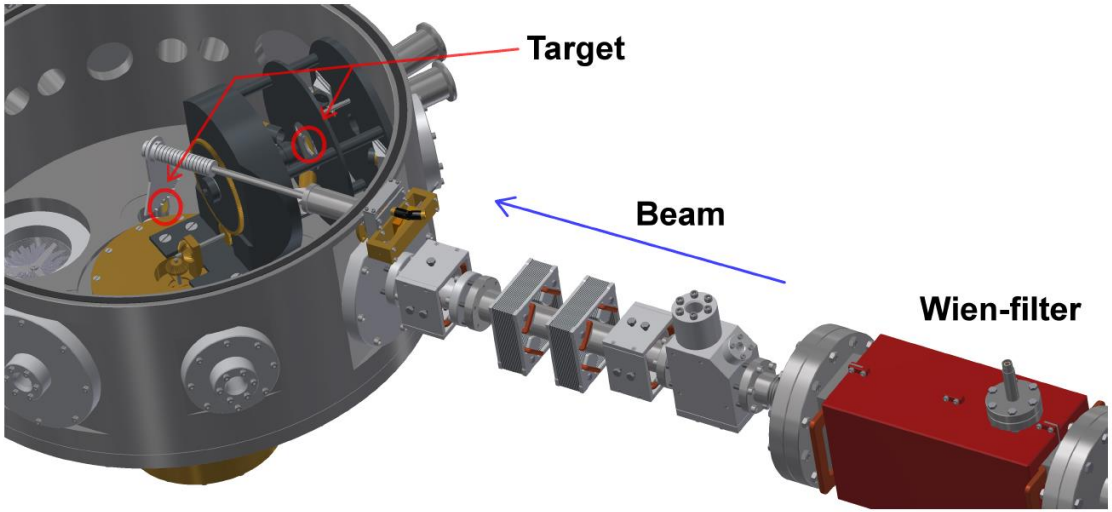

Systematic studies:

- Long term stability, reproducibility : o.k.
- Operation with olarized beam, + Wien filter allows to do different single/double scattering experiments with different directions of polarization.
- Redundant set of observables (5 Observables, four unknowns)
- Results in 5 independent methods to extract analyzing power: measurements done
- Depolarization factor not yet taken into account, **-- work in progress**

Calculation of the effective analyzing power in 5 different ways.

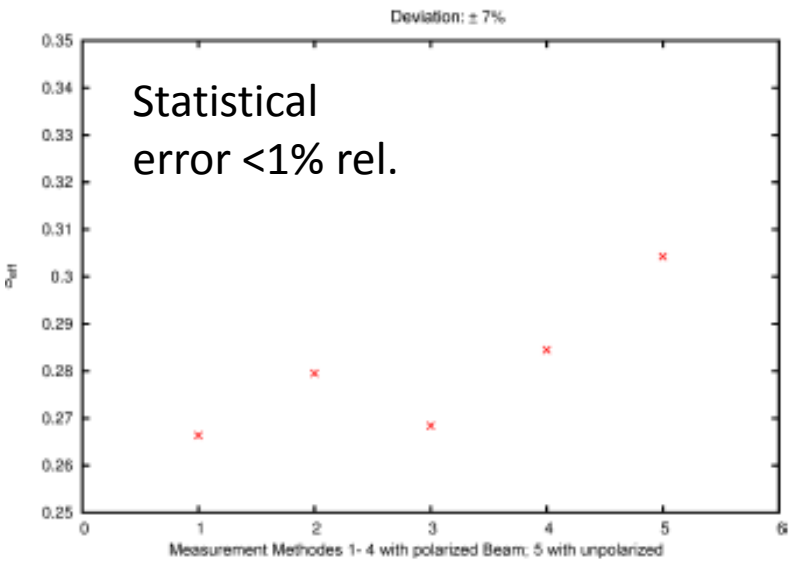

1 $S^2_{\text{eff}} = \frac{A_0}{A_T}\left[A_\uparrow(1+A_T) - A_0\right]$

2 $S^2_{\text{eff}} = \frac{A_0}{A_T}\left[A_\downarrow(1-A_T) + A_0\right]$

3 $S^2_{\text{eff}} = \frac{1}{4A_T}\left\{\left[A_\uparrow(1+A_T)\right]^2 - \left[A_\downarrow(1-A_T)\right]^2\right\}$

4 $S^2_{\text{eff}} = \frac{A_0 A}{A_T}$

5 $S^2_{\text{eff}} = A$

Hydro Möller

2 m long cryostat Engineering challenge!

refrigerator

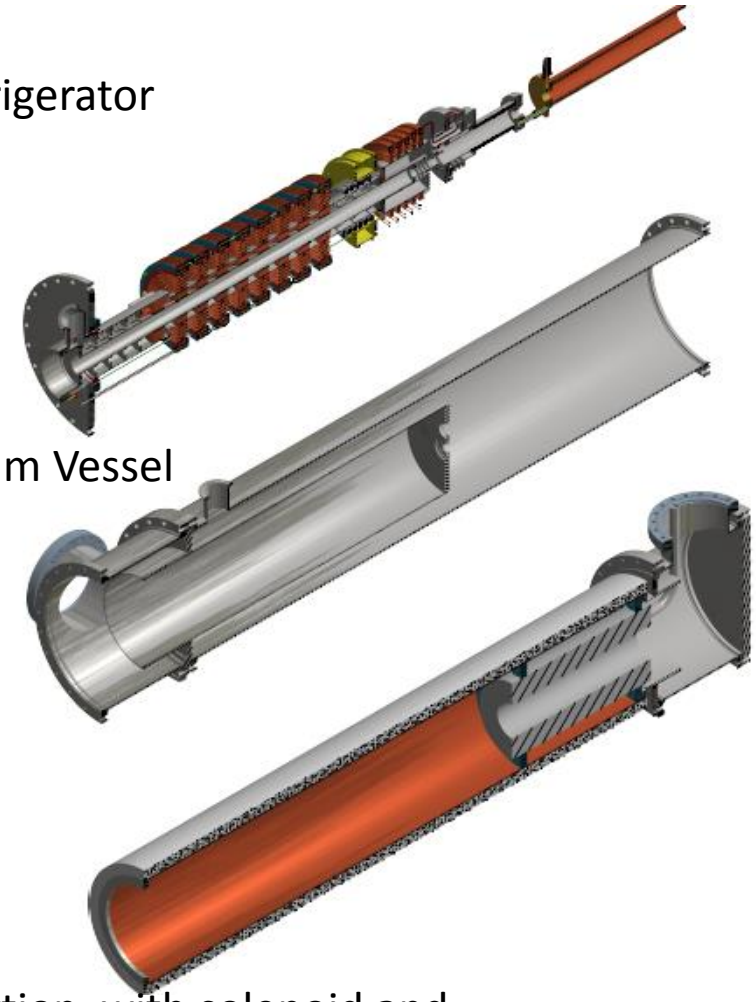

Vacuum Vessel

Insertion with solenoid and hydrogen injector

Design parameters

- Dilution Cryostat – Mixing He3 in He4
- $P_{cooling} \sim 60.0\,\mathrm{mW}$ at $T_{mc} = 0.25\,\mathrm{K}$ and $\dot{n}_{He3} = 22.5\,\frac{\mathrm{mmol}}{\mathrm{s}}$
- $P_{precooling} \sim 150.0\,\mathrm{W}$
- Insert (up)
- Housing (middle)
- Magnet and MLI (down)

Purchase of solenoid and pumping system
Possible if PRISMA+ is succesful.

Topic E: Polarimetry

Mott polarimeter at MESA at 5 MeV

Double Mott polarimeter at 100 KeV

Møller polarimeter with polarized iron target at 100 - 1600 MeV

New: Møller polarimeter with polarized atomic hydrogen target at 50 -1600 MeV
Nondestructive measurement

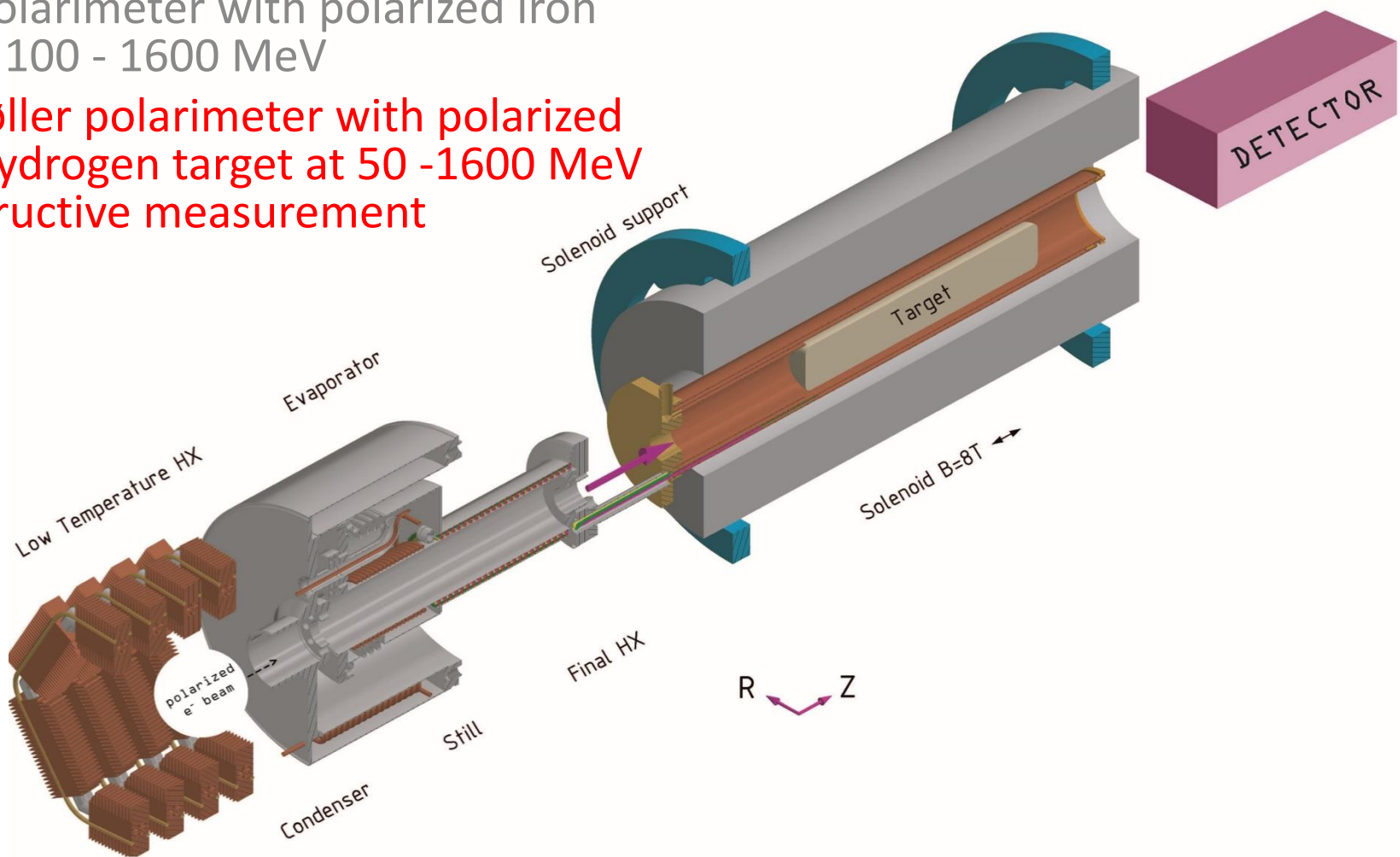

Topic E: Polarimetry

HT-HX from SS
complete welded system

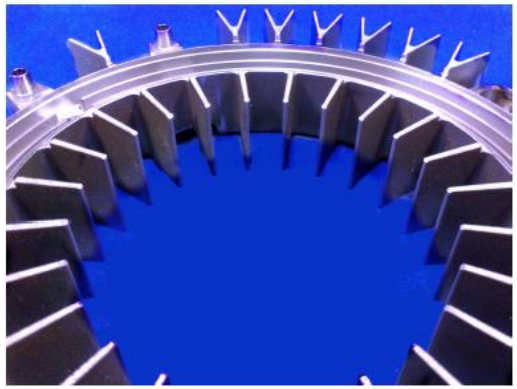

HT-HX from SS
before welding

Dimensions: $D196xH25$ mm, heat transfer between cold ^3He,^4He and warm ^3He

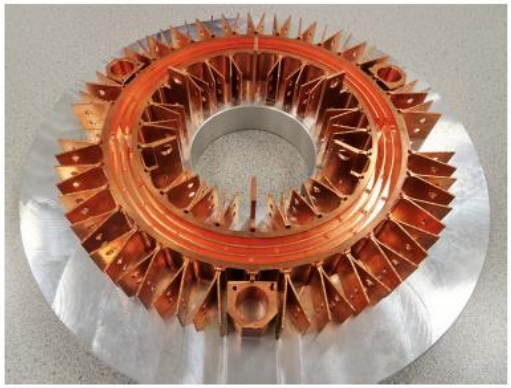

HT-HX plate before soldering

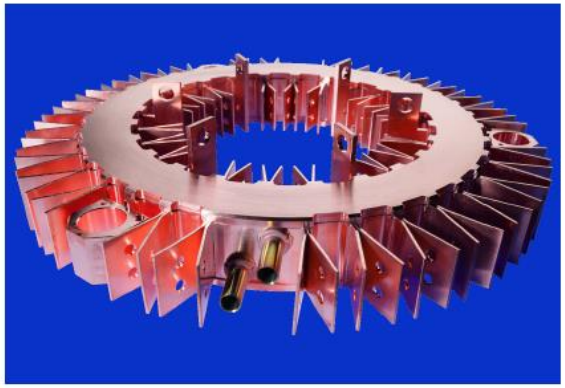

HT-HX from OFHC-Cu

Dimensions: $D196xH25$ mm, heat transfer between cold ^3He,^4He and warm ^3He

goals for the next funding period

- improve accuracy of DSP Mott polarimeter
- Design and construction of additional 5MeV Mott polarimeter for MESA, based on existing Mott at MAMI operating at 3,5 MeV (at present limited in accuracy by theoretical uncertainties)
- Build Hydro Möller atomic trap and test it with beam (MAMI beam useful)
- Assemble and commission MESA until end of funding period
  → first P2 beam at MESA by 2023.

Detector studies

Prototype tests @ MAMI

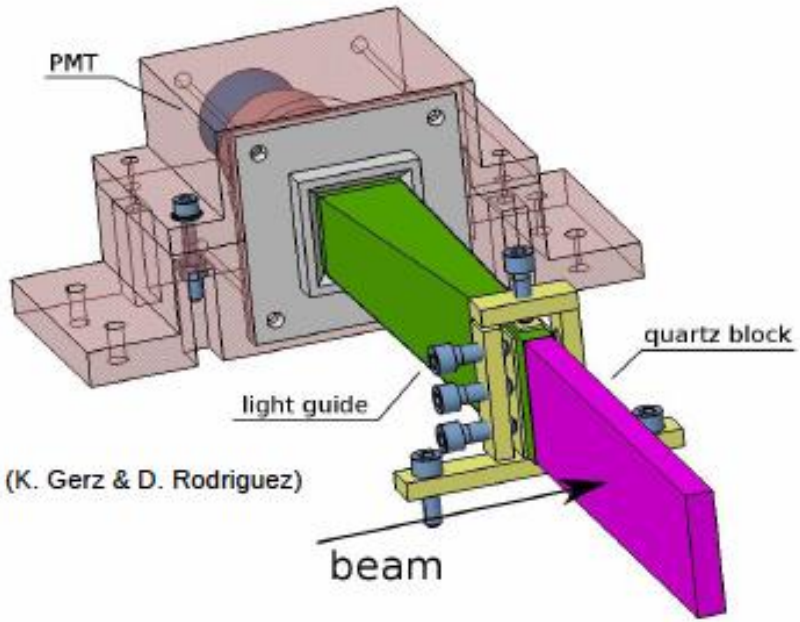

(K. Gerz & D. Rodriguez)

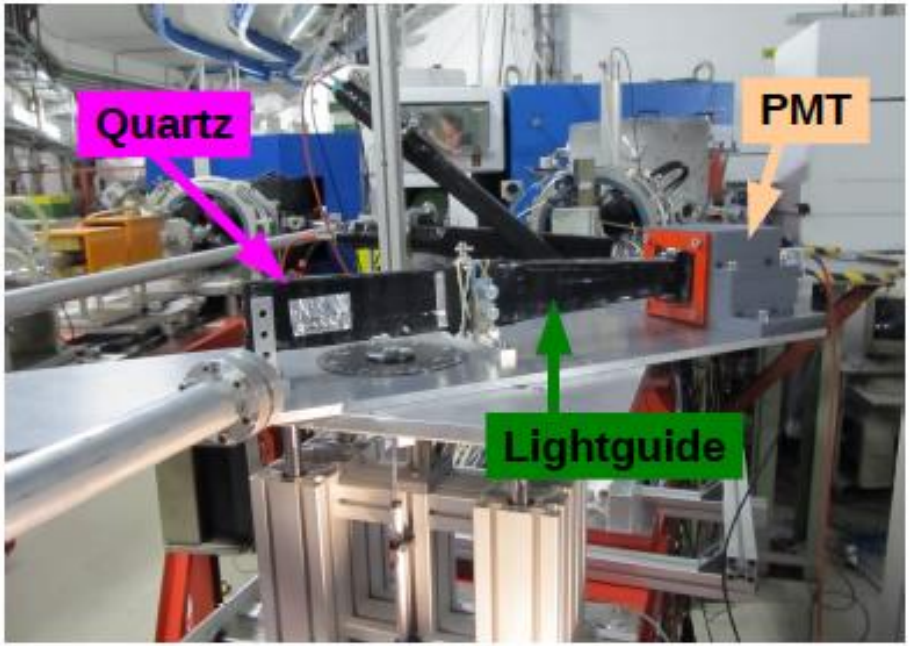

Measured the yield of photo electrons for different

- materials (quartzes, wrappings, lightguids, PMTs)
- geometries
- impact positions
- angles of incidence

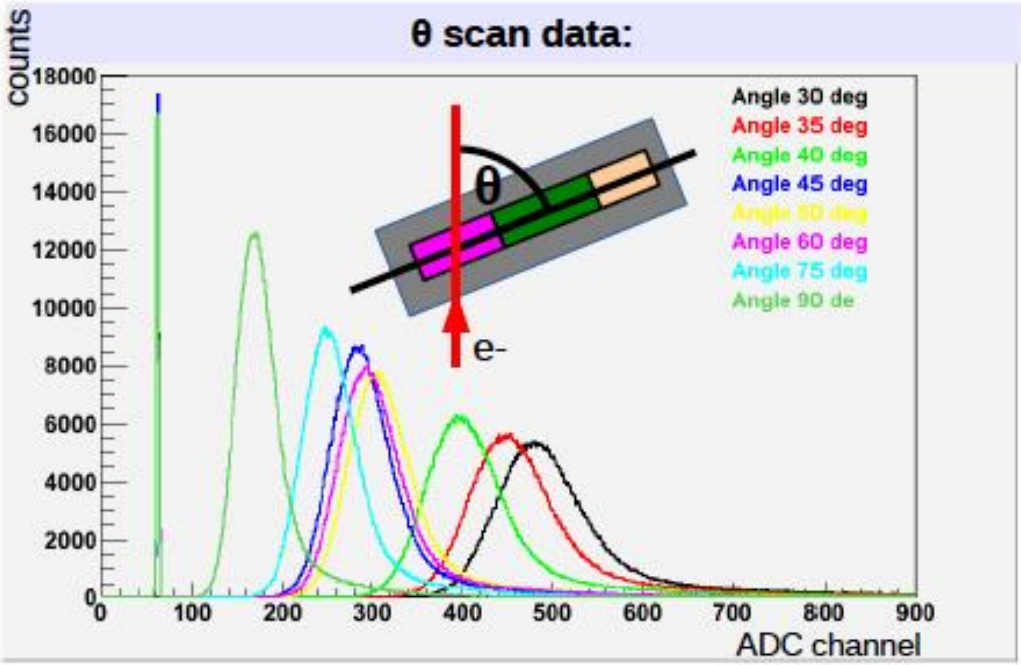

Detector module prototype tested at MAMI

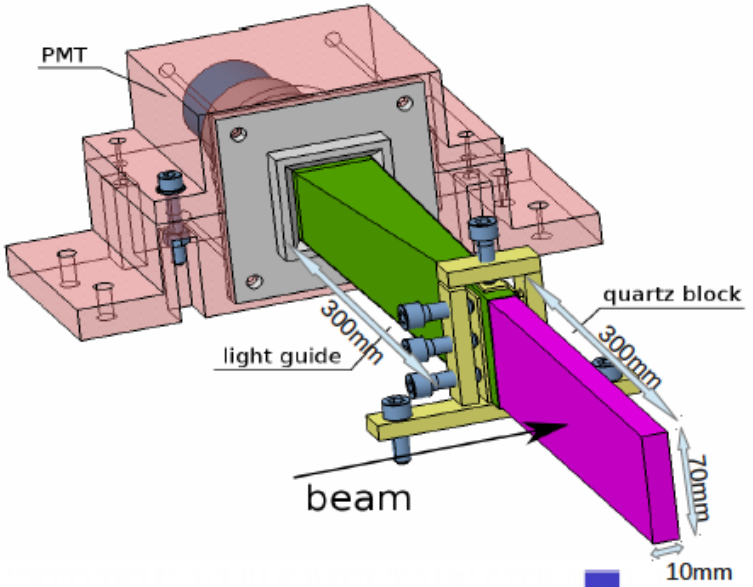

Outline of different setups and scan series 01/2014

Angular scans

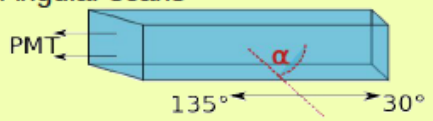

Position scans

Quartz materials
- Heraeus Suprasil 2A
- Heraeus Spectrosil 2000

Geometries
- Quartz bars 10mm / 15mm
- w/ and w/o "outlet optic" (45° cut)
- Measurements w/ and w/o LG

Polishes
- Flamepolished
- Mechanical
- Optical polish

Reflective materials for wrap and LG
- Mylar
- Alanod 4300UP
- Millipore ImmobilonP

~350 runs in January 2014 beam time
~400 runs in December 2015

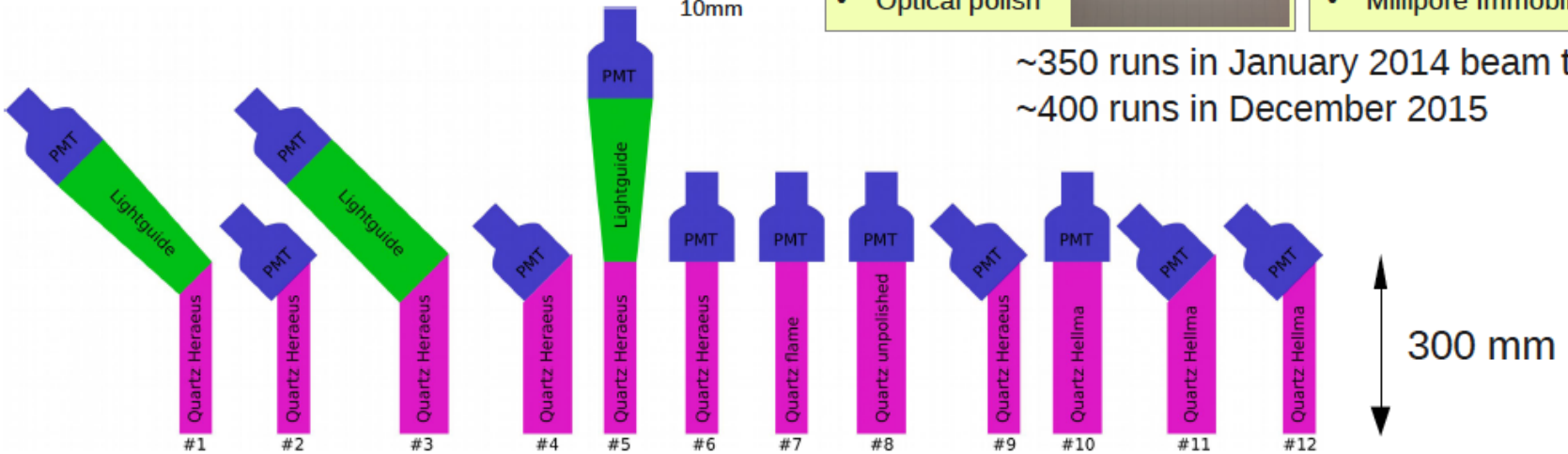

Prototype Cherenkov detector

Prototype Detector test at MAMI

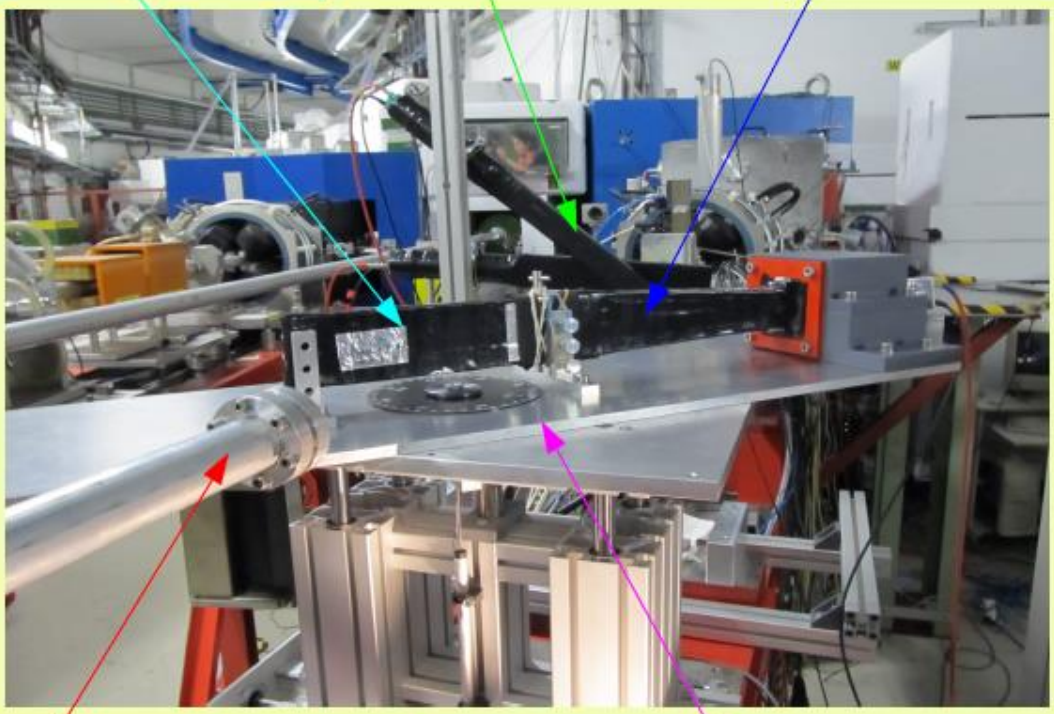

Detector test after 2nd stage of MAMI @855MeV

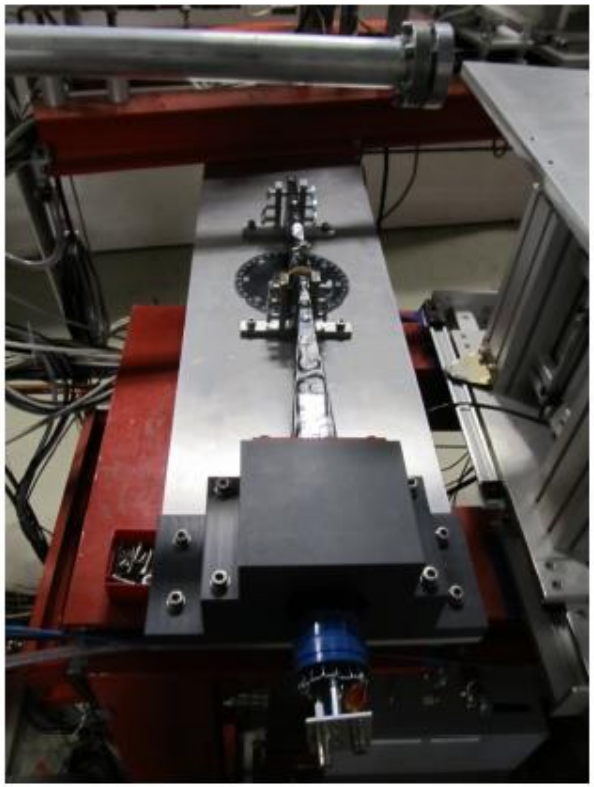

Photomultipliers

Tubes in test:

Hamamatsu R11410

ET Enterprises 9305QKMB

Quantum Efficiencies of Tubes in beam time 01/2014

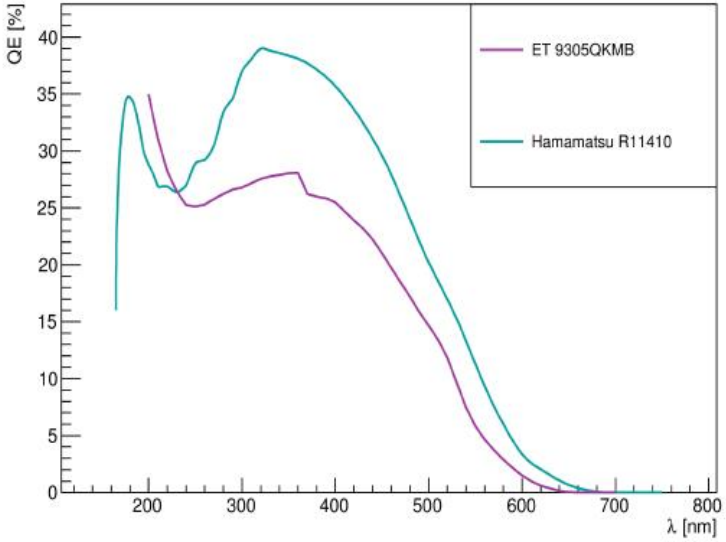

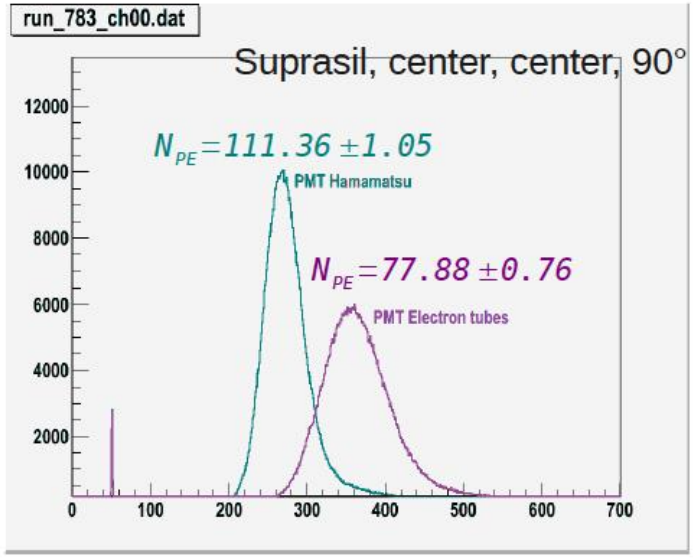

Loss in Light Guide

Our geometry:

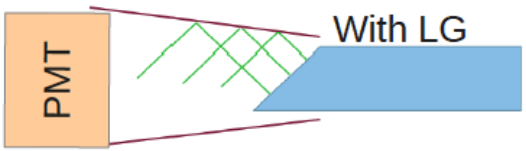

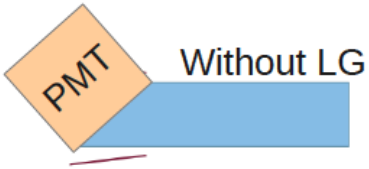

Comparison of Signal with and without use of light guide

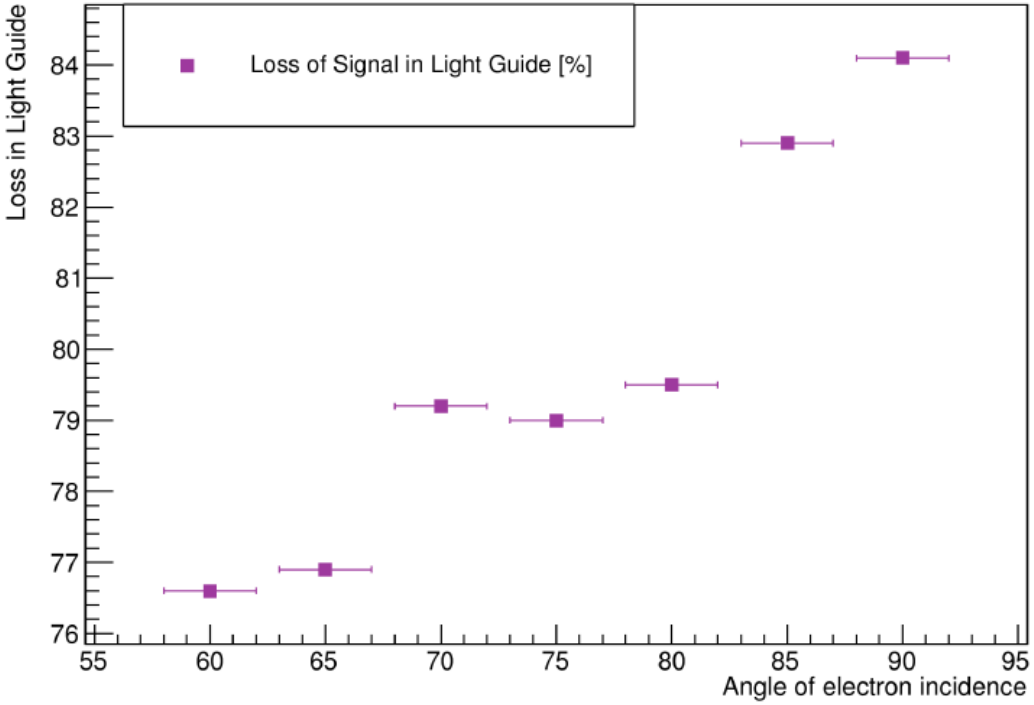

ANGLE	N w/ LG	N w/o LG
60	12.4	53
70	11.6	55.4
80	11.8	56
90	12.8	77.9

Next beam time:
Test other geometry

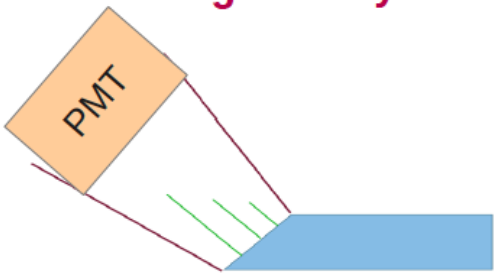

P2 Experimental setup (second testbeam January 2014)

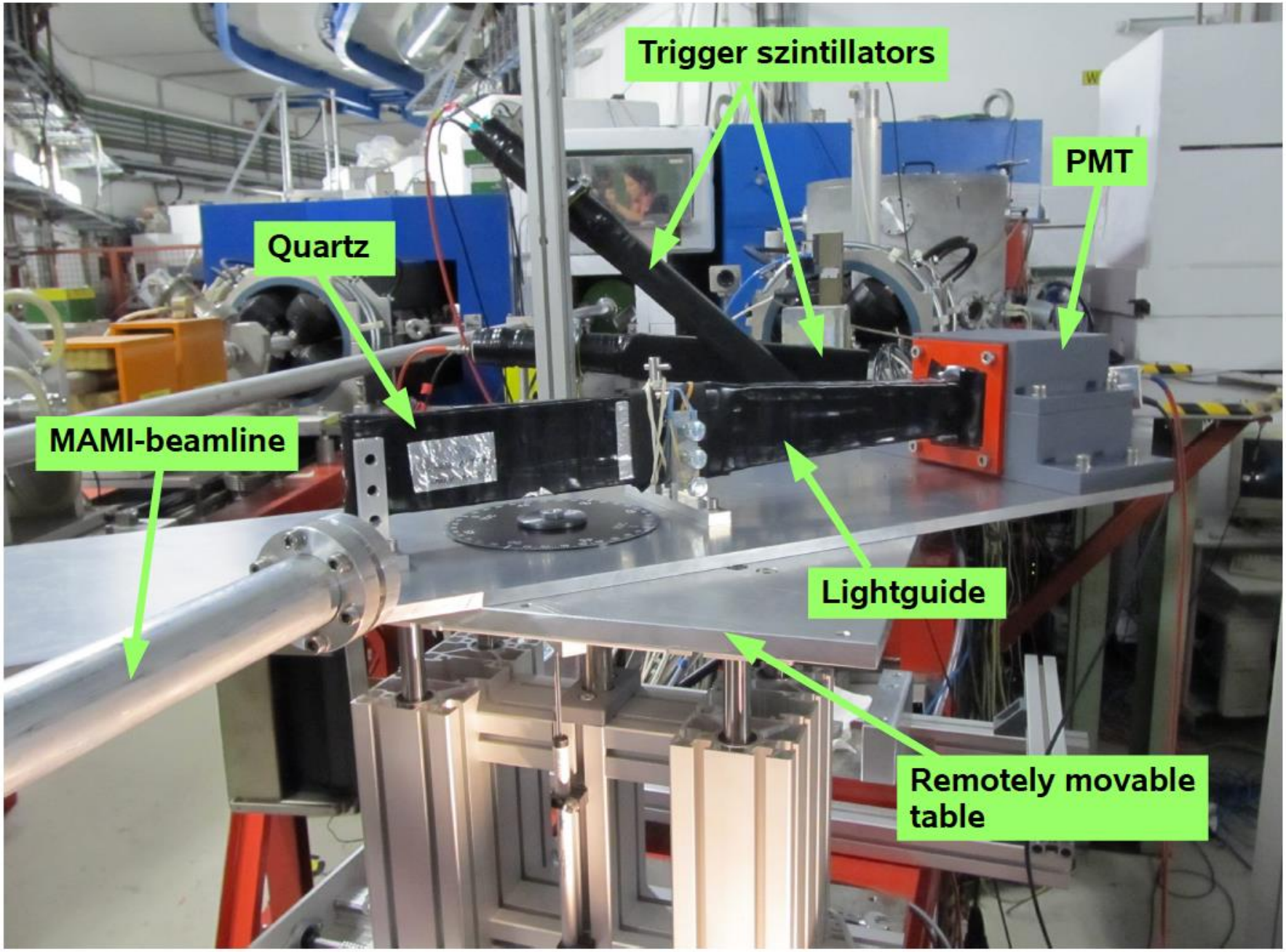

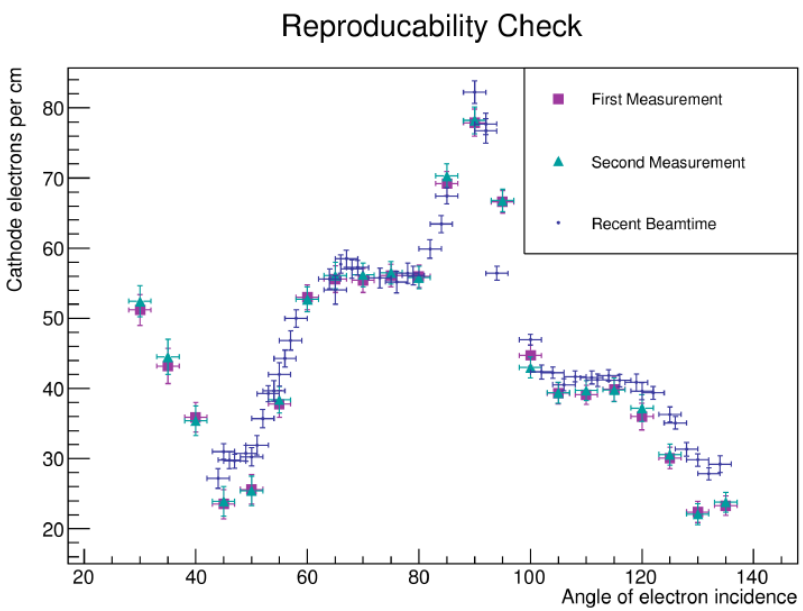

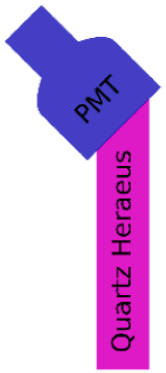

Comparison of experimental data with Simulation:

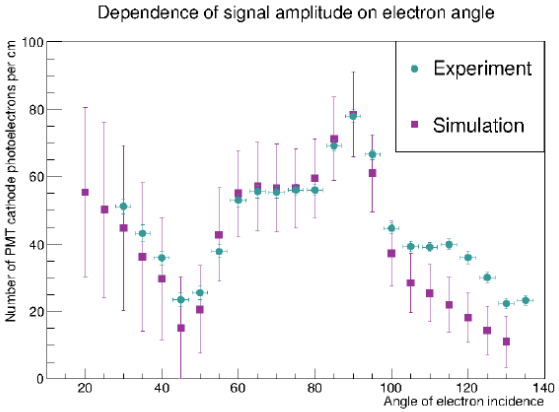

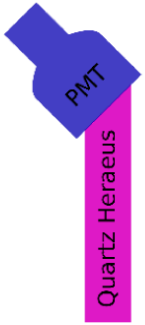

Development of PMT base with remotely switchable gain (high and low current mode)

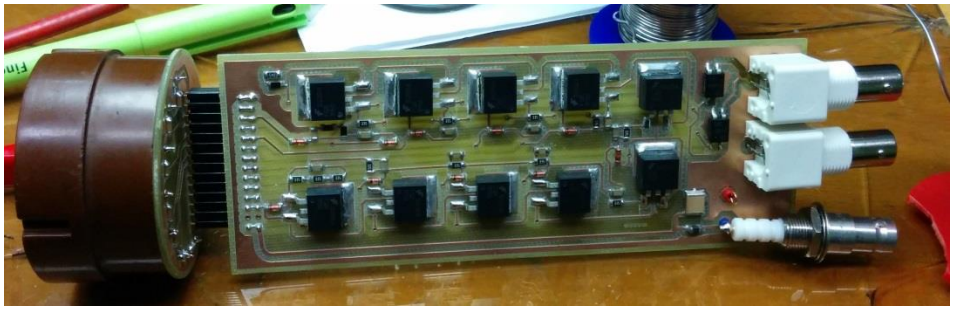

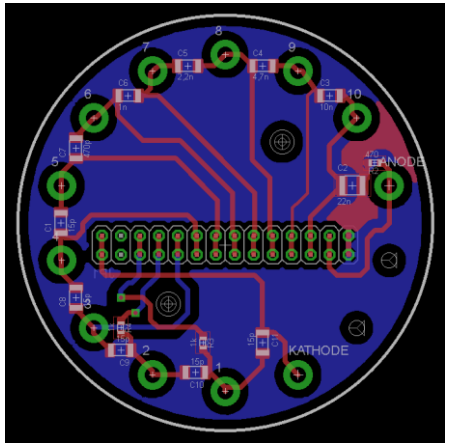

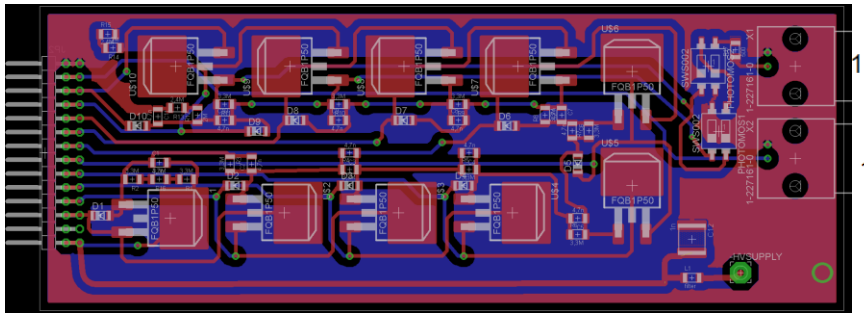

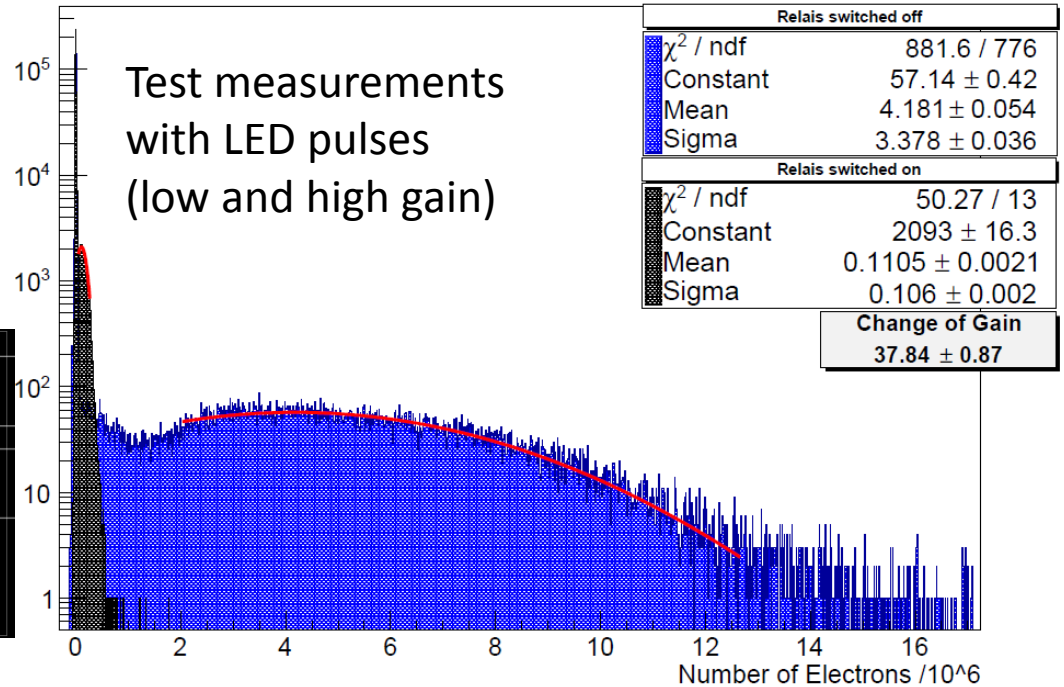

P2 setup overview

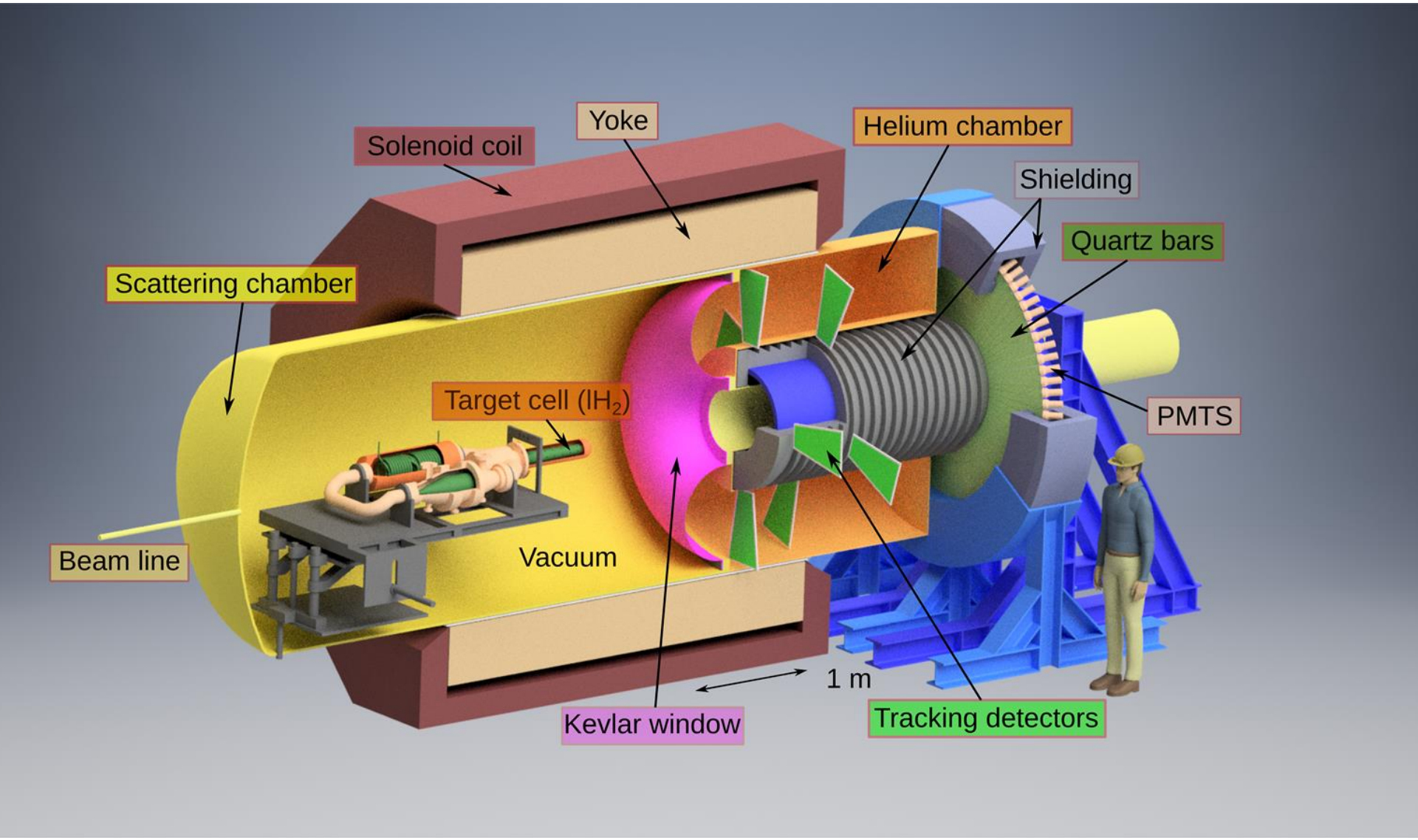

Quartz Cherenkov detector concept

- Cherenkov detector ring consisting of
  - **80 fused silica bars**

- Covering
  - **full azimuth**
  - **25° - 45° polar angle**

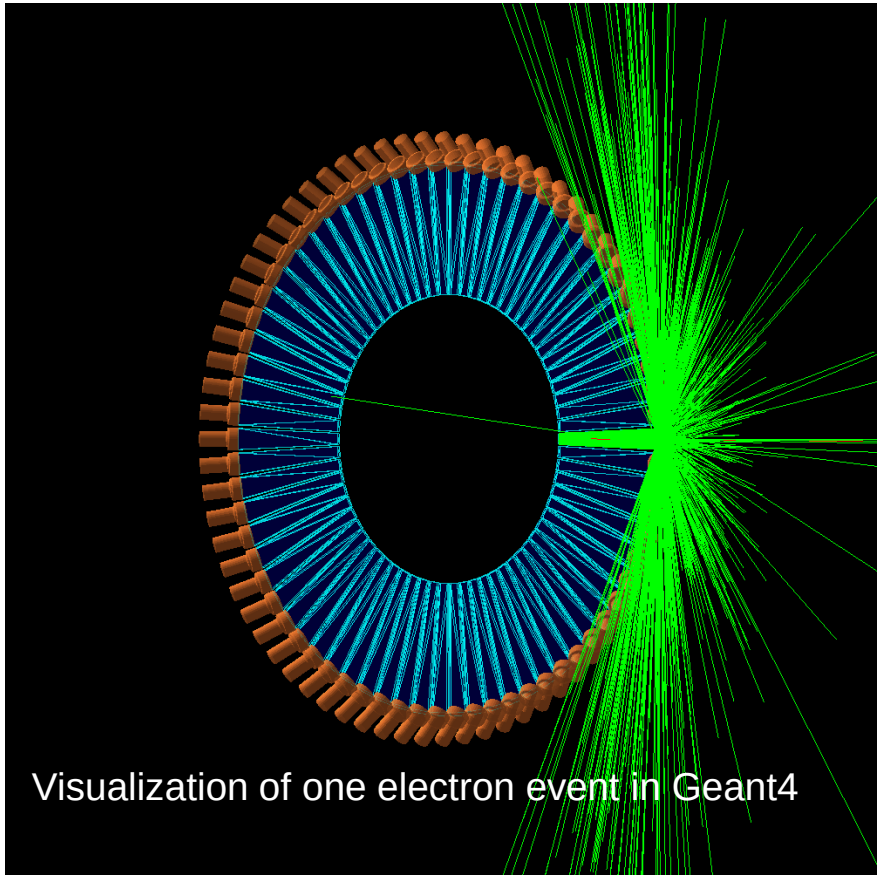

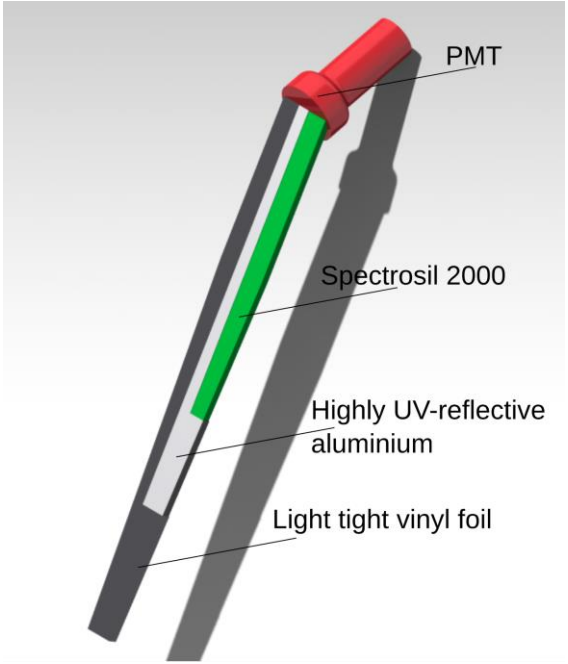

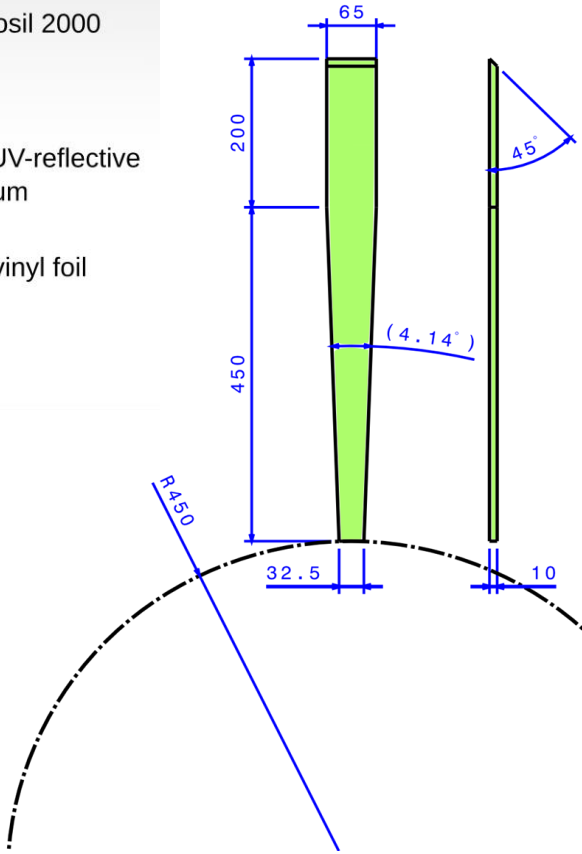

Detector response to signal electrons

Detector prototype tests at MaMi compared to Geant4 simulation results

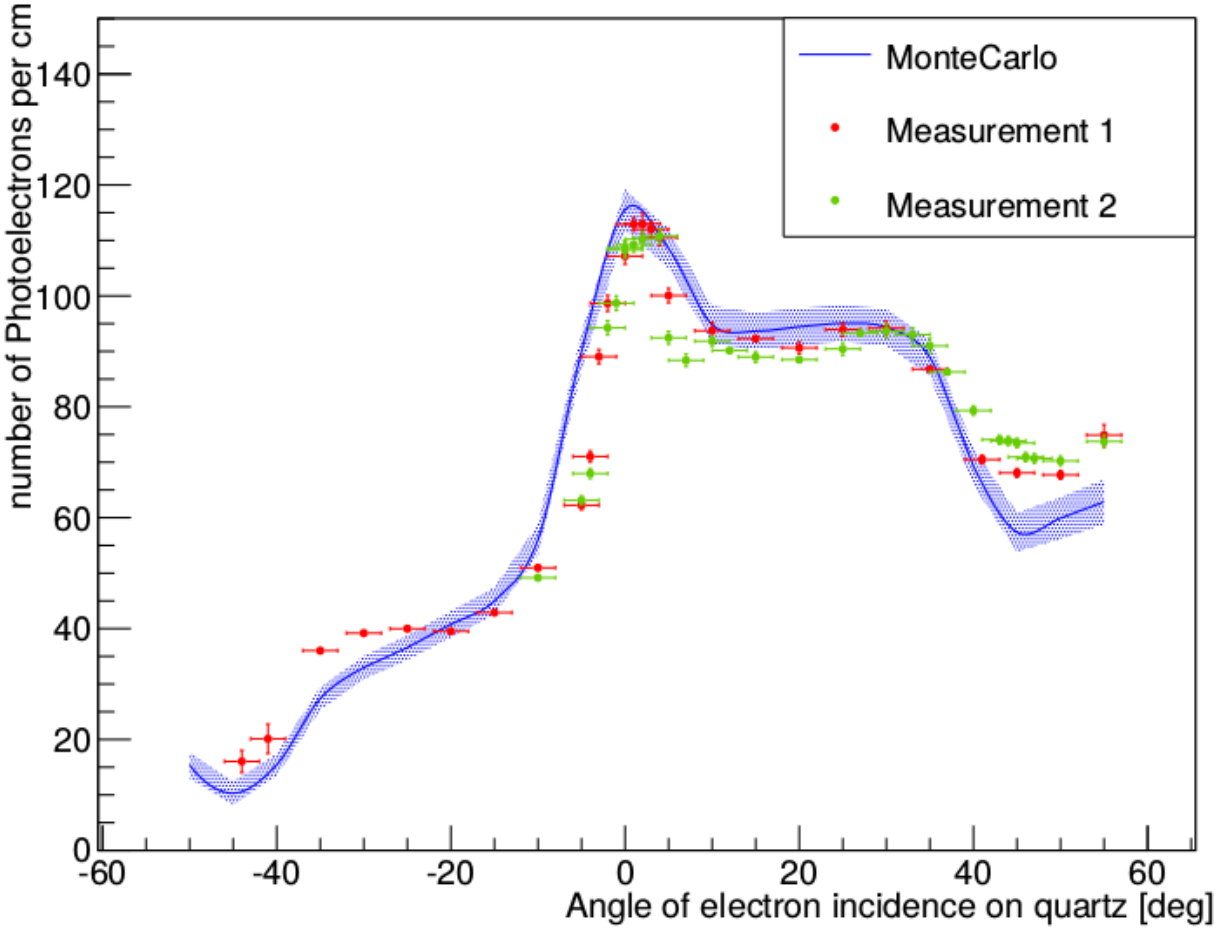

Radiation hardness tests

Hit rates onto Cherenkov detector ring

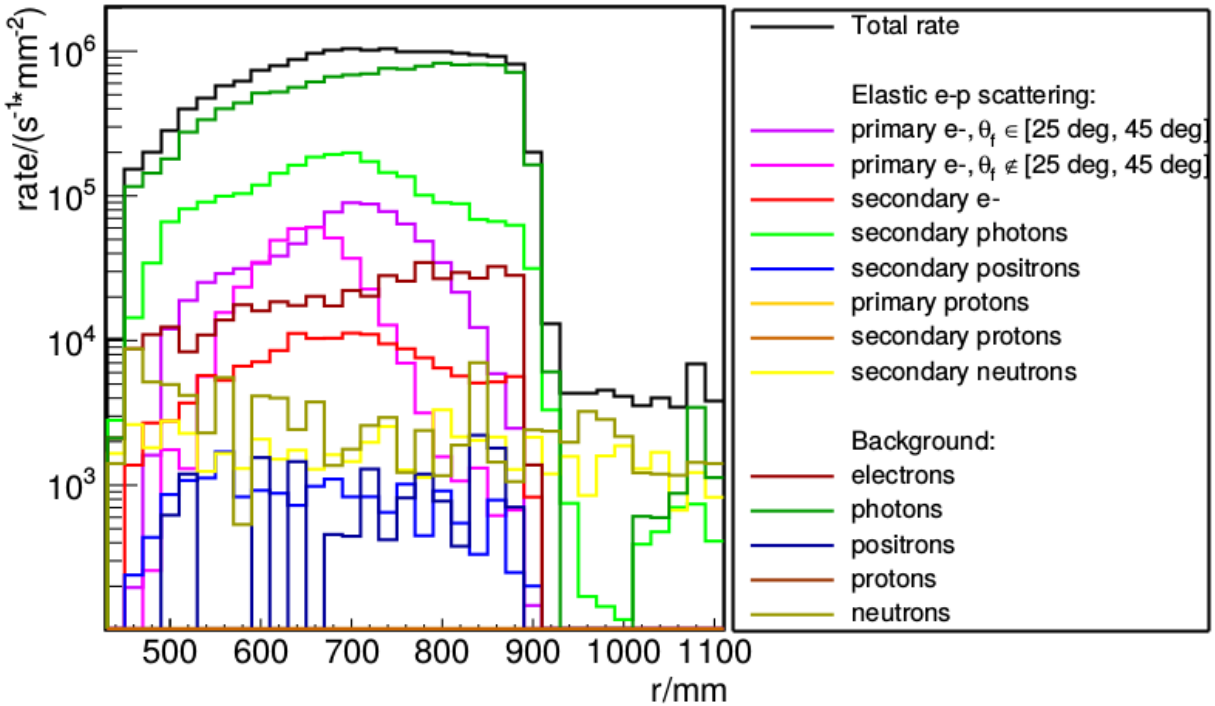

Particle type	Hit rate [s^{-1}]
Primary electrons, $\theta \in [25°, 45°]$	$7.10 \cdot 10^{10}$
Primary electrons, $\theta \notin [25°, 45°]$	$3.21 \cdot 10^{10}$
Secondary electrons	$1.33 \cdot 10^{10}$
Electrons from background processes	$4.05 \cdot 10^{10}$
∑ electrons	**$1.57 \cdot 10^{11}$**

+ neutronic and photonic background

35Mrad
purely from electrons
!

Radiation hardness tests

Samples of Spectrosil 2000 and Suprasil 3A were exposed at the 180MeV MaMi beam

8300s @ 100nA	≙ 10-fold P2 dose
4150s @ 100nA	≙ 5-fold P2 dose
4150s @ 20nA	≙ P2 dose
2075s @ 20nA	≙ half P2 dose

Radiation hardness tests

Samples of Spectrosil 2000 and Suprasil 3A were exposed at the 180MeV MaMi beam

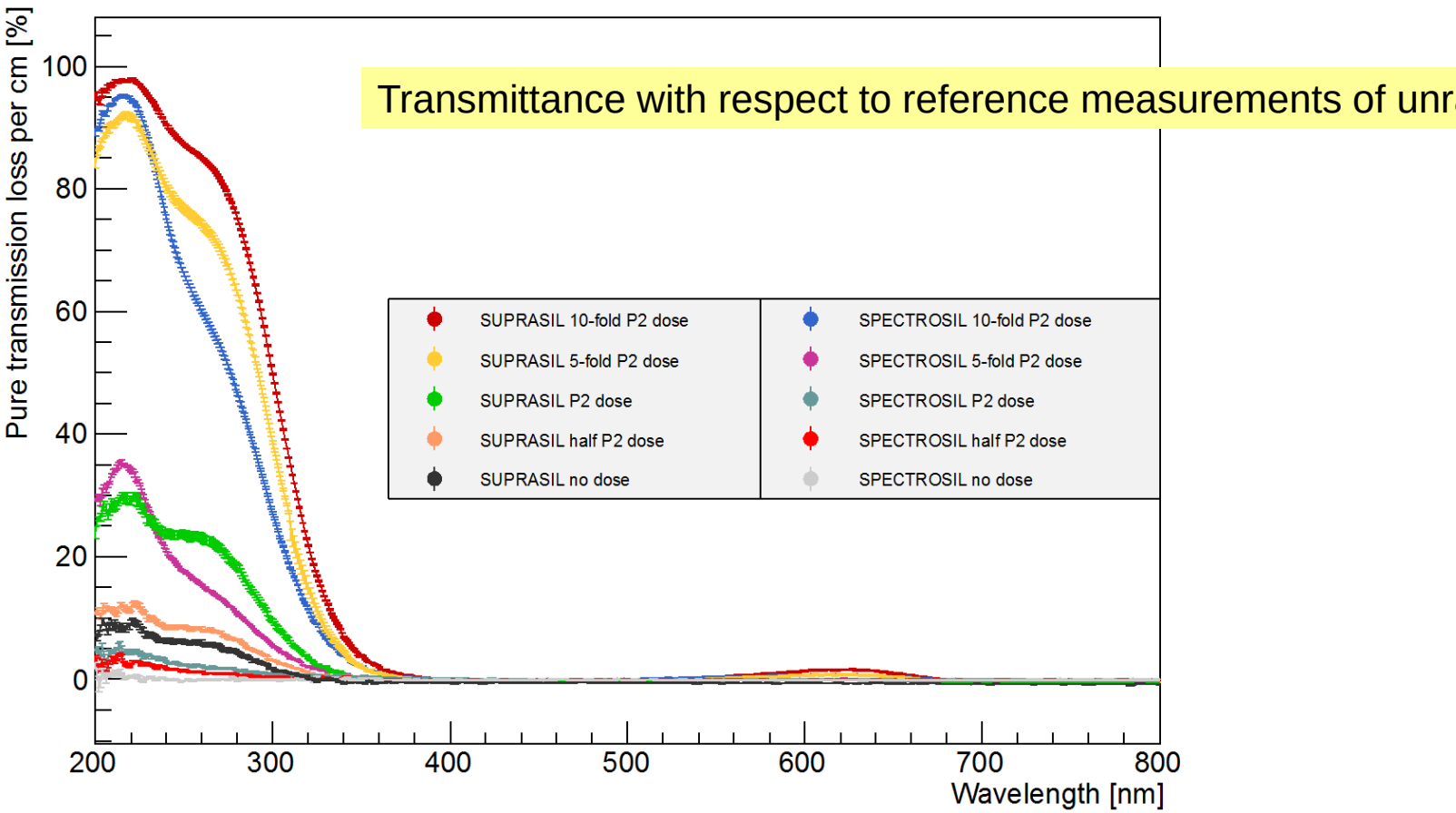

Radiation hardness tests

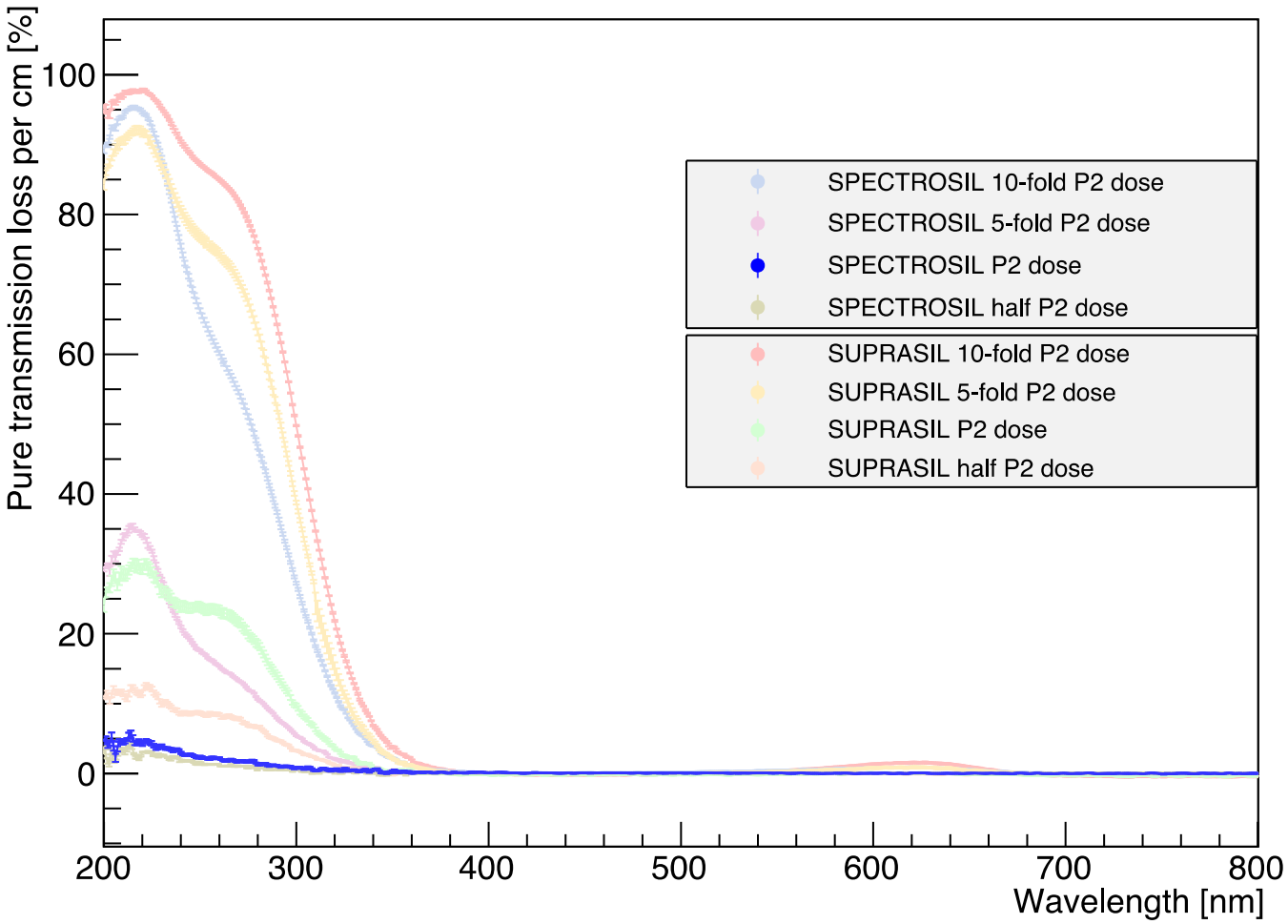

PMT, Electronics

Synergy with MOLLER; University of Manitoba

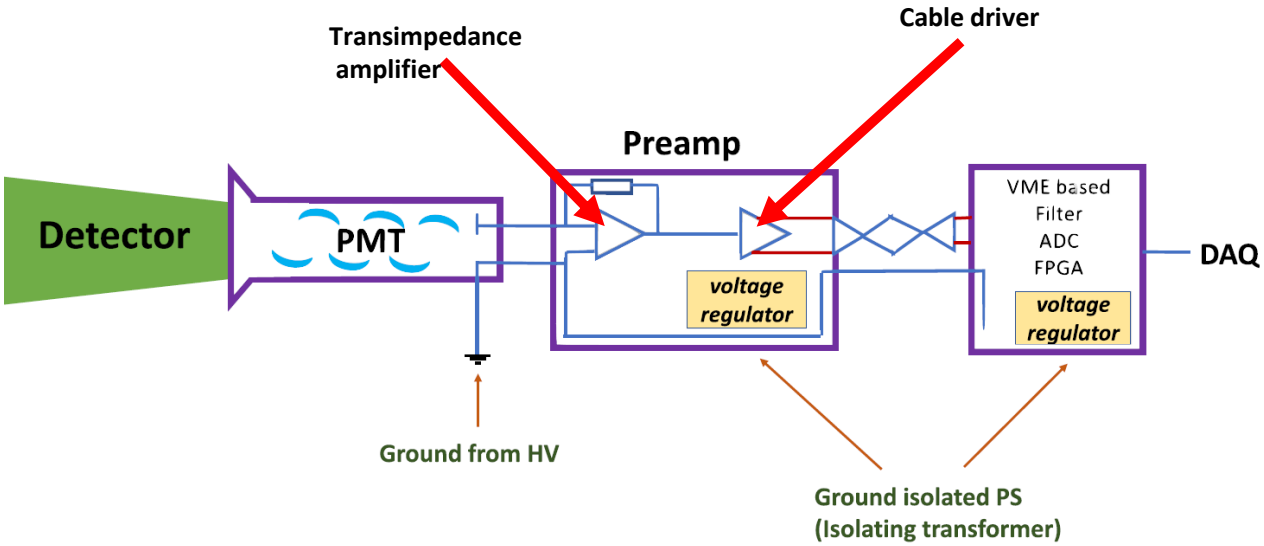

Schematic layout of the read-out signal path for the P2 experiment at MESA

Block Diagram: Principle Of The Front-end Path

Two operation mode:

- high beam current
  → integration mode for asymmetry measurement

→PMT voltage divider can be operated in low gain mode

- low beam current
  → pulse mode for kinematics and background study

→ PMT voltage divider can be operated in high gain mode

- Selectable transimpedance amplifier of the preamplifier controlled and switchable externally by use of a raspberry PI

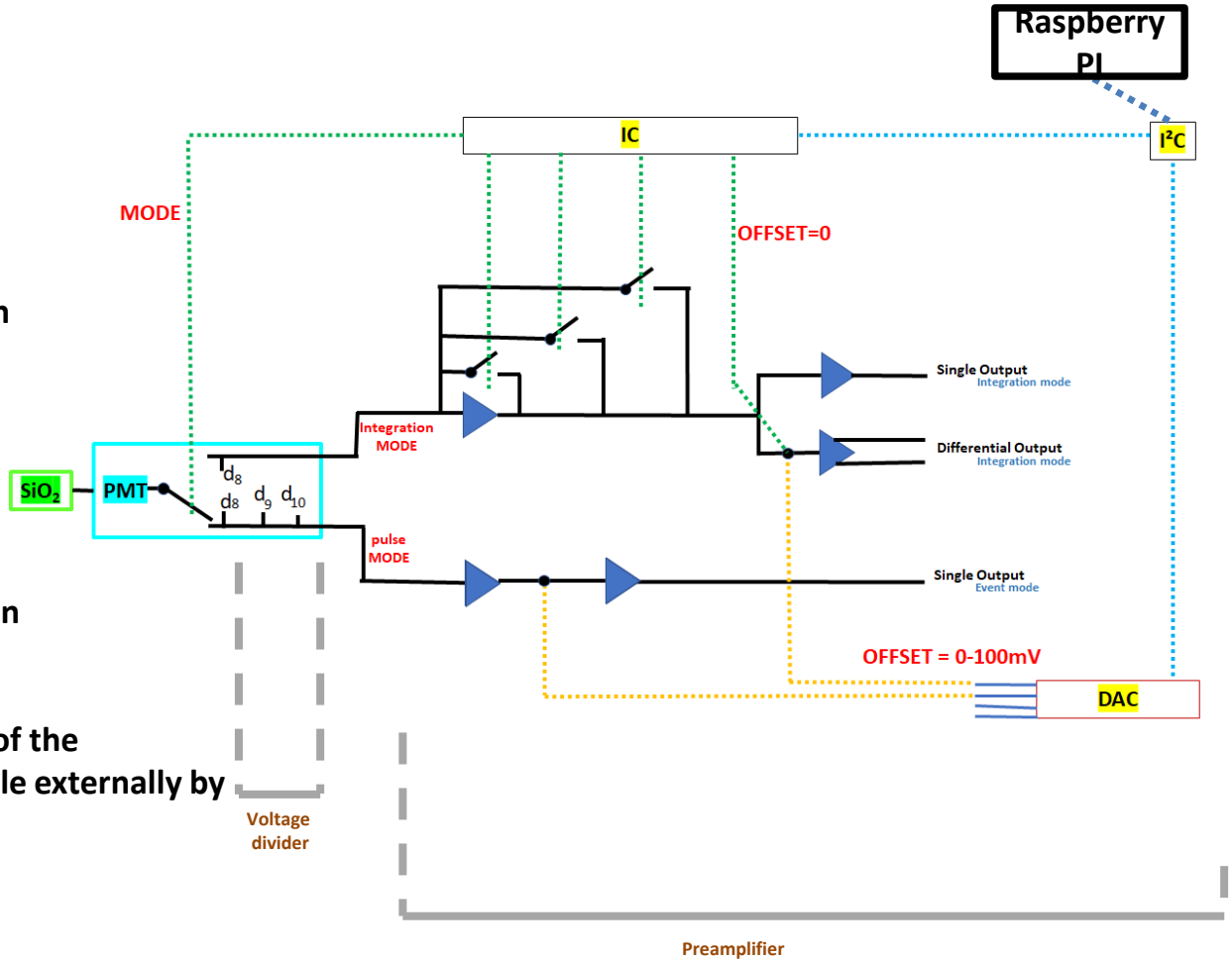

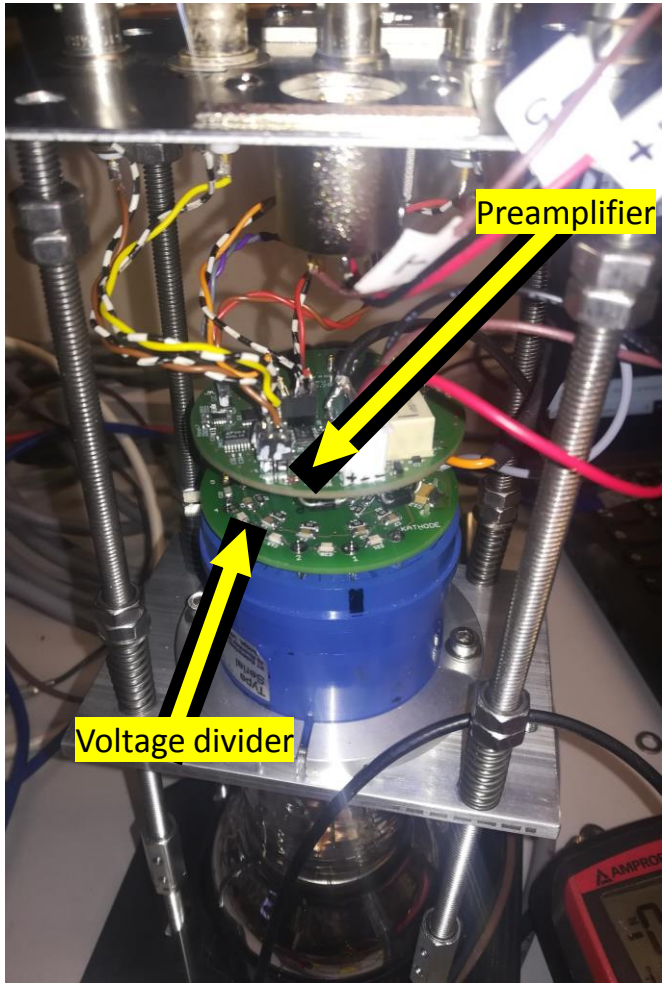
Preamplifier
Voltage divider

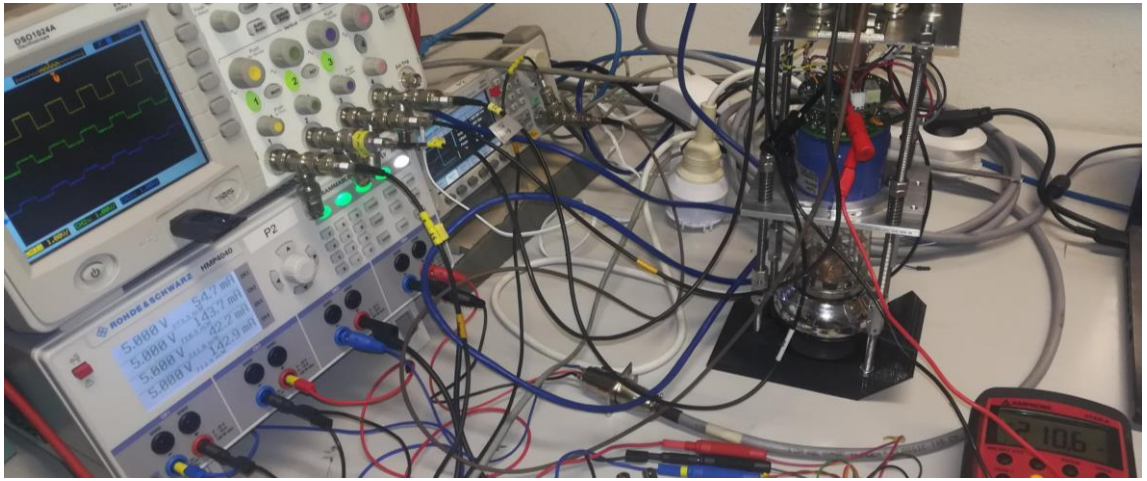
ROHDE&SCHWARZ
5.000 V
5.000 V
5.000 V
5.000 V

Preamplifier test with transimpedance gain =1, pulsed input signal of 1Vpp@600nA feedbacck restistent 1MOhm, 1pF

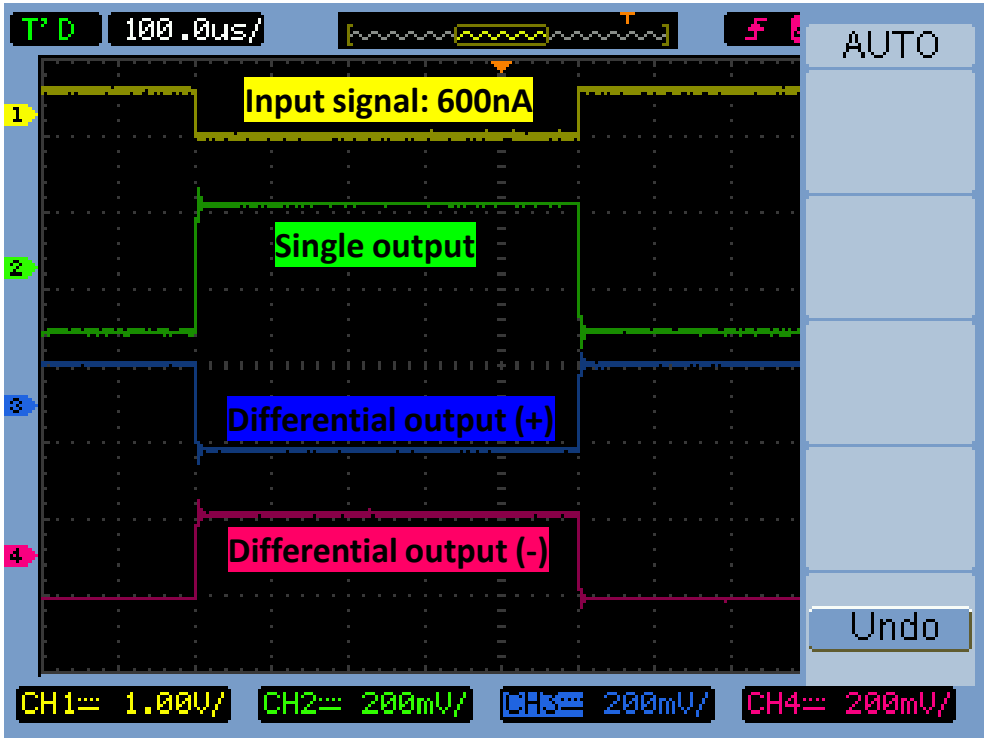

Offset check (without input signal), with supply voltage +/-5 V

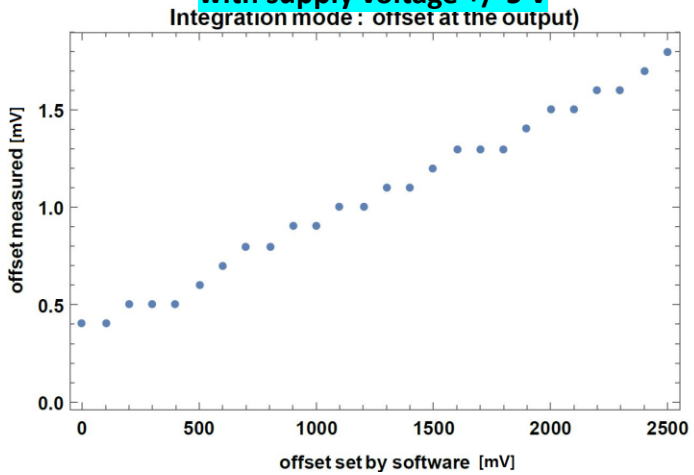

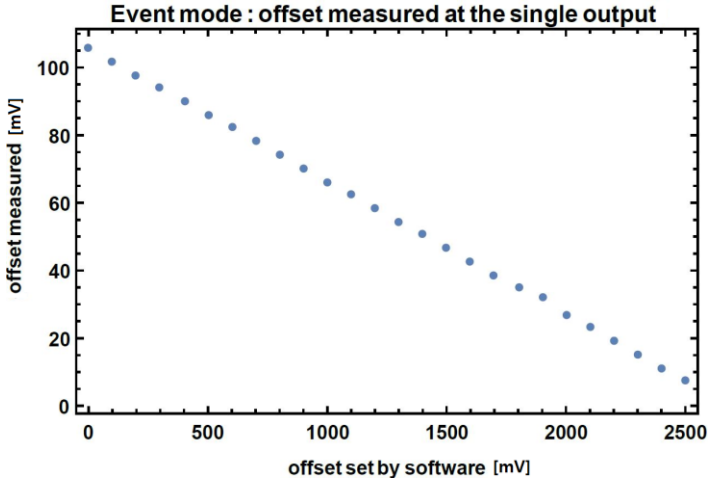

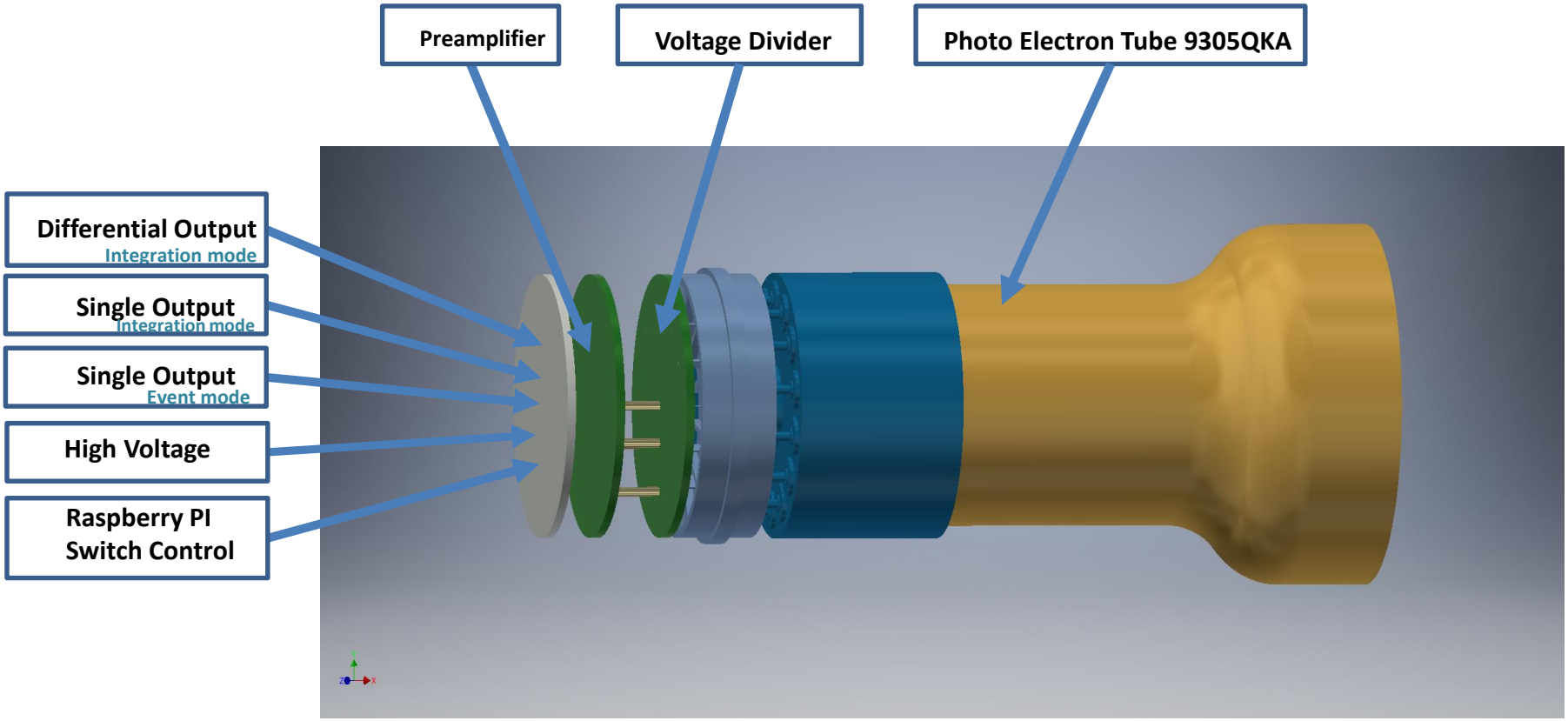
Preamplifier
Voltage Divider
Photo Electron Tube 9305QKA
Differential Output
Integration mode
Single Output
Integration mode
Single Output
Event mode
High Voltage
Raspberry PI
Switch Control

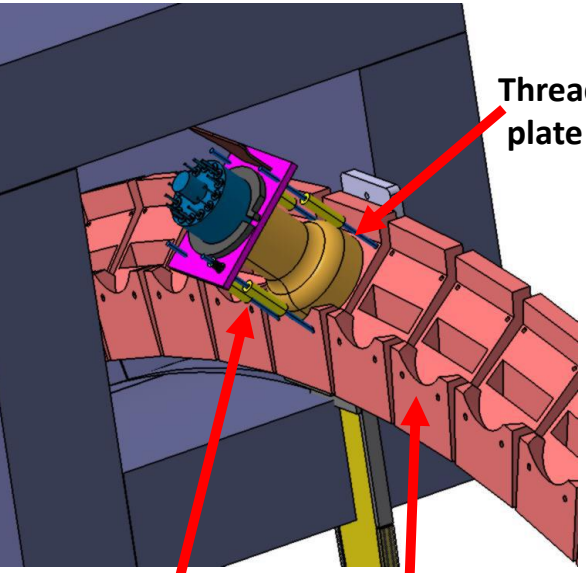

Threaded rods fix the pink plate to the holding block

Spring to gently push the PMT to the quartz

Holding block for the PMT

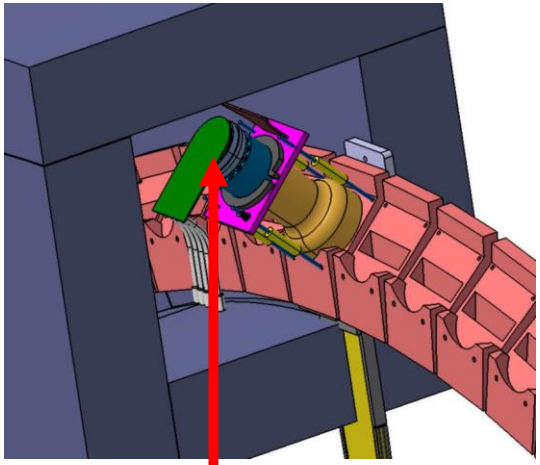

The PMT socket with the electronics (PCB)

Due to lack of space, the preamplifier and the voltage divider will be on the same PCB

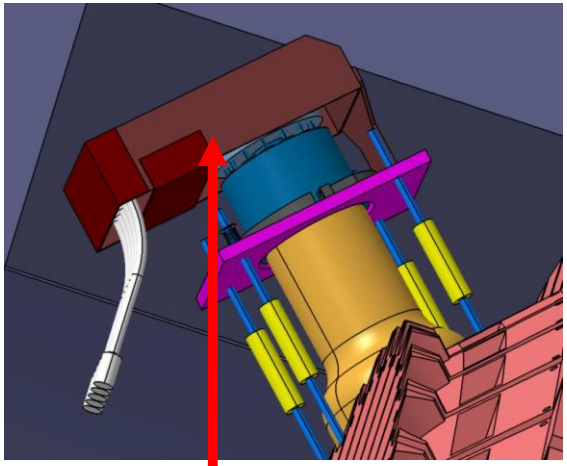

Copper insulation box around the PCB

Topic C: Experimental design

Qweak electronics

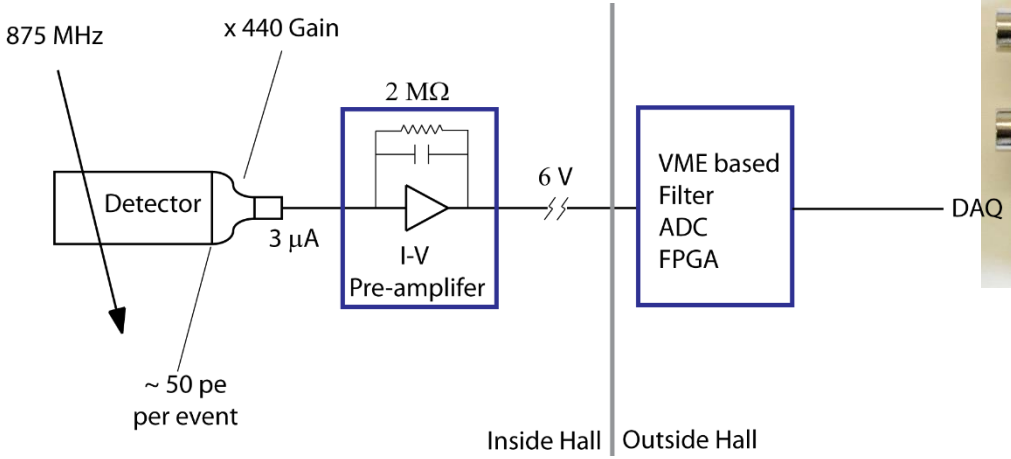

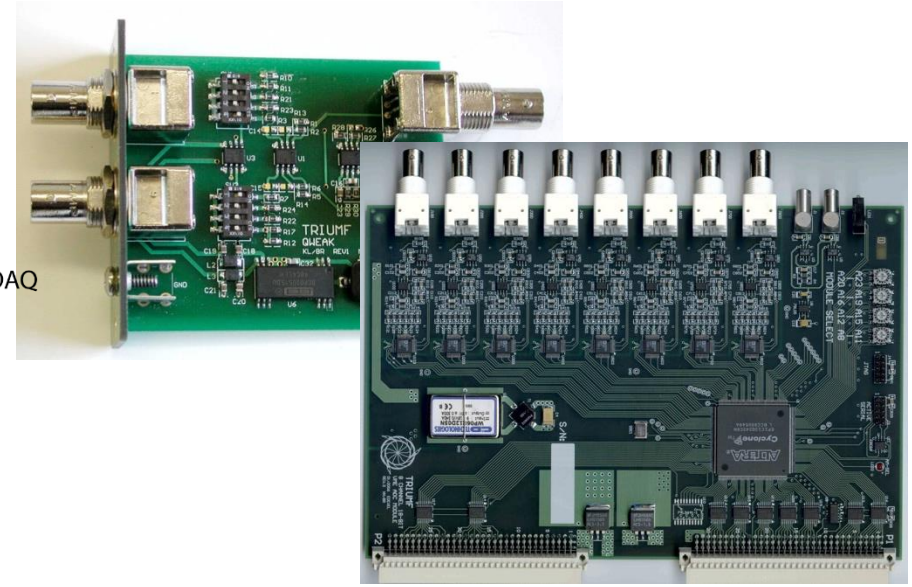

P2 electronics (large synergy with MOLLER)

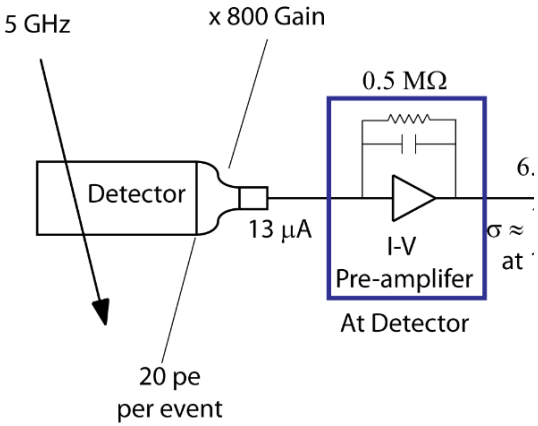

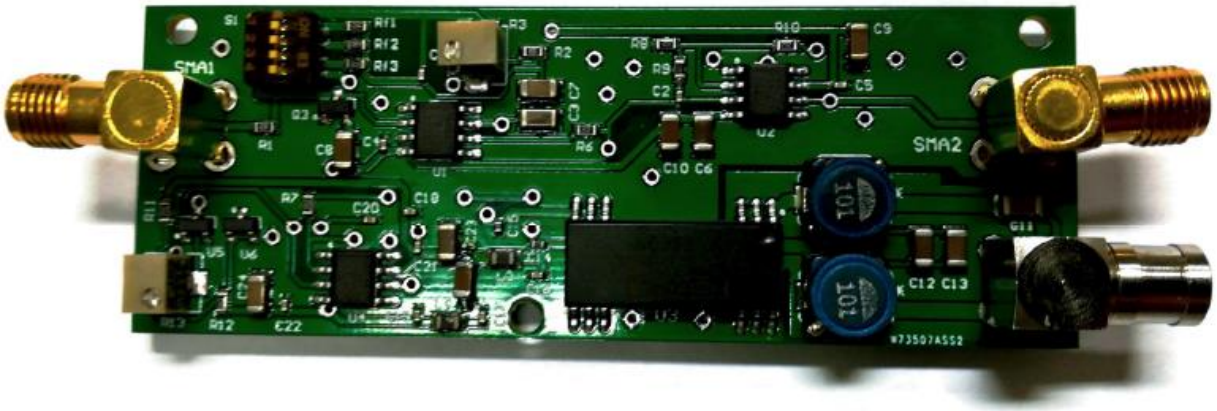

M. Gericke: U Manitoba a

New prototype, as of November 15, 2018

Theory

Shift in momentum transfer due to photon radiation

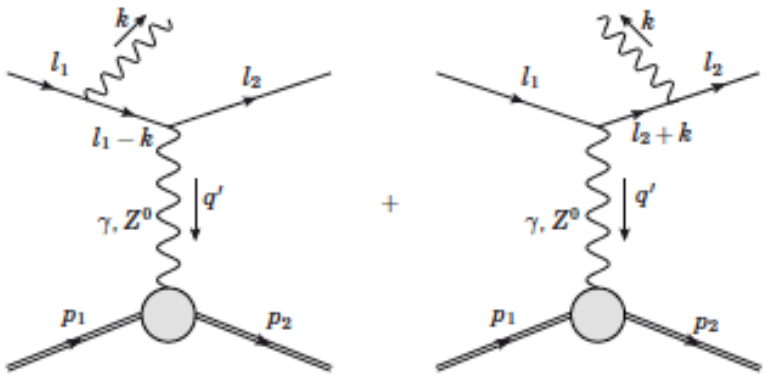

Shifted kinematics:

$$Q^2 = -(l_1 - l_2)^2 \rightarrow Q'^2 = -(l_1 - l_2 - k)^2$$

$\rightarrow Q'^2$ can be on average much smaller than Q^2.

The average shift in momentum transfer squared due to hard-photon bremsstrahlung can be defined as

$$\langle \Delta Q^2 \rangle = \frac{1}{\sigma} \int \frac{\mathrm{d}^4 \sigma^{1\gamma}}{\mathrm{d}E' \mathrm{d}\theta_l \mathrm{d}E_\gamma \mathrm{d}\theta_\gamma} \mathrm{d}E' \mathrm{d}\theta_l \mathrm{d}E_\gamma \mathrm{d}\theta_\gamma \Delta Q^2,$$

with

$$\Delta Q^2 = Q'^2 - Q^2,$$

$$\sigma = \sigma^{1\gamma}_{1-\mathrm{loop}} \Big|_{E_\gamma < \Delta} + \sigma^{1\gamma} \Big|_{E_\gamma > \Delta}.$$

Second-Order QED Corrections

1-loop and 1-photon bremsstrahlung

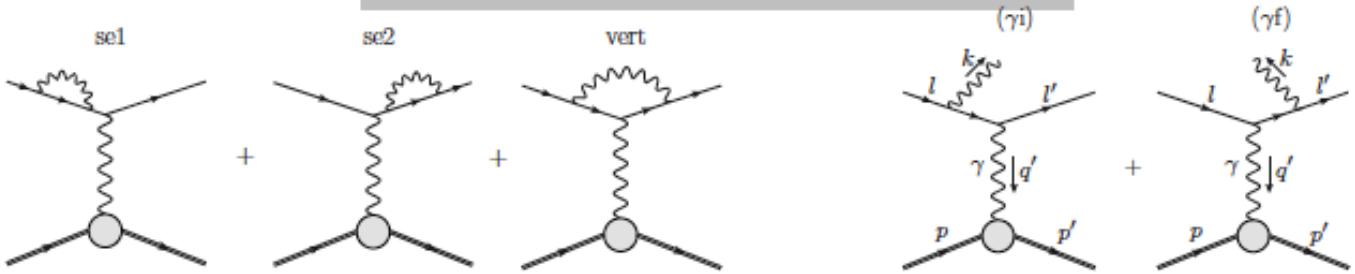

2-loop and 2-photon bremsstrahlung

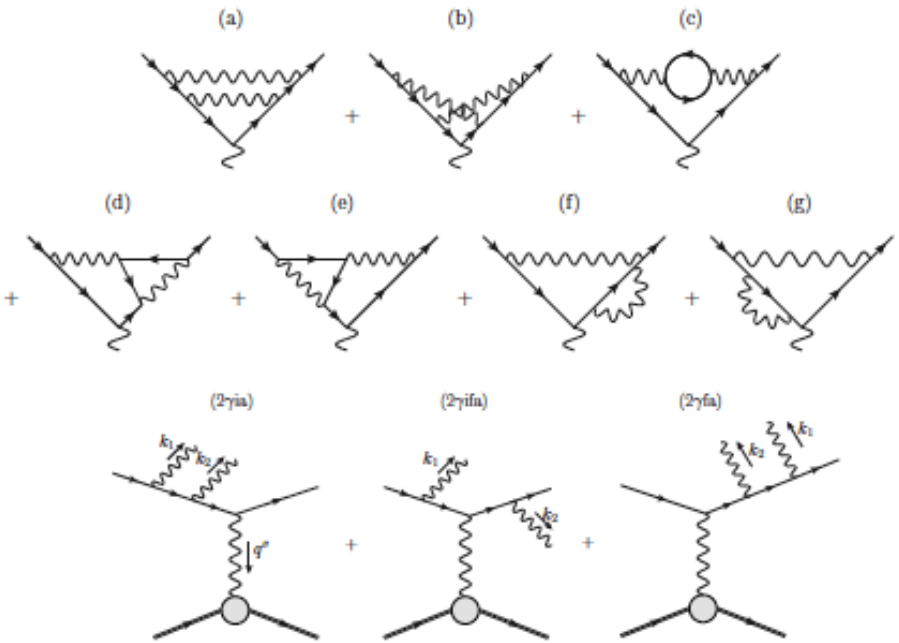

1-loop for 1-photon bremsstrahlung

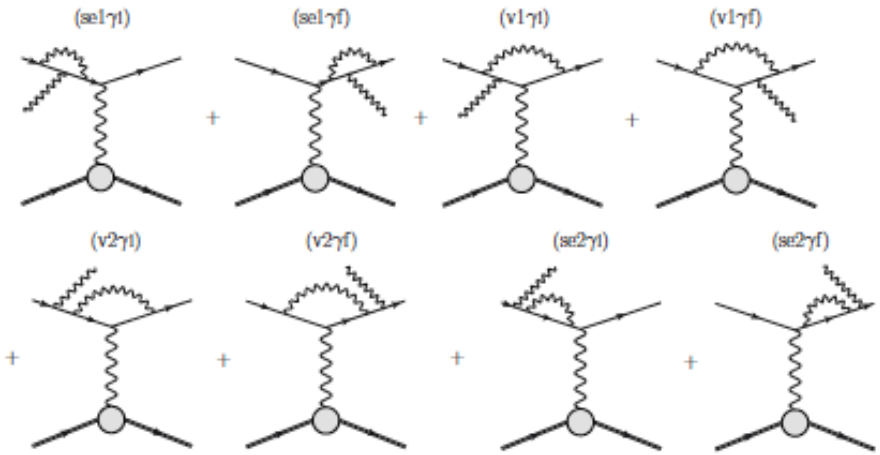

QED at order $O(\alpha^2)$

Leptonic QED second-order corrections: arXiv:1811.04970

Monte Carlo event generator program: Ready to study details of kinematic distributions

dependence on beam energy

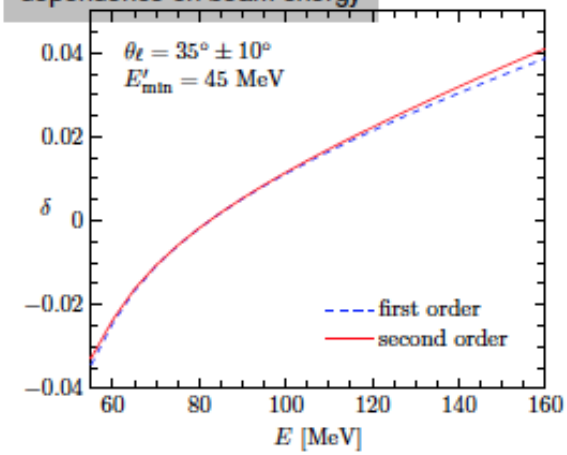

dependence on scattering angle

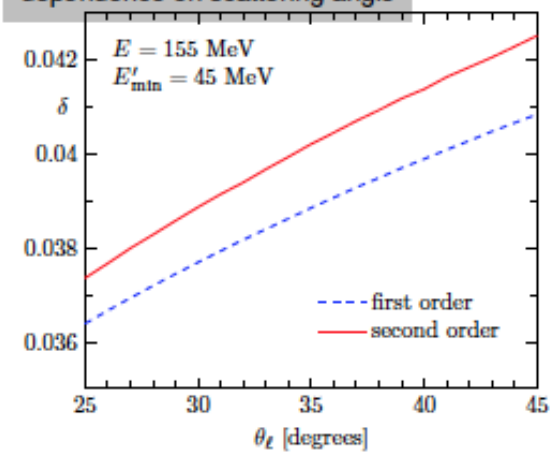

dependence on minimum electron energy

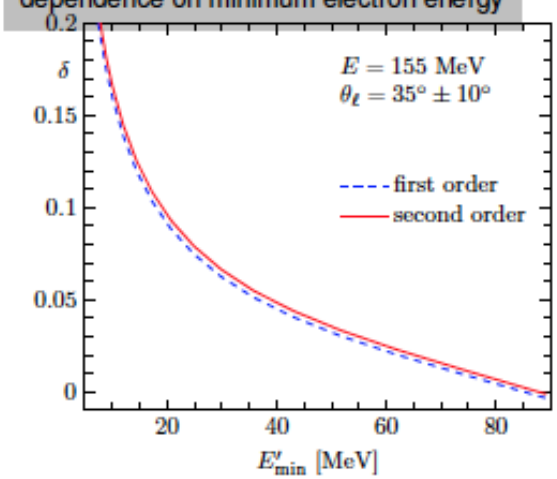

bremsstrahlung photons

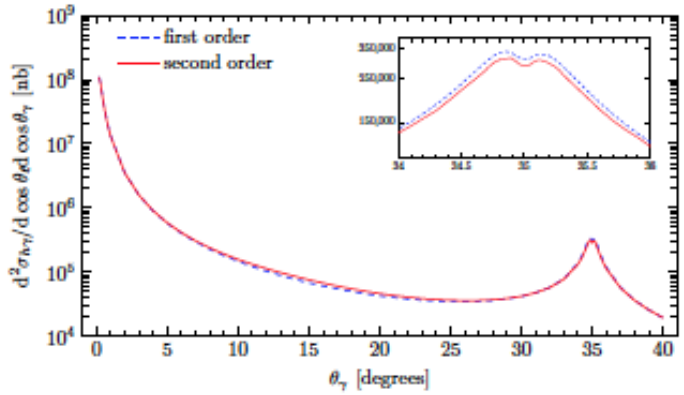

Bremsstrahlung at order $O(\alpha^2)$: Q^2 shift

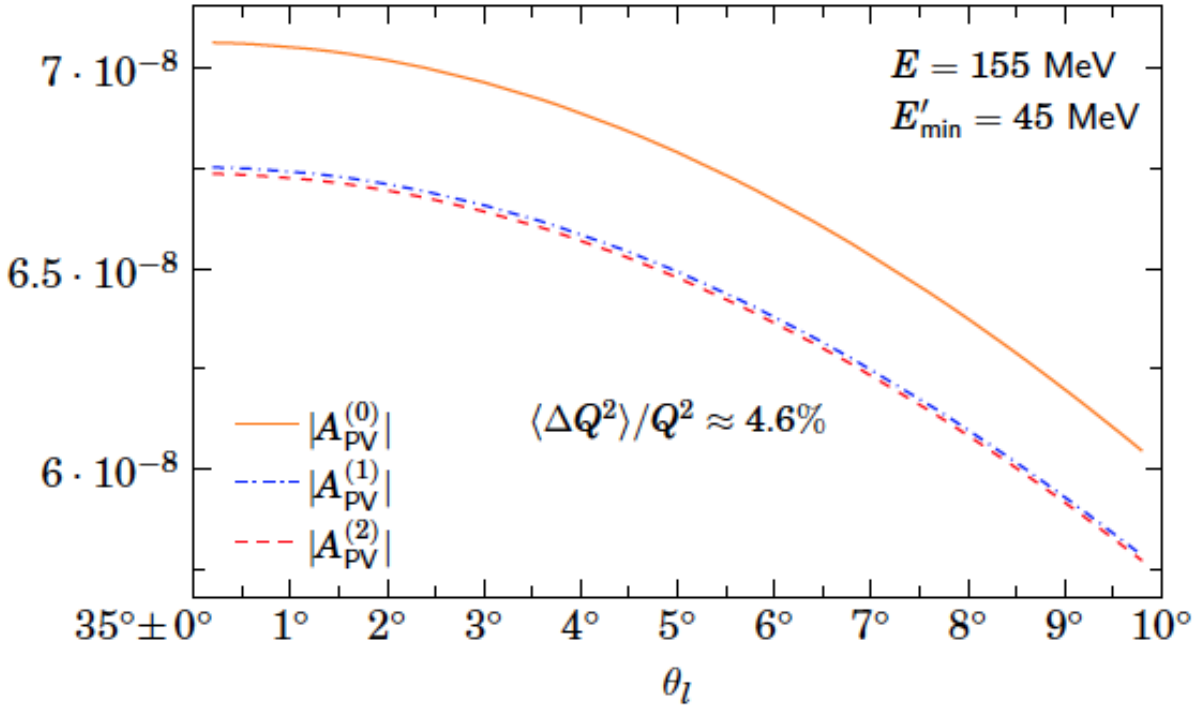

QED corrections for the asymmetry:
Q^2 shift is a kinematic effect: 1γ radiation has it all
Very small $O(\alpha^2)$ correction

Workshop

MITP Scientific program: 23 April 2018 – 4 May 2018

Bridging the Standard Model to New Physics
with the Parity Violation Program at MESA

Organized by
Jens Erler, Mikhail Gorshteyn, Hubert Spiesberger

Executive Summary and talks:
see https://indico.mitp.uni-mainz.de/event/123/

- Weak charge measurements with PVES at MESA
- Parity violation in atomic systems
- Neutron skins
- Ultra-cold neutron beta-decay

Dedicated Workshop on C^{12} at UNAM Mexico in Spring 2019: DFG+CONACyT SP 778/4-1
Instituto de Física de la Universidad Nacional Autónoma de México (IF-UNAM)
March 18 to April 5, 2019.

HPNC @ MESA+

PV πN coupling $\mathcal{L}_{PV} = -ih^1_\pi \pi^+ p^\dagger n \; + \; h.c. \; + \; \ldots$

Non-derivative coupling, dominate at low energies; Origin: effective PV 4-quark operators

Recent result from $\vec{n}p \to d\gamma$ experiment @ Los Alamos: *Blyth et al [NPDGamma] '2018*

$h^1_\pi = (2.6 \pm 1.2 \pm 0.2) \times 10^{-7}$ $A^{PV} \sim 0.1\, h^1_\pi \sim 10^{-8}$ hard to measure; low rate; polarized UCN…

Chen, Ji 2001: semi-inclusive threshold π production w. polarized e-
Larger signal: $A^{PV} \sim 0.5\, h^1_\pi$

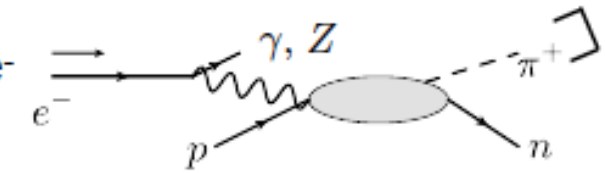

Sensitivity to h^1_π: beam energy close to π threshold
e' undetected - quasi-real photon $\langle Q^2 \rangle \sim 0.001$ GeV^2

Z-exchange suppressed: $A^{PV}_Z \approx -\dfrac{G_F < Q^2 >}{2\sqrt{2}\pi\alpha} \sim -2 \times 10^{-7}$

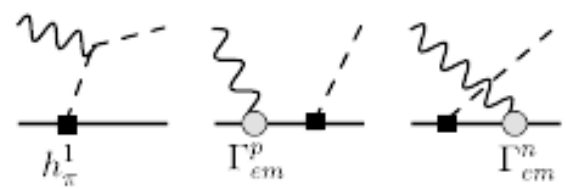

h^1_π partially cancels Z-exchange; but Z-exchange is known (P2 + A2@MAMI)
P2: $A^{PV} = -4 \times 10^{-8}$ to 1.5%; PV π production: $A^{PV} = -2 \times 10^{-7}$ to 10-20%

Z-exchange only

Z-exch. + h^1_π

Shaded band:
uncertainty due to h^1_π